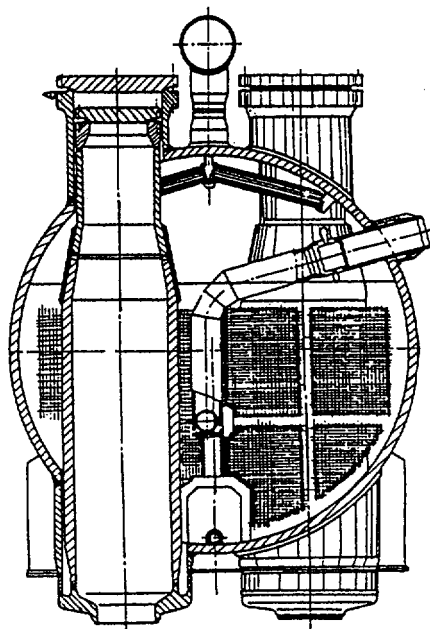




FOURTH INTERNATIONAL SEMINAR ON HORIZONTAL STEAM GENERATORS



LTKK-TJ-67



FI9800021

UDK 621.1

621.039

621.311.25

LAPPEENRANNAN TEKNILLINEN KORKEAKOULU
LAPPEENRANTA UNIVERSITY OF TECHNOLOGY

TIETEELLISIÄ JULKAISUJA
RESEARCH PAPERS

67

FOURTH INTERNATIONAL SEMINAR ON HORIZONTAL STEAM GENERATORS

LAPPEENRANTA
1997

ISBN 951-764-189-3
ISSN 0356-8210

**FOURTH INTERNATIONAL SEMINAR ON HORIZONTAL
STEAM GENERATORS**

11-13 March 1997, Lappeenranta, Finland



FOURTH INTERNATIONAL SEMINAR ON HORIZONTAL STEAM GENERATORS 11-13 March 1997, Lappeenranta, Finland

PREFACE

A series of International Seminars of Horizontal Steam Generator Modelling were initiated by Finnish nuclear organisations a few years ago. Three seminars have been arranged in March 1991, September 1992 and October 1994 in Lappeenranta, Finland. Improvement in understanding of realistic thermal hydraulic behaviour of the horizontal steam generators when performing safety analyses for VVER reactors has been a general objective. The initiated international cooperation has proven to be effective in collecting existing experimental and theoretical knowledge of the behaviour of horizontal steam generators under normal operation, transient and accident conditions. The first two seminars concentrated on thermal hydraulic experiments and analytical modelling of the flow behaviour both in the primary side and in the secondary side. New experimental results, comparisons of existing experimental facilities and approaches to calculational modelling were presented. The scope of the third seminar was widened to structural and aging issues. It turned out to be very beneficial to bring structural and thermal hydraulic experts together and thus decrease the difficulties in governing the interface of these areas. It was agreed to include the same subjects to the fourth seminar.

Consequently, overall objectives for the fourth seminar were set as

- to enhance understanding of horizontal SG behaviour during normal operating and accidental conditions,
- to provide forum for discussion among the experts,
- to collect new experimental and theoretical results, and
- thus enhance safety and economy of VVER operation.

The fourth seminar consisted of six sessions. The topics were thermal hydraulic experiments and analyses, primary collector integrity, feedwater distributor replacement, management of primary-to-secondary leakage accidents and new developments in the VVER safety technology. As in the previous seminars, the organisers were IVO Power Engineering Ltd, Lappeenranta University of Technology (LTKK) and VTT Energy. There were 70 participants in total. They came from 10 countries and 25 papers were presented. The participants represented designers and manufacturers of the horizontal steam generators, plant operators, engineering companies, research organisations, universities and regulatory authorities.

Session I dealt with thermal hydraulic experiments. New results were available from the Finnish PACTEL facility concerning heat transfer degradation and flow distributions during boil-off under natural circulation conditions. Direct measurements of water inventory of the VVER-440 steam generator in operation (measured at Rovno Unit 1) were discussed by OKB Gidropress. Thermal hydraulic experiments were presented by Mitsubishi Heavy Industry on the flow behaviour of the secondary side of the horizontal steam generator designed for the passive next generation PWR concept. Influence of dissolved nitrogen in the ECCS accumulator water on the steam generator heat transfer was discussed based on the

experiments by OKB Gidropress. Finally, the sixth paper of the session introduced the results from experiments in the German HORUS-II facility.

Session II consisted of various papers on modelling the horizontal steam generators with thermal hydraulic system codes and their validation against experiments. Coolant flow distribution in the steam generator primary side was also discussed.

Session III started with papers on mechanical integrity aspects of the primary collectors. The significance of temperature stratification in the collectors under natural circulation conditions was discussed and scoping experiments were presented.

Session IV dealt with the problem of the feedwater distributor experiencing severe erosion-corrosion in the VVER-440 steam generators. Two principally different designs have been applied to replace the eroded pipe sections: one by Gidropress and its modification for Loviisa, and the other by Vítkovice. The first two papers presented the experiments on condensation driven water hammers of the Loviisa designs, and the other papers discussed operating experience and effects on flow distributions of the latter design.

Session V was dedicated to the aspects of primary-to-secondary (PRISE) leakage accidents. Plugging criteria and integrity assessment of the heat transfer tubes were discussed by the first two papers. And there was a presentation of thermal hydraulic analyses to support development of the PRISE management concepts.

Final Session VI was devoted for new developments in the VVER safety technology. The first paper of the session presented the design and construction status of the large scale KMS facility that is an integral facility to model VVER-640 plant concept with passive safety systems. The KMS facility has a volume scaling ratio of 1:27 and it includes the integrated primary circuit with containment. It is being constructed by NITI Institute at Sosnovy Bor near to St. Petersburg, Russia. There was a presentation of the modernisation and power upgrading project of the Loviisa VVER-440 Plant. Finally, mechanical component developments of horizontal steam generators in the Czech Republic were presented.

Final discussion of the seminar started with a proposal by Dr. Trunov of OKB Gidropress concerning continuation of the common code validation exercises. After obtaining new data on the secondary side water inventory a common calculational exercise could be arranged and every participant would calculate by applying various codes the secondary side water inventory e.g. on power levels 0%, 40%, 60%, 80% and 100% The proposal was well taken.

Prof. Blagovechtchenski of St.Petersburg State Technical University proposed that cooperative experimental program of his university, Kalinin NPP, LTKK and VTT at Lappeenranta should be supported. Temperature stratifications make an important input from thermal hydraulics to structural integrity assessments of primary components including steam generators.

There was common agreement among participants that more papers from the plant operators particularly on the operating experience should be emphasized for future seminars.

Dr. Hyvärinen felt that these seminars serve as an excellent forum from the regulator's viewpoint. Organizers should encourage more regulatory authorities to participate and focus even more on operational experience.

It was felt that the next seminar should be organised in the time frame of two to three years. It was emphasized that communication between thermal hydraulic and structural and material experts should be sought even more strongly. Also various stratification phenomena and their significance for various plant operations modes and for plant aging should be further studied. The Finnish organizers volunteered to continue as organizers and they also continue to seek for support from international organisations for the arrangements of the next seminar and proposed tentatively to have the next seminar in Lappeenranta in 1999.

Harri Tuomisto, IVO
Heikki Purhonen, VTT
Virpi Kouhia, LTKK

FOURTH INTERNATIONAL SEMINAR ON HORIZONTAL STEAM GENERATORS

11 - 13 March 1997, Lappeenranta, Finland

PROGRAMME

Tuesday, 11 March 1997

- 8:30 Registration
- 9:00 Opening of the Seminar
- 9:15 Aim and Programme of the Seminar
Dr. Harri Tuomisto, IVO Power Engineering

Session I

THERMAL-HYDRAULIC EXPERIENTS ON HORIZONTAL STEAM GENERATORS

Chair: Dr. N. Trunov, OKB Gidropress, Russia

Co-Chair: Prof. H. Kalli, LTKK, Finland

- 9:30 J. Hyvärinen, J. Kouhia: Experimental Verification of the Horizontal Steam Generator Boil-Off Heat Transfer Degradation at Natural Circulation.
- 10:00 G.A. Tarnkov, N.B Trunov, B.N. Dranchenko, W.W. Kamiagin: Direct measurements of water inventory of steam generator PGV-213 in operation.
- 10:30 *Coffee break*
- 11:00 K. Sakata, Y. Nakamura, N. Nakamori, T. Mizutani, S. Uwagawa, I. Saito, T. Tsuyoshi: Advanced Technologies on Steam generators - Study on Thermal-Hydraulic Behavior of Horizontal Steam Generators.
- 11:30 S.A. Logvinov, Yu.K. Sitnik: Study of Steam Condensation in SG Tubes with Large amount of Nitrogen to be Accumulated.
- 12:00 S. Alt, W. Lischke: Experiments with the HORUS-II Test Facility
- 12:30 Discussion on Session I.
- 13:00 *Lunch*

Session II

THERMAL HYDRAULIC ANALYSES OF HORIZONTAL STEAM GENERATORS

Chair: Mr. P. Matejovic, VUJE, Slovakia

Co-Chair: Mr. J. Miettinen, VTT Energy, Finland

- 14:30 F. D'Auria, M. Frogheri, G.M. Galassi: Modelling of WWER-1000 Steam Generators by Relap5/Mod 3.2. Code.
- 15:00 L. Perneczky: Possible Thermal Shock Events During Large Primary to Secondary Leakage.
- 15:30 *Coffee Break*
- 16:00 N. Agafonova, J. Banati: The Evaluation of Validity of the RELAP5/MOD3 Flow Regime Map for Horizontal Small Diameter Tubes at Low Pressures.
- 16:30 A. Blagovechtchenski, V. Leontieva A. Mitrioukhin,: Coolant Rate Distribution in Horizontal Steam Generator Tubes under Natural Circulation.
- 17:00 W. Lischke, B. Vandreier: Post Test Calculation of the Experiment "Small Break Loss of Coolant Test" SBL-22 at the Finnish Integral Test Facility PACTEL with the Thermohydraulic Code ATHLET.
- 17:30 Discussion on Session II
- 18:00 Social Programme

Wednesday, 12 March 1997

Session III

PRIMARY COLLECTOR INTEGRITY

Chair: Dr. O. Matal, Energovyzkum, Czech Republic

Co-Chair: Mr. J. Pullinen, IVO Power Engineering, Finland

- 9:00 K. Matocha, J. Wozniak: Analysis of WWER 1000 SG Collector Cracking Mechanisms.
- 9:30 K. Matocha, J. Wozniak, K. Pochman: Analysis of WWER 440 Primary Collector Bolted Joint Damage.
- 10:00 *Coffee Break*

- 10:30 A. Blagovechtchenski, V. Leontieva, A. Mitrioukhin: Coolant Stratification and its Thermohydrodynamic Specificity under Natural Circulation in Horizontal Steam Generator Collectors.
- 11:00 V. Mitoukov, A. Mitrioukhine, V. Kortenien: About Technical Possibility to Use VEERA Facility for Investigation of Coolant Stratification Phenomenon in Horizontal Steam Generators.
- 11:30 Discussion on Session III
- 12:00 *Lunch*
- 13:30 Tour to the PACTEL facility

Session IV

FEEDWATER DISTRIBUTOR REPLACEMENT

Chair: Mr. S. Savolainen, IVO Loviisa, NPP, Finland

Co-Chair: Mr. H. Ollikkala, STUK, Finland

- 15:00 S. Savolainen, S. Katajala, B. Elsing, P. Nurkkala, J. Hoikkanen, J. Pullinen: Condensation-driven Water Hammer Studies for Feed Water Distribution Pipe.
- 15:30 P. Nurkkala, J. Hoikkanen: Integrated Experimental Test Program on Waterhammer Pressure Pulses and Associated Structural Responses within a Feedwater Sparger of a Steam Generator.
- 16:00 *Coffee Break*
- 16:30 O. Matal, S. Schmidt, M. Mihalik: EBO Feed Water Distribution System, Experience Gained from Operation.
- 17:00 Ludovit Papp: Feedwater Flow-in to Steam Generators Tube Bundle.
- 17:30 O. Matal, T. Šimo, L. Kucak, F. Urban: Modeling of Soluble Impurities Distribution in the Steam Generator Secondary Water.
- 18:00 Discussion on Session IV
- 18:15 Social Programme

Thursday, 13 March 1997

Session V

MANAGEMENT OF PRISE ACCIDENTS

Chair: Mr. H. Jokineva, IVO, Loviisa NPP, Finland

Co-Chair: Dr. J. Hyvärinen, STUK, Finland

- 9:00 L. Papp, W. Martin, M. Herman: Plugging Criteria for WWER SG Tubes.
- 9:30 K. Šplichal, J. Otruba: Structural and Leakage Integrity Assessment of WWER Steam Generator Tubes.
- 10:00 P. Matejovic, L. Vranka: Support Calculations for Management of PRISE Leakage Accidents.
- 10:30 Discussion of Session V
- 11:00 *Coffee break*

Session VI

NEW DEVELOPMENTS IN VVER SAFETY TECHNOLOGY

Chair: Dr. H. Tuomisto, IVO Power Engineering, Finland

Co-Chair: Mr. J. Kouhia, VTT Energy, Finland

- 11:30 Y. N. Anishevich, V. A. Vasilenko, V. K. Zasukha, Y. A. Migrov, V. B. Khabenski: Large-Scale Experimental Facility for Emergency Condition Investigation of a New Generation NPP WWER-640 Reactor with Passive Safety Systems.
- 12:00 A. Keskinen: Modernization and Power Upgrading of the Loviisa NPP.
- 12:30 *Lunch*
- 14:00 M. Kawalec: Design and Production Upgrades of Steam Generators WWER-1000 Offered to China Republic (Liaoning NPP Project).
- 14:30 F. Cikryt, L. Bednárek, L. Kusýn: Replacement of Nickel Sealing Rings by Expanded Graphite Sealing Rings - Upgrading of SG Primary Collector Flange Connection.
- 15:00 Discussion of Session VI
- 15:30 Closing Remarks
- Adjourn

FOURTH INTERNATIONAL SEMINAR ON HORIZONTAL STEAM GENERATORS**11-13 March 1997, Lappeenranta, Finland****LIST OF PARTICIPANTS***Name**Organisation**Address, telephone, telefax***Czech Republic**

Mr. Pavel Černík

ŠKODA PRAHA a.s.
Jaderná Elektrořna Temelín
37305 Temelín, Czech Republic
Tel. +420 334 421494, fax +420 334 421755

Mr. František Cikryt

VÍTKOVICE, J.S.C.
Division 600
70602 Ostrava 6, Czech Republic
Tel. +420-69-2926135, fax +420-69-2926460

Dr. Miroslav Kawalec

VÍTKOVICE, a.s., Power Engineering Division
Ruska' 101
70602 Ostrava 6, Czech Republic
Tel. +420-69-2926217, fax + 420-69-2922719

Mr. Miloř Kynčl
kym@nri.cz

Nuclear Research Institute ŘEŽ plc
Nuclear Safety Regulation Support Division
25068 Řeř, Czech Republic
Tel. +420 2 6617 2284, fax 420 2 685 7068

Mr. Milan Malačka
mal@nri.cz

Nuclear Research Institute ŘEŽ plc
25068 Řeř, Czech Republic
Tel. +420 2 6617 2376, fax 420 2 685 7954

Dr. Oldřich Matal

Energovřzkum Ltd
Bořetěchova 17, 61200 Brno, Czech Republic
Tel. +420-5-41214660, fax +420-5-41214659

Dr. Karel Matocha

VÍTKOVICE, J.S.C.
Research and Development Division
Pohraniční 31, 70602 Ostrava 6, Czech Republic
Tel. +420-69-2927189, fax +420-69-2928927

Dr. Ludovit Papp

VÍTKOVICE, J.S.C.
Power Engineering Division
70602 Ostrava 6, Czech Republic
Tel. +420-69-2929635

Mr. Karel Šplíchal

Nuclear Research Institute ŘEŽ plc
25068 Řež, Czech Republic
Tel. +420 2 6617 3224, fax 420 2 685 7519

France

Ms. Isabelle Dor
dor@ecrins.alpes.cea.fr

CEA-Grenoble
DRN/DTP/SMTH/LMTL
17 avenue des Martyrs
38000 Grenoble, France
Tel. +04 76 88 59 70, fax +04 76 88 94 53

Germany

Dr. Michael Kiera
kiera00m@erls15.kwu.siemens.de

Siemens, Power Generation Group (KWU)
Siemens AG, KWU NDS1
P.O.Box 3220
D-91050 Erlangen, Germany
Tel. +49 9131 18 5574, fax +49 9131 18 4345

Mr. Wolfgang Luther
luw@grs.de

Gesellschaft für Anlagen- und Reaktorsicherheit
(GRS) mbh
Forschungsgelände
85748 Garching b. München, Germany
Tel. +49 89 32004 426, fax +49 89 32004 599

Mr. Bernd Vandreier
vandreier@novell1.ipm.htw-zittau.de

Hochschule für Technik, Wirtschaft und
Sozialwesen Zittau/Görlitz (FH)
Theodor-Körner-Allee 16
02763 Zittau, Germany
Tel. +49 (0) 3583 61 1547, fax +49 (0) 3583 61 1288

Hungary

Dr. Lázló Perneczky
pernec@sunserv.kfki.hu

KFKI - Atomic Energy Research Institute
P.O.Box 49
H-1525 Budapest, Hungary
Tel. + 36 1 3959-220/1231, fax +36 1 3959-293

Italy

Mr. Edgardo Coda Zabetta

DITEC - University of Genova
via All'Opera Pia 15/A
16145 Genova, Italy
Tel. +39 10 353 2277, fax +39 10 311 870

Ms. Monica Frogheri
monica.f@unige.it

DITEC - University of Genova
via All'Opera Pia 15/A
16145 Genova, Italy
Tel. +39 10 353 2277, fax +39 10 311 870

Mr. Sergio Giusto

DITEC - University of Genova
via All'Opera Pia 15/A
16145 Genova, Italy
Tel. +39 10 353 2277, fax +39 10 311 870

Mr. Paolo Magliolo

DITEC - University of Genova
via All'Opera Pia 15/A
16145 Genova, Italy
Tel. +39 10 353 2277, fax +39 10 311 870

Japan

Dr. Toshiyuki Mizutani
B900230@KIND.kobe.mhi.co.jp

Mitsubishi Heavy Industry Co. (Kobe)
1-1-1 Wadasaki-Cho, Kobe 652, Japan
Tel. +81 78 672 3491, fax +81 78 672 3339

Russia

Ms. Natalia Agafonova
steam@steam.hop.stu.neva.ru

St. Petersburg State Technical University
Polytechnicheskaya, 29, 195251, St-Petersburg
Russia
Tel. +7 812 552 6591, fax. +7 812 552 67 96

Prof. Anatoli Blagovechtchenski
steam@steam.hop.stu.neva.ru

St. Petersburg State Technical University
Polytechnicheskaya, 29, 195251, St-Petersburg
Russia
Tel. +7 812 552 6591, fax. +7 812 552 67 96

Mr. Yuri Kourakov

Minatom Russia
Staromonetmy per, 26, Moscow 109180, Russia
Tel. +7 (095) 233 30 53, fax. +7 (095) 230 24 20

Ms. Veronika Leontieva
steam@steam.hop.stu.neva.ru

St. Petersburg State Technical University
Polytechnicheskaya, 29, 195251, St-Petersburg
Russia
Tel. +7 812 552 6591, fax. +7 812 552 67 96

Dr. Yuri Migrov

Research Institute of Technology, NITI
Sosnovy Bor, Leningrad Region
188537 Russia
Tel. +7 812 69 63343, fax +7 812 69 63672

Mr. Valeri Mitoukov
steam@steam.hop.stu.neva.ru

St. Petersburg State Technical University
Polytechnicheskaya, 29, 195251, St-Petersburg
Russia
Tel. +7 812 552 6591, fax. +7 812 552 67 96

Dr. Nikolai Trunov
trunov@grpress.msk.ru

OKB Hidropress
 Ordzhonikidze 21, 142103 Podolsk, Moscow Region
 Russia
 Tel. +7 095 137 96 52

Mr. Vitaly Zasukha

Research Institute of Technology, NITI
 Sosnovy Bor, Leningrad Region
 188537 Russia
 Tel. +7 812 69 63343, fax +7 812 69 63672

Slovakia

Mr. Peter Andrasko

NPP Mochovce
 SE, a.s. - EMO o.z. Mochovce
 93539 Mochovce, Slovak Republic
 Tel. +421 813 36 33 00, fax +421 813 39 11 45

Mr. Peter Matejovič
matej-p@inst.vujett.sk

VÚJE Trnava
 VÚJE, Okružná 5 91864 Trnava, Slovak Republic
 Tel. +421 805 569 152, fax +421 805 501 471

Mr. Oto Kuchar

NPP Jaslovské Bohunice
 SE a.s. EBO Jaslovské Bohunice
 91931 Jaslovské Bohunice, Slovak Republic
 Tel. +421 805 591 501, fax +421 805 591 527

UK

Dr. George Kimber
george.kimber@aeat.co.uk

AEA Technology
 Winfrith, Dorchester, Dorset
 DT 2 8 DH, UK
 Tel. +44 1305 202354, fax +44 1305 202508

Finland

Mr. József Bánáti
Jozsef.Banati@lut.fi

Lappeenranta University of Technology
 P.O. Box 20, FIN-53851 Lappeenranta, Finland
 Tel. +358 5 621 2732, fax +358 5 621 2799

Mr. Bernhard Elsing
Bernhard.Elsing@ivo.fi

Imatran Voima Oy, Loviisa Power Plant
 P.O. Box 23, FIN-07901 Loviisa, Finland
 Tel. +358 19 550 3161, fax +358 19 550 4435

Ms. Arja Hyvärinen

Lappeenranta University of Technology
 P.O. Box 20, FIN-53851 Lappeenranta, Finland
 Tel. +358 5 621 2701, fax +358 5 621 2799

Dr. Juhani Hyvärinen
Juhani.Hyvarinen@stuk.fi

Finnish Centre for Radiation and Nuclear Safety
 P.O.Box 14, FIN-00881 Helsinki, Finland
 Tel. +358 9 759881, fax +358 9 75988382

Ms. Anitta Hämäläinen
Anitta.Hamalainen@vtt.fi

VTT Energy
 P.O. Box 1604, FIN-02044 VTT, Finland
 Tel. +358 9 456 5023, fax + 358 456 5000

Mr. Heikki Jokineva
Heikki.Jokineva@ivo.fi

Imatran Voima Oy, Loviisa Power Plant
 P.O. Box 23, FIN-07901 Loviisa, Finland
 Tel. +358 19 550 4020, fax +358 19 550 4013

Prof. Heikki Kalli
Heikki.Kalli@lut.fi

Lappeenranta University of Technology
 P.O. Box 20, FIN-53851 Lappeenranta, Finland
 Tel. +358 5 621 2705, fax +358 5 621 2799

Mr. Ismo Karppinen
Ismo.Karppinen@vtt.fi

VTT Energy
 P.O. Box 1604, FIN-02044 VTT, Finland
 Tel. +358 9 456 5027, fax + 358 456 5000

Ms. Satu Katajala
Satu.Katajala@ivo.fi

Imatran Voima Oy, Loviisa Power Plant
 P.O. Box 23, FIN-07901 Loviisa, Finland
 Tel. +358 19 550 3910, fax +358 19 550 4435

Mr. Jyrki Kouhia
Jyrki.Kouhia@vtt.fi

VTT Energy
 P.O. Box 20, FIN-53851 Lappeenranta, Finland
 Tel. +358 5 621 2375, fax +358 5 621 2379

Ms. Virpi Kouhia
Virpi.Kouhia@lut.fi

Lappeenranta University of Technology
 P.O. Box 20, FIN-53851 Lappeenranta, Finland
 Tel. +358 5 621 2781, fax +358 5 621 2799

Mr. Jaakko Miettinen
Jaakko.Miettinen@vtt.fi

VTT Energy
 P.O. Box 1604, FIN-02044 VTT, Finland
 Tel. +358 9 456 5032, fax + 358 456 5000

Mr. Teemu Nevalainen
Teemu.Nevalainen@lut.fi

Lappeenranta University of Technology
 P.O. Box 20, FIN-53851 Lappeenranta, Finland
 Tel. +358 5 621 2713, fax +358 5 621 2799

Mr. Pekka Nurkkala
Pekka.Nurkkala@ivo.fi

IVO Technology Centre, DLM03
 Rajatorpantie 8, Vantaa
 FIN-01019 IVO, Finland
 Tel. +358 9 8561 4717, fax +358 9 563 2225

Mr. Juha Ohvo
Juha.Ohvo@lut.fi

Lappeenranta University of Technology
 P.O. Box 20, FIN-53851 Lappeenranta, Finland
 Tel. +358 5 621 2784, fax +358 5 621 2799

Mr. Hannu Ollikkala
Hannu.Ollikkala@stuk.fi

Finnish Centre for Radiation and Nuclear Safety
 P.O.Box 14, FIN-00881 Helsinki, Finland
 Tel. +358 9 75988 333, fax +358 9 75988 382

Mr. Christer Palsinajärvi
Christer.Palsinajarvi@ivo.fi

IVO Power Engineering Ltd
 Rajatorpantie 8, Vantaa
 FIN-01019 IVO, Finland
 Tel. +358 9 8561 5387, fax +358 9 8561 3403

Mr. Harri Partanen
Harri.Partanen@lut.fi

Lappeenranta University of Technology
 P.O. Box 20, FIN-53851 Lappeenranta, Finland
 Tel. +358 5 621 2741, fax +358 5 621 2799

Mr. Herkko Plit
Herkko.Plit@vtt.fi

IVO Power Engineering Ltd
 Rajatorpantie 8, Vantaa
 FIN-01019 IVO, Finland
 Tel. +358 9 456 5078, fax +358 9 456 5000

Mr. Jaakko Pullinen
Jaakko.Pullinen@ivo.fi

IVO Power Engineering Ltd
 Rajatorpantie 8, Vantaa
 FIN-01019 IVO, Finland
 Tel. +358 9 8561 4123, fax +358 9 563 0432

Mr. Heikki Purhonen
Heikki.Purhonen@vtt.fi

VTT Energy
 P.O. Box 20, FIN-53851 Lappeenranta, Finland
 Tel. +358 5 621 2371, fax +358 5 621 2379

Mr. Markku Puustinen
Markku.Puustinen@vtt.fi

VTT Energy
 P.O. Box 20, FIN-53851 Lappeenranta, Finland
 Tel. +358 5 621 2374, fax +358 5 621 2379

Mr. Hannu Pylkkö
Hannu.Pylkko@lut.fi

Lappeenranta University of Technology
 P.O. Box 20, FIN-53851 Lappeenranta, Finland
 Tel. +358 5 621 2769, fax +358 5 621 2799

Mr. Vesa Riikonen
Vesa.Riikonen@vtt.fi

VTT Energy
 P.O. Box 20, FIN-53851 Lappeenranta, Finland
 Tel. +358 5 621 2376, fax +358 5 621 2379

Ms. Christine Sarrette
Christine.Sarrette@lut.fi

Lappeenranta University of Technology
 c/o TKK, Department of Technical Physics
 Rakentajanaukio 2C, FIN-02150 Espoo, Finland
 Tel. +358 9 451 3205, fax +358 9 451 3195

Mr. Ilkka Saure
Ilkka.Saure@lut.fi

Lappeenranta University of Technology
 P.O. Box 20, FIN-53851 Lappeenranta, Finland
 Tel. +358 5 621 2749, fax +358 5 621 2799

Mr. Samuli Savolainen
Samuli.Savolainen@ivo.fi

Imatran Voima Oy, Loviisa Power Plant
 P.O. Box 23, FIN-07901 Loviisa, Finland
 Tel. +358 19 550 3050, fax +358 19 550 4435

Mr. R. Scott Semken
Scott.Semken@lut.fi

Lappeenranta University of Technology
 P.O. Box 20, FIN-53851 Lappeenranta, Finland
 Tel. +358 5 621 2373, fax +358 5 621 2799

Ms. Sinikka Soirinsuo
Sinikka.Soirinsuo@vtt.fi

VTT Energy
P.O.Box 1604, FIN-02044 VTT, Finland
Tel. +358 9 456 5010, fax +358 621 5000

Mr. Pekka Tolonen
Pekka.Tolonen@lut.fi

Lappeenranta University of Technology
P.O. Box 20, FIN-53851 Lappeenranta, Finland
Tel. +358 5 621 2713, fax +358 5 621 2799

Dr. Harri Tuomisto
Harri.Tuomisto@ivo.fi

IVO Power Engineering Ltd
Rajatorpantie 8, Vantaa
FIN-01019 IVO, Finland
Tel. +358 9 8561 2464, fax +358 9 8561 3403

Dr. Jari Tuunanen
Jari.Tuunanen@vtt.fi

VTT Energy
P.O. Box 20, FIN-53851 Lappeenranta, Finland
Tel. +358 5 621 2372, fax +358 5 621 2379

Mr. Juhani Vihavainen
Juhani.Vihavainen@lut.fi

Lappeenranta University of Technology
P.O. Box 20, FIN-53851 Lappeenranta, Finland
Tel. +358 5 621 2660, fax +358 5 621 2799

Mr. Eero Virtanen
Eero.Virtanen@lut.fi

Lappeenranta University of Technology
P.O. Box 20, FIN-53851 Lappeenranta, Finland
Tel. +358 5 621 2377, fax +358 5 621 2799

Mr. Vesa Yrjölä
Vesa.Yrjola@vtt.fi

VTT Energy
P.O. Box 1604, FIN-02044 VTT, Finland
Tel. +358 9 456 5041, fax + 358 456 5000

CONTENTS

PREFACE	i
PROGRAMME OF SEMINAR	iv
LIST OF PARTICIPANTS	viii
Experimental Verification of the Horizontal Steam Generator Boil-off Heat Transfer Degradation at Natural Circulation. <i>J. Hyvärinen (STUK, Finland)</i> <i>J. Kouhia (VTT Energy, Lappeenranta, Finland)</i>	1
Direct Measurements of Secondary Water Inventory of Steam Generator PGV-213 in operation. <i>G. Tarankov, N. Trunov, B. Dranchenko, W. Kamiagin (OKB Gidropress, Russia)</i>	15
Study on Thermal-Hydraulic Behavior of Horizontal Steam Generators. <i>K. Sakata, Y. Nakamura, N. Nakamori, T. Mizutani, S. Uwagawa</i> <i>I. Saito, T. Matsuoka (Mitsubishi Heavy Industry Co, Japan)</i>	19
Study of Steam Condensation in SG Tubes with Large Amount of Nitrogen to be Accumulated. <i>S. Logvinov, Y. Sitnik (EDO Gidropress, Russia)</i>	26
Experiments with the HORUS-II Test Facility. <i>S. Alt, W. Lischke (University for Applied Sciences Zittau/Görlitz, Germany)</i>	31
Modelling of WWER-1000 Steam Generators by Relap5/Mod 3.2 Code. <i>F. D'Auria, G.M. Galassi (University of Pisa, Italy)</i> <i>G. M. Frogheri (University of Genova, Italy)</i>	54
Possible Pressurized Thermal Shock Events during Large Primary to Secondary Leakage. <i>L. Perneczky (KFKI, Hungary)</i>	72
The Evaluation of Validity of the RELAP5/MOD3 Flow Regime Map for Horizontal Small Diameter Tubes at Low Pressure. <i>N. Agafonova (StPSTU, Russia)</i> <i>J. Banati (LTKK, Finland)</i>	111
Coolant Rate Distribution in Horizontal Steam Generator Tubes under Natural Circulation. <i>A. Blagovechchenski, A. Mitrioukhine, V. Leontieva (StPSTU, Russia)</i>	122
Post Test Calculation of the Experiment "Small Break Loss-of-Coolant Test" SBL-22 at the Finnish Integral Test Facility PACTEL with the Thermohydraulic Code ATHLET. <i>W. Lischke, B. Vandreier (University for Applied Sciences Zittau/Görlitz, Germany)</i>	131

Analysis of WWER 1000 SG Collector Cracking Mechanisms. <i>K. Matocha, J. Wozniak (Vítkovice, J.S.C., Czech Republic)</i>	137
Analysis of WWER 440 Primary Collector Bolted Joint Failure. <i>K. Matocha, J. Wozniak (Vítkovice, J.S.C., Czech Republic)</i> <i>K. Pochman (NPP Dukovany, Czech Republic)</i>	148
Coolant Stratification and Its Thermohydrodynamic Specificity under Natural Circulation in Horizontal Steam Generator Collectors. <i>A. Blagovechchenski, V. Leontieva, A. Mitrioukhin (StPSTU, Russia)</i>	156
About Technical Possibility to Use VEERA Facility for Investigation of Coolant Stratification Phenomenon in Horizontal Steam Generators. <i>V. Mitoukov, A. Mitrioukhine (StPSTU, Russia)</i> <i>V. Korteniemi (LTKK, Finland)</i>	163
Condensation-Driven Water Hammer Studies for Feed Water Distribution Pipe. <i>S. Savolainen, S. Katajala, B. Elsing, P. Nurkkala, J. Hoikkanen (Imatran Voima Oy, Finland)</i> <i>J. Pullinen (IVO Power Engineering Ltd, Finland)</i> <i>S.A. Logvinov, N.B. Trunov, J.K. Sitnik (EDO Gidropress, Russia)</i>	169
Integrated Experimental Test Program on Waterhammer Pressure Pulses and Associated Structural Responses within a Feedwater Sparger. <i>P. Nurkkala, J. Hoikkanen (Imatran Voima Oy, Finland)</i>	189
EBO Feed Water Distribution System, Experience Gained from Operation. <i>O. Matal (Energovýzkum Ltd, Czech Republic)</i> <i>P. S. Schmidt, M. Mihalik (Slovenské Elektrárne, a.s., Slovak Republic)</i>	204
Feedwater Flow-in to Steam Generators Tube Bundle. <i>L. Papp (Vítkovice J.S.C, Czech Republic)</i>	210
Modelling of Soluble Impurities Distribution in the Steam Generator. Secondary Water. <i>O. Matal, T. Šimo (Energovýzkum s.r.o., Czech Republic)</i> <i>L. Kucak, F. Urban (Slovak Technical University, Slovak Republic)</i>	217
Plugging Criteria for WWER SG Tubes. <i>L. Papp, M. Wiliam (Vítkovice J.S.C, Czech Republic)</i> <i>M. Herman (VÚJE, Slovak Republic)</i>	224
Structural and Leakage Integrity Assessment of WWER Steam Generator Tubes. <i>K. Šplíchal, J. Otruba (NRI REZ, Czech Republic)</i>	233
Support Calculations for Management of PRISE Leakage Accidents. <i>P. Matejovic, L. Vranka (VÚJE, Slovak Republic)</i>	243

Large-Scale Experimental Facility for Emergency Condition Investigation of a New Generation NPP WVER-640 Reactor with Passive Safety Systems. <i>Y. N. Aniskevich, V. A. Vasilenko, V. K. Zasukha, Y. A. Migrov, Z. V. B. Khabenski (NITI, Russia)</i>	256
Modernisation and Power Upgrading of the Loviisa NPP. <i>A. Keskinen (IVO Power Engineering, Finland)</i>	262
Design and Production Upgrades of Vítkovice Steam Generators WVER-1000 Offered to China Rep. (Liaoning NPP Project). <i>M. Kawalec (Vítkovice J.S.C, Czech Republic)</i>	269
Replacement of Nickel Sealing Rings by Expanded Graphite Sealing Rings - Upgrading of SG Primary Collector Flange Connection. <i>F. Cikryt, L. Bednárek, L. Kusýn (Vítkovice J.S.C, Czech Republic)</i>	274
Analysis of Kalinin NPP Steam Generator PGV-1000 Thermophysical Characteristics. <i>V.I. Aksyonov, V.F. Bay, L.N. Bogatchek, A. E. Timofeyev (Kalinin NPP, Russia)</i>	282



FI9800022

EXPERIMENTAL VERIFICATION OF THE HORIZONTAL STEAM GENERATOR BOIL-OFF HEAT TRANSFER DEGRADATION AT NATURAL CIRCULATION

Juhani Hyvärinen
Finnish Centre for Radiation and
Nuclear Safety (STUK)
P.O.BOX 14
FIN-00881 HELSINKI
FINLAND

Jyrki Kouhia
VTT Energy
P.O.BOX 20
FIN-53851 LAPPEENRANTA
FINLAND

ABSTRACT

This paper presents highlights of experimental results obtained for VVER type horizontal steam generator heat transfer, primary side flow pattern, and mixing in the hot collector during secondary side boil-off with primary at single-phase natural circulation. The experiments were performed using the PACTEL facility with Large Diameter (LD) steam generator models, with collector instrumentation designed specifically for these tests. The key findings are as follows: (1) the primary to secondary heat transfer degrades as the secondary water inventory is depleted, following closely the wetted tube area; (2) a circulatory flow pattern exists in the tube bundle, resulting in reversed flow (from cold to the hot collector) in the lower part of the tube bundle, and continuous flow through the upper part, including the tubes that have already dried out; and (3) mixing of the hot leg flow entering the hot collector and reversed, cold, tube flow remains confined within the collector itself, extending only a row or two above the elevation at which tube flow reversal has taken place.

The first two findings are in good agreement with theory put forward earlier (Hyvärinen, 1993, 1996); continuous flow through the dry part of the tube bundle is the root reason for the heat transfer degradation. The mixing observations indicate that the mixing of the hot leg flow and cold reversed tube flow in the lower part of the hot collector is not local in a strict one-dimensional sense, but yet sufficiently local as to be of little if any consequence regarding system-wide natural circulation or total primary to secondary heat transfer.

1 INTRODUCTION

Theoretical analysis of VVER horizontal steam generator performance at natural circulation conditions in the primary [Hyvärinen, 1993, 1996] has shown that the primary to secondary heat transfer capability of these steam generators degrades with depleting secondary inventory roughly proportionally to the fraction of tubes still wetted. This phenomenon is specific to horizontal steam generators featuring horizontal U-tubes. Signs of such heat transfer degradation were evident in earlier PACTEL loss-of-feedwater experiment LOF-10 [Kouhia et al, 1995], but that experiment was terminated after having only five of the 14 tube rows uncovered. This issue is of safety significance since heat transfer degrading faster than core decay heat would lead to gradual primary system heatup and pressurisation in events involving total loss of feedwater. For example, in the event of a VVER 440 station black-

out, heat transfer degradation might lead to pressuriser safety valve actuation in less than three hours instead of the six hours or so that would be required to boil the steam generator secondaries completely dry. Additionally, Hyvärinen [1996] has proposed this degradation as the reason for the surprisingly high secondary water levels observed during the later phases of the Greifswald station blackout incident in 1975 (see, e.g. Albrecht and Gelhorst [1996]).

The same theoretical analyses have shown that at natural circulation conditions a circulating flow pattern emerges in the primary side of the tube bundle. This circulation follows from the need to balance the gravity head between the hot and cold collectors, and it involves reversed flow (from the cold towards the hot collector) in the lower part of the tube bundle. The presence of such flow raises the question of the efficiency of mixing between the hot fluid entering from the hot leg and cold fluid coming from the tube bundle lower part. Were the cold fluid able to fall counter the hot leg flow it could markedly affect overall loop natural circulation and potentially give rise to loop flow instability, as discussed in Hyvärinen [1996].

The Finnish Centre for Radiation and Nuclear Safety (STUK) decided to have experiments conducted to build up a comprehensive data base on all the horizontal steam generator natural circulation performance issues mentioned above. This data base is also being used to validate the HSG horizontal steam generator model developed by STUK [Hyvärinen, 1996]. The experiments were performed in the PACTEL facility in 1996, and this paper gives highlights of the most important findings. Section 2 describes the facility configuration and experimental procedures. The main results regarding heat transfer capability, primary flow pattern and collector mixing efficiency are reported in section 3, and conclusions presented in section 4.

2 FACILITY AND PROCEDURES

The PACTEL facility is a volumetrically scaled out of pile model of Loviisa VVER-440/213 type nuclear reactors operated by Imatran Voima Oy. The scaling factor for the integral test facility is 1:305 and the component heights and relative elevations correspond to those of the full scale reactor to match the natural circulation pressure heads in the reference reactor. The pressure vessel is simulated by a U-tube construction consisting of separate core and downcomer sections. Instead of six primary loops of the VVER-440 reactors PACTEL has three loops, hence one PACTEL steam generator corresponds to two nuclear power plant steam generators. The facility is not a full pressure test loop but the maximum pressure in the primary side is 8.0 MPa while the nominal pressure in the reactor is 12.5 MPa.

The core comprises 144 electrically heated fuel rod simulators. The lattice geometry is the same as in the reactor core. The maximum heating power is 1 MW which corresponds to about 22 % of the scaled down reactor thermal power. The length of the primary loops has been reduced in PACTEL in order to have larger diameter pipes which produces better simulation of the stratification phenomenon in the loops. More detailed description of the test rig is included in [Tuunanen et al, 1997].

The PACTEL facility has been in operation as a one loop test rig since 1990 and all the three loops have been operational since 1991. The test facility has been constructed as part of Finnish national reactor safety program and the construction has been financed by Ministry of Trade and Industry, Lappeenranta University of Technology and Technical Research Center of Finland. PACTEL is b-

cated in the laboratory of Lappeenranta University of Technology and operated by VTT Energy which is a research unit of Technical Research Center of Finland.

2.1 Steam generator description

The PACTEL Large Diameter steam generator models used in the tests features 118 heat exchange tubes in 14 layers connected to a hot and a cold collector (see Figure 3). The average length of the U-tubes is 2.8 m which is roughly a third of the full length of the steam generator tubes (average 9.0 m). The inner diameter is 13.0 mm whereas the inner diameter in the reference tubes is 13.2 mm and both the model and the reference tubes has the same outer diameter of 16 mm. In order to have a higher heat exchange tube cluster, the pitch in vertical direction has been increased to 48 mm instead of 24 mm of the power plant. The pitch in the horizontal direction has been maintained prototypic (30 mm).

The shell diameter is one meter and the height of the steam generator tube cluster is 0.68 m when measured from the bottom of the shell. The secondary side free volume of the PACTEL LD steam generator is by a factor of about 2.5 larger than the scaled down volume of two power plant steam generators, whence the time scale of secondary side transients is nonprototypically slow. (Actually, for the purposes of the boil-off experiments this fact is of considerable benefit.) Two compartments has been constructed on each side of the steam generator to decrease the mass of water that is directly involved to the primary to secondary heat transfer process. The compartments are not totally isolated from the rest of the secondary side, but coolant has a number of flow paths in and out of the compartments. Figure 1 shows a PACTEL steam generator.

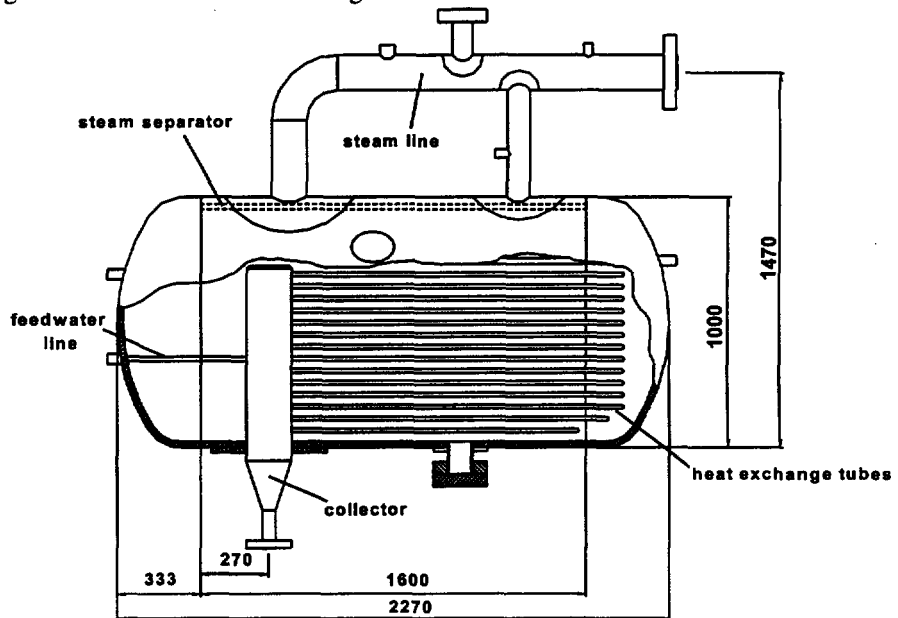


Figure 1. PACTEL steam generator, side view.

2.2 Steam generator measurement instrumentation

Figure 2 shows the cross section of the PACTEL steam generator. The heat exchange tubes with measurements are filled with black color. The instrumented tubes have 1.0 mm mineral insulated thermocouples in three or four different locations along the tube for measuring the primary and secondary side fluid temperatures. These locations are marked as a0, a, b, c, d and e as shown in figure 3. The accuracy of the temperature measurements was ± 2.0 °C in all the tests. Loop mass flow measurement accuracy at the conditions of these experiments was in the order of ± 0.02 kg/s, for primary pressure ± 30 kPa, and for secondary pressure ± 20 kPa.

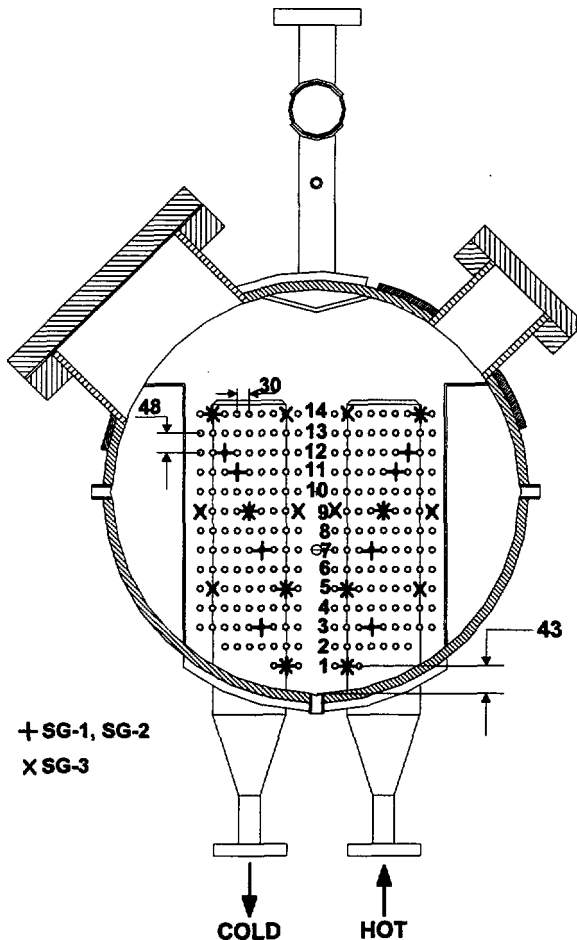


Figure 2. Cross section of the PACTEL steam generator. Tubes marked with + signs are instrumented in steam generators 1 and 2, those marked with X signs are instrumented in SG 3. Instrumented tube feature thermocouples on both the primary and the secondary side.

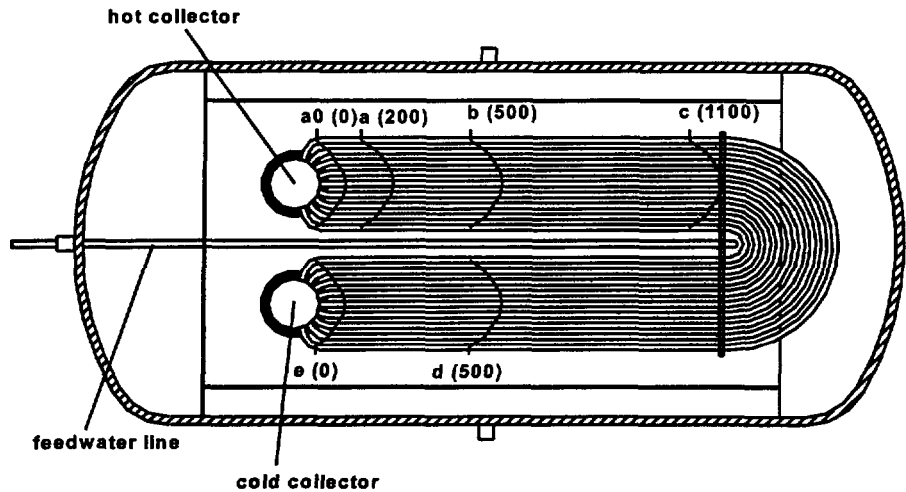


Figure 3. Thermocouple measurement locations in the PACTEL steam generator.

For the boil-off experiments eight thermocouples were added to both the hot and cold collector to produce information on the radial temperature distribution inside the collectors in one steam generator. The measurements were distributed on two different heights in the collectors so that both elevations had four thermocouples. In the hot collector the measurements were at the elevations of the first and the fifth heat exchange tube layer (when bottommost layer is considered as layer one). In the cold collector the corresponding tube layers are one and four. The four radial thermocouples lie in a row at 8, 55, 65 and 70 mm from the center of the collector towards the collector side at which the tubes are. Figure 4 shows the measurement point locations in the hot collector. The cold collector instrumentation is similar to the hot one except for the different axial position of the upper row.

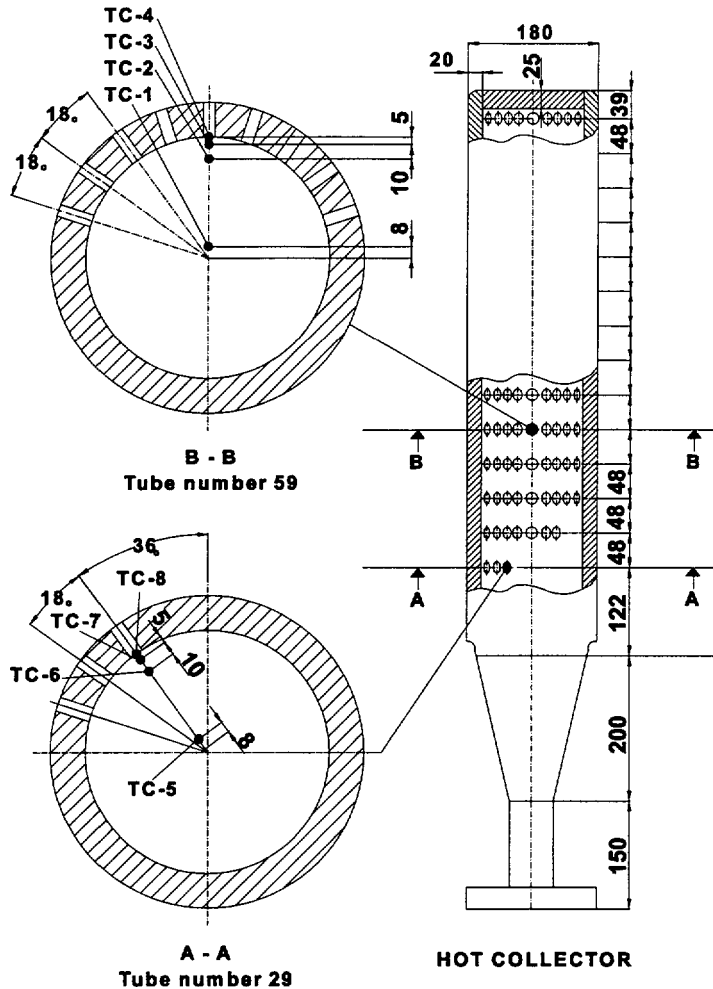


Figure 4. Temperature measurements in the hot collector.

2.3 Procedures

The general test philosophy was developed on the basis of earlier PACTEL boil-off experiments (Kouhia et al, 1995) and pretest analyses using the HSG horizontal steam generator primary side simulation code coupled with a simple natural circulation model. This code system has been developed by STUK (Hyvärinen, 1993, 1996). On the basis of pretest analyses we expected a rather rapid heat transfer degradation as the secondary depletes, and in order to avoid compromising the accuracy of the essential temperature differentials, we decided to attempt to maintain a temperature difference of 20 to 30 °C over the steam generators at all times. To accomplish this we took actions during the experiments, primarily reducing the secondary pressure in a few steps as necessary. Core power was

also adjusted downwards a few times in order to maintain a subcooling margin of at least 5°C in the primary, which was kept at around 7.5 MPa pressure. Towards the end of the experiments we occasionally drained the secondary side by less than the equivalent of one tube row at a time in order to speed up bundle dryout. The actions taken during experiments HSG 1 and 2 are tabulated in Table 1.

Table 1. Main operator actions during experiments HSG 1 and HSG 2.

HSG 1	
Wet rows	Action
11	Power reduction from 92 to 78 kW
9	Power reduction from 78 to 72 kW
8	Secondary pressure reduction from 41 to 33 bar
7	Secondary pressure reduction from 33 to 28 bar
7	Secondary drained by 4 cm
6	Power reduction from 72 to 57 kW
4	Secondary pressure reduction from 28 to 19 bar
4	Secondary drained by 4 cm
3	Secondary pressure reduction from 19 to 10 bar
3	Secondary drained by 4 cm
HSG 2	
Wet rows in SG 3 ^a	Action
11	Secondary pressure reduction from 40 to 28 bar
5	Secondary pressure reduction from 28 to 5 bar
2	Power reduction from 221 to 119 kW

^aNote that in HSG 2 all three loops were involved, but the initial levels differed between steam generators.

Experiment HSG-1 was run in a single loop mode. The heat-up phase before the actual test was performed with the main circulation pump running and when the nominal secondary pressure was reached the pump was stopped. This initiated a one hour period during which the loop flow and temperature reached equilibrium. Data logging was started after this. The primary pressure was maintained using pressuriser heaters throughout the test and secondary side pressure was controlled by a control valve.

In the experiment HSG-2 all the three primary loops were employed to investigate the potential for loop asymmetry effects. The heat-up was performed with the primary circulation pumps running. When the desired secondary pressure, 4.0 MPa, was reached the pumps were stopped. Then we drained the secondary side level of each steam generator to reach the initial conditions: SG-1 42 cm, SG-2 55 cm and SG-3 63 cm. The draining was obtained through the drain valve located in the bottom of the steam generator. After finishing the secondary side draining we waited for a half an hour before starting data logging. This waiting period allowed the loop flow and temperature to equilibrate. The primary pressure was again maintained using pressuriser heaters throughout the test whereas the secondary side pressure was controlled by a control valve.

3 KEY FINDINGS

In this section we present our key findings regarding the overall primary to secondary side heat transfer rate as a function of the secondary water level and sketch the primary side flow pattern deduced from primary temperature measurements in the tubes. As expected, we observed a circulatory flow pattern in the tube bundle, with reversed (cold to hot collector) flow in the lower part of the tube bundle. Reversed flow mixes in the hot collector with hot coolant arriving from the hot leg, and we present measured radial temperature profiles that illuminate the efficiency of this mixing

3.1 Power throughput

The steam generator primary to secondary side heat transfer rates were calculated on the basis of the measured loop mass flows and steam generator inlet and outlet temperatures. These results were checked using the steam generator boil-off rate and the known core power and facility heat losses and found to match well. We present the transferred powers in dimensionless form, where the enthalpies h are computed from system pressures and inlet/outlet temperatures:

$$Q' = \frac{h_{in} - h_{out}}{h_{in} - h'_{(p_{sec})}} \quad (1)$$

This allows an easy comparison with both between experiments with variable secondary pressures and pretest predictions with the HSG code. The results are summarised in Figure 5.

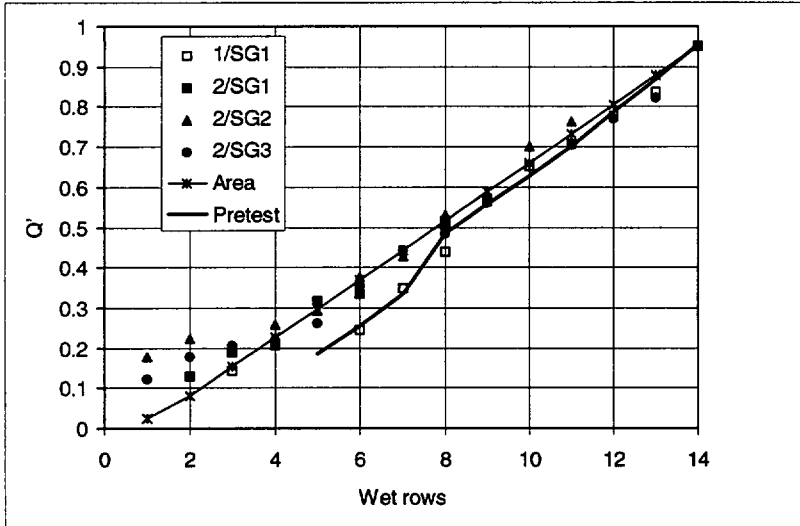
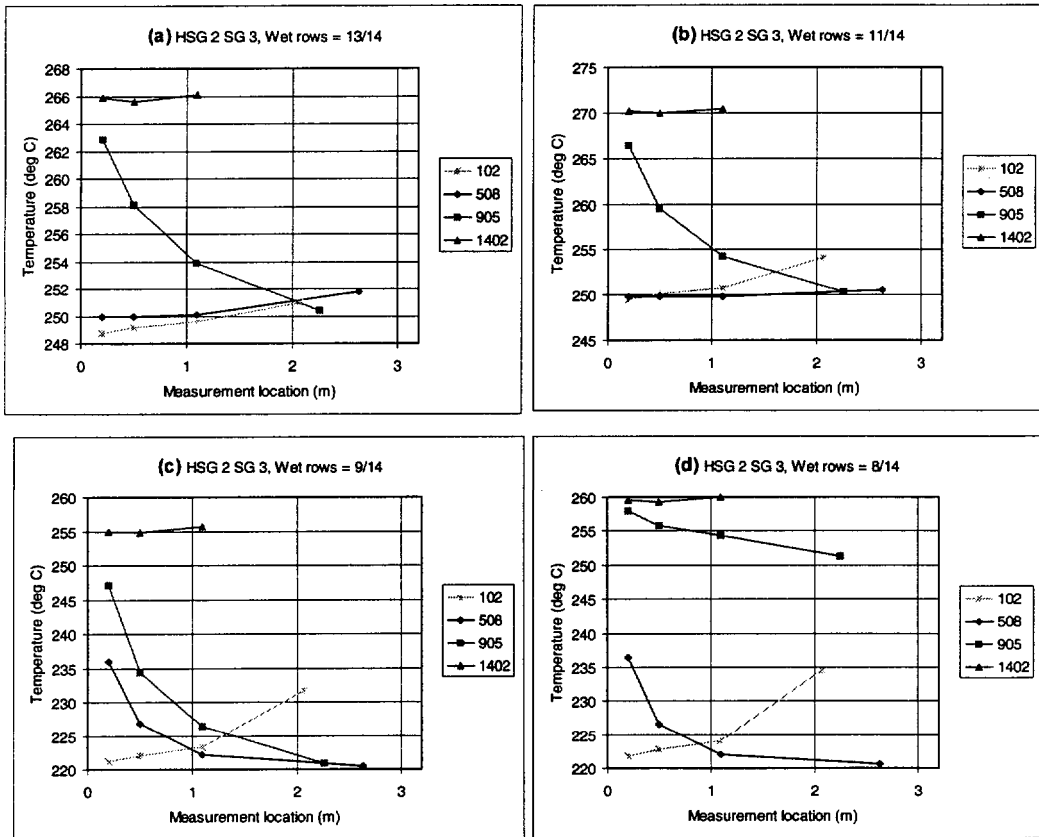


Figure 5. Dimensionless power throughputs from experiments HSG 1 and HSG 2 as a function of the number of wetted tubes, and compared with the corresponding wetted heat transfer area and pretest prediction by the HSG code.

As can be seen, the pretest prediction is generally somewhat below the available area curve, and single loop experiment HSG 1 results agree very well with the prediction. However, the triple loop results from experiment HSG 2 show more scatter and deviate to higher power throughputs especially at lower secondary levels (less than eight wetted rows). This happens because at the very high primary to secondary temperature difference (which prevails there owing to the secondary depressurisation), recirculation continued until the end of the experiment, and its effect at low secondary side level is to increase power throughput markedly (see Figure 6 of (Hyvärinen, 1996b) and the associated discussion). Cooling of the upper tube bundle, due to superheating of steam, is also taking place, but its effect is at most in the order of 10% of the wetted region power throughput.

3.2 Primary side flow pattern

As an example of the four steam generator depletion cases collected from experiments HSG 1 and 2 we present here the samples of the boil-off history of steam generator 3 during experiment HSG 2. This case begins with 13 of the 14 rows wetted and the secondary side at 4.0 MPa pressure. We give tubewise temperature measurements for a representative tube of each of the four instrumented rows in SG 3 in Figures 8a through 8g and inlet and secondary temperatures in Figure 9.



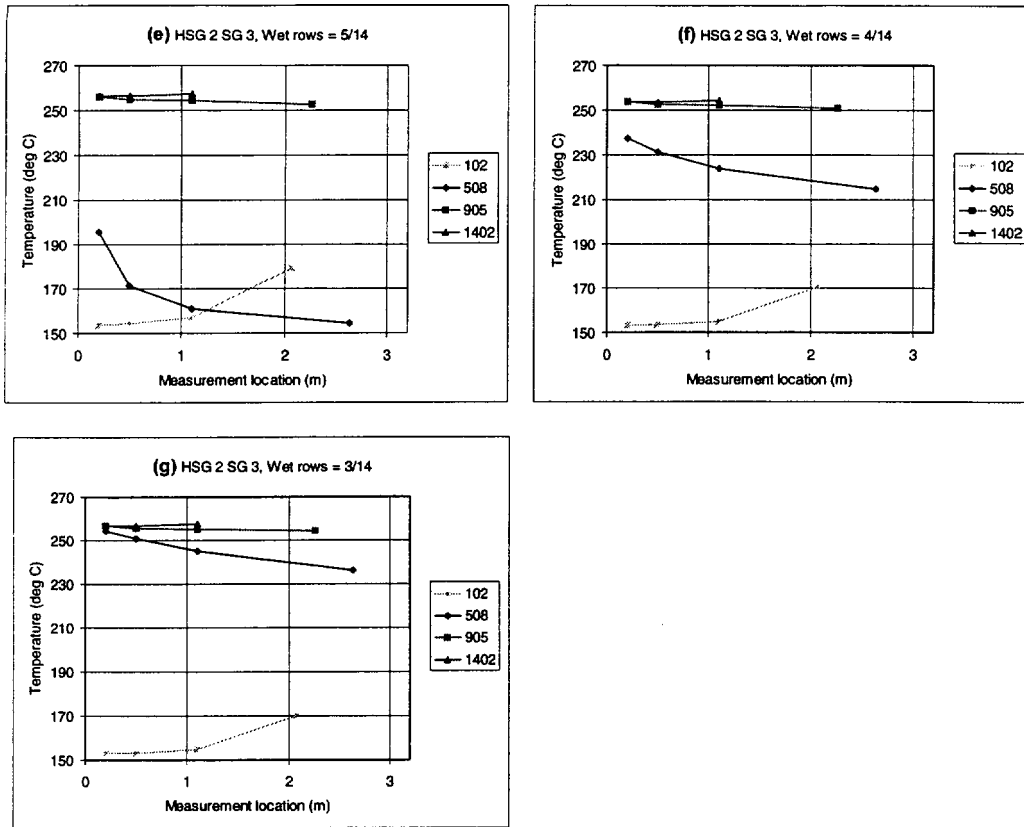


Figure 8. Samples of the tubewise temperature profiles during boil-off in SG 3 during experiment HSG 2. The legend indicates tube position as RRXX, where RR denotes the tube row (from bottom up) and XX lateral column in the bundle (from inside out). Observe how the flow reversal, which initially occurs above row 5 (a), moves below row 5 (b and c), how row 9 dries out (d) and how row 5 dries out (e,f,g).

From Figure 8 one sees the presence of the circulatory flow pattern, with backflow at the bottom of the bundle, and continuous flow through all the topmost tubes, even those that have dried out. This latter fact is best evidenced by the ever increasing gap between the secondary saturation temperature and SG outlet temperature. Top tube uncooled flow is responsible for the cold collector temperature rise with decreasing secondary level; that is clearly visible in the lower (reversed) tube temperature profiles. Furthermore, Figures 8f and g suggest that convective heat transfer to steam is fairly the efficient – steam superheat reaches equilibrium with the hot tubes over the elevation of 2 to 3 tube rows. Backflow at the lowest tube row persists throughout the experiment.

We also observe that when the row 5 flow turns from reversed to forward mode, Figure 8 (b) to (c), its inlet temperature increases only slowly towards the hot collector average temperature (Figures 8 (c) to (f)). This happens because the backflow forms a thin, cold wall layer in the hot collector, as will be detailed below in section 3.3.

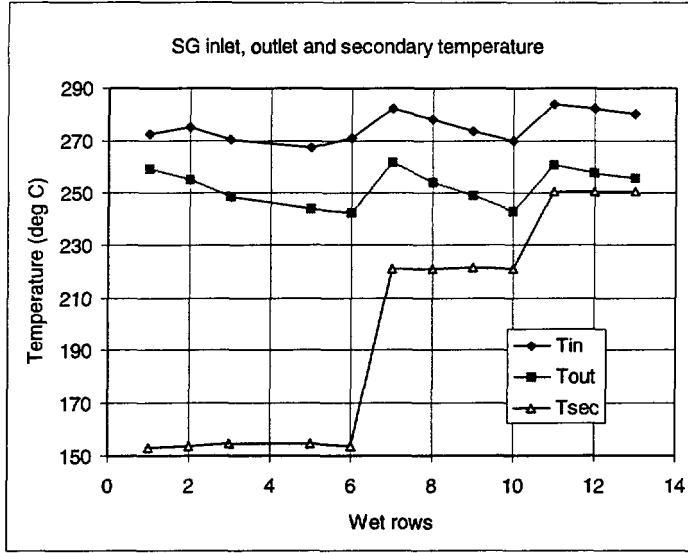


Figure 9. SG 3 inlet, outlet and secondary (saturation) temperatures. See Table 1 for the operator actions performed during the experiment.

3.3 Mixing in the hot collectors

During all the experiments we observed in all steam generators that the steam generator inlet temperature, measured from the hot leg at the flange joining the SG to the leg, was equal to core exit temperature well within measurement accuracy. We interpret this as a clear indication that no cold fluid falldown into the hot leg occurred during these experiments, despite the substantial net reversed flow at the tube bundle bottom part - according to HSG analyses, the net reversed flow was initially in the order of the inlet flow itself, but decreased with decreasing secondary level.

The reason for the absence of cold fluid falldown lies in the geometry of the hot leg to collector joint. As is clear from Figure 4, the joint comprises a conical expansion piece 200 mm long; over this distance the inner diameter increases from 52 to 140 mm, that is, opening at 12.5° half-angle. At typical natural circulation velocities ranging from 0.25 to 0.40 m/s in the hot leg, at such an expansion angle it is certain that the boundary layer will separate and a roughly doughnut-shaped separation vortex will likely form in the expansion piece. Such a vortex would enhance local mixing, and entrain the cold liquid falling down at the wall, thus preventing it from entering the hot leg itself.

We present the radial temperature measurements in the hot collector during experiment HSG 1. The data is given in dimensionless form, since this allows for an easy identification of the mixing efficiency evolution during secondary depletion. The temperatures are nondimensionalised as follows and given for selected number of dry tube layers in Figure 10.

$$T' = \frac{T - T_{sec}}{T_{in} - T_{sec}}; \quad T_{sec} = T_{sat}(p_{sec}) \quad (2)$$

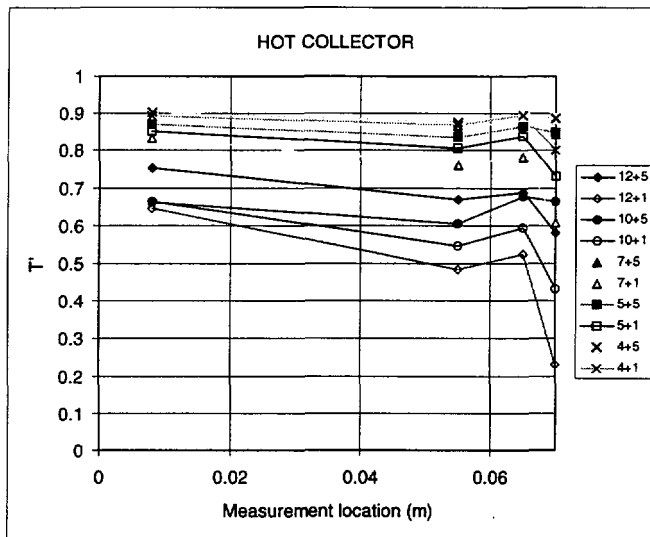


Figure 10. Experiment HSG 1 hot collector temperature profiles. Legend NN+Z indicates both the number of wetted tube rows (NN) and the elevation Z (in terms of tube rows) of the thermocouple rake.

Two observations are readily made: there is a relatively thin strongly cooled layer very near the wall, within some 5 millimeters, and the three "midflow" measurements indicate a 10 to 20% difference between the upper and lower stations (it is recalled that the upper station is at row 5 and the lower at row 1 elevation). This suggests that there is a wide circulation loop from the tube side of the collector towards the blind side, an asymmetry one might expect in PACTEL on the ground that all the tubes join the collector on one side only.

Judging by these data and tube measurements such as were shown in section 3.2 (witness the evolution of row 5 inlet temperature in Figures 8 (c) through (f)), we infer that the thin cold layer extends one or two tube row spacings (about 50 to 100 mm) above the elevation of flow reversal, gradually vanishing. This explains the "anomalously" low tube temperatures immediately above the reversal elevation noted in the the PACTEL LOF-10 analysis (Hyvärinen 1996). The extent of the upward "creep", as well as the relative coldness of the thin layer, decrease with secondary level, as the net reversed mass flow decreases.

We conclude that mixing between the flow entering from the hot leg and the cold reversed flow is confined to the hot collector, inside and above the conical expansion piece and below the reversal elevation plus roughly one tube row. Such mixing is not, strictly speaking, local in the one-dimensional sense (such as in present HSG code versions), but owing to the relatively small height difference between the tip of the cone and bottom of the tube bundle (some 0.32 m), its influence on the overall loop natural circulation is small.

3.4 A Scaling Remark

We remind the reader that the only results which scales more or less directly to plant scale is the fact that the overall primary to secondary heat transfer roughly follows wetted tube area. Tube flow patterns exhibited by the PACTEL LD steam generator are qualitatively similar to those to be expected in the VVER 440 steam generator, but prototypic (plant scale) recirculation mass flows are smaller, in the order of 20% of the inlet flow at conditions similar to the initial conditions of the tests reported here. However, the ranges of flow velocities in PACTEL LD and VVER 440 steam generators are practically equivalent, whence at equal thermodynamic conditions representative flow and heat transfer regimes are present in the PACTEL LD model (Hyvärinen, 1996b).

Thanks to the excessive recirculation mass flow, the cold flow mixing question could be resolved in a bounding fashion: the Froude numbers of the cold streams from tubes in the prototypic and PACTEL LD steam generators do not differ essentially. By virtue of its large reversed mass flow, PACTEL LD steam generator has a greater potential to cause cold liquid falldown into the hot leg. Finally, the expansion angle of the VVER 440 hot leg to collector joint is much larger than the PACTEL LD expansion angle (the half angles being about 37° and 12° , respectively), implying that the formation of a separation vortex at the expansion piece is inevitable at all natural circulation flows occurring in practice. The hot inflow would effectively entrain the cold waterfall from the wall in such a vortex.

4 CONCLUSIONS

Steam generator boil-off experiments were performed with the PACTEL facility using Large Diameter steam generator models. The experiments were designed to yield a comprehensive data base on horizontal steam generator heat transfer degradation with boil-off, primary side tube bundle flow pattern, and collector mixing phenomena. The highlights of the experimental results that are presented in this paper confirm the following:

1. Primary to secondary heat transfer rate generally follows the wetted tube area. At higher secondary levels ($> 50\%$ in the PACTEL LD model) the power throughput tends to decrease slightly faster with the secondary level than the wetted area does; at lower levels ($< 50\%$) experimental data show, despite some scatter, that the continuing recirculatory flow greatly enhances primary to secondary heat transfer.
2. Circulatory flow pattern in the tube bundle is characteristic to natural circulation conditions, with continuous flow from the hot to the cold collector in the upper part, dry or wetted, and reversed flow at the bundle bottom. Ample data is now available on the movement of the reversal elevation as a function of the key boundary conditions, (primary inlet temperature and mass flow, secondary water level and temperature).
3. Mixing of the reversed, cold, flow in the hot collector is confined to inside and above the conical expansion piece and below the reversal elevation plus roughly one tube row.

Such mixing is not, strictly speaking, local in the one-dimensional sense, but owing to the relatively small height difference between the tip of the cone and bottom of the tube bundle (some 0.32 m), its influence on the overall loop natural circulation is small.

A full experiment report with more detailed analysis will be made available as a STUK-YTO-TR report in near future. Recall that the only results to scale relatively directly is the fact that primary to secondary heat transfer follows wetted tube area as the secondary depletes. More elaborate analysis is needed to scale the tube bundle flow patterns, but the theory to do this exists.

REFERENCES

- L. Albrecht und E. Gelhorst, Charakterisierung des Kabeltrassenbrandes im Block 1 des Kernkraftwerks Greifswald, *Kerntechnik* 61(1996)2-3 pp. 77-85. (Characterisation of the Cable Tray Fire in Unit 1 of Nuclear Power Plant Greifswald, in German.)
- J. Hyvärinen, Primary side flow distribution of a horizontal steam generator under low flow conditions, Second International Seminar of Horizontal Steam Generator Modelling, September 29-30, Lappeenranta, Finland (1992). See Lappeenranta University of Technology Research papers 30, Lappeenranta (1993) pp. 17-57.
- J. Hyvärinen, Heat Transfer Characteristics of Horizontal Steam Generators under Natural Circulation Conditions. *Nuclear Engineering and Design* 166(1996)191-223.
- J. Hyvärinen, Horizontal Steam Generator Primary Side Scaling (Appendix 4 of J. Hyvärinen, "On the fundamentals of nuclear reactor safety assessment: inherent threats and their implications", Dr. Tech. thesis, STUK-A135, Finnish Centre for Radiation and Nuclear Safety (STUK)), (1996b).
- J. Kouhia, V. Riikonen, H. Purhonen, PACTEL: Experiments on the Behaviour of the new Horizontal Steam Generator, The 3rd International Seminar on Horizontal Steam Generators, Oct. 18-20, Lappeenranta, Finland (1994). See Lappeenranta University of Technology Research papers 43, Lappeenranta (1995) pp. 1-9.
- J. Tuunanen et al., PACTEL facility for studies of nuclear safety in VVER type reactors. 1997. Espoo: Technical Research Centre of Finland. (VTT Research Notes). To appear.



Ministry of Nuclear Energy of Russia
OKB Hidropress

Direct measurements of secondary water inventory of steam generator PGV-213 in operation

Tarankov G.A., Trunov N.B., Dranchenko B.N., Kamiagin W.W.

Abstract

Results of weight measurement of PGV-213 steam generator during filling in, heating-up and power increase are described. Special measurement system based on stress gauges has been developed. Method of derivation of secondary water inventory is described. Comparison of the data for two steam generators prove accuracy of the measurements.

Introduction

Comparison of experimental and calculated data of void fraction in water volume of horizontal steam generator (SG) is one of the important elements of codes validation. Solving this problem we faced with contradiction between real 3D picture of SG hydrodynamic and its reflection in a model implemented in the code. Unfortunately nodalization level obtained nowadays don't let us perform quantitative comparison because of extremely complicated distribution of void fraction. Available data of void fraction is local. At the same time integral value of the void fraction determine swelled level and feedwater controller operation i.e. heat transfer for transients with level drop. Using of simplified models for dynamic transients could be justified only in case of results verification at least on value of void fraction (water inventory).

One of methods of determination of water inventory could be calculation on the basis of the analysis of level behavior in SG in a transient with load decrease. The attempt of such analysis was undertaken for example in /1/. A problem of a given method is necessity of the exact account of flowrates of water supplied in a SG and steam produced for a time of transient. Moreover high accuracy of level measurement in a SG is necessary. The existing means of measurement do not permit such measurements to be conducted with sufficient accuracy, first of all because of accuracy of flowmeters on steam line, which work correctly only at the flowrates close to nominal. Large uncertainties of this method were marked by author of estimations /1/.

Value determining integral void fraction in water volume or water inventory is the SG weight. In present paper measurements of weight of a SG are described. This data let us to determine with high accuracy integral void fraction at nominal load.

Description of measuring system.

The specified system was mounted on SG 5,6 of unit 1 of Rovno NPP during planned shutdown of 1995. Steam generator PGV-213 is mounted on four suspenders with cross-section of 300 x 30 mm. Thus the weight of a SG and water in it create strains in suspenders. The strains from weight of water in SG are extremely small (on the average 2.8 Kg/cm² on 1 t of weight) and can not be measured by existing strain gauges. For the given task special measurement gauges were developed enabling to multiply value of measured displacement. From two types of developed gauges only one type has appeared serviceable.

The specially developed sensitive element was placed in a gauge, which was fixed on each of 4 suspenders of SG by means of welding and was covered by heat insulation with the purpose to exclude the temperature difference between suspender and sensor. The calibration of gauges on a stand has shown linearity of their characteristics in a working range.

The procedure of weight derivation

While measuring weight of a water in a SG by a strain method there exists a problem of recalculation of value of strains in suspenders in weight of a water. The problem is complicated by the fact that SG together with suspenders and pipelines represent statically undeterminable system. Weight of a water and strains in suspender are connected ambiguously, since the part of a load is accepted by pipelines, which in the same time create additional load and rotation moment in process of heating-up. Other problem is determination of influence of weight of primary and secondary water separately, as far as for achievement of high accuracy of measurements it is required to take into account small density change in primary loop during load increase.

For overcoming of mentioned problems there was conducted calibration of a measuring system, first during filling of a SG from the primary side, and then during filling from the secondary side. During filling from the primary side a load was applied by pressure of 1 MPa for determination of air volume remaining in the loop. During filling of a SG from the secondary side level was measured directly by meter inside of SG, since existing level gauges do not provide required accuracy of measurement in a cold condition.

As a result of calibration procedure calibration factors were derived connecting weight of water in a SG with readings of the strain gauges. Weight load is distributed on suspenders non-uniformly, but during filling-in essential redistribution of a load does not occur. Suspenders have a large length in comparison with their cross-section and with temperature shift of a SG, that gives to us the right to neglect bending strains. For determination of influence of temperature lengthening of pipelines comparison of weight derived by two ways was conducted for nominal temperature condition. First way by the readings of strain gauges using obtained calibration factor and second way by readings of level gauges and calculation by geometrical data. The divergences were found for SG-5 -480 kg, for SG-6- 280 kg, that does not exceed error of measurement. This fact testifies that the strains arisen during heat-up of pipelines introduce negligible small contribution in vertical component of the load.

We shall note, that before the beginning of measurements calibration of level gauges was conducted on nominal parameters by decrease of SG level below the lower tap of the level gauges.

The value of relative error of determination of weight loss has been estimated 8% at confidence level of 95%.

Results of measurements

The measurements were conducted on SG 5-6 during load increase, and for SG-6 additionally in transients with MCP trip at 76.8 % of nominal load, load decrease by 10% and level decrease by 250 mm from nominal value at loads close to nominal. On the plot Fig 1. water inventory versus loop load for SG 5-6 is shown. The points for modes with switched on - off feedwater heater are designated separately. The deviation of a number of points in modes with working feedwater heater is explained by discrepancy of determination of loop load. Because of undetermined problems with a measuring computing system of the unit there were divergences between values of loop load determined at primary and secondary sides. The points with inexactly determined load are made in brackets and direction of their probable displacement is shown. The difference of values of weight for SG-5 and SG-6 is explained by different values of a level maintained in SG-5 and SG-6, that was confirmed during the calibration of level gauges. Difference of levels was 50-70 mm. In this case in both SGs the level above tubes was higher than it is required.

Let us notice that in fact half of the weight loss happens at load higher than 80%.

At Fig 2. water inventory versus level in SG-6 is shown at load close to nominal. Data were obtained by level decrease at 250 mm from nominal. We can see that curve is practically straight that means that tubes are still covered by water. Weight decrease is approximately 20 kg per mm of level drop.

Conclusion

Measurements performed let us derive dependency between water inventory in SG and power from minimal controlled power to almost nominal value. Accuracy of measurement is $\pm 8\%$. It is shown that in range of 80-100% of nominal power increase of void fraction is about 50%. Dependence between water inventory and water level was obtained for load conditions.

The data obtained could be used for codes validation.

References

1. H. Tuomisto. Secondary side water inventory in the Loviisa steam generators. Proceedings of International seminar of horizontal steam generator modelling, vol. 1. Lappeenranta, Finland, 1991.

Water inventory versus load

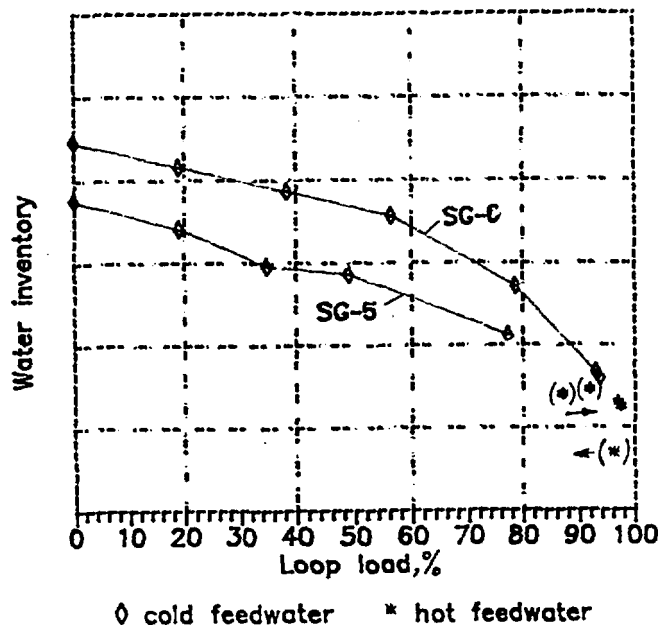


Fig.1

Water inventory versus level

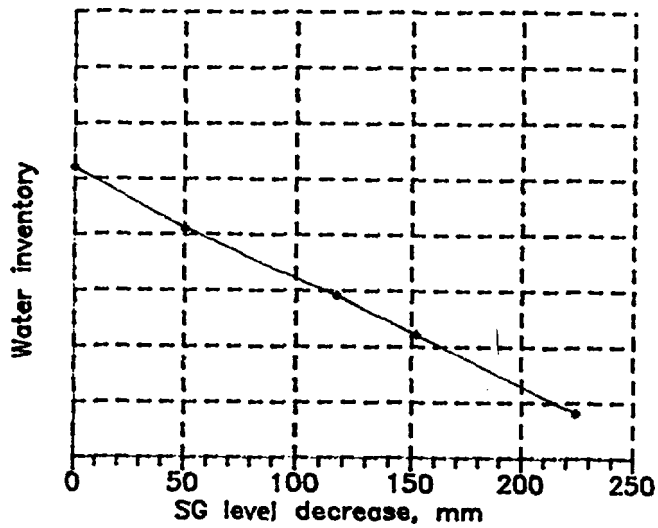


Fig.2



ADVANCED TECHNOLOGIES ON STEAM GENERATORS

(Study on Thermal-Hydraulic Behavior of Horizontal Steam Generator)

Kaoru SAKATA¹, Yuuki NAKAMURA¹, Nobuo NAKAMORI²,
Toshiyuki MIZUTANI², Seiichi UWAGAWA², Itaru SAITO²,
and Tsuyoshi MATSUOKA³

- 1 Mitsubishi Heavy Industry Co. (Takasago), 2-1-1 Shinham Arai-Cho, Takasago, Hyogo Pref. 676 Japan
TEL +81-794-45-6757, FAX +81-794-45-6947
- 2 Mitsubishi Heavy Industry Co. (Kobe), 1-1-1 Wadasaki-Cho, Kobe 652 Japan
TEL +81-78-672-3491, FAX +81-78-672-3339
- 3 Mitsubishi Heavy Industry Co. (Yokohama), 3-3-1 Minatomirai Nishi-Ku, Yokohama 220-84 Japan
TEL +81-45-224-9237, FAX +81-45-224-9920

ABSTRACT

The thermal-hydraulic tests for a horizontal steam generator of a next-generation PWR (New PWR-21) were performed. The purpose of these tests is to understand the thermal-hydraulic behavior in the secondary side of horizontal steam generator during the plant normal operation. A test was carried out with cross section slice model simulated the straight tube region. In this paper, the results of the test is reported, and the effect of the horizontal steam generator internals on the thermalhydraulic behavior of the secondary side and the circulation characteristics of the secondary side are discussed.

1. INTRODUCTION

Responding to the growing need for new concepts to produce nuclear power plants with improved safety, higher reliability and improved economy, Mitsubishi is now developing a next-generation PWR (New PWR-21) which has the innovative feature of hybrid safety systems incorporating the following new concepts [1, 2].

- (1) Conventional active safely systems and passive safety systems using new technologies are combined in a way that optimizes reliability and economy.
- (2) For Non-LOCA events, such as loss of external power, powerful and flexible active

safety systems are used similar to conventional PWR (Pressurized Water Reactor) plants.

- (3) Passive safety systems operate if the active safety systems are not available and also in a LOCA event.
- (4) Passive safety systems include horizontal steam generators (SGs), advanced accumulators, improved automatic depressurization systems, a gravity injection pit and a condensate storage tank as shown in Fig. 1.

The hybrid safety system uses horizontal steam generators which provide natural circulation cooling under accident conditions as part of the passive safety design. The horizontal arrangement avoids the possibility of accumulation of noncondensable gas in the U-tubes which could obstruct natural circulation.

In order to confirm the feasibility of the hybrid safety system, various kinds of safety analyses and tests are performed for LOCA events [3, 4].

On the other hand, a steam generator is one of the most important components of PWR nuclear power plant from the viewpoint of its reliability. Heat transfer tubes of the vertical steam generators used in the existing PWR nuclear power plants were experienced tube degradation due corrosion and wear related to the thermal-hydraulic behavior in the secondary side of steam generator. Therefore, authors performed the thermal-hydraulic tests for the design of horizontal steam generator.

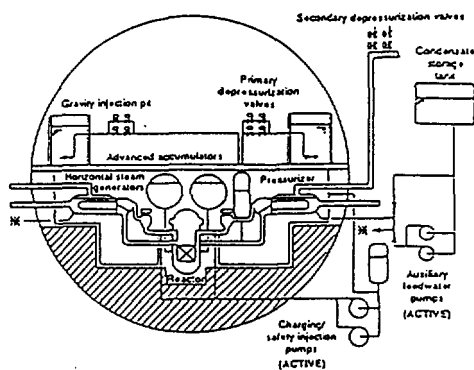


Fig. 1 Hybrid safety systems in New PWR-21

II. DESCRIPTION OF EXPERIMENT

The outline drawing of Horizontal steam generator is shown in Fig. 2. U-bend type tube bundle is applied to the horizontal steam generator, and then the thermalhydraulic behavior test was carried out by cross section slice model simulated the straight tube region.

The purpose of the cross section slice model test is to establish the database on the effect of the horizontal steam generator internals on the thermal-hydraulic behavior and the circulation characteristics in the secondary side of horizontal steam generator.

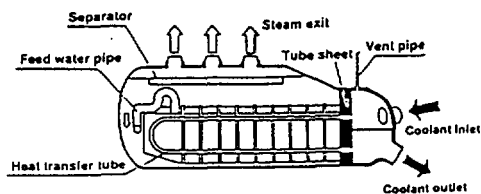


Fig. 2 Outline drawing of horizontal steam generator

The picture of cross section slice model is shown in Fig. 3. The model is the two-dimensional slice model to laterally cut the straight tube region of horizontal steam generator and the 1/2-scale model equipment with $\varnothing 21.7$ mm diameter tubes. Some of tubes are made of porous material tube to supply air, which simulate the void fraction distribution in the horizontal steam generator.

The explanation of internals in slice model is shown in Fig. 4.

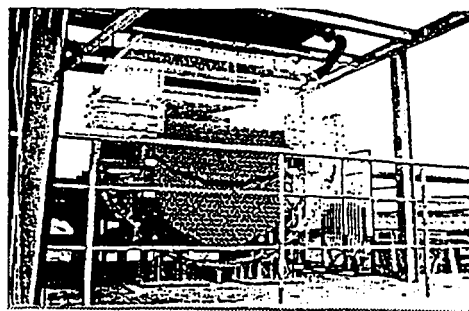


Fig. 3 View of cross section slice model

This test consists of a single-phase flow test and a air-water two-phase flow test under the conditions of a room temperature and an atmospheric pressure. The experimental apparatuses of the single-phase flow test and two-phase flow test are shown in Fig. 5 and Fig. 6, respectively.

In the single-phase flow test, a water or an air is supplied from the downcomer entrance (with the downcomer partition plate) through the orifice flow meter by the pump or the blower, respectively. Then it flows through the downcomer and the tube bundle, and flows out from the water exit or the air exit, respectively.

In the two-phase flow test, a forced circulation test and a natural circulation test are performed. In the forced circulation test, the downcomer partition plate is installed and a water is supplied from the downcomer entrance and an air is supplied through porous material tube. On the other hand, in the natural circulation test, the downcomer partition plate is removed and tested under the condition natural circulation.

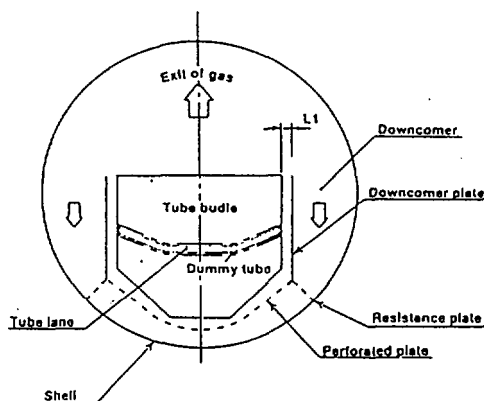


Fig. 4 Cross section slice model internals

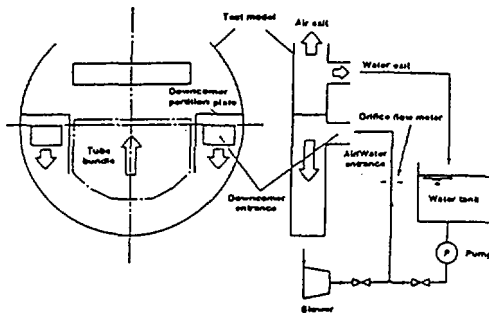


Fig. 5 Experimental apparatus of single-phase flow test

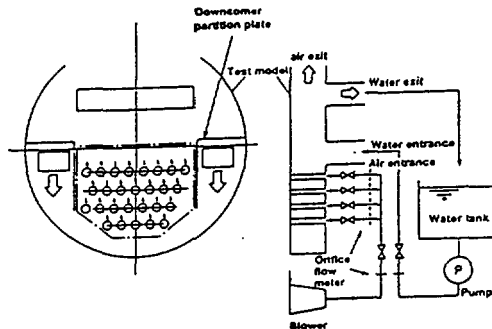


Fig. 6 Experimental apparatus of two-phase flow test

III. TEST RESULT AND DISCUSSION

1. Effect of internals on thermal-hydraulic behavior

Tests were performed with the following parameters of internals. (See Fig. 4)

- (1) Downcomer plate
- (2) Gap between downcomer plate and tube bundle (L1)
- (3) Perforated plate at entrance of tube bundle
- (4) Dummy tubes in tube lane

The difference of flow pattern between with and without downcomer plate is shown in Fig. 7, which were taken in the natural circulation test. These pictures show that the downcomer plate reduces the amount of carried-under gas. The reduction of carried-under gas increases the circulation ratio because of increasing a circulation head and reduce the high void fraction region and corrosion potential. In addition, the visualization due to dye injection indicates that the downcomer

plate is effective to normalize the velocity distribution in tube bundle. So the downcomer plate plays an important role in improving the thermalhydraulic behavior in tube bundle.

The effect of gap (L1) between downcomer plate and tube bundle for the velocity distribution in tube bundle, was tested in the single-phase flow test, as shown in Fig. 8. These test results show that the reduction of L1 is to increase the velocity in tube bundle, especially upper part of tube bundle, because of restricting the by-pass flow between downcomer plate and tube bundle. The increasing of velocity in tube bundle is contributed to reduce the high void fraction region, which reduces the corrosion potential.

The effect of perforated plate at entrance of tube bundle for the velocity distribution in tube bundle, was tested in the single-phase flow test, as shown in Fig. 9. Test results shows that the perforated plate at entrance of tube bundle is not much effect to normalize the velocity distribution at the vicinity of tube bundle entrance.

The effect of dummy tubes in tube lane to normalize the velocity distribution and the void fraction distribution in tube, which are measured in the single-phase flow and the two-phase flow, are shown in Fig. 10 and Fig. 11, respectively.

The comparison of Fig. 10 with Fig. 9 shows that the dummy tubes slightly reduce the by-pass flow between downcomer plate and tube bundle in the upper part of tube bundle and slightly increase the velocity in tube bundle, especially upper part of tube bundle. And also void fraction in tube bundle slightly increases, especially upper part of the tube bundle as shown in Fig. 11.

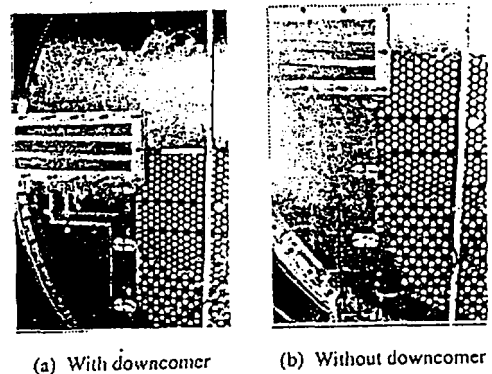


Fig. 7 Difference of flow pattern between with and without downcomer plate (Natural circulation test)

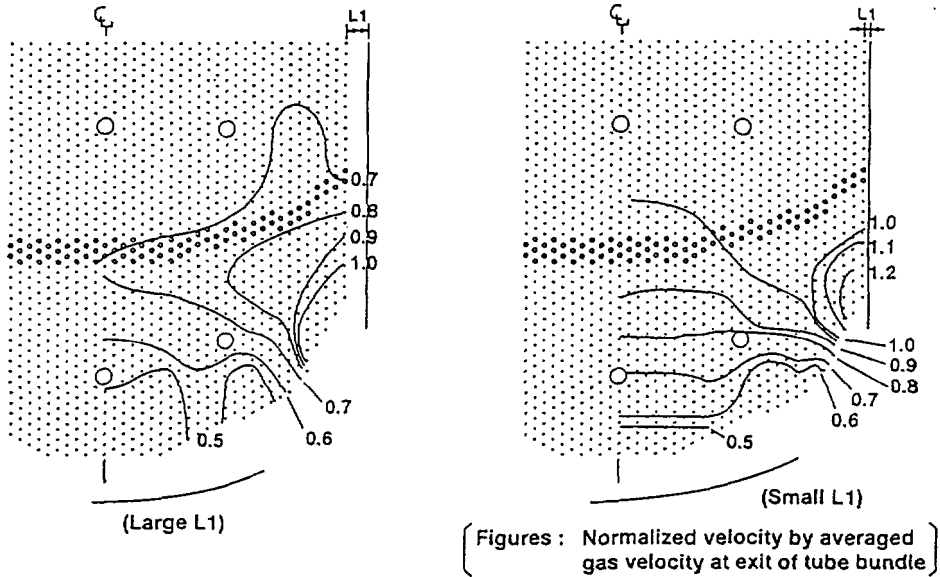


Fig. 8 Effect of gap ($L1$) between downcomer plate and tube bundle for the velocity distribution in tube bundle(Single-phase flow test)

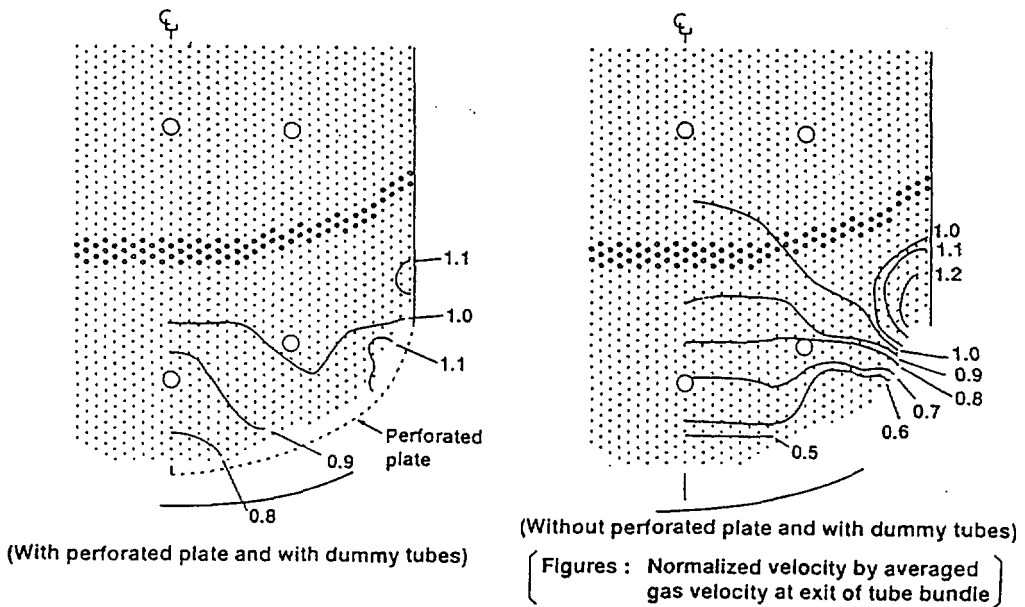


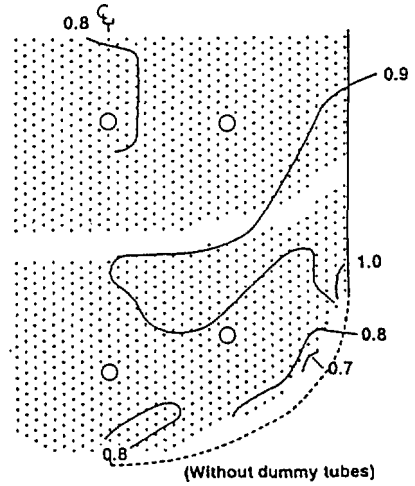
Fig. 9 Effect of perforated plate at entrance of tube bundle for the velocity distribution in tube bundle(Single-phase flow test)

2. Circulation characteristics of secondary side

Tests were performed with the parameter of the opening ratio of resistance plate (See Fig. 4) in the downcomer.

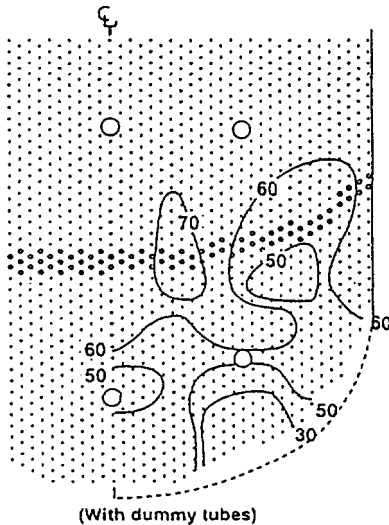
In order to evaluate the effect of opening ratio at resistance plate on the circulation ratio and the critical air flow rate on the occurrence of circulation instability, which was performed in the natural circulation test, and the test results are shown in Fig. 12. To reduce the opening ratio at resistance plate is to increase the critical air volume flow rate and to reduce the circulation ratio. For example, in case of 5 % opening ratio at resistance plate, circulation ratio is about 4 and the critical air flow rate is more than 2 times of the 100 % air volume flow, which is corresponding to the operating steam flow rate in actual Horizontal steam generator.

Concerning the circulation instability, the pressure fluctuation in tube bundle after the instability occurrence, which was also measured in the natural circulation test, is shown in Fig. 13. The period of this instability is about 1 second and is the same order as the passage time of fluid through the tube bundle. This fact indicated that this instability corresponds to the density wave oscillation.

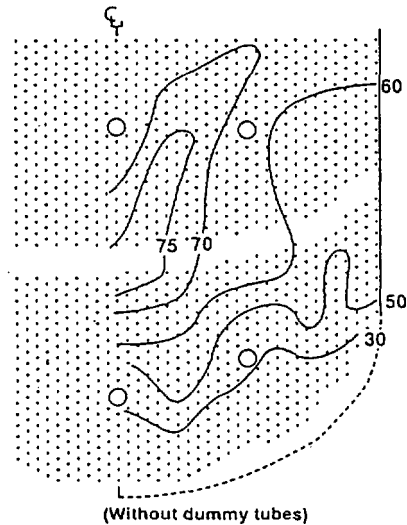


{ Figures : Normalized velocity by averaged gas velocity at exit of tube bundle }

Fig. 10 Effect of dummy tubes in tube lane for the velocity distribution in tube bundle (Singlephase flow test)



{ Figures :Void fraction (%)}



{ Figures :Void fraction (%)}

Fig. 11 Effect of dummy tubes in tube lane for the void fraction distribution in tube bundle (Two-phase flow test)

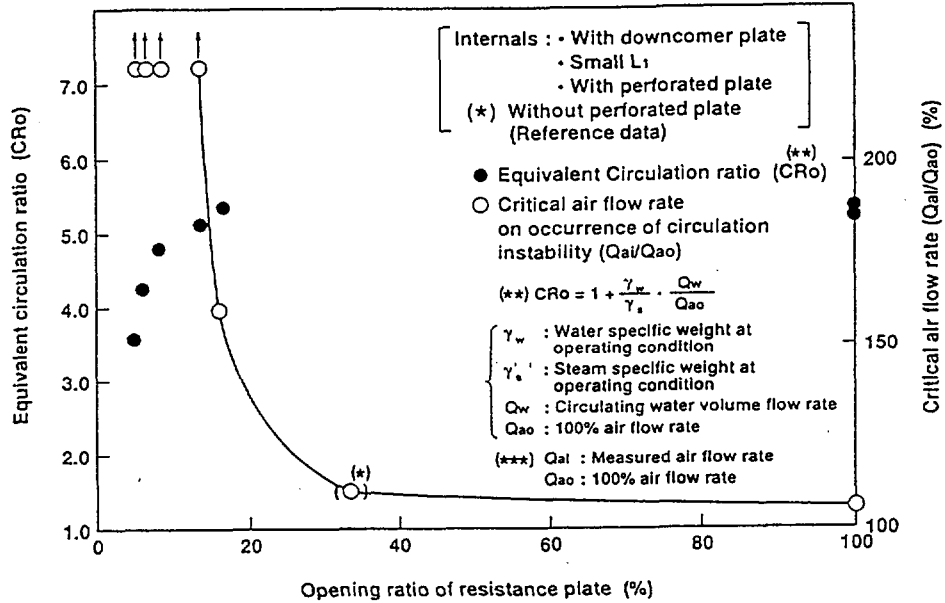


Fig. 12 Effect of opening ratio of resistance plate for the circulation ratio and critical air flow rate

IV. CONCLUSION

The experimental study on the thermal-hydraulic behavior of horizontal steam generator was performed using the cross section slice model. As a result, the thermal-hydraulic behavior in the secondary side of horizontal steam generator has been understood, and the database on the effect of internals on the thermal-hydraulic behavior and the circulation characteristics of the secondary side has been established.

The main results are as follows:

- (1) The installation of the downcomer plate and the reduction of gap (L₁) between downcomer barrel and tube bundle are effective to improve thermal-hydraulic behavior of the secondary side of horizontal steam generator
- (2) On the other hand, the effect of perforated plate at entrance of tube bundle and dummy tubes in tube lane is small. Therefore, the installation of perforated plate and dummy tubes should be carefully designed from the viewpoints of the thermal-hydraulic behavior, the complexity of internals structure and the cost.

- (3) It is confirmed that adjusting the opening ratio at resistance plate in downcomer, the target value of circulation ratio around 4 is established without pressure fluctuation.

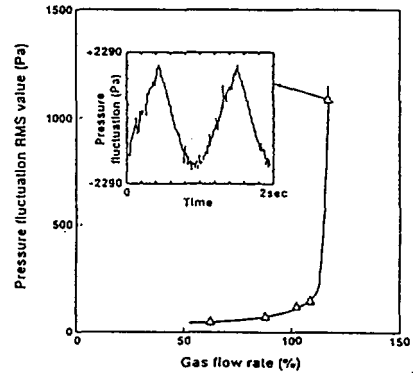


Fig. 13 Pressure fluctuation in tube bundle after instability occurrence (Natural circulation test)

REFERENCES

- [1] T. Matsuoka et al., Nuclear Safety, Vol. 33 No. 2 (1992).
- [2] T.Sugisaki et al., Proceedings of NURETH-5(1992).
- [3] K. Okabe et al., Proceedings of International Conference of Design and Safety of Advanced Nuclear Power Plants (1992). [4] T. Ueno et al., Proceedings of ICON-3 (1995).



FI9800025

STUDY OF STEAM CONDENSATION IN SG TUBES WITH LARGE AMOUNT OF NITROGEN TO BE ACCUMULATED

S.A.Logvinov, Yu.K.Sitnik
(EDO Hidropress, Podolsk, Russia)

Abstract

The effect of nitrogen during SG heat transfer under SBLOCA conditions have been studied. Depressurization of the primary side leads to release of nitrogen dissolved in the hydroaccumulator water. Nitrogen can accumulate in SGs and affect adversely heat transfer under reflux condenser conditions. The main objective of the study was to show that nitrogen does not prevent heat transfer in SGs of the VVER-640 which is reactor plant of new generation.

INTRODUCTION

Design of the new generation reactor VVER-640 makes provisions for the safety systems based on passive actuation. During SBLOCA at first the high pressure hydroaccumulators (HA) start to actuate which contain water in amount of about 270 m³ under pressure of 40 bar and temperature of 40-50°C. After the primary pressure decreases down to 7 bar, the rapid depressurization valves (RDV) open to equalize the reactor and containment pressures. Further, water from the atmospheric tanks of volume 2000 m³ is injected into the reactor by gravity preventing the core from uncover. This water after passing through the reactor forms external emergency pool whereas in the reactor there arises natural circulation through the pool and the depressurization lines.

The SG significance under SBLOCA depends on break size. If the leak is compensable, the primary-side natural circulation is kept with normal heat removal via the SGs. If break size is rather large, the primary-side pressure decreases down to 7 bar independently of the SG contribution. However, break may be of such size that the core-generated steam can not be discharged entirely through the break because of critical velocity. Passive pressure decrease is possible only due to steam condensation in the SG tubes with simultaneous decrease in the

passive heat removal system used to remove heat from the SG via the heat exchangers submerged in boiling water.

In the course of primary depressurization release of large amount of nitrogen dissolved in HA water is possible. The saturated solution could contain about 200 kg of nitrogen. Gas accumulation within the SG deteriorates heat transfer. If break is in the hot leg of the loop there is possible progressive gas accumulation in the SG. This phenomenon is capable of blocking up heat transfer completely. When break is in cold leg nitrogen is not accumulated and is carried away into the break.

To evaluate whether the mentioned gas amount could block the SG heat transfer, the tests have been carried out.

DESCRIPTION OF TEST FACILITY AND MAIN RESULTS

Test facility scheme is shown in Fig.1. It consists of reactor model, one short loop and 4-tube SG model. The SG U-shape tubes are 16x1,5 mm in diameter and 11 m in length. Tubes spacing (2,1 m) corresponds to the SG tube bundle height. Each tube is enclosed in a housing of tube 32x3 mm through which cooling water passes with temperature of 100-120°C. Extending outwardly tube ends are connected to two vertical collectors (tube 32x3 mm). Tube slope is 20 mm in the collectors direction. To prevent deformation due to gravity each tube has 5 additional supports.

Steam from reactor model enters SG model. Water level in the loop is set below outlet collector. After reaching steady state conditions nitrogen is injected into steam with a flow rate of 40-50 g/h. During nitrogen accumulation the SG model pressure starts to increase. Test is stopped when pressure rises up to 6,5 bar. Then the SG model is cut off and cooled. In cold state the residual pressure is measured and using the known volumes we calculate the amount of accumulated nitrogen.

The main objective of the tests was to define nitrogen amount in SG at pressure near threshold of FDW actuation (7 bar) and secondary side temperature of 100-110°C. If this amount exceeds the above 200 kg than heat removal from SG is possible in spite of gas accumulation. Otherwise, full blockage of SG could occur.

To transfer the test results for the real SG the following ratio between volumes of test rig and SG were taken into account (volumes in liters):

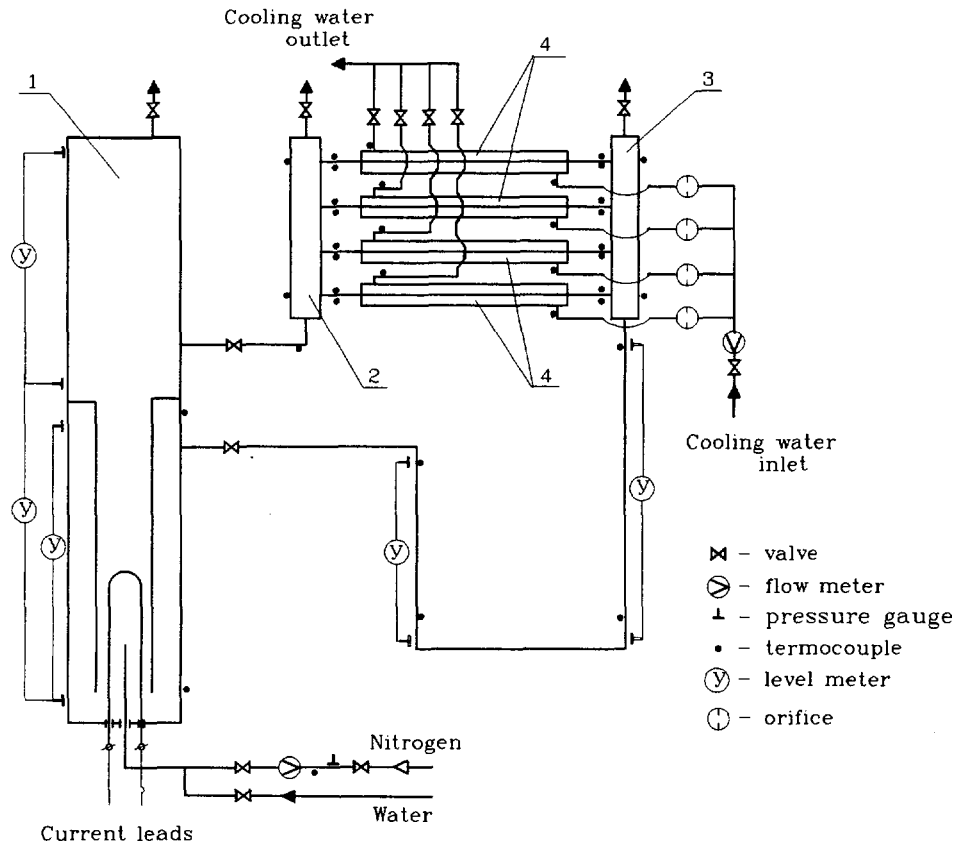


Fig.1. Flow diagram of test rig for steam condensation study in SG tubes

	SG	Model
Tubes	$11,1 \cdot 10^3$	5,74
Two collectors	$4 \cdot 10^3$	2,28
Volume below outlet collector	$2,52 \cdot 10^3$	1,20
Total	$17,65 \cdot 10^3$	9,24
Tubes volume to the total one ratio	0,63	0,62

As one can see from comparison, the volume ratios in the both cases are similar that permits to transfer the test results for the SG by scaling related to tubes quantity (8310:4).

Volume below the outlet collector represents a part of the cold leg which lies above the hot leg as shown in Fig.2. This part will be empty under SBLOCA in the hot leg and it could accumulate large amount of gas as the outlet collector.

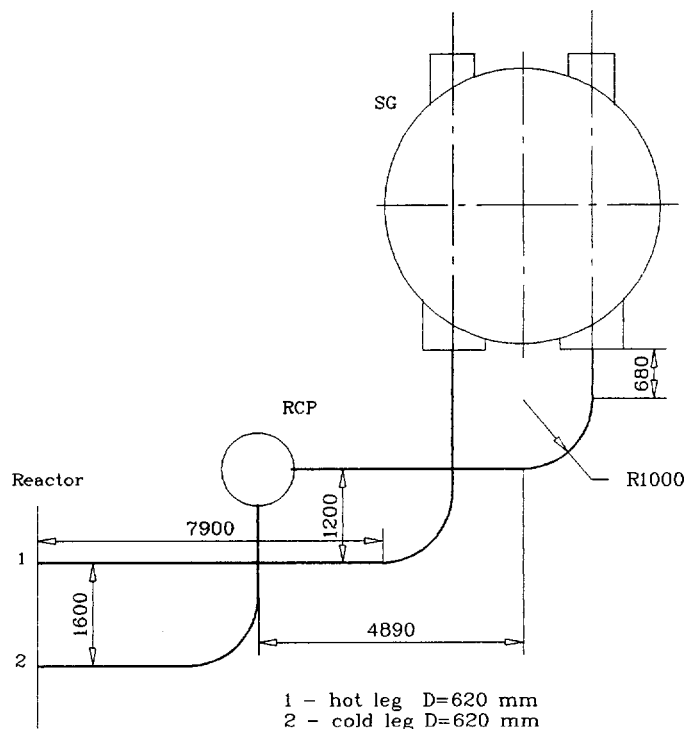


Fig.2. Layout of primary piping in VVER-640

Under decay power 2% of nominal rating (1800 MWt for VVER-640) the SG model must consume power of 4,3 kW. Power of electric heater was set

by 15% higher to compensate heat losses. These losses were defined beforehand.

Three tests have been carried out with the results as follow:

Test number	1	2	3
Heat power on SG model, kW	8,77	4,50	4,51
Pressure at test end, bar	6,3	6,7	6,2
Cool water temperature at inlet/outlet, °C	95/111	97/115	102/108
Amount of gas accumulated, g	30,9	35,2	35,7
Scaled to four SGs amount, kg	257	292	296

From the data presented one can see that for the given combination of the primary and secondary parameters four SGs of VVER-640 plant are capable to accumulate entire amount of nitrogen (200 kg) released without loss of heat transfer. This guarantees passive pressure decrease in the primary side up threshold of FDV actuation in case of SBLOCA.

Also, the tests have been carried out under constant pressure about 5 bar and temperature difference of 3-4°C between the primary and secondary sides. Pressure was maintained by partial blowdown of gas-steam mixture from the hot leg. It follows from results that in scaling for four SGs, 130 kg of nitrogen accumulated could block the heat transfer completely. To keep heat transfer during nitrogen accumulation of 200 kg a larger temperature difference is need as shown above. Such difference is provided by the passive heat removal system which is able to cool the SG secondary side rather rapidly.

Evaluations above are to be conservative because it is supposed that entire gas is accumulated in the SGs. In reality, portion of nitrogen is discharged into the break. Another portion could be separated in HA itself during pressure decrease. Cushion gas from HA can not enter the primary side because till the moment of their emptying HA pressure falls to 3 bar. At this moment FDVs have been opened already.

CONCLUSION

It is shown that nitrogen which is dissolved in the HA water does not prevent passive primary pressure decrease under SBLOCA and subsequent actuation of FDVs in the new generation plant VVER-640.



EXPERIMENTS WITH THE HORUS-II TEST FACILITY

Soeren Alt, Wolfgang Lischke

Department of Nuclear Engineering
University for Applied Sciences Zittau/Goerlitz
Theodor-Koerner-Allee 16, 02763 Zittau, Germany
Phone: ++49/3583/611-642 or 611-601
Fax: ++49/3583/611655
E-mail: saalt@orion.hrz.htw-zittau.de

Keywords: nuclear engineering, VVER, reactor safety, thermohydraulics, experiments

1 Introduction

Within the scope of the German reactor safety research the thermohydraulic computer code ATHLET which was developed for accident analyses of western nuclear power plants is more and more used for the accident analysis of VVER-plants particularly for VVER-440, V-213. The models for the thermohydraulic processes of the western codes like the ATHLET-code are verified by a large number of integral and separate effect experiments performed at test facilities constructed for western reactor type geometries. The conception of the VVER-440 design differs from the western PWR-constructions essentially. The constructional features of the VVER's primary circuit are for example (see Fig. 1):

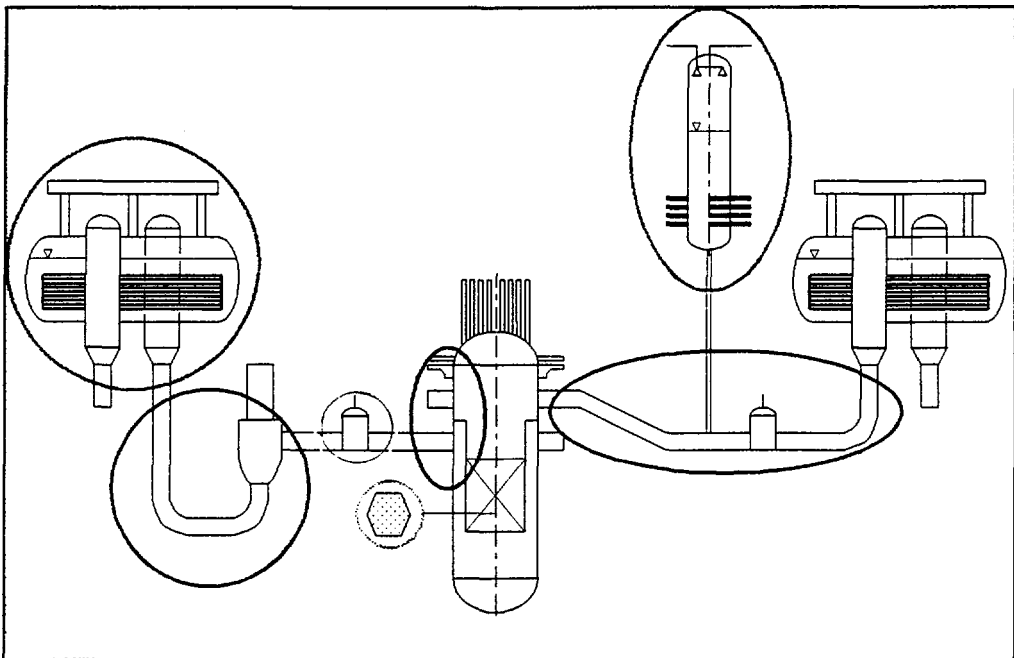


Fig. 1: Constructional features of VVER primary systems

- the outlet connection over the inlet,
- the loop lowering in both hot and cold legs,
- the design of the pressurizer,
- the hexagonal fuel elements,
- the steam generators with vertical collectors and horizontal heater tubes,
- the main slide valves and
- the six coolant loops.

These peculiarities determine the accident behaviour of the VVER reactors. A distinct deviating behaviour occur particularly in the final phase of a small break loss of coolant accident (SBLOCA) due to the condensation processes in the horizontal steam generator heater tubes in comparison to the condensation processes in the vertical tubes of western plants. The verification level of the western code models was not sufficient to simulate the thermohydraulics in VVER-geometries in these cases. A code adaptation which was based on special experiments included in the CNSI-matrix was necessary for using the ATHLET code for the VVER- plants. Regarding this reasons a main investigation field constituted the condensation behaviour of steam in the horizontal steam generator heater tubes without and with parts of noncondensing gases. It was known that separate effect analyses were necessary to complement the integral experiments on typical VVER integral test facilities. The separate test facility HORUS-II is supposed to close this gap and is the basis for the experimental analysis of accident behaviours of VVER plants together with the integral facilities PACTEL, PMK and ISB-VVER.

The experiments with the HORUS-facilities and the analyses with the ATHLET-code have been realized at the Technical University Zittau/Goerlitz since 1991 [1], [2]. The aim of the investigations was to improve and varify the condensation model particularly the correlations for the calculation of the heat transfer coefficients in the ATHLET-code for pure steam and steam-noncondensing gas mixtures in horizontal tubes.

2 The Test Facility HORUS-II

2.1 Geometry, Parameter, Scaling

The facility HORUS-II (test facility of **HOR**izontal **U**-tube **S**tream generators) is a separate effect test facility for VVER-440 and VVER-1000 steam generators with a single U-tube equipped with intensive measurements as primary side and a pressure vessel as secondary side.

	Primary side	Secondary side
Diameter	16 x 1,5 mm	219,1 x 8,2 mm
Length	9065 mm	4620 mm
Parameters	8 MPa, 300 °C	6,4 Mpa, 300 °C

Tab. 1 Geometrical Data and Parameters of HORUS-II

The simulation tube's dimensions correspond to an average tube in the original plant as well as to the geometrical similarity criterion

$$(\text{length/diameter})_{\text{Original}} = (\text{length/diameter})_{\text{Model}}$$

The test tube is made of original material (stainless steel). The installed collectors at the tube which connect the simulation tube with the necessary operating facility are volumetric scaled 1:1400. The collectors agree on principle with the original inlet and outlet collectors but they essentially serve as separator for the absorption of the condensate. The resulted condensate mass flow is collected in the rising mains of the collectors (see Fig. 2).

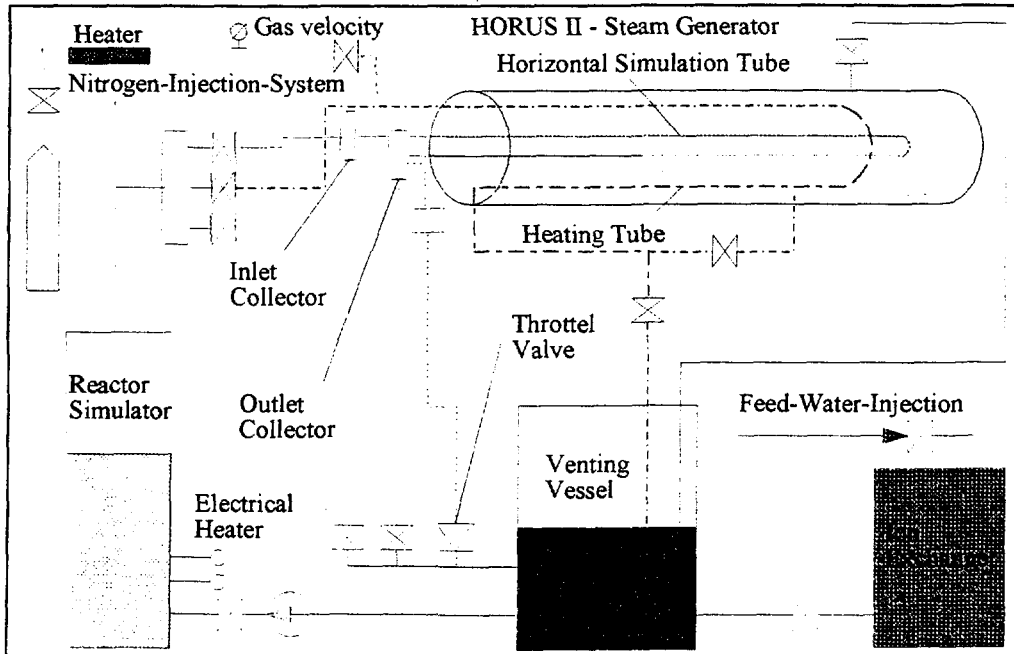


Fig.2: Flow diagram of the HORUS-II rig

2.2 Instrumentation And Data Acquisition

The HORUS-II facility is equipped with extensive measurements for the registration of the thermohydraulic processes (see Appendix). The measurement requirements depend on the issues to be studied. However, in this case the instrumentation of the HORUS-II facility consists of

- pressure, temperature and mass flow rate transducers for the measurement of steam and gas feeded in,
- 37 type K thermocouples for the measurement of fluid temperatures in the tube, material temperatures in the tube wall as well as on the tube surface (outside),
- 2...3 differential pressure transducers for the measurement of pressure drops along primary tube sections,
- condensate level measurements in the tube with ultrasonic probes,
- thermocouples and differential pressure transducers for the measurement of the level in the collector's rising mains, i.e. for the determination of the condensate mass flow rate out of the tube,
- pressure, temperature distribution and level transducers of the secondary side.

The data acquisition system consists of measurement scanners supported by IBM-compatible personal computers, e.g. scanner in connection with PCI-measuring cards. The data of most experiments are recorded with 5 Hz. The data are available in various data formats on standard floppy disks.

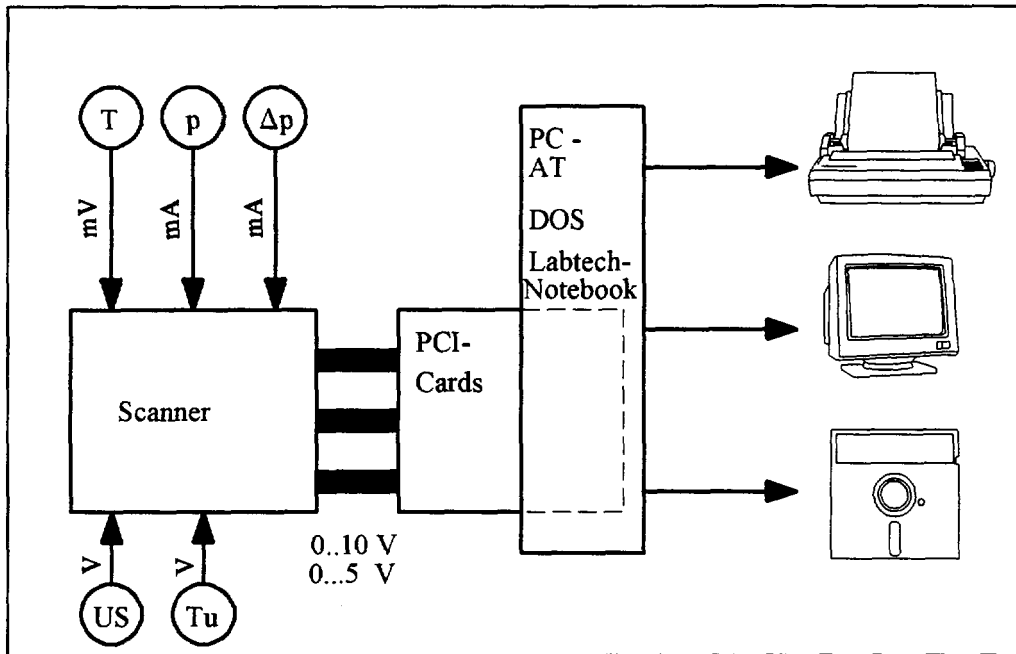


Fig.3: Data acquisition system of HORUS-II rig

3 Experiments at HORUS-II

About 130 condensation experiments have been performed at the HORUS-II facility. The experiments have been carried out with pure steam as well as with noncondensing gas injections into the steam mass flow. The experimental simulations are characterized as accident simulation tests for SBLOCA for VVER-conditions. The simulation conditions of the experiments had been adjusted correspondingly to the parameters of a postulated SBLOCA's fourth phase at the original plant. The fourth phase of the postulated accident is characterized through following conditions:

- The water level in the reactor pressure vessel lies under the hot leg connections.
- One loop seal is cleared at least.
- The heat removal out of the core is realized by steam condensation in one or more steam generators.

It especially contained the observance of the primary temperature, pressure and flow conditions and the secondary temperature and pressure conditions during the experiment.

- The experimental secondary pressure ranged from the operation pressure up to the pick up pressure of the secondary safety valves (4,5...4,9 MPa).
- The secondary temperature at the simulation tube surface agreed with the saturation temperature.
- The secondary conditions had been varied by different water levels and temperatures.
- The temperature differences between primary and secondary side amounted 4...40 Kelvin.
- The experiments had been realized with closed and opened throttlet valve at the outlet collector.

The closed throttlet valve produced a steam flow velocity which was only caused by the cooling conditions, i.e. the condensation rate only depended on the temperature difference between primary and secondary side. This condition simulated a cold leg loop seal (break is in the hot leg section).

With the opened throttlet valve pressure drops had been given in the simulation tube that simulated free flow conditions (break is in the cold leg section).

- The experiments with a gas mixture (Helium-Oxygen) dosages simulated the condensation behaviour with released gaseous radiolyses products.
- The dosages of nitrogen into the steam mass flow simulated the entry of gas into the primary system during safety accumulator injection.

Experiments are also realized in extended parameter ranges [3].

The titles of the experiments results from the nomenclature used for HORUS-rigs and mean:

A	- atmospherical secondary conditions (HORUS-I)
P	- pressurized secondary conditions (HORUS-II)
C	- closed outlet collector
O	- opend outlet collector
H	- horizontal tube position
L	- lowered tube position
R	- raised tube position
S	- only steam injection
G	- steam and noncondensing gas injection (Helium-Oxygen-Mixture)
N	- steam and Nitrogen injection

no - Number of the experiment.

Experiments with the first letter A had been realized at HORUS-I which was characterized by an open secondary side. This facility was used for testing the experimental procedure and the instrumentation as well as for the investigation regarding the influence of a raised or lowered tube in comparison with the horizontal position of the tube on the condensation process. Table 2 shows an overview about the HORUS-II experiments.

Type of experiments	Quantity of realized experiments	Remarks
PCHS - Phase A	19	original parameters, closed outlet collector, horizontal tube position, pure steam injection, tube without advanced thermocouple assembling and without ultrasonic probes
PCHS - Phase B	27	original parameters, closed outlet collector, horizontal tube position, pure steam injection, tube with advanced thermocouple assembling and with ultrasonic probes
POHS	15	original parameters, open outlet collector, horizontal tube position, pure steam injection, tube without advanced thermocouple assembling and without ultrasonic probes
PCHG - Phase A	19	original parameters, closed outlet collector, horizontal tube position, steam-Nitrogen-mixture injection, tube without advanced thermocouple assembling and without ultrasonic probes
PCHG - Phase B	20	original parameters, closed outlet collector, horizontal tube position, steam-noncondensing gas-mixture (He, O ₂) injection, tube with advanced thermocouple assembling and with ultrasonic probes
POHG	11	original parameters, open outlet collector, horizontal tube position, steam-Nitrogen-mixture injection, tube without advanced thermocouple assembling and without ultrasonic probes
PCHN	15	original parameters, closed outlet collector, horizontal tube position, steam-Nitrogen-mixture injection, tube with advanced thermocouple assembling and with ultrasonic probes
BaF	11	original parameters, closed outlet collector, horizontal tube position, pure steam injection, different secondary conditions simulating secondary bleed and feed procedures, advanced thermocouple assembling and with ultrasonic probes

Tab. 2 Overview about HORUS-II experiments

4 Example of Experimental Results on Experiment PCHS.25

The conditions for the condensation experiment PCHS.25 that had been also calculated with the ATHLET code had been adjusted correspondingly to the parameters of the SBLOCA's final phase at the original plant. The experiment contained the simulation of the primary temperature ($T=266^{\circ}\text{C}$) and pressure ($p=5.17\text{ MPa}$) conditions which representing saturation conditions as well as the secondary temperature ($T=259^{\circ}\text{C}$) and pressure ($p=4.66\text{ MPa}$) conditions. The power of the reactor simulator was constant. The secondary side was only cooled by heat losses to the surrounding. The tube was cooled by diving into the secondary boiling water. The tube was situated in horizontal position and the valve of the outlet collector was closed after the pre-test-phase. The experiment was performed with pure steam injection into the test tube.

Figure 4 shows the primary and secondary pressure during experiment PCHS.25. The levels in the inlet and outlet collector's raising mains are presented in Fig.5.

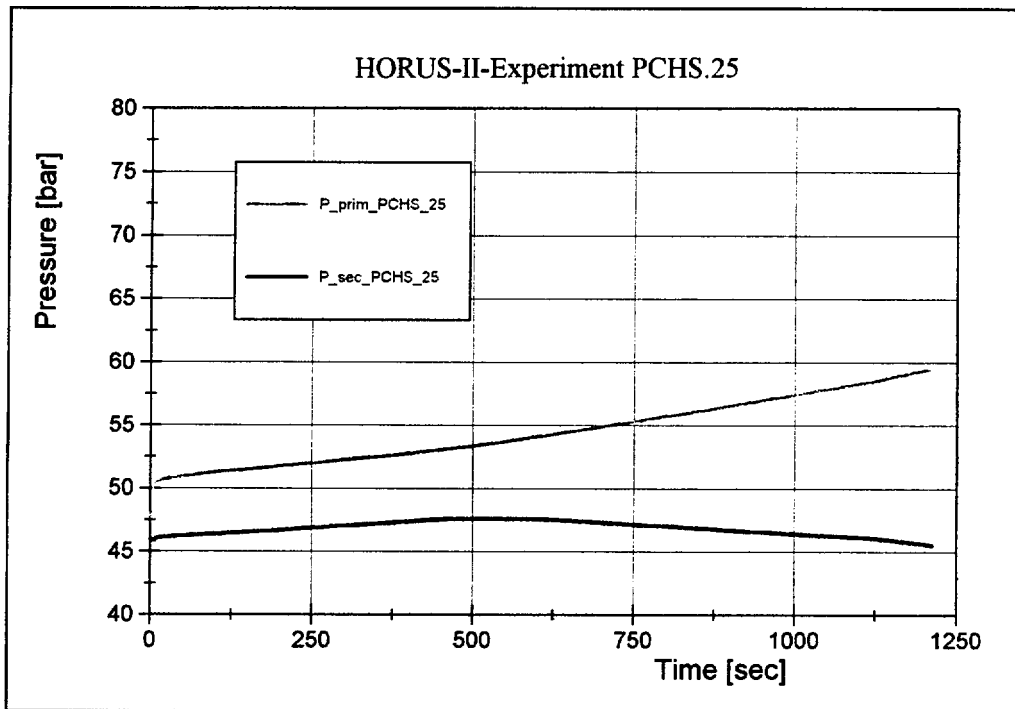


Fig.4: Primary and secondary pressure during experiment PCHS.25

The chronological course of the experiment PCHS.25 can be divided into four phases.

The *pre-test-phase* is the *first phase* before closing the valves in the collectors.

The *second phase* is characterized by a stationary condensate mass flow into the outlet collector until the outlet collector is filled about at 400 seconds. The pressure and temperature differences between the primary and secondary side are nearly constant in this phase.

In the *third phase* the condensate is stacked up in the U-tube. The heat transfer area is reduced by filling the U-tube which can be observed by pressure decreasing on the secondary side and a faster pressure increasing on the primary side before the condensate flows back into the inlet collector during the *fourth phase* of the experiment.

These effects can be also observed by the level measurement in the collectors.

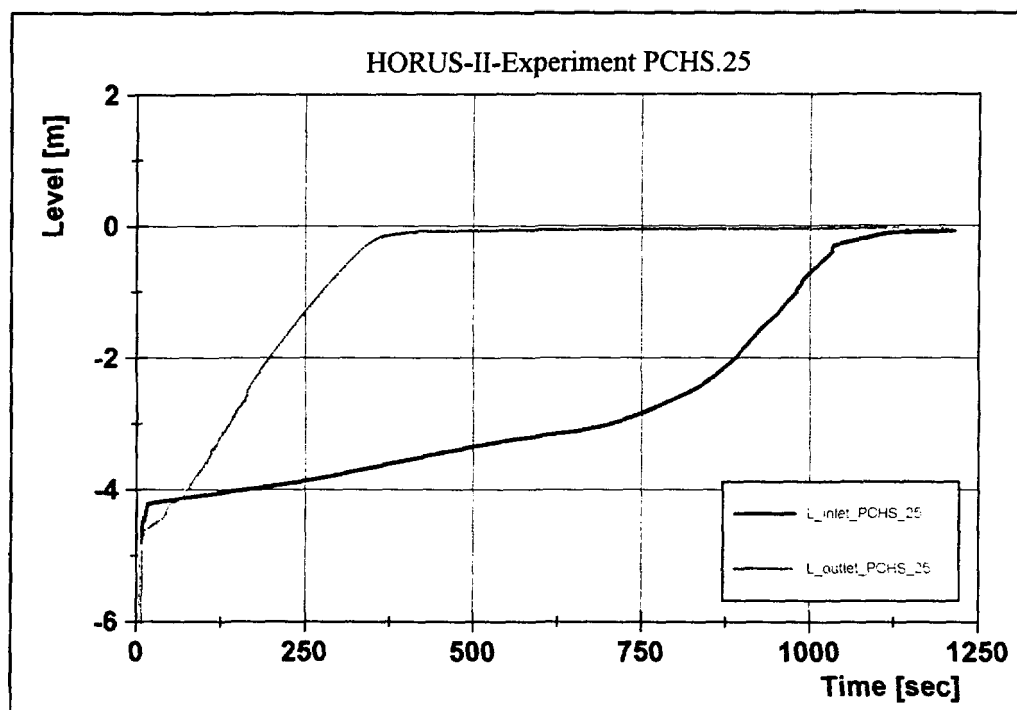


Fig.5: Condensate level in the collectors during experiment PCHS.25

Figure 6 shows temperature datas measured along the tube length in different parts of the tube.

In the second phase of the experiment the temperatures which were measured in the entry section and the middle of the test tube are at saturation temperature. The measuring points which are located in the end of the tube vary between the steam saturation temperature and the little lower subcooled condensate temperature. This effect can be explain by the appearance of waves at the surface of the condensat layer during the stratified flow of the condensate into the outlet collector.

In the third phase of the experiment between about 400 to 700 seconds the tube was filled with condensate from the outlet collector to the inlet collector.

During the fourth phase counter current flow of steam incoming and condensate back flow into the inlet collector can be observed.

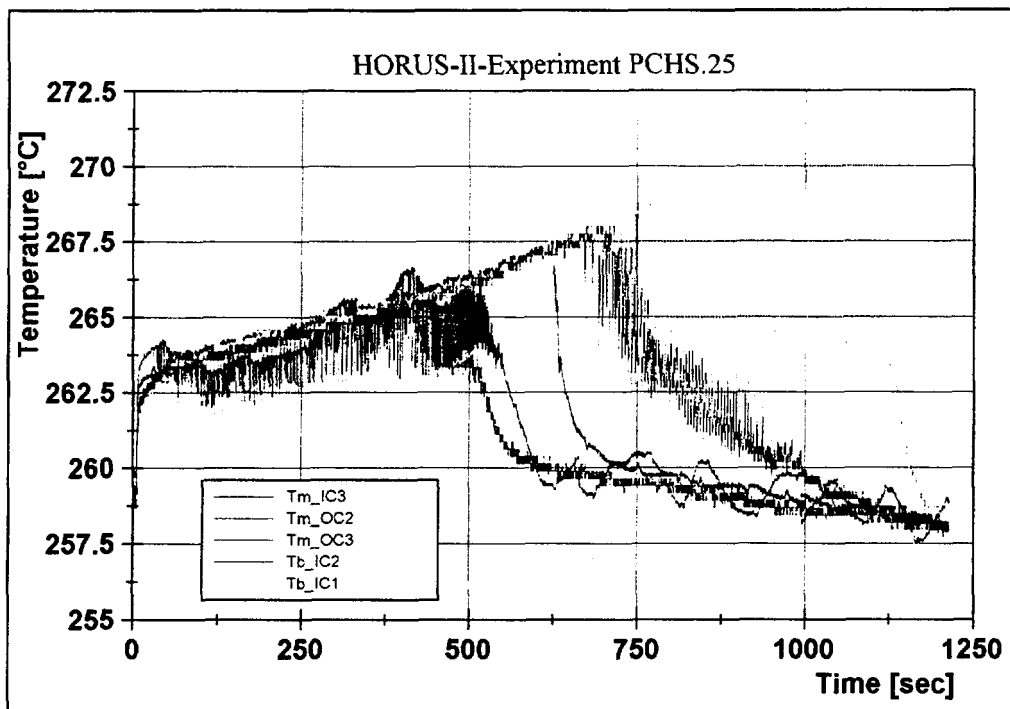


Fig. 6: Primary temperatures along the tube length during experiment PCHS.25

The behaviour of the experiment PCHS.25 is also confirmed by the differential pressure and ultrasonic measurement in the primary side of the test tube.

The experimental results were the basis for the code verification. In the original ATHLET version great differences had been observed between the experiment and the calculation regarding the underestimation of the heat transfer coefficients. The code was improved with the implementation of new options for the calculation of the heat transfer relations and good agreements between experimental data and calculated parameters had been got. The used correlations and heat transfer models are physical exact established. In Fig. 7 is shown the comparison between the measured temperatures and the calculated values in the reactor simulator and at the secondary side during experiment PCHS.25. The new developed condensation model was used for this calculation [4]. The curves show a good agreement between calculated and measured parameters.

The new developed model for the whole spectrum of horizontal flow conditions get a code improvement of the ATHLET-code for VVER conditions which are also verified by PACTEL integral experiments.

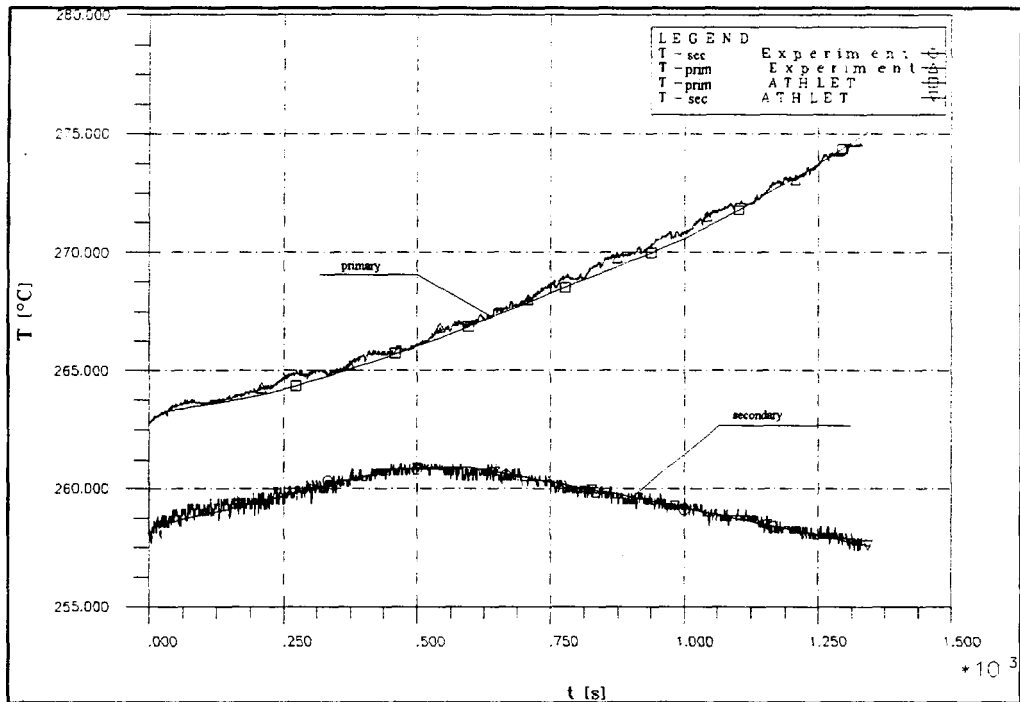


Fig.7: Calculated and measured temperatures in the reactor simulator and at the secondary side during experiment PCHS.25

5 Conclusions

The HORUS-II rig is designed, constructed and erected for the experimental simulation of thermohydraulic separate effects in horizontal U-tubes which are installed for example in VVER steam generators. The U-tube presents in the dimensions an average tube of the original steam generators. The maximum design parameters of the test facility allow to investigate SBLOCA scenarios of VVER with original parameters. The data of the experiments are phenomenological understandable and the results of the various measurement techniques are suited for model verification, improving of models and validation of thermohydraulic computer codes like the ATHLET-code.

6 Acknowledgments

The investigations described in this paper have been sponsored by the German Federal Ministry of Education, Science, Research and Technology.

7 References

- [1] S. Alt, Fessel, M., Lischke, W.:
 'Experimentelle Untersuchungen zum thermohydraulischen Verhalten der Heizrohre liegender Dampferzeuger von Kernkraftwerken mit WWER unter Störfallbedingungen'
 Final report, THZ-61202-10, Zittau, June 1995

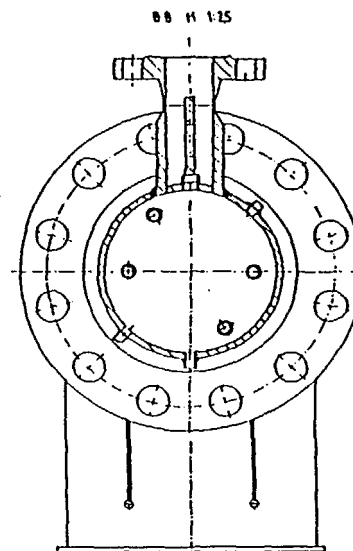
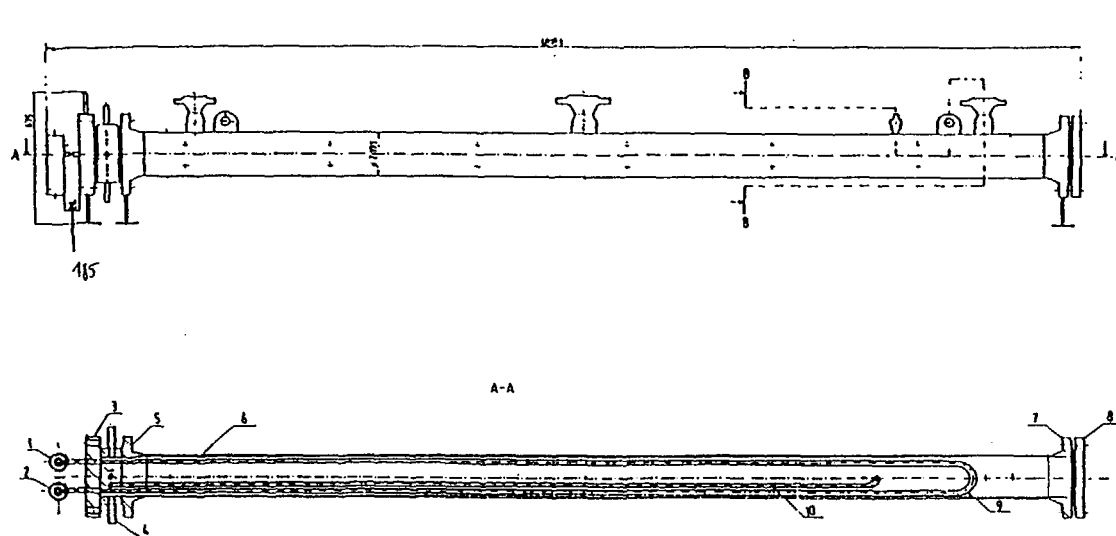
- [2] S. Alt, Fessel, M., Fjodorov, A., Kraus, B., Lischke, W., Vandreier, B.:
 'Beiträge zur Verifikation des Rechencodes ATHLET - Analyse und Nachrechnung der Experimente an den Einzelrohrversuchsständen HORUS-I/HORUS-II und am Integralversuchsstand PACTEL'
 Final report, THZ-61205-17, Zittau, May 1996

- [3] S. Alt, Lischke, W.:
 'Experimente mit der Einzeleffektversuchsanlage HORUS-II Versuchsphase B'
 Final report, THZ-601202-03, Zittau, February 1997

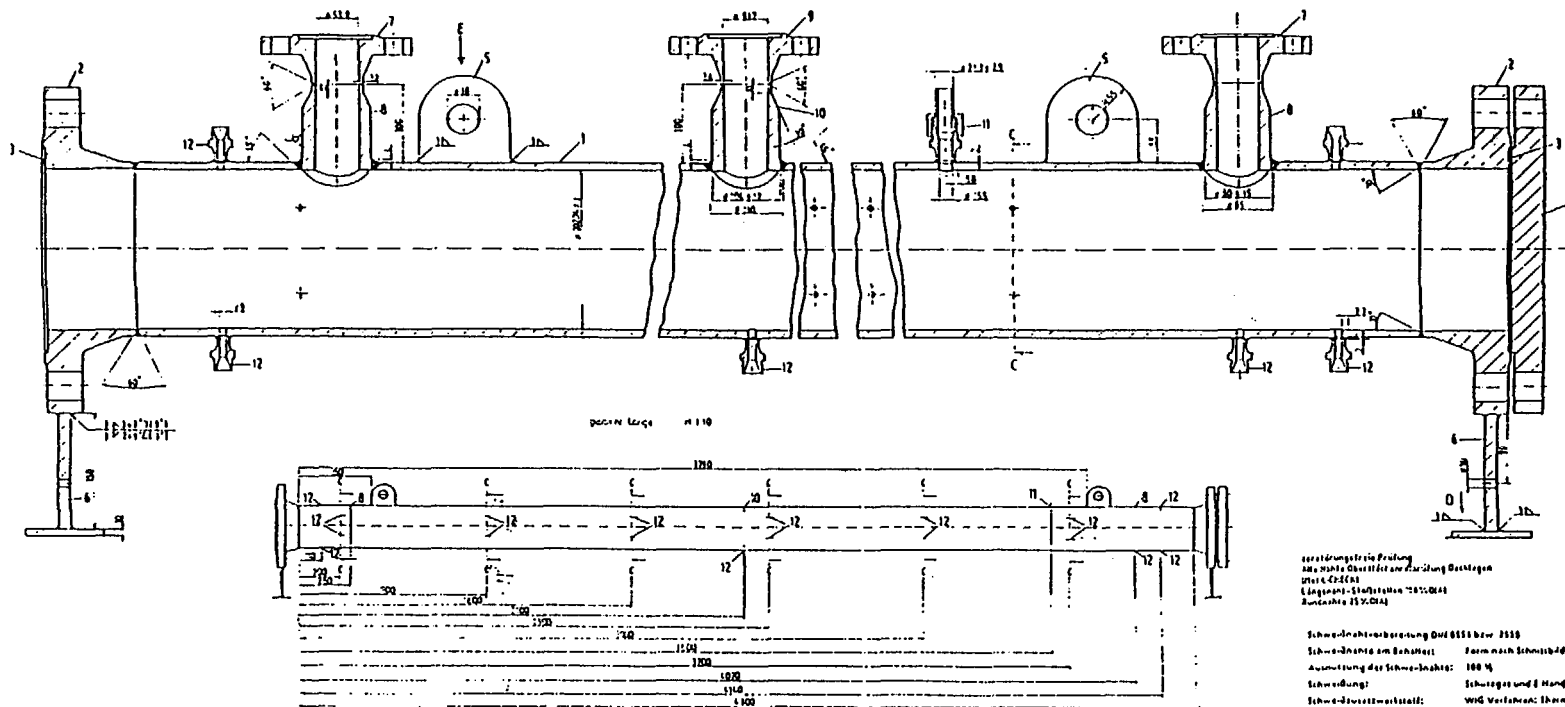
- [4] A. Fjodorov, Lischke, W.:
 'Modellierung der Wärmeübergangsvorgänge bei der Dampfkondensation in den Heizrohren liegender Dampferzeuger von WWER-Anlagen unter Störfallbedingungen'
 Annual Meeting on Nuclear Technology, Mannheim, May 21-23 Mai 1996,
 Proceedings p.151-154.

Appendix

- A1 Assembling drawing of HORUS-II
- A2 Pressure vessel of the secondary side
- A3 Detail drawing of the inlet and outlet collectors
- A4 Instrumentation of the reactor simulator during operation
- A5 Instrumentation of the secondary side during operation
- A6 Instrumentation of the inlet and outlet collectors during operation
- A7 Position of the thermocouples locating in and at the U-tube
- A8 Vertical positions of the thermocouples in the U-tube
- A9 Vertical positions of the thermocouples inside and outside of the wall
- A10 Positions of the primary differential pressure measurements
- A11 Positions of the primary ultrasonic probes



A1: Assembling drawing of HORUS-II



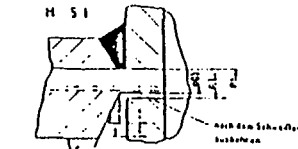
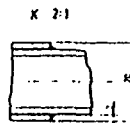
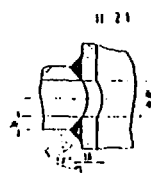
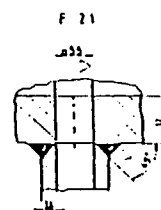
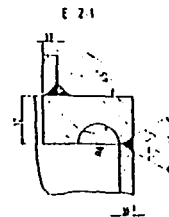
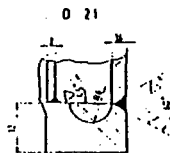
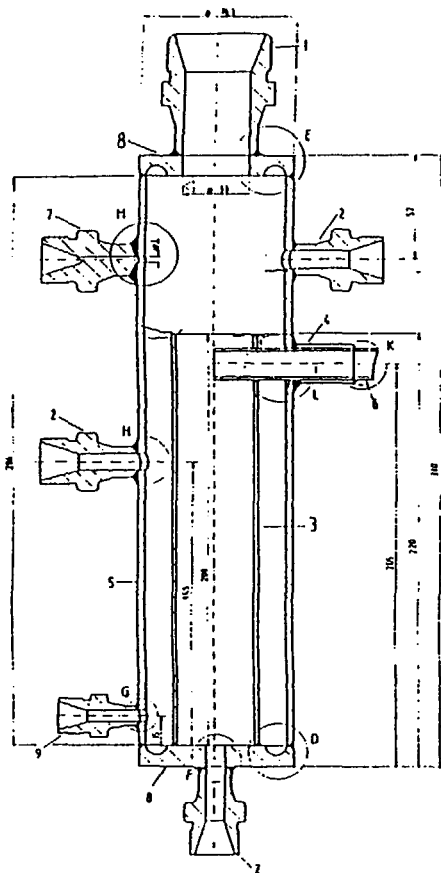
A2: Pressure vessel of the secondary side

zerstörungsfreie Prüfung
mit Röntgen-Strahlung nach DIN EN 4555
(Längs- und Querschnitte 10% DGS)
Röntgenstrahlung 15 kV, 0,1 mA

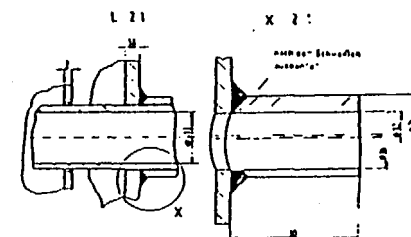
Schweißnahtüberprüfung nach DIN 6850 bzw. 2550
Schweißnaht am Behälter: Form nach Schweißnaht
Auswertung der Schweißnaht: 100 %
Schweißung: Schweißerg und 2 Hand
Schweißnahtwerkstoff: Werkstoff: Chromnickel 18/10
Mit Verfahren: Thermomessung 18/10
Zul. Schweißnahtdruck: 64 bar
Hochstzul. Betriebsdruck: 100 °C
Prüfdruck: 64 bar
Medium: verdampfendes Wasser (Dampfdruck < 10 bar)
Inhalt: 150 dm³

Flanschschliffe dürfen keine Feststellwunde anweisen

Herstellung und Prüfung nach den AD-Merkblätter der Reihe HP



Teil 3 und Teil 4 zusammenbohren $\varnothing 16$ zu L, X



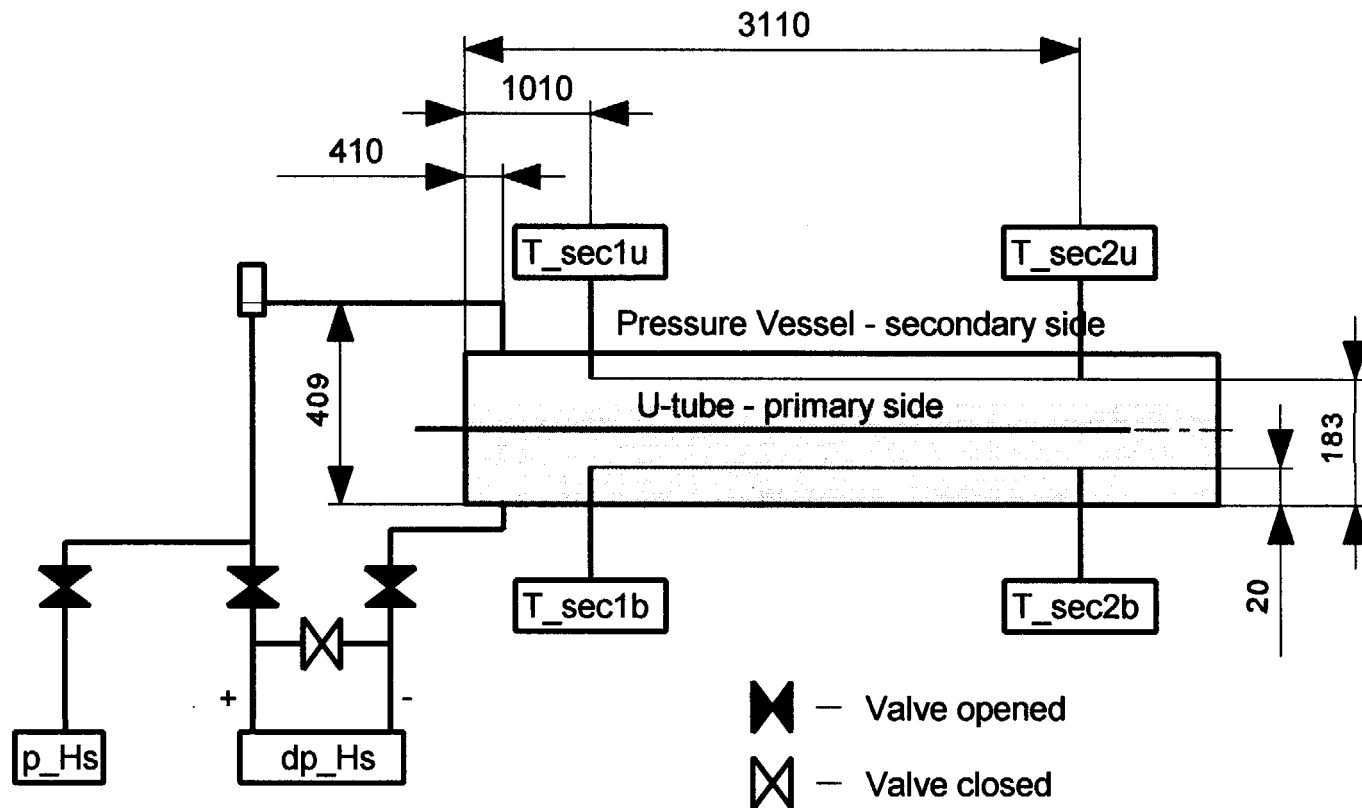
zerstörungsfreie Prüfung
Alle Metall-Oberflächenprüfung (Teil 4 - ZND 62)
Längsschnitt-Streifen 100% DZ 4
Rundstift 10% DZ 4
nicht bearbeitete Oberflächen sind 100% geprüft

Schweißnahtüberprüfung DIN 5511 bzw. 5515
Schweißnaht am Behälter: 100% nach Schweißbild
Auswertung der Schweißnaht: 100%
Schweißnaht: Schweißgut und 8 Hand
Schweißnahtwerkstoff: VWS Verfahren: Schweißnaht 100%
VWS Verfahren: Schweißnaht 100%
Zul. Betriebsdruck: 100 bar
maximale Betriebstemperatur: 100 °C
Prüfdruck: 100 bar
Medium: reines Wasser (Reinigungs-
mittel)
Inhalt: 1,1 dm³

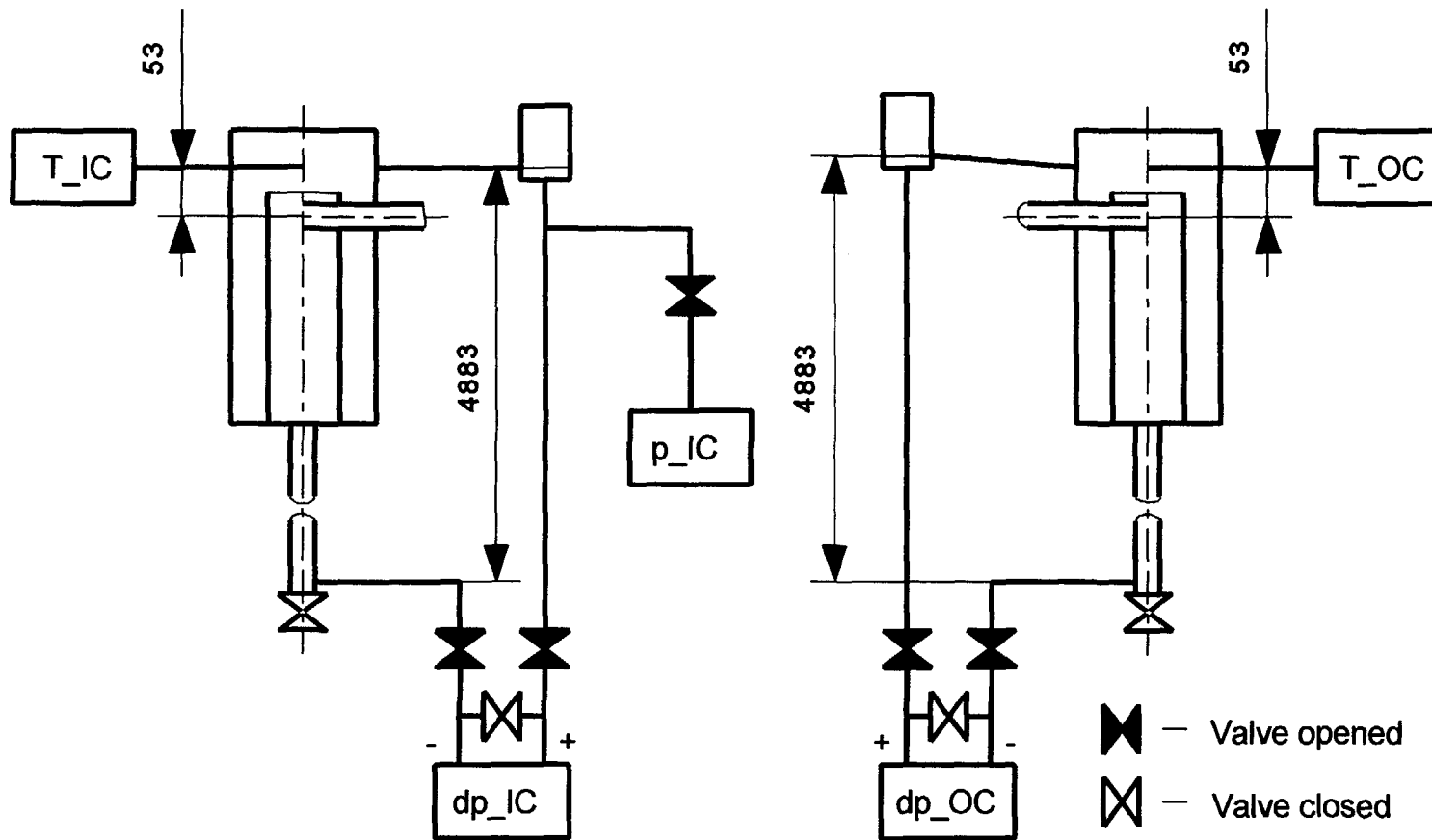
Flanschanschlüsse dürfen keine Kesselschweißnaht angeschlossen

Herstellung und Prüfung nach den AD-Merkblättern
der Reihe III

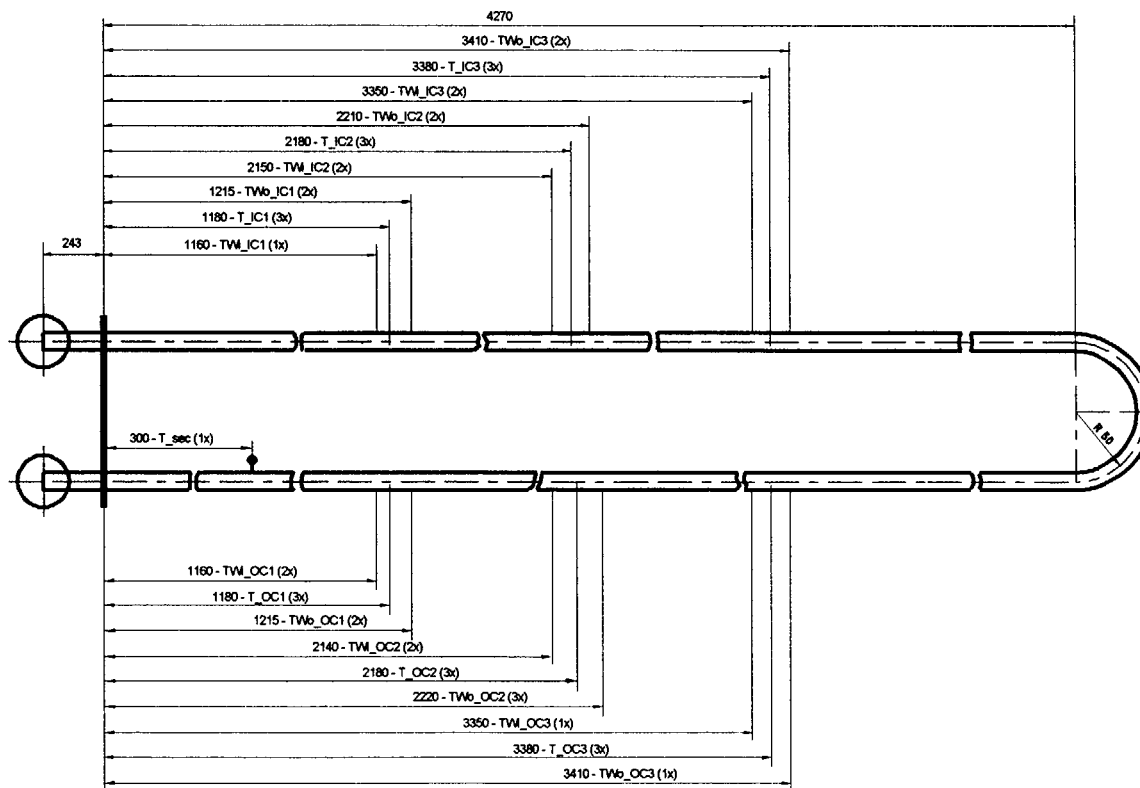
A3: Detail Drawing of the inlet and outlet collector



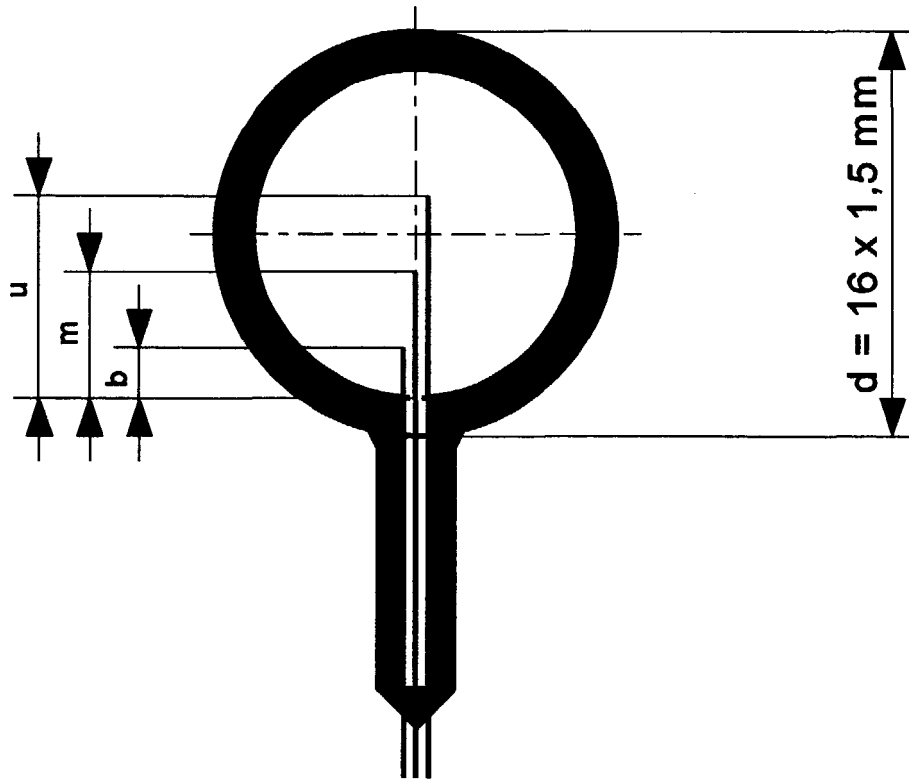
A5: Instrumentation of the secondary side during operation



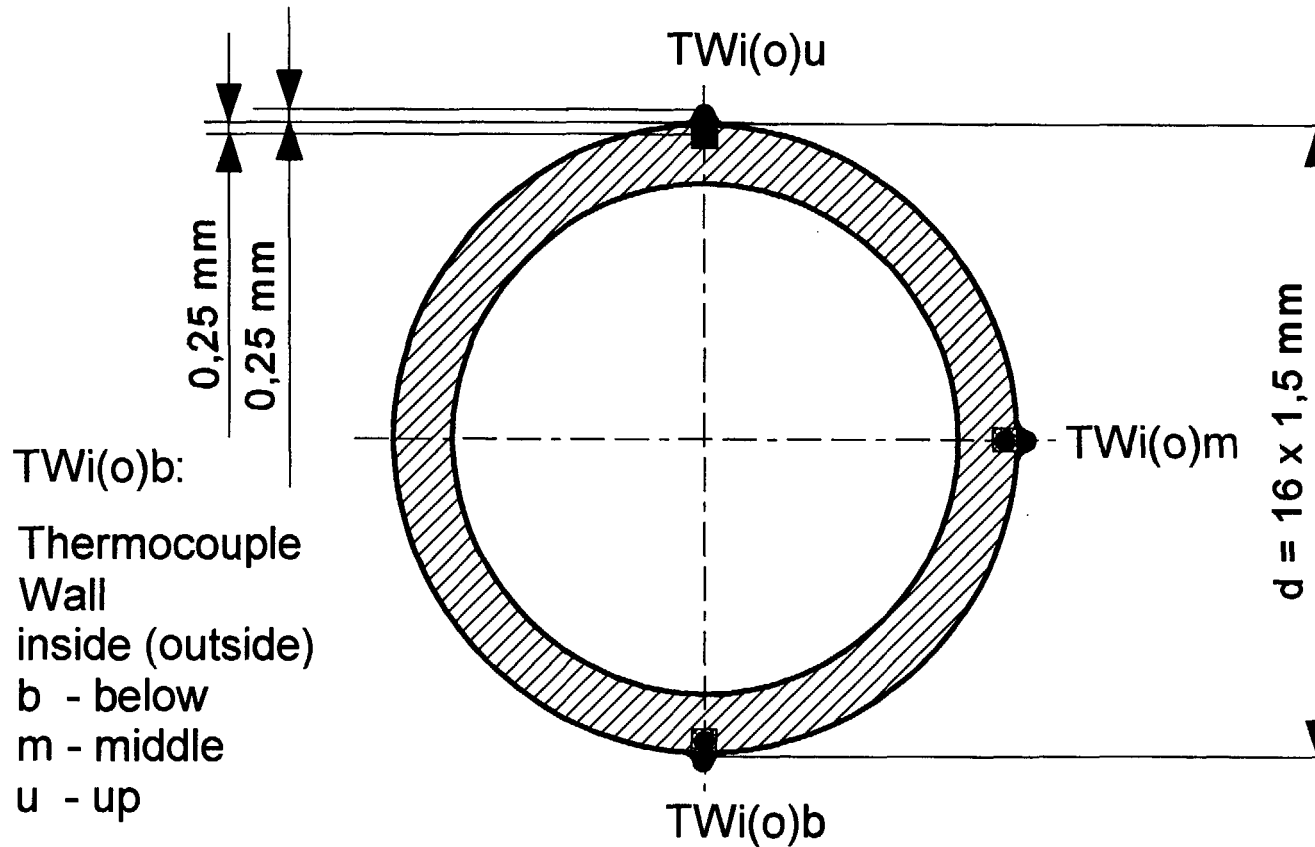
A6: Instrumentation of the Inlet and Outlet Collectors during Operation



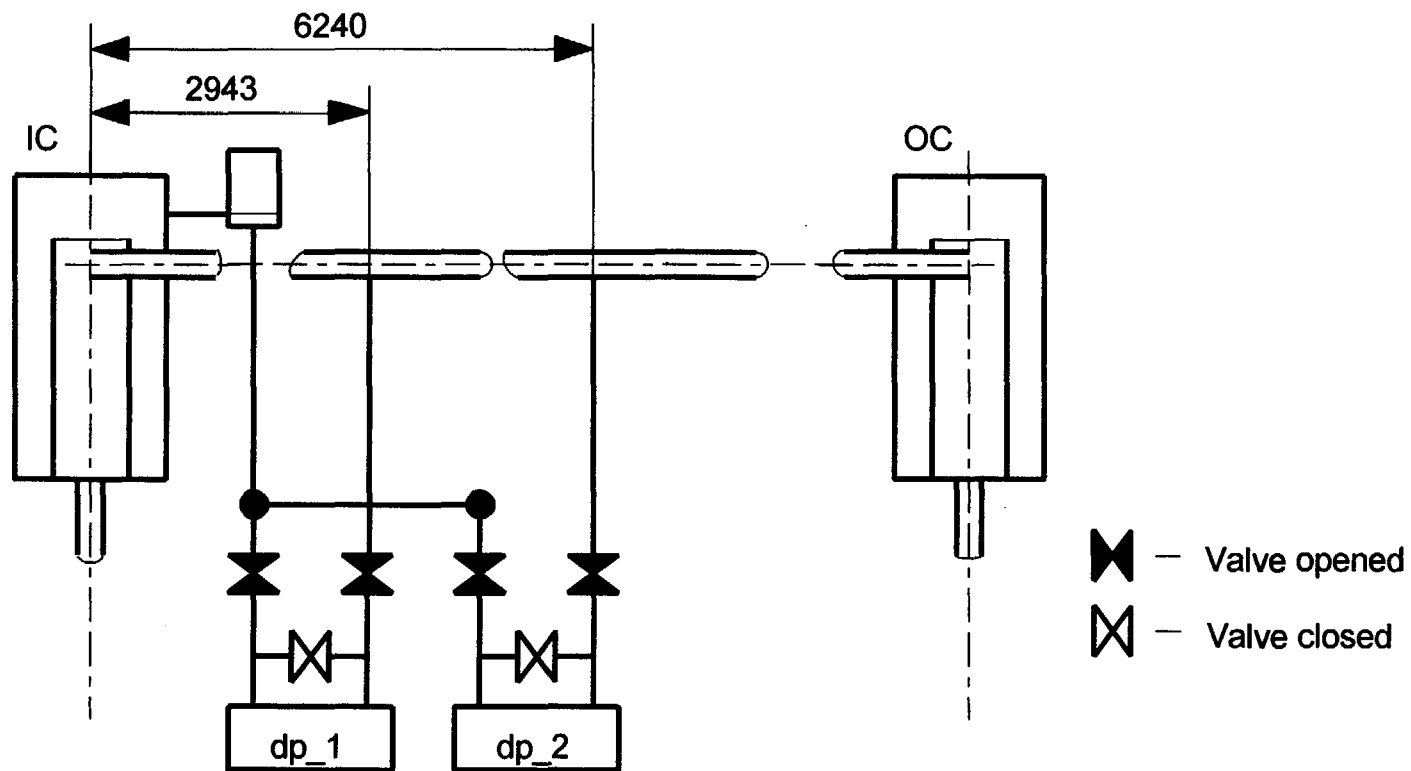
A7: Positions of the Thermocouples locating in and at the U-Tube



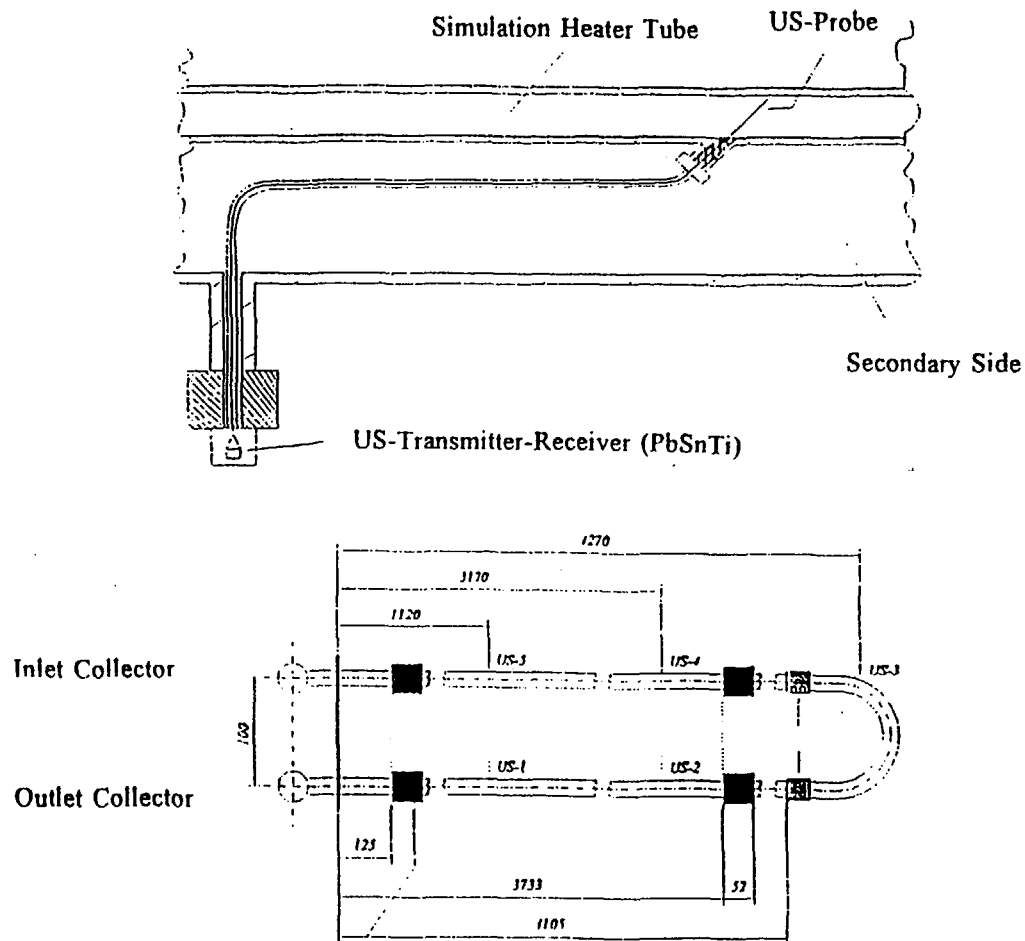
A8: Vertical Positions of the Thermocouples in the U-Tube



A9: Vertical Positions of the Thermocouples inside and outside of the Wall



A10: Positions of the primary differential pressure measurements



A11: Positions of the primary ultrasonic probes



**MODELLING OF WWER-1000 STEAM GENERATORS
BY RELAP5/MOD3.2 CODE**

F. D'Auria[°], M. Frogheri*, G.M. Galassi[°]

[°] DCMN - University of Pisa, Italy

* DITEC - University of Genova, Italy

Presented at

Fourth International Seminar on Horizontal Steam Generator

Lappeenranta, Finland, March 11-13, 1997

ABSTRACT

The present paper deals with the results of best estimate calculations carried out with reference to the WWER-1000 Nuclear Power Plant, utilizing a qualified nodalization set-up for the Relap5/Mod3.2 code.

The nodalization development has been based on the data of the Kozloduy Bulgarian Plant. The geometry of the steam generator imposed drastic changes in noding philosophy with respect to what is suitable for the U-tubes steam generators. For the secondary side a symmetry axis was chosen so to separate (in the nodalization) the hot and the cold sides of the tubes. In this way the secondary side of the steam generators was divided into three zones: a) the hot zone including the hot collector and the hot 1/2 parts of the tubes; b) the cold zone including the cold collector and the cold 1/2 parts of the tubes; c) the downcomer region, where down flow is assumed. As a consequence of above in the primary side more nodes are placed on the hot side of the tubes.

Steady state and transient qualification has been achieved, considering the criteria proposed at University of Pisa, utilizing plant transient data from the Kozloduy and the Ukrainian Zaporosche Plants.

The results of the application of the qualified WWER-1000 Relap5/Mod3.2 nodalization to various transients including large break LOCA, small break LOCA and steam generator tube rupture, together with a sensitivity analysis on the steam generators, are reported in this paper.

Emphasis is given to the prediction of the steam generators performances.

1. INTRODUCTION

The safety of nuclear power plants constitutes a global concern on the planet. This justifies interchanges of competencies and information between Western and Eastern Countries in the nuclear technology area. Specifically, application of advanced best estimate system codes to the evaluation of safety margins of Russian type WWER plants, are part of such a context.

Considering the experience gained in the validation and the use of the Relap5 and Cathare codes /1, 2, 3/, including application to WWER related phenomena /4, 5/ and the scientific cooperation with Energoproekt of Sofia (BG), the decision was taken to develop a WWER-1000 detailed nodalization.

In the initial stage of the activity, Relap5/Mod3.2 code /6/ was selected. The reference plant hardware information is included in refs. /7/, /8/ and /9/ and nominal operating conditions and Emergency Core Cooling System are also described into detail in the same report.

The nodalization was set up in the frame of a cooperation also involving the Italian Licensing Authority (ANPA), the vendor Ansaldo and the University of Roma "La Sapienza", e.g. refs. /10/, /11/ and /12/, the last one also including the qualification of Kozloduy transient data.

The resulting nodalization consists of more than one thousand nodes; among the other things, each of the four loops of the plant is modelled independently. The qualification of the nodalization was attained in the frame of the activity documented at ref. /13/, utilizing previously defined criteria /14/ and the plant transient data described in refs. /12/ and /15/.

The purpose of the present paper is to show significant results related to the prediction of steam generators performance.

Following the illustration of few results coming from previous analyses, /16, 17/, the attention is focused toward:

- a) characterization of steady state and transient performance of steam generator secondary side;
- b) comparison between predicted quantities and data available in literature /18, 19, 20, 21/.

2. NODALIZATION QUALIFICATION

2.1 Outline of the plant

The Kozloduy WWER-1000/320 plant, shown in Fig. 1, basically consists of (refs. /7/ to /10/):

- a pressurized water reactor vessel of 3000 MWt rated power with 163 hexagonal fuel assemblies, which are open to permit cross flows among the bundles. The fuel is UO_2 in annular pellet form, clad in a zirconium-niobium alloy. There are 10 banks of control rods, without fuel followers, located in 61 fuel assemblies;
- four primary loops equipped with horizontal tubes steam generators (Fig. 2) and main circulation pumps of centrifugal type;
- one turbogenerator with 1500 rpm and 1000 MW electric power;
- an emergency core cooling system including three High Pressure Injection pumps, four accumulators (SIT = Safety Injection Tank) and three Low Pressure Injection pumps;
- two independent feedwater systems connected with the four steam generators; each loop includes a turbine driven pump and piping connecting the feedwater line to four different locations in each steam generator; several valves are part of the system. The two feedwater systems feed a common header upstream the four steam generators.

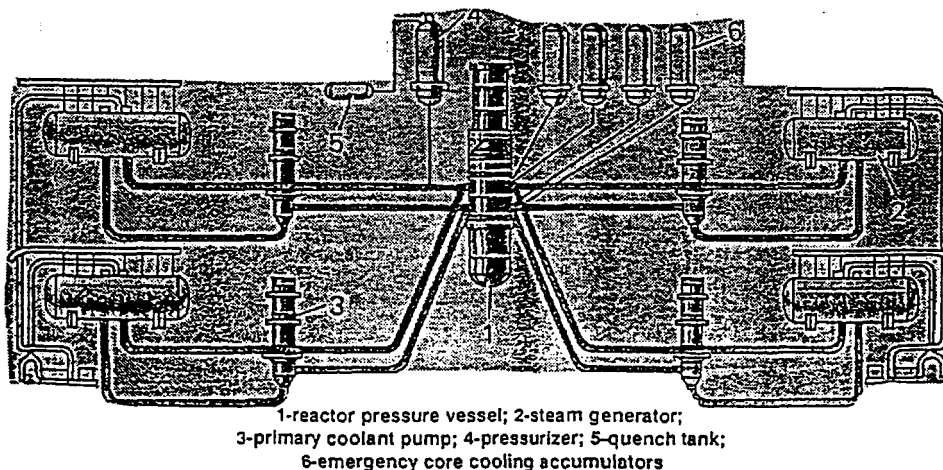


Fig. 1 - Kozloduy NPP: primary system

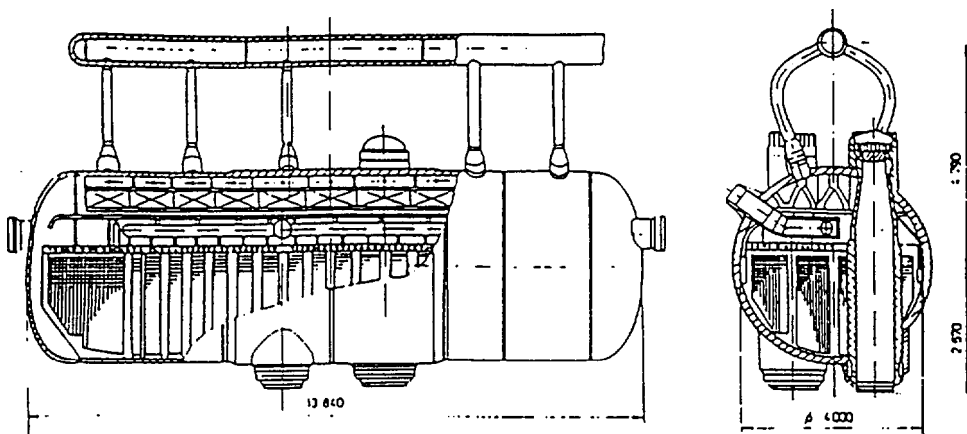


Fig. 2 - Kozloduy NPP: steam generator detail

2.2 Nodalization description

A detailed nodalization was developed considering the guidelines of the code User Manual and the criteria reported on ref. /14/. The sketch of the noding scheme can be seen in Fig. 3; information about adopted code resources is given in Tab. 1.

The vessel and the piping do not represent any particular challenge for the code, being quite similar to the corresponding ones in the Western type PWR. However, the bypass flow paths configuration inside the vessel is different: in the case of the WWER-1000 the upper part of the downcomer is not directly connected with the upper head; instead, a bypass flow path exists from the lower plenum to the upper head through the control rods housing and guide tubes.

The active core has been modelled adopting four parallel stacks (three core regions and one hot rod) characterized by different linear power.

Steam generator geometry imposes drastic changes in noding philosophy with respect to what is suitable for the U-tubes steam generators. As "symmetry axis" for the secondary side (and consequently for the primary side), a line was taken connecting the center between the two collectors with the average (virtual) position of the centers of the horizontal tubes, with the aim to separate (in the nodalization) the hot and the cold sides of the tubes. In this way, the secondary side of the steam generators was divided into three zones: a) the hot zone including the hot collector and the hot 1/2 parts of the tubes; b) the cold zone including the cold collector and the cold 1/2 parts of the tubes; c) the downcomer region gathering different zones of the secondary side: essentially, the regions where down flow is assumed (e.g. the boundaries and the location of feedwater nozzles). Four positions were distinguished for the feedwater nozzles, as results from Fig. 3. The node subdivision in the primary side was a consequence of the above: more nodes are placed on the hot side of the tubes; six axial levels, lumping six groups of tubes, can be noted.

The Emergency Core Cooling System (ECCS) consists of three High Pressure, three Low Pressure Injection systems (HPIS and LPIS, respectively) and four accumulators (SIT, Safety Injection Tank).

These are directly connected with the downcomer and with the upper plenum of the main vessel. All the ECCS have been modelled together with the AFW (Auxiliary Feedwater System) and the relief valves at the top of the pressurizer and in the secondary side of the steam generators (PORV and SRV).

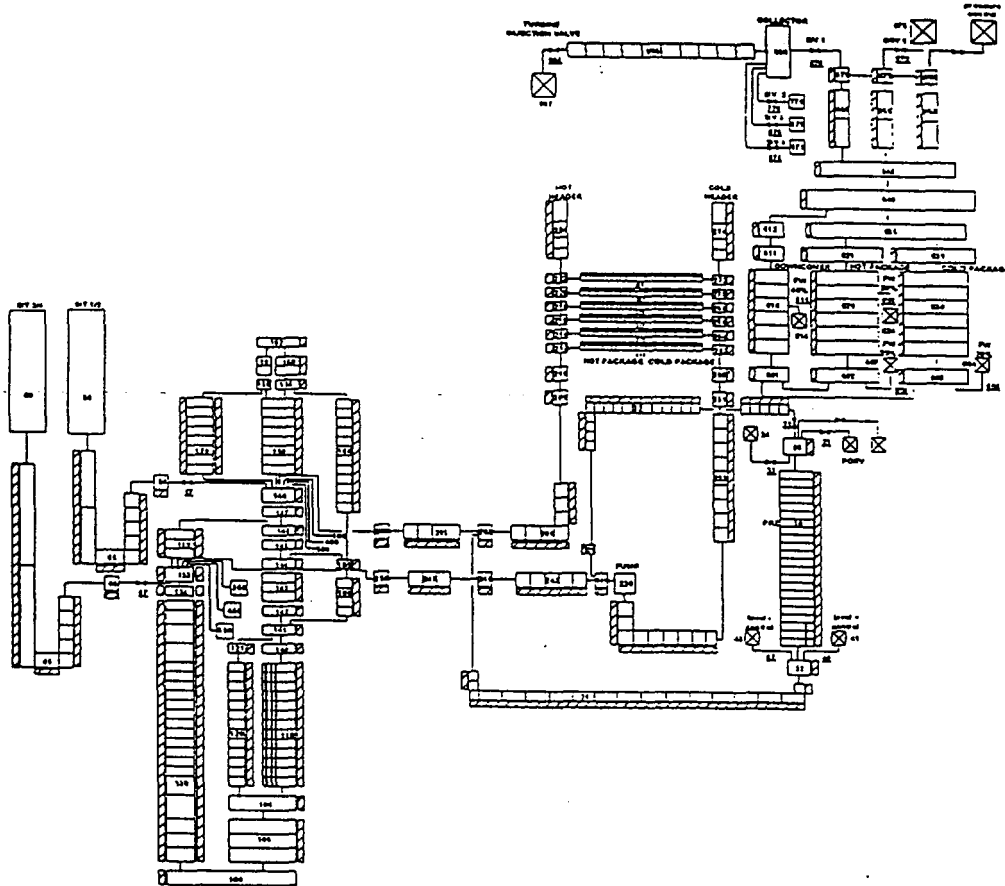


Fig. 3 - WWER-1000 NPP: noding scheme for Relap5/Mod3.2

Number of nodes	1102
Number of junctions	1148
Number of heat structures	1028
Number of mesh points	5590
Number of core active structures	42

Tab.1 - Adopted code resources for the WWER-1000 nodalization

2.3 Qualification

The nodalization qualification consists of the following two main steps:

a) steady state level

Two sub-steps can be identified /14/: development of the nodalization and achievement of the steady state.

Criteria like those recommending the maximum node length, the number of mesh points necessary to simulate the conduction heat transfer in the fuel rods and across the steam generator tubes, the connection between neighbouring nodes etc. have been used. The first sub-step concludes with the check that various dimension of the nodalization coincide with the design or reference values. An example of this is given by Fig. 4 that shows the correspondence between the volume and the height of the secondary side of one steam generator.

The second sub-step deals with the achievement of the steady state. Typically 100 s are considered sufficient, running the code in the transient mode. Again, criteria dealing with the time derivative and the absolute values of relevant time trends are available and have been matched (in the last case, design or reference values are used for defining the acceptable error). Some results are shown in Tab. 2.

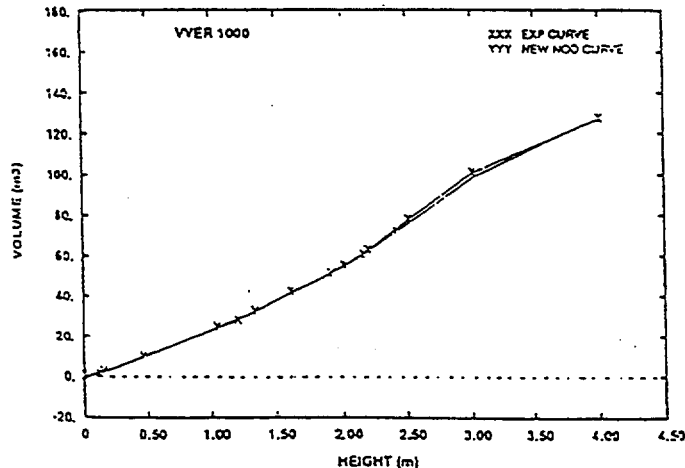


Fig. 4 - Nodalization qualification at steady state level: calculated and measured volume/height curve for SGs

b) transient level

The NPP transient adopted for qualifying the nodalization at the "on transient" level are outlined in Tab. 3. It can be noted that the Kozloduy transients were operational transients ("planned", /8/), while an unplanned event occurred in Zaporosche (April '95, /15/). In this last case, the intervention of three High Pressure Injection Systems and the accumulators was sufficient to recover the NPP in a few tens of minutes. The available NPP data were qualitatively and quantitatively well predicted by the nodalization /13/.

The nodalization was also qualified through the comparison of results from the same (i.e. same sequence of events and properly scaled boundary conditions) small break LOCA transient in a Western type PWR and in related experimental facilities, Tab. 3 /11/.

PARAMETER	UNIT	EXP.	CALC.
Primary side pressure	MPa	15.7	15.7
Hot leg temperature	°C	320.1÷3.5	322
Cold leg temperature	°C	289.8÷2	287.2
Primary side mass	kg	240000	235100
PRZ level	m	8.77	8.75
Core power	MW	3000	3000
Reactor flow	kg/s	15704	15450.6
SG power	MW	750	748
Secondary side mass	kg	160000	159900
Feedwater temperature	°C	220	220
Secondary side pressure	MPa	6.28	6.27

Tab. 2 - Nodalization qualification at steady state level: calculated and measured boundary condition values

Transient	Plant	Type	Description	Initial power (%)	Initial pressure (MPa)
KZ-1	Kozloduy-5	planned	1 pump trip	72	15.7
KZ-2	Kozloduy-5	planned	2 pumps trip	54	15.7
KZ-3	Kozloduy-5	planned*	Partial loss of feedwater	72.1	15.8
ZAP	Zaporosche	unplanned	PORV stuck open	1.0**	18.8
PWR	Krsko	calc.°	Small break LOCA	100.	15.

* unplanned sequence of events

** estimated

° with the support of experimental data in test facilities

Tab. 3 - Transients utilized for the "on-transient" qualification of the Relap5/Mod3 WWER-1000 nodalization

3. SIGNIFICANT RESULTS INVOLVING STEAM GENERATORS PERFORMANCES

The main purposes of system codes is to perform accident analyses, in order to confirm the design choices also in relation to emergency planned guidelines /22, 23/.

A matrix of accidents was fixed and is reported in Tab. 4. It essentially consists of simplified sequences of events, without having in mind the results of probabilistic safety studies. Rather, the selected events, put a challenge to the code and the nodalization, include a wide range of phenomena and make possible the comparison with the results of similar transients in Western PWR.

N°	NPP TRANSIENT	TYPE	SG SIGNIFICANT CONDITIONS	HPIS	ECCS LPIS	SITS	RCP	AM PROCEDURE
1a	VV-SGT-01	SGTR 1 tube	Isolation at scram (AFW off)	off	in CL at 2.15 MPa	4 at 5.9 MPa	off	-
1b	VV-SGT-02	SGTR hot coll. 100% br.	Isolation at scram (AFW off)	off	in CL at 2.15 MPa	4 at 5.9 MPa	off	-
1c	VV-SGT-03	SGTR 5 tubes	Isolation at scram 30k/hr (intact SG)	off	in CL at 2.15 MPa	4 at 5.9 MPa	off	-
1d*	VV-SGT-04	SGTR 20 tubes	Isolation at scram 40k/hr (intact SG)	off	in CL at 2.15 MPa	4 at 5.9 MPa	off	-
2a*	VV-LFW-01	LOFW	Isolation at scram AFW delayed	off	off	4 at 5.9 MPa	on	AFW
2b	VV-LFW-02	LOFW	Isolation at scram AFW delayed	off	off	4 at 5.9 MPa	off	AFW
3	VV-PTR-01	LOFA 4 pumps	Isolation at scram off	off	off	off	off	-
4a	VV-SBP-00	PORV Stuck Open	15K/hr after scram AFW off	at 8.9 MPa	in CL at 2.15 MPa	4 at 5.9 MPa	off	-
4b	VV-SBP-01	PORV Stuck Open	15K/hr after scram AFW off	off	in CL at 2.15 MPa	4 at 5.9 MPa	off	-
4c	VV-SBP-02	PORV Stuck Open	15K/hr after scram AFW off	off	in CL at 2.15 MPa	4 at 5.9 MPa	off	SIT° init cond
4d*	VV-SBP-03	PORV Stuck Open	SG SRV opening after dryout AFW off	off	in CL at 2.15 MPa	4 at 5.9 MPa	off	SG BLEED
5a	VV-LFW-A1	LOFW ATWS	Isolation	off	off	4 at 5.9 MPa	on/off	-
5b	VV-LFW-A2	LOFW ATWS	Isolation	off	off	4 at 5.9 MPa	on	HPIS unborated
6a*	VV-SLB-01	SLB/ATWS BA=0.0022 m ²	Isolation	off	off	4 at 5.9 MPa	on	-
6b	VV-SLB-02	SLB/ATWS BA=0.98m ²	Isolation	off	off	4 at 5.9 MPa	on	-
6c*	VV-SLB-03	SLB/ATWS BA=0.5m ²	Isolation	off	off	4 at 5.9 MPa	on	-
6d	VV-SLB-04	SLB/ATWS BA=0.1m ²	Isolation	off	off	4 at 5.9 MPa	on	-
7	VV-LBL-01	LB-LOCA BA=2x80%	Isolation AFW off	off	in CL at 2.15 MPa	4 at 5.9 MPa	on	-
8a	VV-SBL-01	SB-LOCA BA=1 %	Isolation AFW off	off	in CL at 2.15 MPa	4 at 5.9 MPa	on	-
8b	VV-SBL-01	SB-LOCA SIT line break	Isolation AFW off	off	in CL at 2.15 MPa	4 at 5.9 MPa	on	-
8c	VV-SBL-01	SB-LOCA BA=10 %	Isolation AFW off	off	in CL at 2.15 MPa	4 at 5.9 MPa	on	-
9a*	VV-SGC-01	SG1 FW isolation	1 SG isolated	off	-	-	off	-
9b*	VV-SGC-02	loop1 pump trip	1 SG thermal power trip	off	-	-	off	-
9c*	VV-SGC-03	500 s steady state	-	off	-	-	on	-

° N₂/H₂O ratio changed from 1/5 to 7/5

* considered in the present paper

Tab. 4 - Imposed main events for Relap5/Mod3.2 calculation

Almost all the selected scenario can be classified as "beyond DBA - before core melt"; namely "beyond DBA" testifies that not all the Emergency Systems (ECCS) were assumed to operate as from the respective design, and "before core melt" indicates that the analysis is stopped, eventually, when any fuel cladding surface temperature reaches the licensing limit.

A detailed analysis of the results of each calculation is well beyond the purposes of the present paper. Some significant results are summarized hereafter.

3.1 Loss of feedwater (LOFW)

The studied transient (Figs. 5 and 6) is originated by a complete loss of feedwater without the availability of AFW when requested. HPIS is also assumed to fail.

In these conditions primary and secondary side pressure reach the PORV and SRV set points causing mass depletion in the primary loop and emptying of steam generators, respectively.

AFW is assumed available more than one hour after the transient beginning; its intervention is required following extended core dryout. AFW actuation causes cooling of steam generator tubes, void collapse of primary side, pressurizer liquid draining that is effective for the top-down core cooling and, definitely, leads to pressure decrease in the primary loop. The last effect brings the pressure to the actuation set point of the accumulators causing further pressure decrease down to the LPIS set point.

3.2 PORV stuck open

The original considered transient was used for the nodalization qualification (case VV-SBP-00 in Tab. 4). Sensitivity studies include hypothetical scenarios without the HPIS. In this case the transient evolution look similar to the 1% Small Break LOCA, with the rod surface temperature reaching unacceptable values. AM possibilities were investigated including different initial conditions for two of the accumulators and secondary side depressurization (cases VV-SBP-02 and VV-SBP-03). The secondary side depressurization led to a complete recovery of the plant (see Figs. 7 and 8).

3.3 Steam line break without scram (SLB ATWS)

Four steam line break transients without scram (SLB/ATWS in Tab. 4) were analyzed (Figs. 9 to 12). The boundary and initial conditions are the same as adopted in the LOFW/ATWS, the only difference being the introduction of the break in one steam generator top collector, instead of stopping the feedwater flow.

The results indicate that large break areas (0.98 and 0.5 m^2) cause very rapid power excursion, while break area less than 0.1 m^2 , even though leading to power excursion, may not endanger the integrity of the system. In addition, around ten minutes may be available for operators to take actions for recovering the plant.

3.4 Steam generator tube ruptures

The typical accident time sequence selected for the SGTR studies includes the scram and the secondary side mutual isolation at the start of the transient. In all cases the break is assumed at the bottom of the hot collector and is of double ended type. Sensitivity analyses were carried out to evaluate the effect of the break. In all cases no flowrate inversion was calculated at the break and the core levels remained relatively high in the considered time spans of the transient (Figs. 13 to 15).

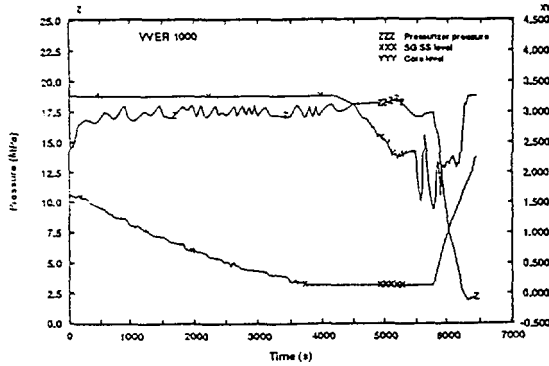


Fig. 5 - WWER-1000 LOFW: PRZ pressure and core and SG levels

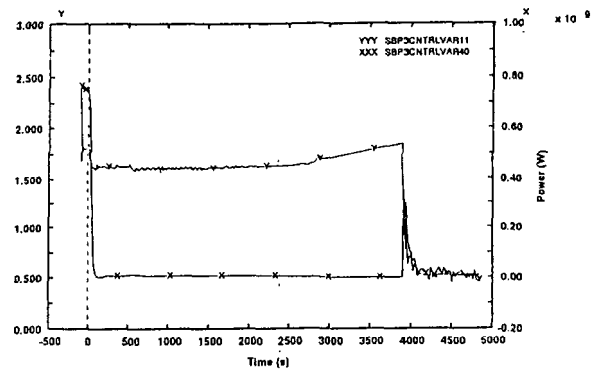


Fig. 8 - WWER-1000 PORV stuck open: SG level and exchanged power

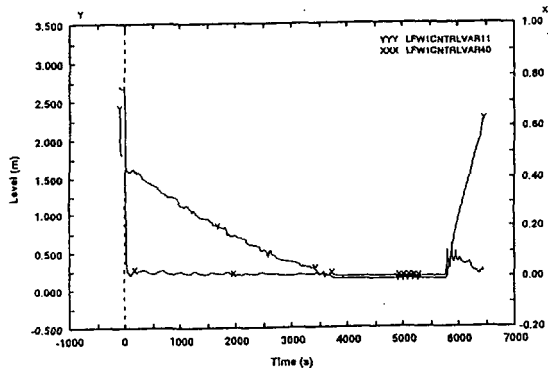


Fig. 6 - WWER-1000 LOFW: SG level and exchanged power

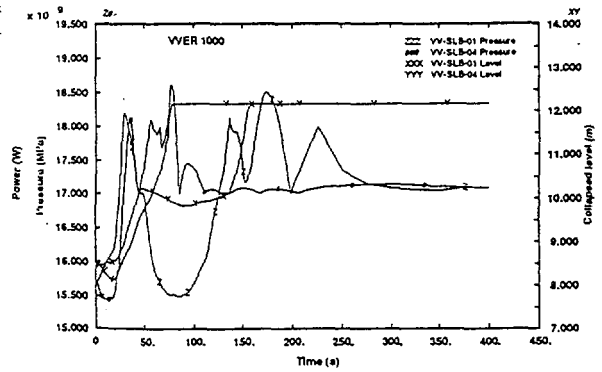


Fig. 9 - WWER-1000 SLB/ATWS: PRZ pressure and level

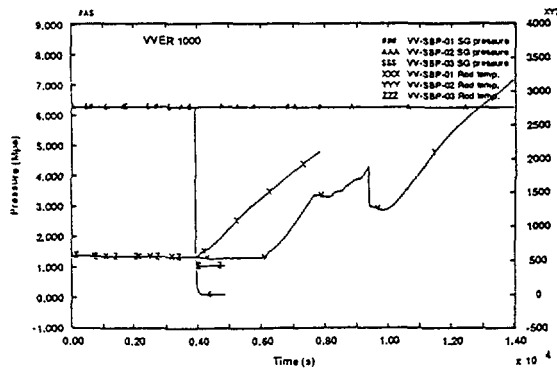


Fig. 7 - WWER-1000 PORV stuck open: SG pressure and rod surface temperature

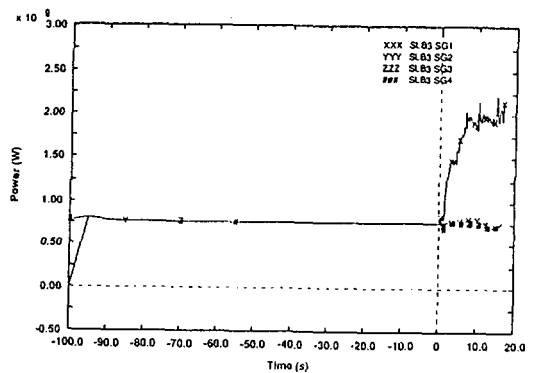


Fig. 10 - WWER-1000 SLB03: SGs exchanged power

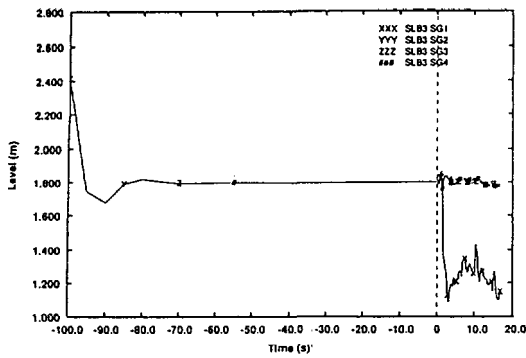


Fig. 11 - WWER-1000 SLB03: SGs levels

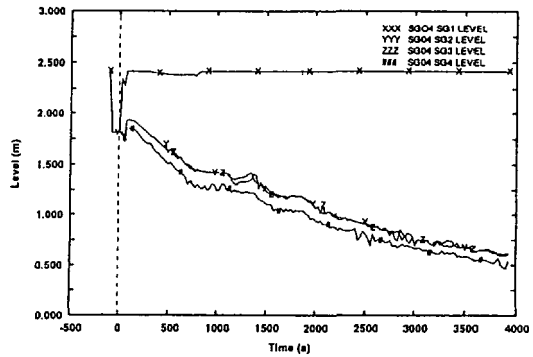


Fig. 14 - WWER-1000 SGTR: SGs level

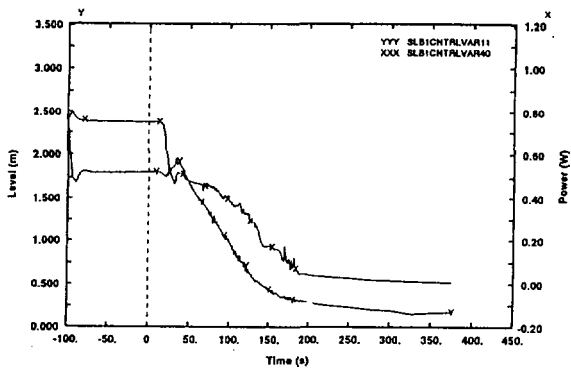


Fig. 12 - WWER-1000 SLB01: SG level and exchanged power

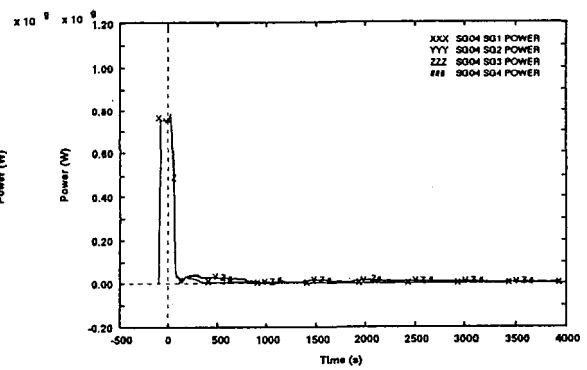


Fig. 15 - WWER-1000 SGTR: SGs exchanged power

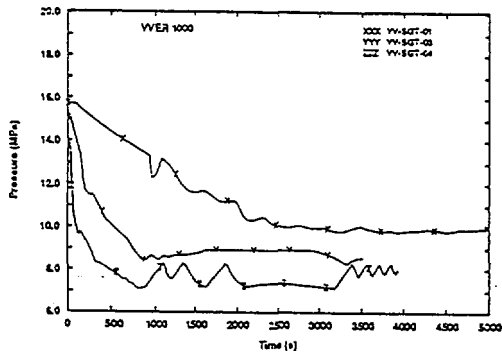


Fig. 13 - WWER-1000 SGTR PRZ pressure

4. STEADY STATE AND TRANSIENT STEAM GENERATOR PERFORMANCES

4.1 Steady state data and comparison with literature data

The characterization of the steady state performance of steam generators has been made with reference to nominal operating conditions. In order to achieve more precise steady state values, 500 seconds of code calculation have been considered (instead of 100 seconds, normally assumed as sufficient for achieving the steady state with a qualified nodalization).

All the considerations below are related to the nodalization configuration that has been selected and here is assumed as reasonable (see section 2.2).

The steady state performance can be characterized by fluid mass, level in downcomer, void fraction, fluid velocities and /or quality distribution in hot and cold package, recirculation ratio and temperature distribution in the primary side. All these information is given in Tab. 5 and Figs. 16 to 18.

The lack of time variation of any data reported, constitutes the only qualification level for the data themselves, because:

- nodalization is very rough, compared with the physical situation;
- there is not possibility so far for the comparison with qualified experimental data (see below).

An overview of the literature reveals the existence of experimental data. The most relevant information in this connection has been found in ref. /20/ and are reported in Fig. 19 and in Tabs. 6 and 7.

NODE	LEVEL (m)					
	0.31	0.6	0.89	1.18	1.47	1.76
QUALITY						
610	0.013	0.013	-1.8E-3	-1.9E-3	-1.9E-3	-2E-5
620	0.0019	0.054	0.089	0.124	0.144	0.177
630	0.021	0.055	0.089	0.123	0.158	0.193
GAS VELOCITY (m/s)						
610	0.333	0.34	0.409	0.441	0.863	-
620	0.685	0.92	1.17	1.4	1.37	1.57
630	0.358	0.451	0.597	0.768	0.774	0.868
FLUID VELOCITY (m/s)						
610	0.464	0.46	0.511	0.497	0.898	0.881
620	0.239	0.267	0.296	0.321	0.285	0.295
630	0.09	0.098	0.104	0.105	0.087	0.088
GAS VELOCITY/FLUID VELOCITY						
610	-	-	-	-	-	-
620	2.87	3.44	3.95	4.36	4.8	5.32
630	3.98	4.6	5.74	7.31	8.89	9.86

Tab. 5 - Steady state characteristics of steam generator performances

It appears clear that the local experimental information (transducer measuring situation in zones of cubic millimetres) can not be used for comparison with calculated data related to cubic meters.. In addition, the 3-D features of steam generator design are not simulated by the adopted nodalization scheme. However, it seemed interesting to compare our results with those provided in the same ref. /20/ and obtained by a specifically developed code. This comparison is given in Figs. 20 and 21.

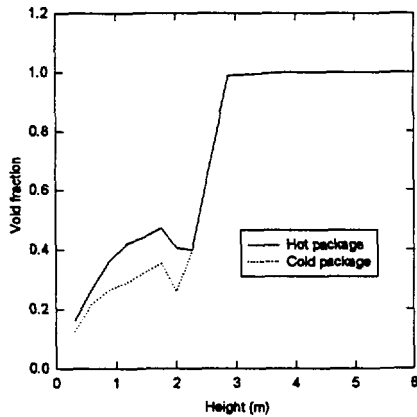


Fig. 16 - VV-SGC-03: void distribution along the height

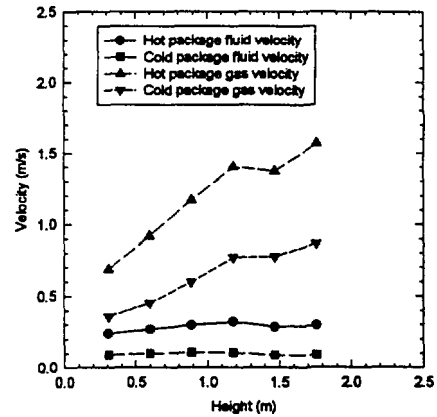


Fig. 17 - VV-SGC-03: gas and fluid velocity distribution along the height

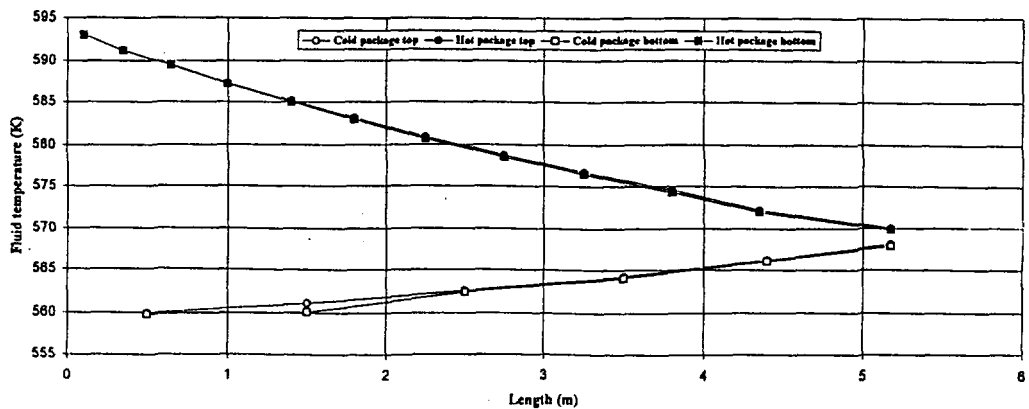


Fig. 18 - VV-SGC-03: temperature distribution

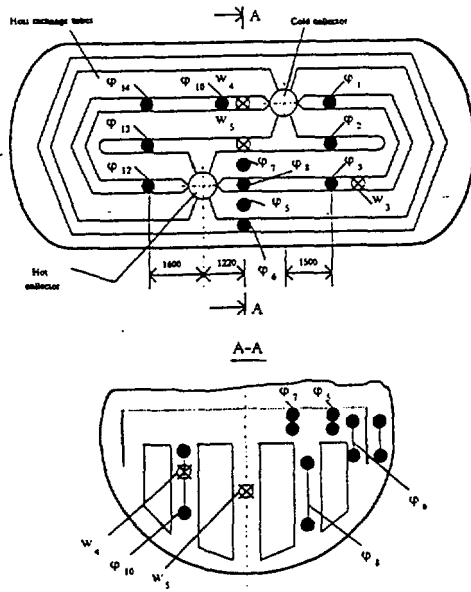


Fig. 19 - Position of velocity and void fraction gauges in steam generators

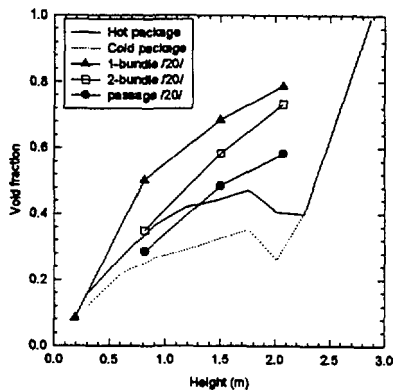


Fig. 20: Comparison between Relap5 and mathematical model /20/ results

Velocity	Experiment	Calculation
w_3	0.35	0.45
w_4	0.7	0.60
w_5	0.3	0.38

Tab. 6 - Comparison of exp. and numerical data on steam - water mixture

Void fraction	Experiment	Calculation
ϕ_1	0.3	0.55
ϕ_2	0.45	0.63
ϕ_3	0.45	0.54
ϕ_5	1.0	0.84
ϕ_6	0.7	0.77
ϕ_7	1.0	0.89
ϕ_8	0.55	0.55
ϕ_{10}	0.47	0.56
ϕ_{12}	0.52	0.51
ϕ_{13}	0.5	0.63
ϕ_{14}	0.55	0.54

Tab. 7 - Comparison of exp. and numerical data on void fraction

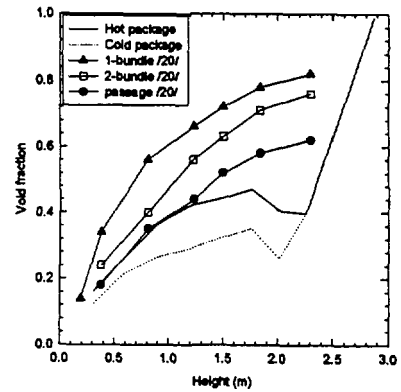


Fig. 21: Comparison between Relap5 and STEG-01 /20/ results

4.2 Transient performances

The purpose of this section is the characterization of the transient performance of steam generators. Only time dependent results (status approach) are reported and complete information for this section also includes the data discussed under section 3, specifically making reference to variables characterizing steam generators behaviour.

The transient steam generator performance has been characterized through four graphs (Figs. 22 to 25), obtained from runs VV-SGC-01 and VV-SGC-02 of Tab. 4. In these runs actual operating conditions for steam generators have been taken as reference.

The results reported in Figs. 22 and 23 show that around 40 % of power can be removed with very low values of level or mass (about 20 % of the nominal value). In both cases the abrupt fall of the exchanged power at value close to the nominal operating conditions is connected with the evolution of the transients, essentially stop of the feed water and pressure increase up to the SRV set point.

The recirculation flow (see Fig. 24) depends upon the level only for values above 1.2 m, below such value the recirculation flow is close to zero and the steam generator behaviour is essentially like a "once-through" one.

The data in Fig. 25 show a nearly linear relationship between thermal power and primary circuit mass flowrate, in a mass flow range 10% - 100% and in a power range 20% - 100%. It is interesting to note that removed power holds not less than 5 %, whatever is the flow rate in the primary side; in other terms, natural circulation seems very effective.

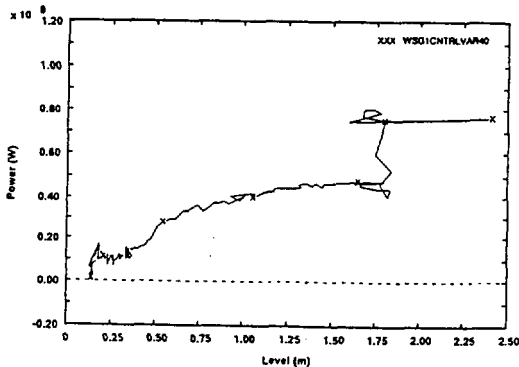


Fig. 22 - VV-SGC-01: SG exchanged power vs. level

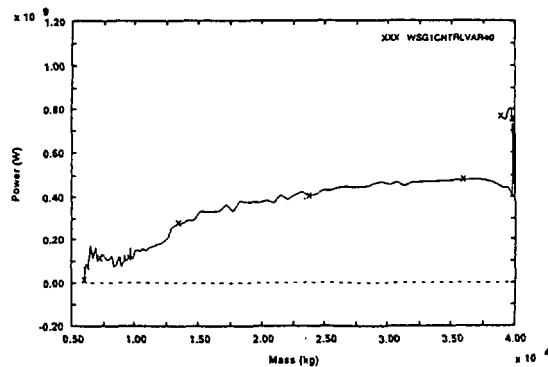


Fig. 23 - VV-SGC-01: SG exchanged power vs. mass

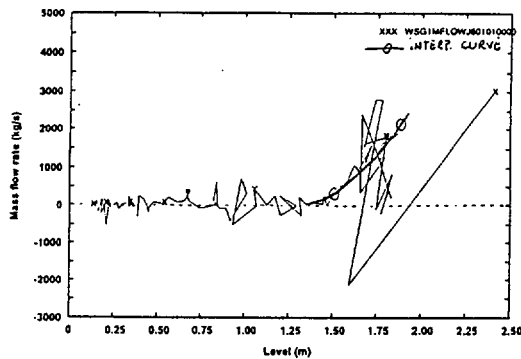


Fig. 24 - VV-SGC-01: SG flow rate vs. level

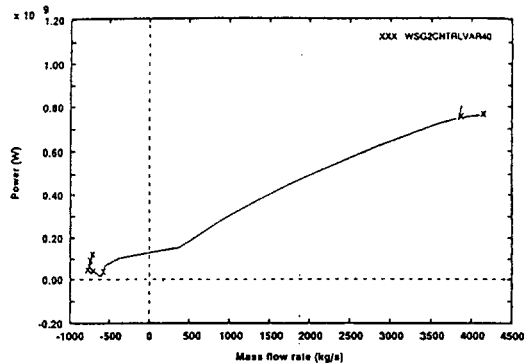


Fig. 25 - VV-SGC-02: SG exchanged power vs. primary circuit flow rate

Additional comments related to steam generator performance can be drawn from section 3:

- there is a clear relationship (see Figs 6 and 8) between the exchanged power and the start of depressurization: power increase is a follow up of the Accident Management procedure, steam generator depressurization (Fig 8) and Auxiliary Feedwater injection (Fig 6), respectively;
- Fig. 10 shows that the maximum removable power is of the order of 250%;
- from Fig. 15 it can be noted that the exchanged power is constant in the first couple of minutes of the transient.

5. CONCLUSIONS

The performed activity is part of a research aiming at qualifying the input deck for WWER-1000. For the sake of completeness a few conclusions reached in the papers in refs. /16/ and /17/ are recalled hereafter:

- the consideration of hot rod with a power peak factor (equal to 2.4) caused unacceptable high temperature for the rod surface;
- the design of the operating conditions for SIT appears suitable for Large Break LOCA, but not for Small Break LOCA: essentially a too high value of the ratio initial liquid mass/initial nitrogen mass characterizes the SIT operating conditions;
- Accident Management procedure based on steam generator depressurization or (even) delayed actuation of Auxiliary Feed Water are very effective for cooling the primary circuit owing to the large heat transfer area available in steam generators;
- the main Steam Line Break accidents (break area > 50%) combined with an ATWS situation brings to unacceptable power rise; however this condition is also expected in Western PWR.

In this paper special emphasis has been given to the prediction of the behaviour of the steam generators.

Main conclusions are as follows:

- 1) Relap5/Mod3.2 code appears robust and suitable in calculating transients evolving at high pressure in WWER-1000 steam generators;
- 2) a calculated data base has been proposed in this paper, that is suitable for further development of the activity, though for different reasons limited comparison with experimental data could be completed;
- 3) it is recommended experimental information gathered from operation of steam generators should be put in a form suitable for comparison with code data;
- 4) a mechanistic detailed evaluation of 3-D/two phase natural circulation in secondary side of steam generators is well beyond the capabilities of existing qualified codes; however, the experience gained so far, demonstrates that the rough noding scheme adopted is sufficient for safety and design optimization calculation related to WWER-1000 (this mostly comes from analyses of transients in plants and of experimental data in facilities like PMK and Pactel, not discussed in the present paper).

REFERENCES

- /1/ D'Auria F., Galassi G.M., 1990, "Assessment of Relap5/Mod2 on the basis of experiments performed in Lobi facility", J. Nuclear Technology, Vol. 90, N° 3.
- /2/ D'Auria F., Galassi G.M., 1990, "Code assessment methodology and results", IAEA/TCM Workshop on Computer Aided Safety Analyses, Moscow (Ru), May 14-17.
- /3/ Bernard M., D'Auria F., 1990, "Validation of Cathare on the basis of Lobi experiments", CEC Seminar Contribution to Reactor Safety Research, Varese (I), November 20-24.
- /4/ Mavko B., Prosek A., Parzer I., Frogheri M., D'Auria F., Leonardi M., 1995, "Application of the FFT method to the IAEA SPE-4 experiment simulation", Annual Meeting on Nuclear Technology, Nurnberg (G), May 16-18.
- /5/ D'Auria F., Frogheri M., Vigni P., 1995 "Natural circulation in Candu, WWER and PWR type nuclear plants", 13th. Conf. of Italian society of Heat Transport, Bologna (I), June 22-23.
- /6/ Fletcher C.D., Schultz R.R., 1995, "Relap5/Mod3 code manual - User guidelines", NUREG/CR-5535, INEL-95/0174.
- /7/ Kolev N.P., Tomov E., Ovchatova I., Angelov D.K., 1992, "Kozloduy Nuclear Plant analyzer. Specification of a WWER-1000 reference plant for NPA modelling purposes", Energoproekt report, Sofia (BG).
- /8/ Hinovsky I., 1995, "Personal communications to F. D'Auria", Sofia, March and June 1995.
- /9/ US. DOE, 1987, "Overall plant design descriptions WWER", DOE/NE-0084, rev 1, Washington (US).
- /10/ Gatta P., Mastrantonio L., 1995, "Thesis in nuclear Engineering", Università di Roma "La Sapienza".
- /11/ D'Auria F., Galassi G.M., Gatta P., Mastrantonio L., Marsili P., 1996, "Comparison between small LOCA scenarios in Eastern and Western type PWRs", ICONE-4 Conference, New Orleans (US), March 10-14.
- /12/ Cerullo N., D'Auria F., Frogheri M., Hinovsky I., 1996, "Data base for transient analyses in WWER-1000 Nuclear Plant", ICONE-4 Conference, New Orleans (US), March 10-14.

- /13/ Aprile G., 1996, "Thesis in Nuclear Engineering", Università di Pisa.
- /14/ Bonuccelli M., D'Auria F., Debrecin N., Galassi G.M., 1993, "A methodology for the qualification of the thermalhydraulic codes nodalization", Proc. of NURETH-6 Conf., Grenoble (F), October 5-8.
- /15/ Kolochko W., 1995 "Personal communication to F. D'Auria", Kiev, December 1995.
- /16/ Aprile G., D'Auria F., Frogheri M., Galassi G.M., 1996, "Application of a qualified WWER-1000 plant nodalization for Relap5/M3.2 computer code", Int. Conf. on Nuclear Option in Countries with Small and Medium Electricity Grid, Opatija (Croatia), Oct. 7-9.
- /17/ D'Auria F., Galassi G.M., Mastrantonio L., 1997, "Accident management studies in the WWER-1000 plant", ICONE-5 Conference, Nice (F), May 26-30.
- /18/ Belijaev Y. V., Trunov N.B., Shumsky A.M., 1992, "Calculation of conditions with drop of the level over PGV-1000 secondary side using Dinamika-5 code", Second Int. Seminar on Horizontal Steam Generator Modelling, Lappeenranta (SF), September 29-30.
- /19/ Ubra O., Doubek M., 1994, "Horizontal steam generator PGV-1000 thermal-hydraulic analysis", Third Int. Seminar on Horizontal Steam Generator Modelling, Lappeenranta (SF), October 18-20.
- /20/ Melikhov V.I., Melikhov O.I., Nigmatulin B.I., 1994, "Numerical modelling of secondary side thermohydraulics of horizontal steam generator", Third Int. Seminar on Horizontal Steam Generator Modelling, Lappeenranta (SF), October 18-20.
- /21/ Karppinen I. , 1994, "Modelling studies of horizontal steam generator PGV-1000 with Cathare", Third Int. Seminar on Horizontal Steam Generator Modelling, Lappeenranta (SF), October 18-20.
- /22/ Aksan N., D'Auria F., Glaeser H., Pochard R., Richards C., Sjoberg A., 1993, "Separate effects test matrix for thermalhydraulics code validation", OECD/CSNI Report, OCDE/GD (94), Paris (F).
- /23/ D'Auria F., Debrecin N., Galassi G.M., 1995, "Outline of the Uncertainty Methodology based on Accuracy Extrapolation (UMAE)", J. Nuclear Technology, Vol. 109, N° 1.



F19800028

**FOURTH INTERNATIONAL SEMINAR ON HORIZONTAL
STEAM GENERATORS**

11 - 13 March 1997, Lappeenranta, Finland

**POSSIBLE PRESSURIZED THERMAL SHOCK EVENTS
DURING LARGE PRIMARY TO SECONDARY LEAKAGE**

**THE HUNGARIAN AGNES PROJECT AND PRISE ACCIDENT
SCENARIOS IN VVER-440/V213 TYPE REACTOR**

by L. Perneczky

**KFKI Atomic Energy Research Institute
H-1525 Budapest, P.O.Box 49, Hungary**

Budapest, February 1997

ABSTRACT

Nuclear power plants of VVER-440/213-type have several special features. Consequently, the transient behaviour of such a reactor system should be different from the behaviour of the PWRs of western design.

The opening of the steam generator (SG) collector cover, as a specific primary to secondary circuit leakage (PRISE) occurring in VVER-type reactors was occurred first time in Rovno NPP Unit 1 on January 22, 1982 [1]. Similar accident was studied in the framework of IAEA project RER/9/004 [2] - [4] in 1987-88 using the RELAP4/mod6 code.

The Hungarian AGNES project [5] - [10] was performed in the period 1991-94 with the aim to reassess the safety of the Paks NPP using state-of-the-art techniques. The project comprised three type of analyses for the primary to secondary circuit leakages: Design Basis Accident (DBA) analyses, Pressurized Thermal Shock (PTS) study and deterministic analyses for Probabilistic Safety Analysis (PSA). Major part of the thermohydraulic analyses has been performed by the RELAP5/mod2.5/V251 code version with two input models.

In the DBA type medium size LOCA calculations and the PTS studies, as well as in the deterministic study in support of PSA the six loops (six primary coolant loops and six secondary steam lines) of the VVER-440 system were modelled by three loops (a single, a double and a triple loop). In the further developed version of the input model used in small break LOCA, primary to secondary circuit leakages and other DBA analyses the six reactor cooling loops were modelled separately [11], [15]. The nodalisation schemes of the reactor vessel and the pressurizer, moreover the single primary loops are identical in the two input models. The six-loop input model for VVER-440/V213 system was verified by the data of two operational transients measured in Paks NPP: loss of one main circulating pump and transient after scram (reactor protection operation) [13], [14]. According to the results the two input decks was used in the primary to secondary circuit leakages calculation cases with complete success.

The accident scenarios following the SG heat transfer tube failure and collector failure in VVER-440/V213 type reactor are presented in the paper. It is pointed out that the relevant acceptance criteria are satisfied for the analysed scenarios. The analyses were continued for evaluating the radiological consequences, or - for PTS study - to investigate the behaviour of the pressure vessel wall from the point of view of fracture mechanics.

Since reactor repressurization is a prohibited action as long as the temperature is below the critical temperature of the vessel, these scenarios are considered as a combination of a transient and an operator mistake. It is important to note, however, that there are very many valves in the VVER-440 primary circuit compared to the Western PWRs and the present operating procedures give absolute priority to the isolation of breaks.

The PTS analyses pointed out in a unique and unambiguous way that the isolation of primary circuit breaks should not be given priority over the cold repressurization of the reactor vessel. The necessity to give priority to the leakage isolation in case of a steam generator collector cover opening, represent further problems to be solved.

1 INTRODUCTION

The Paks Nuclear Power Plant is the only NPP in Hungary, it consist of four units, equipped with VVER-440/V213 type reactors. The units were put into operation between 1982 and 1987. The general opinion on Paks NPP is positive in Hungary as well as internationally. The operating experience is fairly good, in the last years two of the four units were among the top ten individual reactors in terms of cumulative load factors. During the 42 reactor years of operation no serious safety related problem occurred [6].

The Safety Analysis Reports (PSAR and FSAR) for Paks NPP were completed on the basis of the Technical Design Document delivered by the vendor. At that time they could be accepted, but also criticised because of important deficiencies of analyses as

- the list of initiating events of accidents is not complete,
- input data of the analyses are not fully known, uncertainties of data are not available,
- detailed information concerning the codes, tools of analyses are missing,
- conservatism applied to the calculations is generally not known, e.t.c.

Since the start-up of the plant an amount of experience has been gained in the field of nuclear safety, knowledge concerning the safety assessment of NPPs has significant improved. This valuable information been well supplemented by the results obtained in the Hungarian research institutes, were partially realized in the acknowledged high level operation of Paks NPP and in the already performed safety enhancement measures as well. In the last few years the nuclear safety of Soviet designed reactors has become a major factor of interest world-wide. In 1993 the Hungarian Atomic Energy Commission prescribed the periodic renewal of the licence of all Hungarian nuclear facilities.

With all this in mind, by means of the systematic utilisation of the above mentioned knowledge the reassessment of the nuclear safety of the plant was considered necessary, this reassessment has become linked with the periodic licence renewal, outlined finally a new project.

2 THE AGNES PROJECT

The Hungarian Atomic Energy Commission in February 1992 officially launched the AGNES project (Advanced General and New Evaluation of Safety) [6] by conforming the aims as follows:

- a state of art report on the reassessment of the nuclear safety of Paks NPP by using internationally acknowledged up-to-date techniques on the level of the nineties has to be prepared,
- those deterministic analyses of design basis accidents (DBA) and severe accidents as well as probabilistic safety analysis (PSA) should be carried out that are necessary for the preparation of the report,
- the priorities of safety enhancement and backfitting measures should be determined,
- preparation of a revised Safety Analysis Report satisfying the requirements of the expected new Hungarian regulations should commence.

The AGNES project was performed in the period 1991-94 with success. Experts of Hungarian institutes were taking part in various aspects of the works. Same parts were performed by organizations from abroad (GRS-Germany, IVO-Finland, VTT-Finland, TRACTEBEL-Belgium). The quality assurance of the tools for analyses was provided in accordance with the international standards by involving foreign experts. Results were confirmed by IVO-Finland. A Final Report [5] summarizes the results of the project, detailed analyses of possible incidents and accidents are given with summarizing main results and evaluations, and further recommendations for essential and possible safety enhancement measures are included. The project answered all questions what are in the focus of

interest of the international nuclear community and, on the other hand, the non-investigated problems do not influence significantly the statements of the project concerning the safety of Paks NPP.

So far the AGNES project has been the first comprehensive and systematic safety analysis for a Russian designed NPP containing system analyses, DBA, severe accident analyses and PSA Level 1 performed with the help of the most advanced techniques [5] - [10].

3 ACCIDENT ANALYSIS IN THE AGNES PROJECT

The accident analyses performed in the course of the project are practically identical to the analyses which would represent the content of the corresponding chapters of a Safety Analysis Report (SAR). The analyses include - in addition to DBA - the pressurized thermal shock (PTS) analyses, deterministic analyses for Probabilistic Safety Analysis (PSA) and some anticipated transients without scram (ATWS) scenarios. The analyses are normally related to the full power state if the Unit 3 of the NPP, starts at decreased power level and shut-down states have been treated but without the demand for completeness.

The set of initiating events for DBA covers every initiating events considered world-wide to affect plant safety and also specific cases occurring in VVER-type reactor (e.g. horizontal steam generator collector cover opening). The most advanced computer codes were applied in the reactor safety studies and when a system-specific validation was needed to ensure quality of results or to assess their uncertainties, this validation was performed. The data base was established on the basis of all the data which are needed for the complete technical description of the plant in the analyses to be performed. Any data of the data base is associated with a reference to design drawings and other technical documents. The general input data of the codes applied to the analyses are presented in Handbooks, The TRASS (Transient and Accident Summary Sheet) reports summarize the initial and boundary conditions and the information of parameter study, regarding the initial event in question.

The loss of coolant accident (LOCA) analyses and other thermohydraulic studies of the system were made basically by means of the RELAP5/mod2.5/V251 code version, the exceptions are the large break LOCAs, the steamline break and the ATWS events. The code version is originated from Siemens and it was obtained from TRACTEBEL with the permission of Siemens and US-NRC. The analysis of large break LOCAs, where the combined simultaneous upper plenum and downcomer injection results in a rather complicated process during reflooding phase, was carried out by using the ATHLET mod 1.1 Cycle code version (developed by GRS) in the framework of a bilateral German-Hungarian cooperation agreement. The analysis of steamline break was made by IVO using the SMABRE code (developed by VTT) which applies a special mixing model and the three-dimensional reactor kinetic HEXTRAN code. The ATWS analysis was performed by SMATRA code (developed by VTT too). In the evaluation of PTS problems calculated by RELAP5 and ATHLET, the stagnation of coolant should also be modelled, this type of process is analysed by the REMIX code. After the thermohydraulic analysis special fracture mechanical calculations for actual pressure vessel material had to be performed. In order to assess the severity of LOCAs the containment behaviour studies by CONTAIN code and dose calculations were performed to verify whether the acceptance criteria are fulfilled.

4 INPUT MODELS FOR RELAP5 CODE

For the RELAP5 calculations two input models of VVER-440/V213 primary and secondary coolant systems were developed and used in the AGNES project.

In the medium size LOCA calculations [7], deterministic cases for PSA [23] and the PTS studies [17], [22] the six loops (six primary coolant loops and six secondary steam lines) of the VVER-440 system

were modelled by three loops - a single, a double and a triple loop -, one of the turbines is fed by the steam lines of the single and double loops, the other one is fed by the steam line of the triple loop. This so-called 1+2+3 model is based on results of an international cooperation organized and coordinated by IAEA, Vienna, in framework of the "IAEA Technical Co-operation Project RER/9/004 on Evaluation of Safety Aspects for WWER440 Model 213 Nuclear Power Plants". The nodalization of systems consists of 250 volumes, 284 junctions and 248 heat slabs with 1144 mesh points.

In the further developed version of the input model used in small break LOCA and other DBA analyses the six reactor cooling loops were modelled separately [11], [15], [20], [21]. The nodalisation schemes of the reactor vessel and the pressurizer, moreover the single primary loops are identical in the two input models.

4.1 Nodalization in the six-loop model

The base of the six-loop input model is the nodalization conception. The numbering of control volumes and pipes (even numbers), as well as of junctions and valves (odd numbers) are as follows [11]:

- reactor vessel	001 - 099
- coolant loops (* = 1,2,3,4,5,6)	
- primary side	*00 - *59
- secondary side with feed lines	*60 - *99
- steam line system from main isolating valves with steam header and turbines (* = 7,8)	*00 - *99
- pressurizer with spray and surge lines	901 - 949
- emergency core cooling systems (ECCS)	950 - 999

The main characteristics of the reactor vessel (see Fig. 4.1) are as follows:

- the downcomer consists of five volumes in one channel,
- the lower plenum is divided into four volumes vertically,
- the core is represented by three channels, consisting of 7-7 volumes, one channel corresponds to the hot fuel rod assembly, two represents the peripheral region (1/3) and the central region (2/3) of the average assemblies,
- parallel to the core a 3-volume by-pass can be found,
- the upper plenum is divided into six volumes vertically, the outlet ring is connected to the third one,
- four times five heat slabs representing heated part of fuel rods are used for modelling the fuel rod of highest power rate in the hot assembly, the average 125 fuel rods of the hot assembly and the average fuel rod bundles of the two average channels,
- 19 heat slabs represent the heat capacity of structural elements including walls, plates and guide tubes and heat losses through the vessel wall,
- the heat source in active core is modelled by the RELAP5 point kinetic model with feedback.

The pressurizer vessel model (see Fig. 4.2) contains 14 volumes with heat slabs for wall and heaters, the surge line four elements, while the spray system consists of 8 components. The ECCS model including four hydroaccumulators and 3 independent active systems is composed of 45 elements.

The primary U-tubes of horizontal steam generator (SG) are divided axially into 5 nodes (the length of the nodes are different corresponding to a similar temperature drop in the nodes), while vertically into 3 bundles. Each of the vertical collectors is divided into five volumes. The junctions between the

collectors and U-tubes are cross-flow type. On the SG secondary side 5 layers can be found, 3 in the liquid part (tube bundle region) with a parallel channel providing the simulation of internal recirculation (downcomer region) and 2 layers in steam part. Heat slabs in SG model represent the walls of collectors, U-tubes and vessel.

The nodalization of the steam line and feedwater systems consists of relatively few control volumes but all isolation, steam dump and safety valves are comprised in schemes. The two turbines are modelled by time dependent volumes (Fig. 4.3).

The total number of elements in the input model are: 512 volumes, 581 junctions and 417 heat slabs with 1869 mesh points.

4.2 The control and protection systems

The boundary conditions like reactor protection systems and control logic can be specified in RELAP5 input model by using control variables, trip cards and general tables. In the six-loop model these elements are generated in a unified manner on the basis of the detailed control schemes of the Paks NPP unit No 3 by using a RELAP5 object-oriented preprocessing interactive code with high level graphic functionalities, the TROPIC 4.0 code received from TRACTEBEL Belgium [12].

The TROPIC code is intended to meet the following objectives:

- reduction in code syntax knowledge,
- permanent documentation of the input data set,
- reduction of the user reluctance to modify his input deck,
- possibility of performing restart sessions very easily,
- availability of a user friendly tool.

In the six-loop input deck for VVER-440/V213 system we have 4510 cards representing 229 trips, 1032 control variables and 95 tables due to TROPIC code describing the following protection and control systems:

- first level unit protection system (scram),
- complete ECCS logic,
- pressurizer pressure control and protection system,
- SG protection and level control,
- turbine protection system.

We have got very favourable experiences in use of this preprocessing code.

4.3 Experiences in use of input models

The six-loop input model for VVER-440/V213 system was verified by the data of two operational transients measured in Paks NPP: loss of one main circulating pump and transient after scram (reactor protection operation) [13], [14]. It was proven that the models in the "master input deck" developed for the six loop system of VVER-440/V213 unit seem to work correctly, the measured data are matched with sufficient accuracy. The possible reasons for differences could be pointed out.

The first results obtained in the field of medium size LOCA analyses using the 1+2+3 loop RELAP5 input model in the AGNES project were presented on the RELAP5 Users' Seminar in 1993 [7]. It has

to be mentioned that the six-loop model with more than double dimensions encountered difficulties in the repetition of these medium size break LOCAs (if the diameter of break was greater than 70 mm), due to time step convergence failure in the early phase of transients (water property failure at the minimum time step). Nevertheless according to the results in the AGNES project and other tasks the six-loop input deck was used in more than 30 DBA calculation cases with complete success.

The six-loop RELAP5 input model of the Paks NPP and an illustrative part of the analysis results obtained for the group of accidents initiated by the decrease of secondary side heat removal were reported in two papers [15], [16]. Some calculations applying the three-loop input model were made for the PTS study [17]. Experiences gained in use of RELAP5 input models of VVER-440/V213 reactor were presented on 1996 RELAP5 Users Seminar in Dallas [18].

5 RESULTS OF PRIMARY TO SECONDARY LEAKAGES CALCULATIONS

In the AGNES project three type of analyses for the primary to secondary circuit leakages were performed: Design Basis Accident (DBA) analyses, Pressurized Thermal Shock (PTS) study and deterministic analyses for Probabilistic Safety Analysis (PSA).

5.1. Design Basis Accident (DBA) analyses

DBA analyses aimed at proving whether for the processes following the selected initiating events, the safety systems of the plant are capable of preventing severe consequences. Correspondingly, acceptance criteria were formulated and the fulfilment of these criteria was to be proven in the analyses.

The DBA analyses can be further divided into three groups based on the processes following the initiating events: Reactivity Initiated Accidents (RIA), Thermohydraulic Transients (TH), and analysis of auxiliary systems from the point of view of radioactive releases (AUX).

Analysis of thermohydraulic transients caused by various initiating events requires the use of specific codes, depending on the nature of the process. If the primary circuit is dehermetised in the analysed process, then generally activity transport, release and dose calculations were performed.

5.2. Pressurized Thermal Shock (PTS) analyses

Pressurized thermal shock is a serious problem of the older US and Soviet RPVs as a consequence of the poor material quality. In spite of the excellent quality of the Paks NPP RPVs the extended accident analysis of the AGNES project also covers PTS analyses.

On the broad scale of presumable transients and accidents which may occur during the lifetime of the plant the RPV may suffer a very fast and significantly large temperature decrease while, at the same time the high system pressure may be maintained. According to the regulatory practice it has to be proven that the RPV may not be damaged due to a PTS event during its entire designed lifetime, taking into account the embrittlement due to radiation damage.

5.3. Deterministic analyses for Probabilistic Safety Analysis (PSA)

The probabilistic safety analysis has an obvious great significance since it reveals the weak points of

the plant and gives a sound basis for prioritizing interventions.

In the PSA the event trees comprising the possible scenarios corresponding to the initiating events selected for the accident analysis are analysed. The success criteria (i.e. if core melt is avoided) of the single event sequences belonging to an event tree can be determined by using the computer programs used in DBA analysis. In these analyses best-estimate, normal operating condition data were used.

5.4. Survey of initiating events

The first step of the analyses was to determine the initiating events. Based on the many decades of NPP operating and regulatory experience, the list of initiating events as given in the US NRC Regulatory Guide 1.70 [19] covers the set of presumable transients and accidents which are relevant for the safety of the plant and environment, if probabilities and consequences are assessed. In the framework of the AGNES project these initiating events were analysed, supplemented with initiating events which are specific for VVER-type plants, as the SG collector cover opening [6].

In the following tables the 6th group of initiating events of DBA (grouped into seven classes) including primary to secondary leakages are presented (Table 5.1) together with the initiating events of PTS group (Table 5.2). It is also shown which cases were deterministically analysed to support PSA analyses (Table 5.3). The "US NRC" column indicates the number of the list [19]. The numbers of the cases show the total number of studied cases and the number of cases calculated by RELAP5/mod2.5.

Table 5.1.

Group 6 of initiating events: DBA cases for decrease of reactor coolant inventory

Initiating event	US NRC	Number of cases
6.1 Inadvertent opening of pressurizer safety or relief valve	15.6.1	2 / 2
6.2 Primary circuit line break outside the containment	15.6.2	1 / -
6.3 Steam generator tube break	15.6.3	3 / 3
6.4 Steam generator collector cover opening	-	3 / 3
6.5 Spectrum of loss of coolant accidents	15.6.5	20 / 12
6.6 MCP leak into intermediate circuit at loss of power	-	1 / -

Table 5.2.

Group 9 of initiating events: Pressurized thermal shock (PTS) cases

Initiating event	Number of cases
9.1 Inadvertent opening of pressurizer safety valve	4 / 2
9.2 Small and medium size LOCAs	4 / 4
9.3 200 % cold leg break	3 / -
9.4 Steam generator collector cover opening	3 / 3
9.5 Steamline break	2 / 2
9.6 Inadvertent ECCS operation	2 / -

5.4.1. DBA cases

In group of the initiating events for decrease of reactor coolant inventory two type of primary to secondary leakages are included:

- Steam generator tube failure;
- Opening of the SG collector cover.

Table 5.3.

Group 10 of initiating events: the deterministic analyses in support of PSA

Initiating event	Number of cases
10.1 Rupture of the control assembly housing	3 / 3
10.2 Large break LOCA in the cold leg	4 / 1
10.3 Large break LOCA in the hot leg	4 / 3
10.4 Medium size LOCAs in the cold leg	11 / 11
10.5 Inadvertent opening of pressurizer safety valve	2 / 2
10.6 Spray line break in pressurizer	2 / 2
10.7 Steam generator collector cover opening	3 / 3

Three cases were analysed for the double-ended rupture of single SG tube in order to maximize the radiation consequences, to determine the time available for the SG isolation so that the radiological consequences for the neighbourhood of the plant remain acceptable [20], [27].

In the accident of SG hot collector cover opening - due to the opening of the SG safety valves, too - the primary activity passing through the secondary circuit reaches the environment. At the analysis conservatism and boundary conditions of thermohydraulic calculations had to be chosen taking into account the radiation consequences. Two cases were investigated [21], [28]:

- with maximum ECCS injection (3 HPIS and 4 HA's)
- assuming a single failure (2 HPIS and 3 HA's).

The results of the dose calculations have shown that the corresponding acceptance criteria are not violated.

A third case, the most unfavourable from the point of view of core cooling - with minimum ECCS injection (1 HPIS and 2 HA's) - was also investigated. The core cooling criteria are fulfilled by the emptying of the ECCS tanks. If isolation of the break does not happen in due time and the supplementary source of primary coolant is not ensured, then the process leads to core melt. A safety enhancement measure is needed for the solution of this problem.

5.4.2. PTS analyses

The following anticipated initiating events were analysed in the AGNES project from the point of view of primary to secondary circuit leakages [22], [28]:

Steam generator collector cover opening:

Case 1 - the steam generator is isolated after 7200 s

Case 2 - the steam generator is isolated after 1800 s

Case 3 - the steam generator is isolated after 3600 s and flow stagnation is assumed

Since reactor repressurization is a prohibited action as long as the temperature is below the critical temperature of the vessel, these scenarios are considered as a combination of a transient and an operator mistake. It is important to note, however, that there are very many valves in the VVER-440 primary circuit compared to the Western PWRs and the present operating procedures give absolute priority to the isolation of breaks.

The PTS analyses pointed out in a unique and unambiguous way that the isolation of primary circuit breaks should not be given priority over the cold repressurization of the reactor vessel. The necessity to give priority to the leakage isolation in case of a steam generator collector cover opening, represent further problems to be solved.

5.4.3 The deterministic analyses in support of PSA

In accordance with the relevant PSA workplan among others the accident sequences for 3 cases of the SG hot collector rupture having an equivalent diameter of 100 mm were studied [23], [28]. The question was whether only one high pressure injection system is enough to reach the success criteria without and with secondary bleed and feed procedure. It was found, that the success criterion is fulfilled in all cases including the last one, when primary and secondary isolation in broken loop at 600 s after the break and bleed and feed action, but no available ECC system were assumed.

6 STEAM GENERATOR TUBE FAILURE

After one or more SG U-tubes rupture the primary coolant discharges into the secondary circuit, so activity appears in the secondary coolant as well, and from there through the secondary safety devices it is released into the environment. From the point of view of core cooling this case is covered by opening of SG collector cover, where no direct cooling problems emerged. Naturally with SG tube rupture the total water inventory of ECCS is not needed because the primary pressure can be reduced in time below the opening pressure of the SG safety valve.

Thermohydraulic analysis - referring to the double-ended rupture of one tube - was performed in order to maximize the radiation consequences, to determine the time available for the SG isolation in case of rupture of a single tube so that the radiological consequences for the neighbourhood of the plant remain acceptable. Three subcases were treated, which differ in the means of emergency feedwater supply. Detailed information and calculation results can be found in [20] and [27].

7 DBA ANALYSES FOR PRIMARY TO SECONDARY LEAKAGES AT SG COLLECTOR

The opening of the steam generator collector cover, as a specific primary to secondary circuit leakage case occurring in VVER-type reactors was studied first time in the framework of "IAEA Technical Co-operation Project RER/9/004 on Evaluation of Safety Aspects for WWER440 Model 213 Nuclear Power Plants" in 1987-88 using the RELAP4/mod6 code. The results were presented on workshops held in Sofia and Piestany [2], [3]. At the same time the Safety Enhancement Programme (SEP) at Paks NPP was enlarged with new item, where the results were utilized [4]. A new activity is going on at the Paks NPP on this topic on the basis of the results of the AGNES project [29] and other international programmes [32].

The accident analyses performed in the course of the AGNES project are practically identical to the analyses which would represent the content of the corresponding chapters of a Safety Analysis Report (SAR). The analyses include - in addition to DBA - the PTS analyses and some deterministic analyses in support of PSA (see Chapters 8 and 9).

DBA analyses aimed at proving whether for the processes following the selected initiating events, the safety systems of the plant are capable of preventing severe consequences. Correspondingly, acceptance criteria were formulated and the fulfilment of these criteria was to be proven in the DBA analyses of the AGNES project.

Opening of the hot-leg collector cover results in deterioration of core cooling conditions, but no state violating acceptance criteria regarding safe core cooling will directly come about [21]. Having both turbines tripped the relief valves into the atmosphere start to operate and the secondary circuit safety valves open. Taking it into account that during the process not only steam leaves through the secondary safety valves but water as well, it has to be supposed that one of them does not reclose automatically. If it is not possible to close this safety valve, then in the long run one has to consider the likelihood of the ECCS tanks emptying and the core running dry. This situation has to be changed, its priority being defined by the probabilistic analyses.

The present study aims to analyse the consequences of the opening of the hot collector cover in one SG. The analysis consists of two parts. First the thermohydraulic response of the system is calculated using the system code RELAP5/MOD2.5. Then the analysis is continued for evaluating the radiological consequences by using the TIBSO and CRAC2 programs [30], because it should be also investigated, whether the radiological consequences are below the limits during the transient caused by the opening of the SG collector cover, without isolation of broken SG for 30 minutes and with the

single failure that one of the SG safety valves remains stuck open.

Results show that from thermohydraulic point of view the transient does not represent any danger for the reactor. Dose values remain within the limits given in the acceptance criterion.

7.1 Definition of the accident

The postulated accident analysed in the present study assumes the opening of the SG collector cover. After the initiating event the primary pressure in the system decreases quickly near to the pressure of the secondary circuit. The secondary pressure reaches the setpoints of the steam dump and SG safety valves. The analysis is performed with the assumption that one safety valve remains stuck open. Reactor scram is initiated earlier by "last turbine tripped" signal. To make up the loss of water inventory the ECC system injects cold water into the primary circuit. The HPIS injection into the cold leg and the direct cold water feed from the HAs into the downcomer result in an overcooling of the system.

The effect of the number of ECC systems on the situation produced by the opening of one SG collector cover has been investigated in two cases for radiological consequences and a third case regarding the core cooling aspect (see SA8 in [25]).

Case 1: 3 HPIS and 4 accumulators are available (maximum configuration of ECCS)

Case 2: 2 HPIS and 3 accumulators are available

Case 3: 1 HPIS and 2 accumulators are available (minimum configuration of ECCS).

7.2 Acceptance criteria

Acceptance criteria were chosen in accordance with [24] (compare [25]). A short summary of the acceptance criteria is given below.

- C1** The analysed transient does not generate a more serious accident.
- C4** Neither fuel cladding nor fuel pellets should be overheated. Excessive fuel enthalpy should not be produced. Other mechanisms of rod failure modes should not occur.
- C5,(PA2)** The primary reactor coolant system should be maintained in a safe status so that fuel coolability can be maintained.
 - a) The maximum fuel cladding temperature does not exceed 1200°C. The total cladding oxidation does not exceed 17% of the total cladding thickness before oxidation. The total amount of generated hydrogen does not exceed 1% of the hypothetical amount that would be produced if all the metal were to react.
 - b) The radially averaged fuel enthalpy shall not exceed 963 J/g UO₂ at any axial location in any fuel rod.
- C7,(PA4)** The resulting doses are below the limits for postulated accident.
- C9,(PA3)** Pressure in the reactor coolant and main steam systems is maintained below acceptable design limits, considering potential brittle as well as ductile failures, and considering the fuel.

The dose limits proposed in [30] are applied as far as radiological consequences are concerned.

7.3 System initial conditions

Conservative initial conditions (nominal values \pm uncertainty) are taken into consideration (compare [25]):

Core power	1430.0	MW
Core inlet temperature	269.1	°C
Primary pressure	12.38	MPa
Core flowrate	7934.0	kg/s
SG pressure	4.71	MPa
Feedwater flowrate (for 1 SG)	129.3	kg/s
Feedwater inlet temperature	221.8	°C
Pressurizer level for Case 1 and Case 2	7.1	m
for Case 3 (6.9 - 0.2 m)	6.7	m
Water temperature in HAs	55.0	°C
Water temperature in HPIS tanks	35.0	°C

7.4 Core conditions

Core conditions are determined in a conservative way. The power distribution has an EOC top skewed shape.

The hot channel power is calculated by using the following distribution factors:

$$\begin{aligned} k_q &= 1.35 \quad \text{hot assembly} \\ k_k &= 1.15 \quad \text{hot rod in the hot assembly} \\ k_{eng} &= 1.17 \quad \text{uncertainty factor.} \end{aligned}$$

Point kinetics for EOC conservative conditions is applied without thermal feedback. The decay power is considered as EOC. The core by-pass flow is 7.3 % of the total downcomer flow.

7.5 Control and protection systems

The first part of the transient process is so fast that the reactor is quickly scrammed and the pressurizer becomes rather soon empty. As a result none of the control systems has influence on the process.

The following protection signals and systems are relevant in the actual scenarios:

SG level increase > 0.2 m	→	turbine trip
last turbine tripped	→	scram
pressurizer level < 0.47 m	→	SI signal
pressurizer level < 0.17 m	→	HPIS IV opening
SI signal + 16 s delay	→	HPIS start
primary pressure < 5.88 MPa	→	HA actuation
secondary pressure > 5.4 MPa	→	steam dump control valve actuation
secondary pressure > 5.75 MPa	→	SG safety valve actuation

7.6 Thermohydraulic models and codes

The analysis was performed by means of the RELAP5/mod2.5 for the system thermohydraulic response. The six-loop input model of VVER-440 reactor was used, the nodalisation scheme for RELAP5 simulation is presented in Chapter 4. The break is in loop No. 1. at the top of SG hot collector.

From the RELAP results a special file is created for the dose calculations. The transferred data are:

- primary mass inventory,
- break outflow,
- coolant enthalpy at the break,
- secondary outflow,
- secondary outflow enthalpy.

7.7 Results of the thermohydraulic analysis

Table 7.1 provides the chronology of events for Case 1. The transient is initiated at $t=0$ s after a steady-state calculation of 100 s, by opening the break area, corresponding to the rupture of a tube, having an inner diameter of 100 mm. This is a medium size break from primary to the secondary system resulting in fast discharge of coolant.

The first safety signal is the secondary coolant level increase in the broken steam generator by 0.2 m in the narrow range measurement system. As a consequence, the turbine isolation begins at 25.68 s. The scram is initiated by the "last turbine tripped" signal. The "small leak" signal - primary pressure less than 11.8 MPa and pressurizer level less than 2.4 m - occurs about 13 s later and SI signal is also generated. Diesel units start as a consequence of the SI signal and it is followed by the start of the ECC system pumps in LPIS and HPIS. The HPIS injection begins immediately because the isolation valves are open at low pressurizer level.

The primary pressure as a function of process time is presented in Fig. 7.1. After the transient initiation the pressurizer pressure is sharply decreasing during the subcooled blow-down. The slope is changed at less than 8 MPa, when the system pressure drops to the saturation pressure. Then it is affected by the secondary side pressure which shows an increase up to 5.76 MPa, reaching the opening pressures of BRU-A valves and the first safety valves in all SGs (Fig. 7.2). The secondary pressure is always lower than the primary pressure providing heat sink in the intact steam generators.

The discharge flow through the break is shown in Fig. 7.3. In the second part of the process the flow rate is the same order of HPIS injection rate (Fig. 7.7). The steam generator in the broken loop is filled up at about 105 s. From the process time of about 130 s, when SITs start to work, the primary mass inventory is slightly increasing (Fig. 7.4).

The core inlet and outlet temperatures show similar behaviour, they follow the primary system pressure behaviour and significantly drop during the injection of HAs. After that there is a lower decrease rate up to the end of calculation. Similar statement is true for the time variation of hot channel cladding temperature (Fig. 7.6), because the collapsed coolant level in reactor vessel does not decrease below the hot leg elevation, as shown in Fig. 7.5. No heat transfer crisis is expected as high vessel level and forced circulation is maintained after the scram. For the accident consequences the released coolant mass is shown in Fig. 7.8.

As a parametric study Case 2 and Case 3 were analysed. From thermohydraulic point of view there is no significant difference between the cases. Due to the lower value of the break flow (Figs. 7.10 and 7.12), energy released through the break with lower ECC injection (Figs. 7.9 and 7.11) a bit higher values of pressures and temperatures can be observed, but the conclusion is the same as for Case 1 (see Figs 7.13 and 7.14).

The results of the thermohydraulic analysis reveal that the different configuration of the safety system influences the accident consequences through the different released coolant mass originated from the primary system.

Table 7.1

CHRONOLOGY OF EVENTS

Case 1

0.0 s	break on top of SG hot collector
9.0 s	primary pressure < 11.8 MPa
25.6 s	SG1 narrow range level > 0.2 m
25.7 s	turbine trip for both units
25.8 s	reactor scram signal (last turbine tripped)
29.3 s	BRU-A1 opens
29.5 s	BRU-A2 opens
34.9 s	SG1 safety valve opens
35.0 s	SG2-SG6 safety valves open
37.3 s	SG2-SG5 safety valves close, (SG1 safety valve remains open)
38.2 s	pressurizer level < 0.47 m
38.3 s	SI signal, Diesel start
40.1 s	pressurizer level < 0.17 m, HPIS-IVs open
41.7 s	SG6 safety valve closes
43.2 s	primary pressure < 9.3 MPa
47.1 s	pressurizer wide range level = 0 m
48.3 s	Diesel ready, for LIP = 0 s
49.4 s	LPIS pump in operation
53.4 s	HPIS pumps start
54.4 s	HPIS injection begins
104.6 s	SG1 filled up
127.5 s	SITs N° 1,4 injection starts
134.2 s	SITs N° 2,3 injection starts
1997.0 s	SITs N° 1,4 emptied
2156.0 s	SITs N° 2,3 emptied
3600.0 s	integrated secondary out flow (BRU-A + SVs) is 318722 kg, integrated ECC flow is 456760 kg
4704.4 s	$\Delta p > 0.5$ MPa between SG5 and MSH2, MSIV closes and MCP stops in loop 5
4710.3 s	$\Delta p > 0.5$ MPa for SG1 and SG3, MSIVs close and MCPs stop in loops 1 and 3
5400.0 s	end of calculation ($P_{\text{prim}} = 1.02$ MPa, $t_{\text{core in}} = 441.18$ K)

7.8 Conclusions of the thermohydraulic analysis

The results of the present thermohydraulic analysis clearly show that the different configuration of the safety systems, even the minimum configuration of the ECCS can prevent any core damage before operator intervention when the cover of SG collector opens. The HPIS pumps will be switch over after emptying the tanks to the LPIS tanks. There is about 3 to 3.5 hours water reserve for ECCS.

Acceptance criteria given for postulated accidents are fulfilled:

- no more serious accident is generated, if operator action is supposed before 3 - 3.5 hours,
- fuel rod failure is not induced,
- fuel coolability is provided, cladding temperature remains below its value from steady state,
- both primary and secondary pressure remain below the limits.

7.9 Definition of the studied case and calculational assumptions for radiological consequences

In the LOCA scenario studied here the total quantity of water, steam and gas leaking from the primary coolant system flows into the secondary system. Consequently, the corresponding amount of the radioactive isotopes is also flowing into the secondary system. Since it is assumed that the SG safety valve remains stuck open, the radioactivity is released directly into the environment.

It is assumed that the primary circuit nuclide inventory corresponds to the maximum permitted concentrations for normal operation. Since these concentrations are identical with those obtained for 1 % fuel leak, it is further assumed that these permitted values already take into consideration spiking effects.

It is assumed that the radionuclide inventory of the primary circuit flows into the atmosphere at a rate given by the total mass flow resulting from thermohydraulic calculations.

Since the core coolability is not questioned in the given scenarios, no fuel damage occurs.

7.10 Results of release and dose calculations

Release and dose calculations were performed for first two ECCS actuation cases. Results are presented for Case 1 in [21], representing the worse case. Dose values are higher than in case of LBLOCA scenarios [5], however, they remain within the limits given in the acceptance criterion.

8 THE PRESSURISED THERMAL SHOCK STUDY

Pressurized thermal shock (PTS) is a serious problem of the older US and Soviet reactor pressure vessels (RPV) as a consequence of the poor material quality. In spite of the excellent quality of the Paks NPP RPVs the extended accident analysis of the AGNES project also covers PTS analyses.

On the broad scale of presumable transients and accidents which may occur during the lifetime of the plant the RPV may suffer a very fast and significantly large temperature decrease while, at the same time the high system pressure may be maintained. According to the regulatory practice it has to be proven that the RPV may not be damaged due to a PTS event during its entire designed lifetime, taking into account the embrittlement due to radiation damage.

In the framework of AGNES project the investigated 18 cases well cover the full range of PTS events. The present study aims to analyse the overcooling consequences of the opening of the SG collector cover [22].

The PTS analysis consists of 3 parts. First thermohydraulic response of the system is calculated using the system code RELAP5/mod2.5. When the thermohydraulic calculation reveals flow stagnation then the analysis is continued by means of the REMIX program. As the aim of the calculation is to investigate the behaviour of the pressure vessel wall from the point of view of fracture mechanics the analysis is finished with the ACIB-RPV code [31] calculation based on the downcomer pressure and temperature history given by the thermohydraulic part of the analysis. It should be investigated, whether any crack propagation occurs during the transient, either at the welds 5/6 and 3/5 or at the forged ring of the vessel opposite to the reactor core.

8.1 Definition of the accident

The postulated accident studied is the loss of integrity of the primary circuit by opening of the SG collector cover. After the initiating event the pressure in the system decreases quickly to the saturation temperature of the primary circuit, and reactor scram is initiated. The resulting rapid decrease of the primary side water inventory should be compensated by the actuation of the active and passive ECC systems at full capacity each. The HPIS injection into the cold leg and the direct cold water feed from the HAs into the downcomer result in a rapid overcooling of the RPV wall.

The effect of the PTS produced by the opening of one SG collector cover has been investigated in 3 cases with different repressurisation times.

In Case 1 the damaged SG is isolated by the operator at $t=7200$ s. In Case 2 the separation occurs at $t=1800$ s. In Case 3 it has been assumed that at $t=0$ s the electrical grid is lost and isolation of the leaking SG is executed at $t=3600$ s.

8.2 Acceptance criteria

The postulated accident is analysed from the point of view of the fulfilment of the thermohydraulic acceptance criteria in a separate study (Chapter 7). There other kind of conservatism was required than in the present PTS study.

The vessel failure during a PTS event is considered to be acceptable, if no crack propagation occurs during the PTS or the crack is arrested and becomes stable before reaching 75% of the vessel wall thickness. If the safety factor for the finally arrested crack is below 1.1 for any of the three crack models used, then the fracture analysis must be repeated by using a finite element code and the arrested crack stability must be verified.

8.3 System initial conditions

The initial parameters have best estimated nominal values, except the ECCS water temperatures:

Core power	1375.0	MW
Core inlet temperature	265.0	°C
Primary pressure	12.26	MPa
Downcomer flowrate	8207.6	kg/s
SG pressure	4.63	MPa
Feedwater flowrate (for 1 SG)	129.0	kg/s
Feedwater inlet temperature	221.0	°C
Pressurizer level	6.9	m
Water temperature in HAs	40.0	°C
Water temperature in HPIS tanks	20.0	°C

Active and passive ECC systems (SA8) are considered at their maximum capacity, i.e. 3 HPIS and 4 accumulators are available. Core conditions are determined in a conservative way from the point of view of PTS i.e. a BOC distribution has been taken into consideration.

The hot channel power is calculated by using the same distribution factors as in DBA calculations.

8.4 Control and protection systems

The first part of the transient process is so fast that the reactor is quickly scrammed and the pressurizer becomes rather soon empty. As a result none of the control systems has influence on the process. The following protection signals and systems are relevant in the actual scenarios:

Case 1 and 2

pressurizer level < 0.47 m	→	scram + SI signal
scram + 10 s delay	→	turbine trip
SI signal + 16 s delay	→	HPIS start
primary pressure < 5.88 MPa	→	HA actuation
secondary pressure > 5.4 MPa	→	steam dump control valve actuation
secondary pressure > 5.75 MPa	→	SG safety valve actuation

Case 3

loss of electricity	→	scram+SI signal+MCP stop
scram + 10 s delay	→	turbine trip
SI signal + 16 s delay	→	HPIS start
primary pressure < 5.88 MPa	→	HA actuation
secondary pressure > 5.4 MPa	→	steam dump control valve actuation
secondary pressure > 5.75 MPa	→	SG safety valve actuation
SG $\Delta p > 5$ bar	→	MSIV actuation

8.5 Thermohydraulic models and codes

The analysis for the system thermohydraulic response was performed by the means of the RELAP5/mod2.5 code. The 1+2+3 loop input model was used.

The coolant temperature calculated by the RELAP code represents the mixed coolant temperature in the downcomer. For the worst case (Case 3) to consider the effect of cold water separation after stagnation (because of loss of electricity for main circulating pumps) the downcomer temperature has been corrected using the results of the REMIX calculation.

From the RELAP and REMIX calculations the following data are transferred for the analysis of fracture mechanics code ACIB-RPV:

- primary pressure
- downcomer flow
- downcomer temperature
- HA injection temperature
- cold leg entrance temperature.

Table 8.1

CHRONOLOGY OF EVENTS

Case 3

time (s)	
0.0	break on top of SG hot collector
0.0	loss of grid
0.0	MCP run out begins
0.1	reactor scram signal
0.1	SI signal, Diesel start
5.9	primary pressure < 11.8 MPa
10.1	turbine trip signal, isolation begins
10.1	Diesel ready, for LIP t=0
11.1	LPIS pump in operation
15.1	HPIS pumps start
18.0	max. break flow 358.8 kg/s
24.4	pressurizer level < 0.47 m
26.9	pressurizer level < 0.17 m, HPIS-IV open
27.0	HPIS injection begins
32.6	primary pressure < 9.3 MPa
41.1	SG1 narrow range level > 0.2 m
52.1	BRU-A-1 opens
52.6	BRU-A-2 opens
61.0	broken SG1 filled up
63.6	pressurizer level < 0.1 m
122.9	SI Tank No. 1 injection starts
123.3	SI Tank No. 2 injection starts
2725.0	primary pressure minimum (4.803 MPa)
3313.1	SG1 $\Delta p > 5$ bar signal, MSIV closes
3318.0	SG1 safety valve opens first time
3600.0	operator closes the MainGate Valves in broken loop
3870.0	minimum temperature in DC middle point (306.75 K)
3920.0	primary pressure > 12.26 MPa
4835.0	end of calculation (DC middle point t=350.2 K) (primary pressure p=12.87 MPa)

8.6 Results and conclusions of the thermohydraulic analysis

Table 8.1 provides the chronology of the events for the Case 3. The most important thermohydraulic parameters characterizing the postulated accident procedure are presented in [22], from which Figs. 8.1 - 8.6 from Case 1 and Figs. 8.7 and 8.8 from Case 3 are selected for this paper.

The thermohydraulic analysis is used only for preparing data for the PTS study. The assumptions are conservative from the point of view of the PTS event, but they are favourable from the point of view of thermohydraulic parameters. So the results of the thermohydraulic analysis proved again that the ECC system is able to prevent core damage in case of the opening of a SG collector cover.

The calculation showed that after the SITs become empty (Fig. 8.4) a moderate repressurisation of the system can be observed (Figs. 8.1, 8.7 and 8.3), but the isolation of the damaged SG results in a rapid repressurization of the system (Fig. 8.1) and a moderate heating rate of the coolant (Figs. 8.6 and 8.8).

The lowest coolant temperature in downcomer was found in case when no forced circulation was maintained (Case 3).

8.7 Calculation assumptions for PTS consequences

The fracture mechanical integrity analysis of the PTS event was performed by a deterministic analytical calculation method. This method is conservative and fully satisfies the regulatory requirements. The used data is presented in [22] and [28].

Three very conservative postulated cracks were used:

a): Axial semielliptical surface crack $a/c=2/3$, depth is $1/4T = 35$ mm. Location: the forging against the middle of the core.

b): Underclad axial crack in the ferritic welds, 4 mm deep and 50 mm long touching the interface of the clad, which is in complete contact with the vessel wall, and free of defects. Location: weld 5/6; weld 3/5.

c): Elliptical circumferential surface crack with a depth of 4 mm in the 15H2MFA weldment, and the clad is postulated broken. Location: weld 5/6; weld 3/5.

The vessel lifetime used in the calculations was 40 operational years with the same load and core configuration as realised during the first 5 years of operation. It is a conservative assumption due to the use of the low leakage core configuration in use afterwards. The screening criteria were checked according to 10 CFR 50 rules and the analysis was performed according to the ASME code Section XI.

An analytical computer program called Analytical Calculation for Integrity of Beltline (ACIB-RPV) was used for the analysis of the stability of defects in reactor vessel walls during pressurised thermal shock.

8.8 Preparing the input data

Investigating the transient in question it was considered three different cases which are in keeping with the thermohydraulic study. In all cases, after some time, the isolation of the break is assumed. The data for the $p(t)$, $T(t)$ transient are based on RELAP5 (and REMIX calculations for Case 3) before the

isolation of the break, and on model assumptions, after the isolating event (for the worst Case 3 between $t=3600$ s and $t=4400$ s).

In every case all three crack models were calculated and crack tip intensity factor (K_I) and crack tip temperature were determined for each crack model. The clad effect was taken into account too, as it has strong effects on the results in the colder temperature regions.

The core Beltline is treated as a plate during the calculation of the temperature distribution, and as a thick walled shell during the calculation of the stress and strain distribution. The modelling of the temperature distribution is made by Fourier solutions.

8.9 Results of fracture mechanics calculations

Since according to the results of the thermohydraulic calculation no significant difference was detected in the coolant temperature at the location of welds 3/5 and 5/6, the results are valid for the core zone and for weld 3/5, too.

In case of opening of SG collector cover, the lowest temperature is 23.8 °C. This is quite low compared to the RT_{NDT} of the weld which is 61.5 °C. According to the 10 CFR 50 rules the calculations are required, and the vessel failure risk associated to PTS is considered.

The less safety is in Case 3, in the case of the circumferential surface crack, because the depth of the crack is only 13 mm, and the warm prestressing of the cladding influences the stress intensity factor very strongly, and the high inner pressure has much lower importance.

According to the calculated results, the minimum value of the safety factor during the PTS is very sensitive on the transient behaviour in the colder temperature regions and the crack model used. The minimum safety factor is 1.10 and this means that no crack propagation will be initiated during the transient, and there is no need for continuation of the analysis for crack arrest calculations.

9 DETERMINISTIC ANALYSES FOR PSA

The probabilistic safety analysis has an obvious great significance since it reveals the weak points of the plant and gives a sound basis for prioritizing interventions.

In the PSA the event trees comprising the possible scenarios corresponding to the initiating events selected for the accident analysis were analysed [23]. The success criteria (i.e. if core melt is avoided) of the single event sequences belonging to an event tree can be determined by using the computer programs used in DBA analysis. In these analyses best-estimate, normal operating condition data were used.

The objective of the analysis of the LOCA scenario with a steam generator hot collector rupture is to find whether one HPIS with or without secondary side feed and bleed (FB) is enough to reach the success criterion without core damage. The detailed results can be found in [23] and [28]. The conclusions are: one HPIS is enough to get the acceptance criterion, without HPIS the success criterion is fulfilled again due to the secondary bleed.

10 CONCLUSIONS FOR SG COLLECTOR FAILURE ANALYSES

10.1 Design Basis Accident (DBA) analyses

The accident scenarios following the SG collector failure in VVER-440/V213 type reactor were analysed in the course of the AGNES project [21].

Because - due to the opening of the safety valves - the primary activity passing through the secondary circuit reaches the environment not the containment, conservatism and boundary conditions of thermohydraulic calculations had to be chosen taking into account the radiation consequences. Two cases were investigated:

- with maximum ECCS injection (3 HPIS and 4 HA's)
- assuming a single failure (2 HPIS and 3 HA's).

The results of the dose calculations have shown that the corresponding acceptance criteria are not violated.

A third case, the most unfavourable from the point of view of core cooling - with minimum ECCS injection (1 HPIS and 2 HA's) - was also investigated. The core cooling criteria are fulfilled by the emptying of the ECCS tanks. If isolation of the break does not happen in due time and the supplementary source of primary coolant is not ensured, then the process leads to core melt. A safety enhancement measure is needed for the solution of this problem.

10.2 Pressurized Thermal Shock (PTS) analyses

Pressurized thermal shock is a serious problem of the older US and Soviet RPVs as a consequence of the poor material quality. In spite of the excellent quality of the Paks NPP RPVs the extended accident analysis of the AGNES project also covers PTS analyses [6].

On the broad scale of presumable transients and accidents which may occur during the lifetime of the plant the RPV may suffer a very fast and significantly large temperature decrease while, at the same time the high system pressure may be maintained. According to the regulatory practice it has to be proven that the RPV may not be damaged due to a PTS event during its entire designed lifetime, taking into account the embrittlement due to radiation damage.

The investigated 18 cases in AGNES project well cover the full range of PTS events. The following anticipated initiating events were analysed from the point of view of primary to secondary circuit leakages [22]:

Steam generator collector cover opening:

Case 1 - the steam generator is isolated after 7200 s

Case 2 - the steam generator is isolated after 1800 s

Case 3 - the steam generator is isolated after 3600 s and electrical grid lost is assumed at 0 s.

The worst behaviour - lowest coolant temperature in downcomer - was observed in case when no forced circulation was maintained (Case 3).

Since reactor repressurization is a prohibited action as long as the temperature is below the critical temperature of the vessel, these scenarios are considered as a combination of a transient and an

operator mistake. It is important to note, however, that there are very many valves in the VVER-440 primary circuit compared to the Western PWRs and the present operating procedures give absolute priority to the isolation of breaks.

The PTS analyses pointed out in a unique and unambiguous way that the isolation of primary circuit breaks should not be given priority over the cold repressurization of the reactor vessel. The necessity to give priority to the leakage isolation in case of a steam generator collector cover opening, represent further problems to be solved.

10.3 Deterministic analyses for Probabilistic Safety Analysis (PSA)

In the AGNES project deterministic analyses in support of PSA were performed [23] by use of RELAP5 and ATHLET codes.

In accordance with the relevant PSA workplan among others the accident sequences for 3 cases of the SG hot collector rupture having an equivalent diameter of 100 mm were studied. The question was whether only one high pressure injection system is enough to reach the success criteria without and with secondary bleed and feed procedure. It was found, that the success criterion is fulfilled in all cases including the last one, when primary and secondary isolation in broken loop at 600 s after the break and bleed and feed action, but no available ECC system were assumed.

11 REFERENCES

- [1] I. Moguila: The Leak of the Primary Coolant to the Steam Generator (Rovno NPP Accident) IAEA Consultants' Meeting on Primary to Secondary Cooling Circuit Leakages for WWER-1000 and WWER-440 NPPs, Vienna, 3-7 June, 1996.
- [2] L. Perneczky, I. Tóth, G. Ézsöl: Accident Analyses for a Reference Plant with VVER-440 Reactor. Steam Generator Collector Rupture. IAEA Workshop on Calculation Results for Reference Plant, Warsaw, 20-24 June, 1988.
- [3] L. Perneczky: Analysis of the Steam Generator Collector Rupture for the Paks NPP. IAEA Workshop on VVER Design Basis Accident Analysis, Piestany, 5-9 December, 1988.
- [4] L. Perneczky, G. Ézsöl, L. Szabados: Analysis of the accident scenarios following the Steam Generator Collector Rupture. Computer Analysis with RELAP4/mod6 for the VVER-440 Units of Paks NPP. Central Research Institute for Physics, July 1988, (in Hungarian and Russian).
- [5] AGNES Project: Safety Reassessment of the Paks Nuclear Power Plant. Final Report. Budapest, June 1994.
- [6] AGNES Project: Safety Reassessment of the Paks Nuclear Power Plant. Executive Summary. Budapest, October 1994.

- [7] J. Gadó, L. Maróti, L.Szabados: Reassessment of Safety of VVER-440/213-Type NPPs: Application of RELAP5/mod2 for DBA Analyses. RELAP5 International Users' Seminar, Boston, USA, July 6-9, 1993.
- [8] J. Gadó et al.: Safety Reassessment of the Hungarian NPP.(The AGNES Project). INC'93, Toronto, Canada, October, 1993.
- [9] J. Gadó: AGNES - Safety Reassessment of the Paks Nuclear Power Plant. ENS TOPSAFE '95. Budapest, September 1995. Proc. Vol. I. pp. 106-113.
- [10] I. Tóth: RELAP-Based Safety Analysis of the Paks NPP in the AGNES Project. 5th CAMP Meeting, Idaho Falls, USA, October 19-21, 1994.
- [11] L. Perneczky, L. Szabados: Handbook for RELAP5/mod2 Input Model 6-Loop Representation. Rev. 1. AGNES Project Report, Budapest, December 1994.
- [12] F.Bastenaire et al.: TROPIC User's Manual. Version 4.0 TRACTEBEL, Brussels, May 1992.
- [13] A. Guba, L. Perneczky, I. Tóth: Assessment of RELAP5/mod2.5 and mod3 with a Scram Transient in the Paks NPP. 4th CAMP Meeting, Ljubljana, Slovenia, May 16-19, 1994.
- [14] A. Guba, L. Perneczky, I.Tóth: Validation of Six-Loop RELAP5 Model of VVER-440/213 Unit With Transients Measured in the Paks Nuclear Power Plant. 2nd Regional Meeting on Nuclear Energy in Central Europe, Portoro_, Slovenia, September 11-14, 1995. Proc. pp. 474-481.
- [15] L. Perneczky, I. Tóth, A. Guba: Six-Loop RELAP5 Model of the Paks VVER-440/V213 Unit. In-ternational Topical Meeting on VVER Safety, Prague, September 21-23, 1995. Proc. pp. 100-112.
- [16] L. Maróti, L. Perneczky, I. Tóth: Analysis of Scenarios with Decrease of Secondary Side Heat Removal within the AGNES Project. International Topical Meeting on VVER Safety, Prague, September 21-23, 1995. Proc. pp. 50-53.
- [17] T. Fekete, F. Gillemot: Pressurized Thermal Shock Analyses in the Framework of the AGNES Project. International Topical Meeting on VVER Safety, Prague, September 21-23, 1995. Proc. pp. 254-258.
- [18] L. Perneczky, I. Tóth, A. Guba: Experiences Gained in Use of RELAP5 Input Models of VVER-440/V213 Reactor, 1996 RELAP5 Users Seminar, Dallas, Texas, March 17-21, 1996.
- [19] US Nuclear Regulatory Commission: Regulatory Guide 1.70, Standard Format and Content of Safety Analysis Reports for Nuclear Power Plants. Revision 3, November 1978.
- [20] P. Marks, L. Sági, P.Vértes: Analysis of the LOCA scenario with the steam generator tube rupture. TRASS No. 17, AGNES Project Report, 1994.
- [21] L. Perneczky, L. Sági, P.Vértes: Opening of a steam generator collector cover. TRASS No. 18, AGNES Project Report, 1993.
L. Perneczky: Opening of a steam generator collector cover. Attachment. TRASS No. 18, AGNES Project Report, 1994.

- [22] J. Elter, T. Fekete, F. Gillemot, L. Maróti, L. Perneczky, G. Szabolcs: Analysis of the Pressurized Thermal Shock in the course of the SBLOCA scenario caused by the opening of the steam generator collector cover. TRASS No. 51, AGNES Project Report, 1993.
- [23] P. Marks, L. Perneczky, L. Szabados: Report on deterministic studies in support of Level-1 PSA. RELAP5 calculations. AGNES Project Report, 1993.
- [24] L. Maróti, S. Mikó: Acceptance Criteria for Thermohydraulic Transient Analyses. AGNES Project Report, 1992.
- [25] Guidelines for Accident Analysis of WWER Nuclear Power Plants. IAEA-EBP-WWER-01, Vienna, 1995.
- [26] L. Perneczky: Primary to Secondary Leakages: Steam Generator Collector Rupture Experiments on the Hungarian PMK Test Facility and the IAEA-SPE-3. IAEA Consultants' Meeting on Primary to Secondary Cooling Circuit Leakages for WWER-1000 and WWER-440 NPPs, Vienna, 3-7 June, 1996.
- [27] L. Perneczky: Primary to Secondary Leakages in AGNES project, Part I: The Hungarian AGNES project and Accident Scenarios Following the SG Heat Transfer Tube Rupture. IAEA Consultants' Meeting on Primary to Secondary Cooling Circuit Leakages for WWER-1000 and WWER-440 NPPs, Vienna, 3-7 June, 1996.
- [28] L. Perneczky: Primary to Secondary Leakages in AGNES project, Part II: The Accident Scenarios Following the SG Collector Rupture in VVER-440/V213 Type Reactor. IAEA Consultants' Meeting on Primary to Secondary Cooling Circuit Leakages for WWER-1000 and WWER-440 NPPs, Vienna, 3-7 June, 1996.
- [29] Csilla Tóth: Primary to Secondary Leakages Management. Prevention and Mitigation Measures at the Paks NPP. IAEA Consultants' Meeting on Primary to Secondary Cooling Circuit Leakages for WWER-1000 and WWER-440 NPPs, Vienna, 3-7 June, 1996.
- [30] P. Vértes, L. Sági, L. Koblinger: System of Programs for Analysis of Radionuclide Release at DNB of Nuclear Power Plants. AGNES Project Report, 1992.
- [31] J. Elter, F. Gillemot, L. Maróti, PTS Integrity Assessment of Paks Unit 3, AGNES Project Report, 1992.
- [32] Safety Issues and their Ranking for WWER-440 Model 213 Nuclear Power Plants. IAEA-EBP-WWER-03, Vienna, 1996.

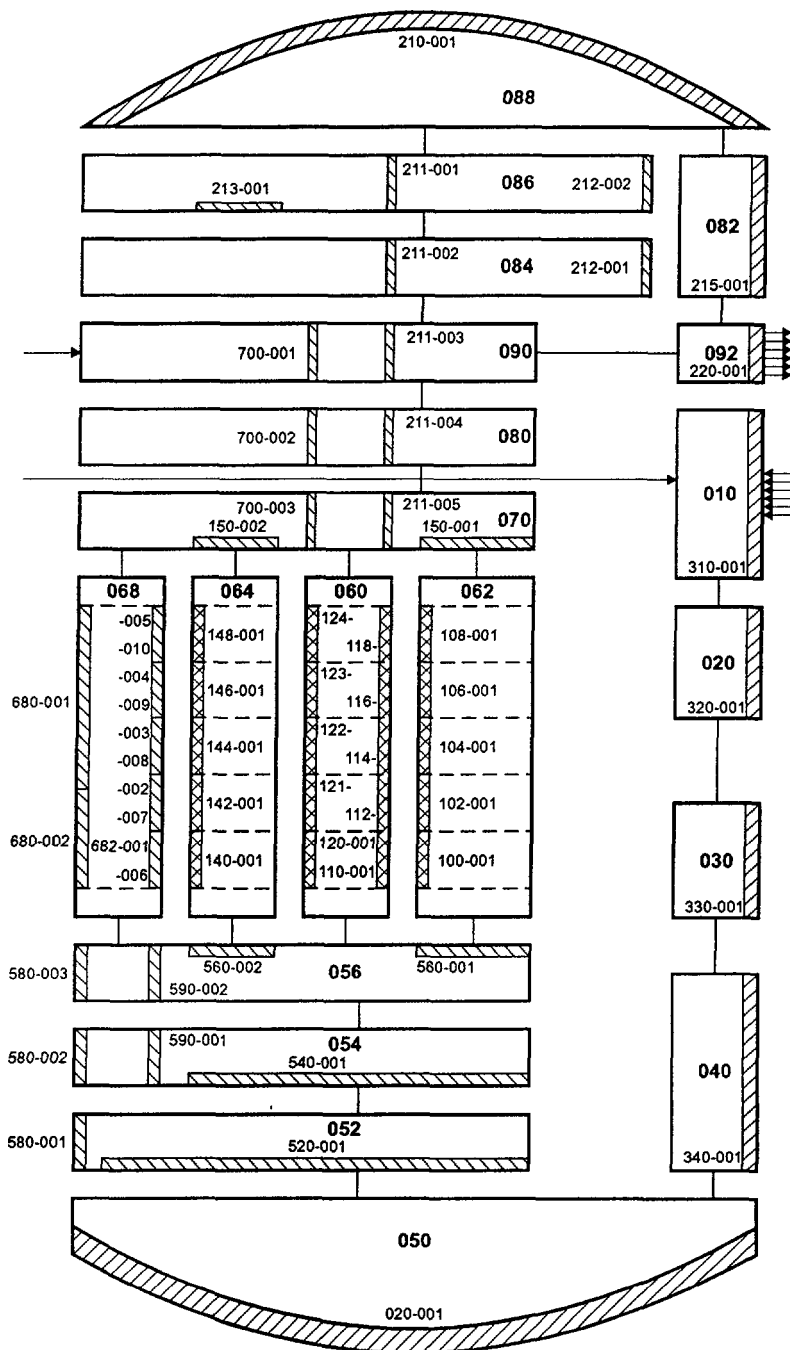


Fig. 4.1 Nodalization of reactor vessel

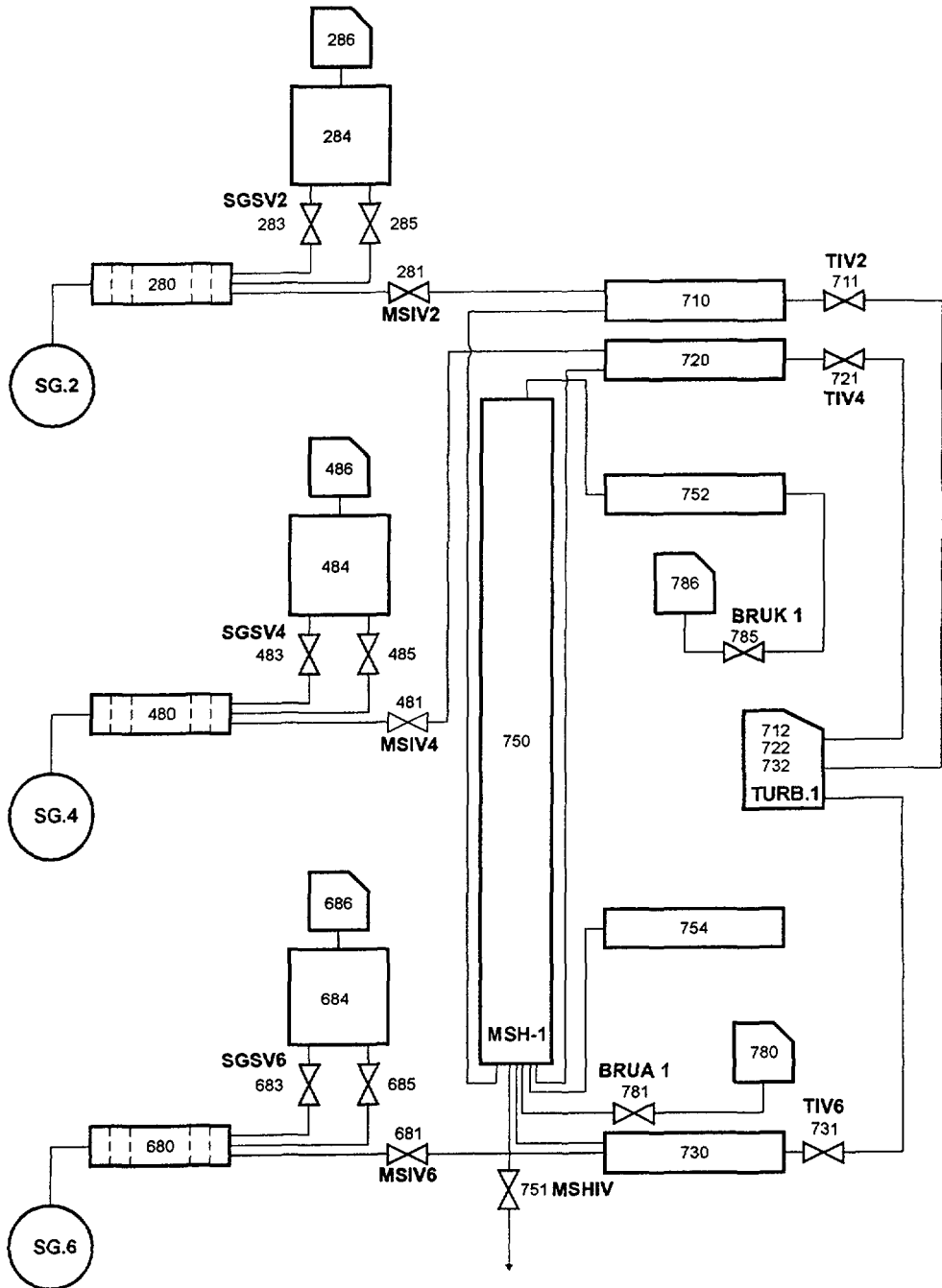


Fig. 4.3 Nodalization in steam line system 1

AGNES/DBA PAKS UNIT 3

TRASS No: 18
AEKI/01

PLOT No: 1.1.
10. 12. 1993

Opening of SG collector cover (Case 1)

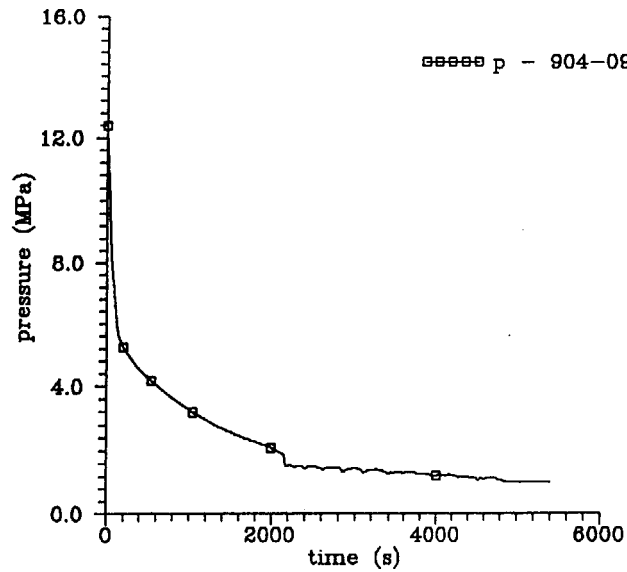


Fig. 7.1 Pressurizer pressure

AGNES/DBA PAKS UNIT 3

TRASS No: 18
AEKI/01

PLOT No: 9.1
10. 12. 1993

Opening of SG collector cover (Case 1)

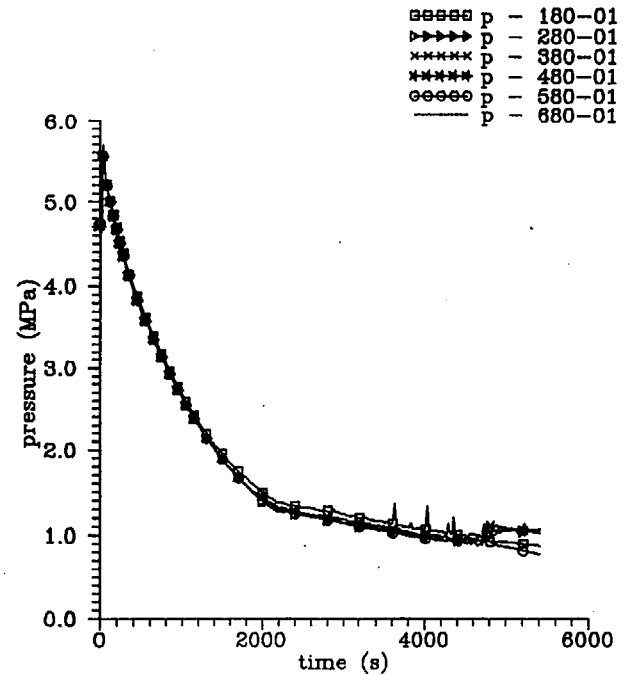


Fig. 7.2 SG pressures

AGNES/DBA PAKS UNIT 3

TRASS No: 18
AEKI/01

PLOT No: 5.7.
10. 12. 1993

Opening of SG collector cover (Case 1)

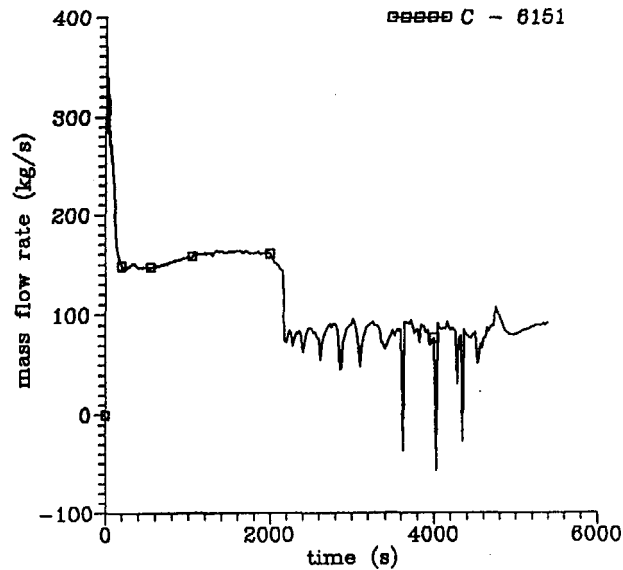


Fig. 7.3 Break mass flow

AGNES/DBA PAKS UNIT 3

TRASS No: 18
AEKI/01

PLOT No: 5.4.
10. 12. 1993

Opening of SG collector cover (Case 1)

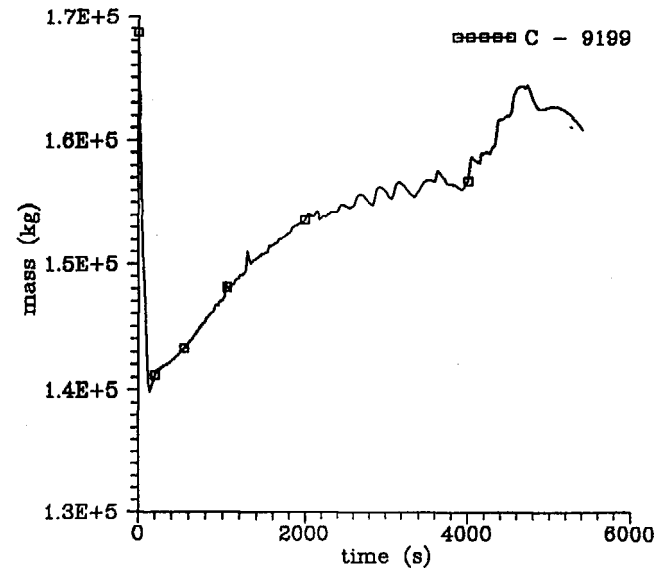


Fig. 7.4 Primary mass balance

AGNES/DBA PAKS UNIT 3

TRASS No: 18
AEKI/01

PLOT No: 8.1.
10. 12. 1993

Opening of SG collector cover (Case 1)

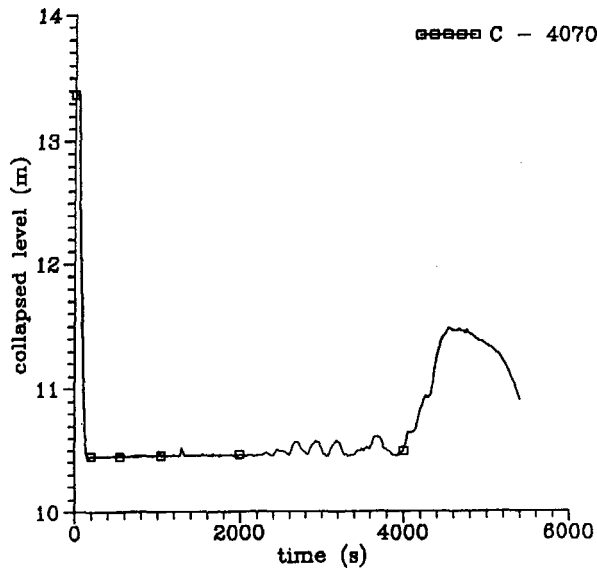


Fig. 7.5 Reactor water level

AGNES/DBA PAKS UNIT 3

TRASS No: 18
AEKI/01

PLOT No: 4.12.
10. 12. 1993

Opening of SG collector cover (Case 1)

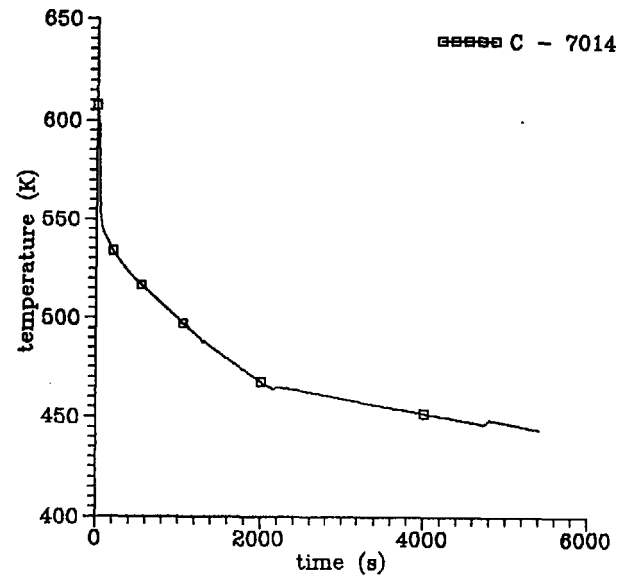


Fig. 7.6 Hot channel cladding temperature

AGNES/DBA PAKS UNIT 3

TRASS No: 18
AEKI/01

PLOT No: 5.10.
10. 12. 1993

Opening of SG collector cover (Case 1)

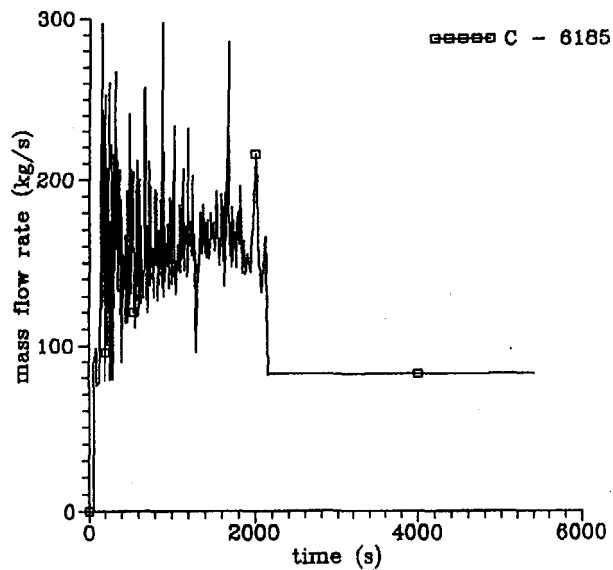


Fig. 7.7 ECC injection rate

AGNES/DBA PAKS UNIT 3

TRASS No: 18
AEKI/01

PLOT No: 12.4.
10. 12. 1993

Opening of SG collector cover (Case 1)

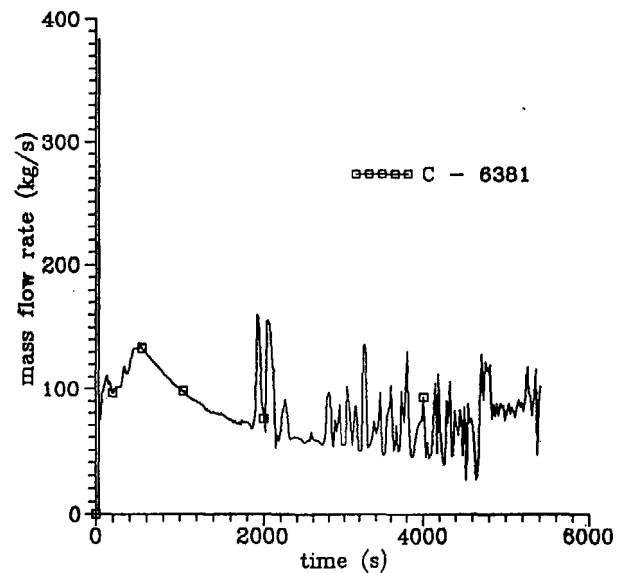


Fig. 7.8 Safety valves 1 flow from SGs

AGNES/DBA PAKS UNIT 3

TRASS No: 18 PLOT No: 5.10.
AEKI/01 09. 12. 1993

Opening of SG collector cover (Case 2)

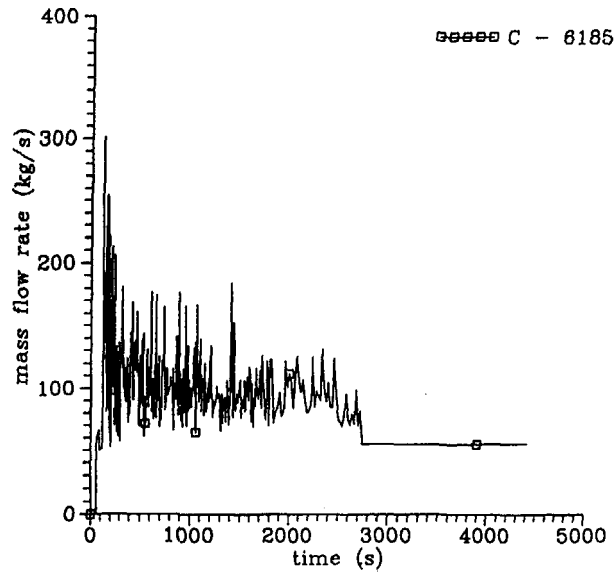


Fig. 7.9 ECC injection rate

AGNES/DBA PAKS UNIT 3

TRASS No: 18 PLOT No: 5.7.
AEKI/01 09. 12. 1993

Opening of SG collector cover (Case 2)

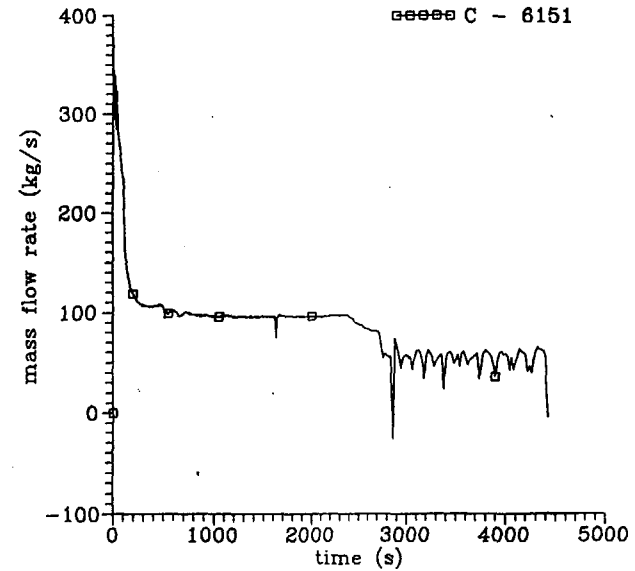


Fig. 7.10 Break mass flow

AGNES/DBA PAKS UNIT 3

TRASS No: 18 PLOT No: 5.10.
AEKI/01 21. 06. 1994

Opening of SG collector cover (Case 3)

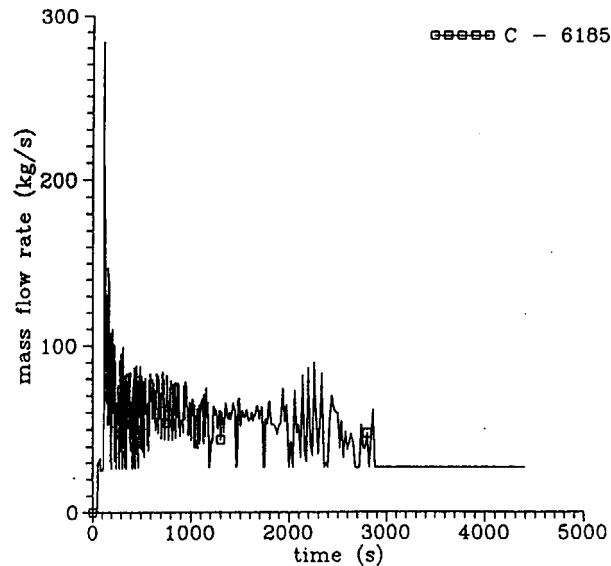


Fig. 7.11 ECC injection rate

AGNES/DBA PAKS UNIT 3

TRASS No: 18 PLOT No: 5.7.
AEKI/01 21. 06. 1994

Opening of SG collector cover (Case 3)

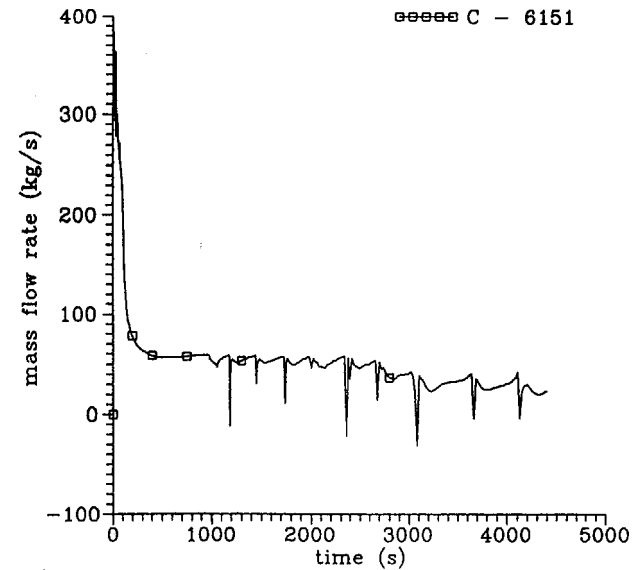


Fig. 7.12 Break mass flow

AGNES/DBA PAKS UNIT 3

TRASS No: 18
AEKI/01

PLOT No: 5.4.
21. 06. 1994

Opening of SG collector cover (Case 3)

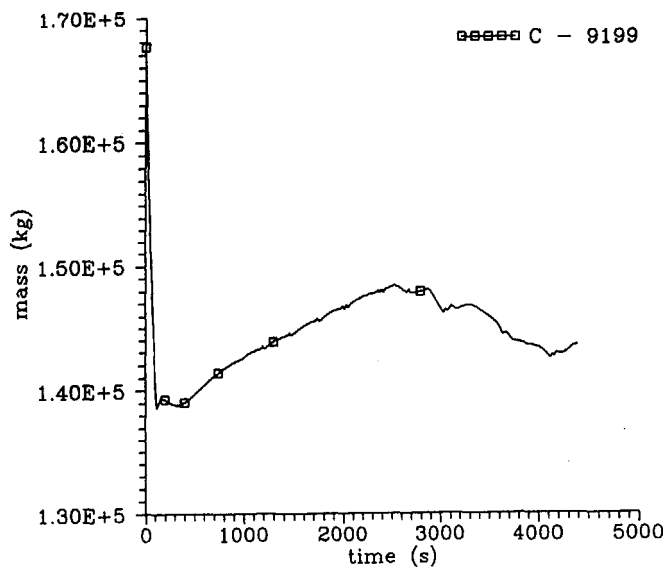


Fig. 7.13 Primary mass inventory

AGNES/DBA PAKS UNIT 3

TRASS No: 18
AEKI/01

PLOT No: 4.12.
21. 06. 1994

Opening of SG collector cover (Case 3)

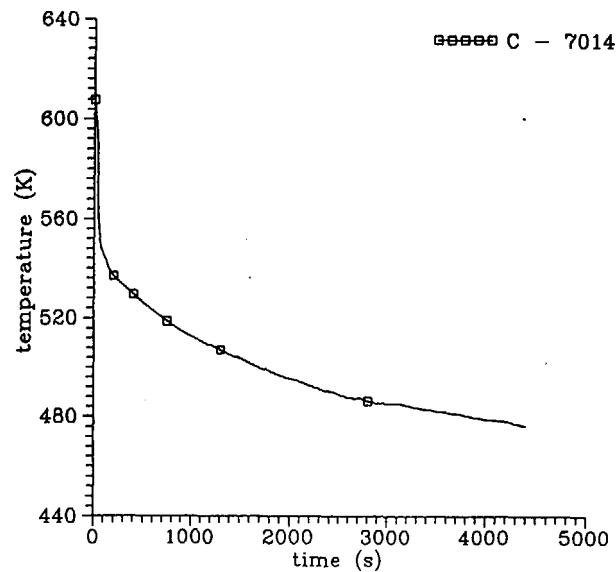


Fig. 7.14 Hot channel cladding temperature

AGNES/DBA PAKS UNIT 3

TRASS No: 51 PLOT No: 1.1.
AEKI/01 16. 11. 1993

Opening of SG collector cover (PTS)
Case 1

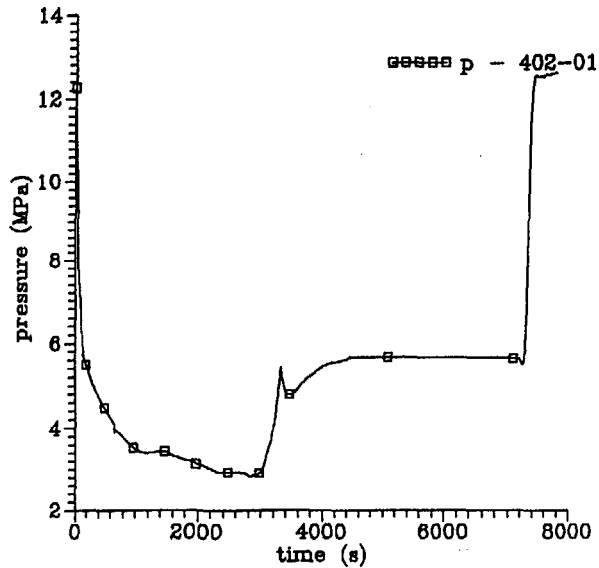


Fig. 8.1 Pressurizer pressure

AGNES/DBA PAKS UNIT 3

TRASS No: 51 PLOT No: 2.1.
AEKI/01 16. 11. 1993

Opening of SG collector cover (PTS)
Case 1

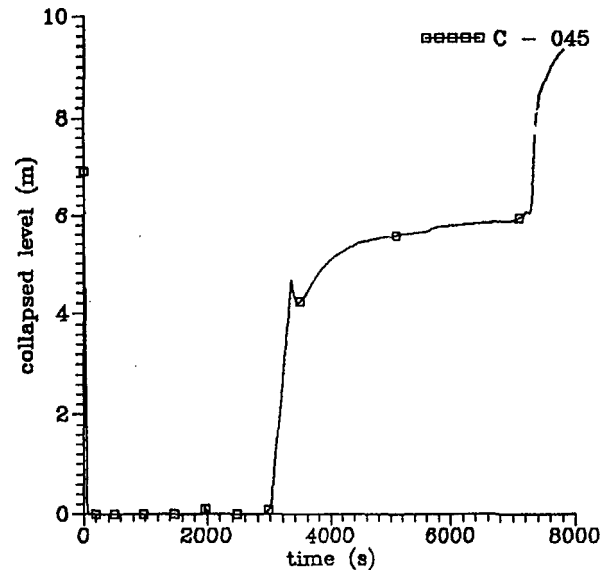


Fig. 8.2 Pressurizer water level

AGNES/DBA PAKS UNIT 3

TRASS No: 51
AEKI/01

PLOT No: 9.1.
16. 11. 1993

Opening of SG collector cover (PTS)
Case 1

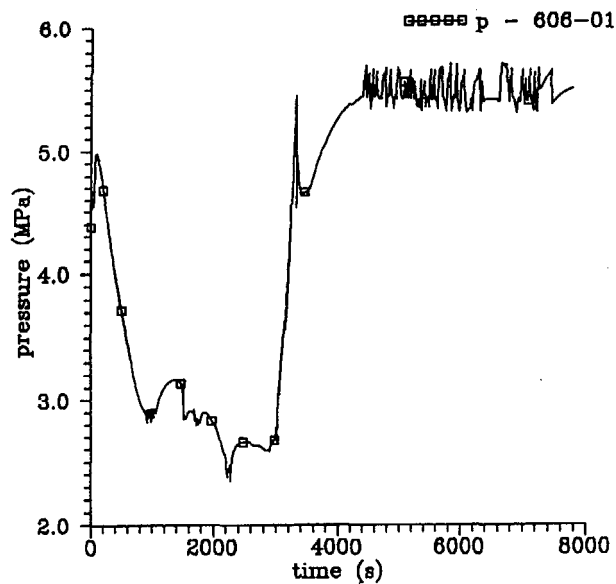


Fig. 8.3 SG pressure in single loop

AGNES/DBA PAKS UNIT 3

TRASS No: 51
AEKI/01

PLOT No: 5.10.
16. 11. 1993

Opening of SG collector cover (PTS)
Case 1

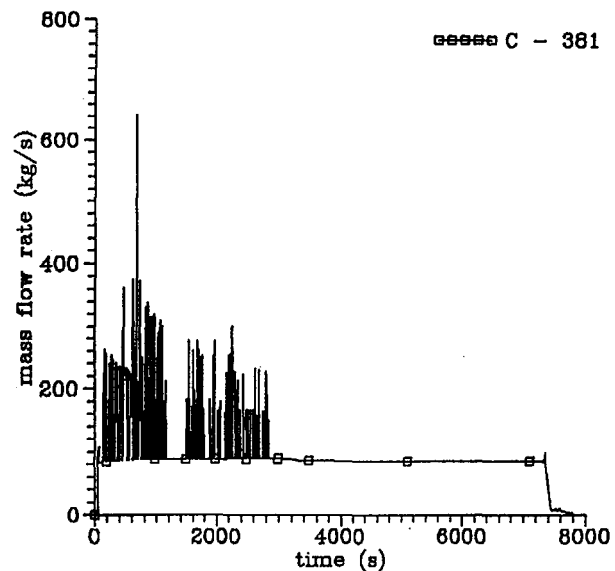


Fig. 8.4 ECC injection rate

AGNES/DBA PAKS UNIT 3

TRASS No: 51
AEKI/01

PLOT No: 5.7.
16. 11. 1993

Opening of SG collector cover (PTS)
Case 1

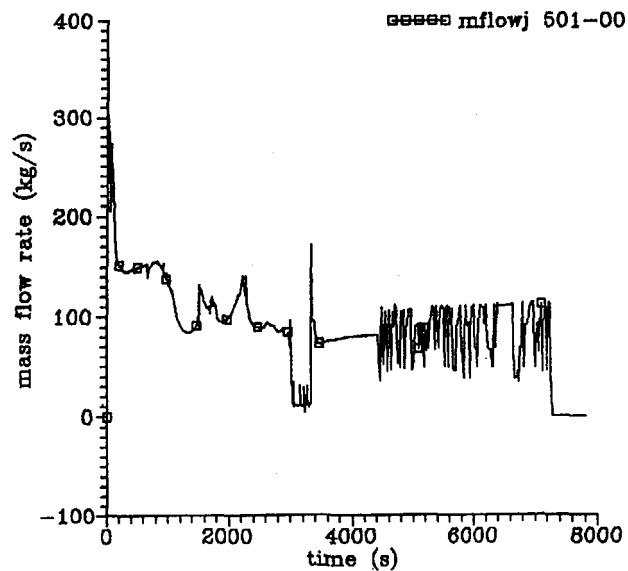


Fig. 8.5 Break mass flow

AGNES/DBA PAKS UNIT 3

TRASS No: 51
AEKI/01

PLOT No: 4.8/b
16. 11. 1993

Opening of SG collector cover (PTS)
Case 1

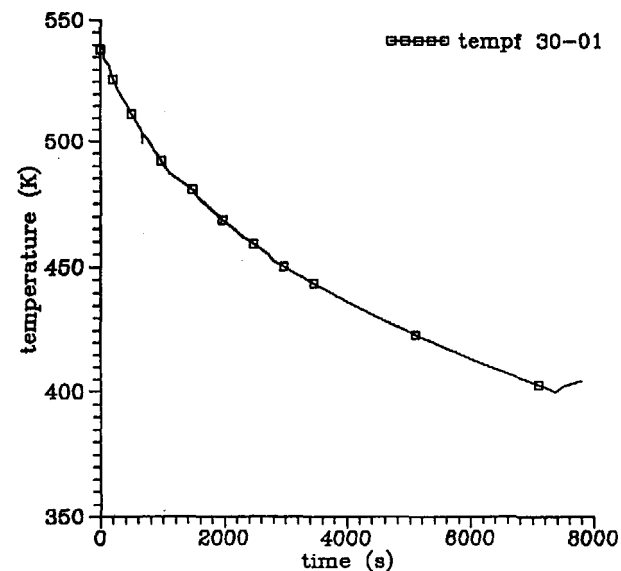


Fig. 8.6 DC middle point temperature

AGNES/DBA PAKS UNIT 3

TRASS No: 51
AEKI/01

PLOT No: 1.1.
07. 12. 1993

Opening of SG collector cover (PTS)

Case 3

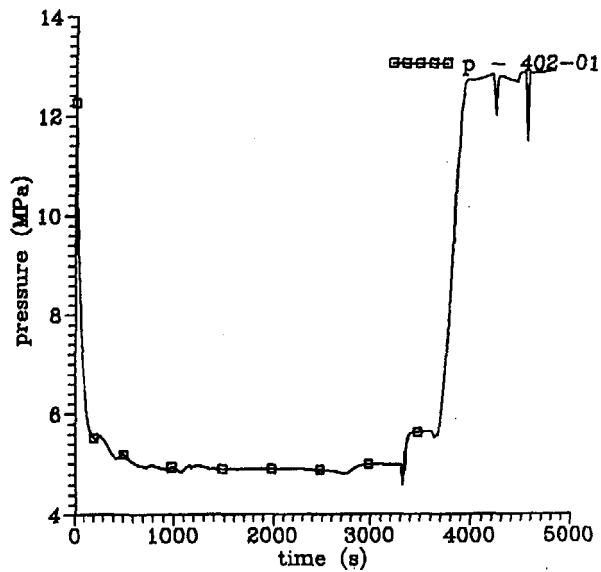


Fig. 8.7 Pressurizer pressure

AGNES/DBA PAKS UNIT 3

TRASS No: 51
AEKI/01

PLOT No: 4.8/b
07. 12. 1993

Opening of SG collector cover (PTS)

Case 3

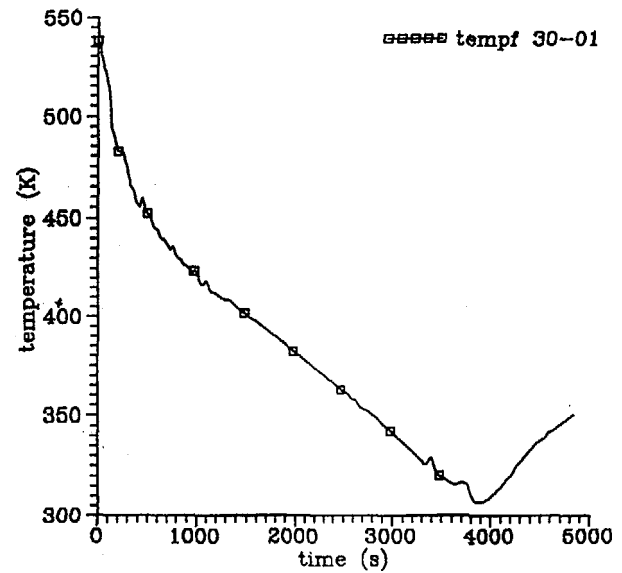


Fig. 8.8 DC middle point temperature



THE EVALUATION OF VALIDITY OF THE RELAP5/MOD3 FLOW REGIME MAP FOR HORIZONTAL SMALL DIAMETER TUBES AT LOW PRESSURE

Agafonova Natalia, St.Petersburg State Technical University,
Banati Jozsef, Lappeenranta University of Technology

RELAP5/MOD3 code was developed for Western type power water reactors with vertical steam generators. Thus, this code should be validated also for VVER design with horizontal steam generators. In application for horizontal steam generators the situation with two-phase flow inside small diameter tubes is possible when the first circuit pressure drops in accident below the pressure level in the boiling water. It is known that computer codes not always modelled correctly the two-phase flow inside horizontal tubes at low pressures (less than 4-6 MPa). It may be the result of erroneous prediction of the flow regime. Correct prediction of the flow regime is especially important for the fully or partly stratified flow in horizontal tubes.

The aim of this study is the attempt of verification of the flow regime map, which is used in the RELAP5/MOD3 computer code for two-phase flow in horizontal small diameter tubes. "Small diameter tube" means according RELAP5/MOD3 that the inner diameter of the tube is less (or equal) than 0.018 m. The inner tube diameter in horizontal steam generators is equal 0.013 m.

RELAP5/MOD3 FLOW REGIME MAP FOR HORIZONTAL TUBES

The flow regime map used in RELAP5/MOD3 for horizontal tubes is following. It consists of horizontally stratified, bubbly, slug, annular-mist and mist-pre-CHF regimes [1]. All these structures are shown in fig.1 except mist-pre-CHF regime. The latest takes place at very high values of void fraction ($\alpha_G > 0.9999$). The value of the void fraction is chosen as the criterion of different regimes: bubbly, slug, annular-mist and mist, and the criterion suggested by Taitel and Dukler [2] is used to define whether the flow is horizontally stratified.

The condition of stratification by Taitel and Dukler [2] is:

$$V_G < V_{crit} = \frac{1}{2} \sqrt{\frac{\rho_L - \rho_G}{\rho_G} \cdot \frac{g \cdot \alpha_G \cdot A}{d \cdot \sin \theta}} \times (1 - \cos \theta), \quad (1)$$

where ρ_L and ρ_G are the densities of liquid and gas respectively, g - the acceleration of the gravity, α_G - the void fraction, A - the total cross section area, d - the diameter of the tube and θ - the angle which defines the liquid level in the tube.

Condition (1) was modified in the RELAP5/MOD3 code to handle situations where the flow is stratified but the liquid is not stagnant as was assumed by Taitel and Dukler [2]:

$$|V_G - V_L| < V_{crit}. \quad (2)$$

Notice that in formulas (1) and (2) V_G is the actual velocity of the gas phase, V_L is the actual velocity of the liquid and V_{crit} is the velocity of the gas phase at which the large waves begin to growth on the surface of the liquid.

The transition region between stratified and slug flow was also postulated: it lies between $0.5 \cdot V_{crit}$ and V_{crit} .

All mentioned flow regimes take place if the total mass flux is less than $3000 \text{ kg}/(\text{m}^2 \cdot \text{s})$. If it is more than $3000 \text{ kg}/(\text{m}^2 \cdot \text{s})$, then the flow undergoes a transition to corresponding flow regime defined with flow regime map for vertical tubes used in a computer code.

PROBLEMS OF RELAP5/MOD3 FLOW REGIME MAP VERIFICATION

To verify the flow regime map is to compare it with reliable experimental data. There are several difficulties while doing this job.

- Traditionally experimental flow regime maps have been constructed using superficial velocities or some other such parameters of two-phase flow. There is an opinion among the scientists working on this subject that superficial velocities are suitable for flow regime mapping for only steady, developed flow. The same is not true for transient or developing conditions that arise frequently for nuclear reactor thermal-hydraulics. So the scientists recommend to use the void fraction as a criterion of different flow regimes in the computer codes. Moreover the void fraction is not so sensitive as superficial velocities to the varying of the pressure in the flow. Void fraction is taken into account in the RELAP5 code. Therefore while comparing flow maps constructed with using of different parameters it is necessary to have a reliable correlation between void fraction and quality. It is a complicated problem to select this reliable correlation especially for small values of void fraction and low pressures. As may be seen from fig.2, different correlations give different values of the void fraction for the same value of quality. This problem was mentioned also by Weisman et al. [3]. In fig.2 several relationships are used for calculation of the void fraction. These relationships are:
 - the correlation of Lockhart and Martinelli [4],
 - the correlation of Martinelli and Nelson [5],
 - the correlation of Smith [6],
 - the correlation of Budrik et al. [7].

All these correlations were derived for adiabatic flows.

- To verify the flow regime map of RELAP5 we need the reliable experimental data on this subject for steam-water flows in a small diameter tube. The majority of known flow regime maps was obtained for gas-liquid flows at low pressures. Unfortunately, there is no systematic investigation of flow regime maps in steam-water adiabatic and diabatic flows at different pressures for horizontal tubes. But there are some interesting results devoted to the definition of boundaries between isothermal and anisothermal zones in circumferential temperatures of heated pipes. These results may be used for verification of boundaries between stratified and nonstratified flow in tubes. Also there are some flow regime maps using the data for cryogenic flows. In the case of heated flow it is necessary to have a corresponding correlation between void fraction and quality.

COMPARISON WITH AVAILABLE DATA

The first stage of this verification is the comparison of RELAP5 flow regime map with existing data for air-water flows and other available data for adiabatic flows. There are two reliable experimental flow regime maps of Mandhane et al. [8] and Weisman et al. [3] which are usually referred to in literature. The map of Mandhane [8] was very carefully constructed with using almost 6000 (namely 5935 and among them 1178 points for air-water flows) experimental data on flow patterns. But the authors did not give any correlations for the boundaries. Such correlations were obtained in the work of Weisman [3]. Those correlations included the effect of fluid properties (consequently pressure) and tube diameter on the boundaries. The flow regime map proposed by Budrik et al. [7] may be used according the authors recommendations for different adiabatic two-phase one-component systems in the wide range of pressures up to critical value.

In this study the calculations of boundaries between different flow regimes were done with using the mentioned maps for pressures 0.1, 2.0 and 4.0 MPa. The results of calculations are shown in fig. 3 .

The most widely accepted theoretical (or semi-theoretical) model for definition of the boundaries between the various flow regimes in horizontal tubes was proposed by Taitel and Dukler [2]. This map and the RELAP5/MOD3 map are also shown in fig.3.

All boundaries were calculated in the given work for the inner tube diameter 0.013 m. The correlation between the void fraction and quality by Lockhart and Martinelli [4] was used here to represent all maps in coordinates of superficial velocities. Fig.3 shows, that all boundaries agree quite well except the boundary separating the intermittent and dispersed bubble regimes from annular regime. The locus of this boundary in superficial velocity coordinates has been found to have a different slope: positive (Taitel and Dukler [3]), positive with more large angle (Mandhane [8] and Budrik [7]) and negative (Weisman [3]). Later investigations of Bar-Cohen et al. [9, 10] showed however that the Weisman's relation for this boundary matches more nearly the locus of the minimum circumferential wall temperature zone than Taitel and Dukler's expression. In their work Bar-Cohen et al. have done sufficiently successful attempt to correlate thermal and hydrodynamic phenomena in a horizontal, uniformly heated steam-generating pipes. In the other side the corresponding boundary given by [7] agrees well with those of Taitel and Dukler.

Besides this according the RELAP5/MOD3 flow regime map bubbly flow is situated in the region of intermittent flow according the other maps.

It is necessary to notice that the flow regime map used in RELAP5/MOD3 is based upon the model of Taitel and Dukler in definition of stratified flow. It may be explained so that this model deals with the description of some physical phenomena and the relations of Weisman are simply a successful treatment of the experimental data. Taitel and Dukler [2] solved too simplified problem for the boundary between stratified and non stratified flow. There are some late works where this problem is being solved in the more realistic conditions, for example the works of Lin and Hanratty [11], Brauner and Maron [12]. Moreover, it is shown by Barnea [13] that even small pipe inclinations ($+1^\circ$ or -1°) influence very strongly on the flow regime map.

It may be seen from fig.3 that the discrepancy in the flow regime boundaries calculated with different maps is decreasing while pressure is increasing.

The validity of the flow regime maps of Mandhane [7], Taitel and Dukler [2] and Weisman et al. [3] is discussed in details by Rouhani and Sohal [14] in their review. It is mentioned there that since all these maps were received for steady state adiabatic flows they fail to describe the transitional data. There is also mentioned that the existing flow regime maps and theoretical criteria are found somewhat inadequate for flow regime prediction in boiling channels.

As was said above, there is no systematic investigation of steam-water mixture flow regimes in horizontal heated tubes at different pressures. But such investigation was done for steam-water flow in vertical tubes by Levitan and Borevski [15]. Some general conclusions were done in this work:

- the results of investigations of air-water flows can not be used directly for steam-water flows;
- the bubbly flow begins in subheated water in the heated tubes and the transition to slug flow may exist at very small or even negative qualities, so the using of logarithmic scale for the flow regime maps is not valid;
- the main parameters which define the flow regime (or the structure of the interfacial surface) of steam-water flow are the quality, the pressure and the total mass flux, so flow regime maps may be constructed with using these values or their combinations as coordinates.

To compare the RELAP5/MOD3 flow regime map with experimental data for heated tubes we examine some undirect data on the beginning of stratification [9, 10, 16, 17, 18]. Unfortunately, the majority of data applies to intermediate diameter tubes (more than 0.018 m but less than 0.08 m). This comparison was carried out in two ways. The first way was the using of correlations from the leading technical material for thermohydraulic calculations of atomic equipment [19]. The second way was the numerical experiment with using of RELAP5/MOD3 code. It is necessary to mention that modeling with RELAP5/MOD3 code is possible only if we have the detail description of the physical experiment.

Ding, Kakac and Chen [17] established the correlation between the existing flow regime in horizontal tube and the temperature difference between the top and the bottom walls. Six different flow patterns were identified, which gave rise to six distinct wall temperature profiles along the tube. The experiment was carried out in a stainless steel tube with inside diameter 10.9 mm and length 1060 mm. Refrigerant-11 was used as the working liquid. It was found in this work that a dimensionless number K represents a particular flow pattern inside the tube:

$$K = \frac{q}{G \cdot h_{fg}}, \quad (3)$$

where q is the applied heat flux, G is the total mass flux and h_{fg} is the fluid latent heat at inlet conditions. So this number may be corresponded to the dimensionless enthalpy or quality used by many researchers and the boundaries between different flow patterns correspond to the

constant values of K . (Notice that such approach is the same of Levitan and Borevski [15]). Flow regime map was received when the numerator and denominator of K were used as coordinates. This map is not a general order map because of using freon-11 as a liquid and absence of data about varying the pressure in the tube.

Styrikovitch and Miropolski [16] investigated circumferential wall temperature variations and becoming stratification in a heated horizontal boiler tubes at different pressures. The result of comparison the data of [16] with RELAP5/MOD3 flow regime map is represented in fig.4. RELAP5/MOD3 flow regime map was calculated with using correlations [19]. It is seen from fig.4 that the stratification boundary given by the RELAP5/MOD3 flow regime map lies more lower than experimental boundary.

In fig.5 the comparison of data from the work of Flores et al. [18] and the flow regime map of RELAP5/MOD3 is represented. The boundary between dry and wet walls in horizontal tube is investigated in [18]. The experimental boundary points of Crowe from [18] were compared with points calculated with RELAP5/MOD3. The numerical experiment was carried out for the same conditions that were used in physical experiments. The values of void fraction obtained with the RELAP5/MOD3 code lie more higher than calculated with formulas of [19] and Lockhart and Martinelli. Moreover these calculations showed that it is necessary to check the influence of heat flux on void fraction. It is seen from fig.5 that the RELAP5/MOD3 flow regime map may be wrong in prediction of annular flow.

CONCLUSION

1. The review of published material on flow regime maps in horizontal tubes has shown that there is a few experimental data on flow regimes in horizontal steam-water flows at nonatmospheric pressures.
2. The comparison of RELAP5/MOD3 flow regime map with existing experimental data at low pressures (less than 0.4-0.5 MPa) is not quite reliable because recommended correlations are usually unreliable at pointed out pressures.
3. It would be desirable to carry out a special experiment on this problem.

REFERENCES

1. RELAP5/MOD3 Code Manual, NUREG/CR-5535 INEL-95/0174 (Formerly EGG-2596), 1995, in four volumes
2. Taitel Y., Dukler A.E. A model for predicting flow regime transitions in horizontal and near horizontal gas-liquid flow. AIChE Journal, 1976, v.22, No 1, pp.47-552.
3. Weisman J., Duncan D., Gibson J., Crawford T. Effects of liquid properties and pipe diameter on two-phase flow patterns in horizontal lines. Int. J. Multiphase Flow, 1979, v.5, No 6, pp.437-462
4. Lockhart R.W., Martinelli R.C. Proposed correlation for isothermal two-phase, two-component flow in pipes. Chem. Engng. Prog., 1949, v.45, No 1, pp.39-48
5. Martinelli R.C., Nelson D.B. Prediction of pressure drop during forced circulation boiling of water. Trans. of ASME (C), 1948, v.70, No 6, pp.695-702

6. Tandon T.N., Varma H.K., Gupta C.P. (1982) A new flow regime map for condensation inside horizontal tubes. *Journal of Heat Transfer*, v.104, No 4, pp.763-768
7. Budrik V.V., Yeliseev A.B., Tonchak N.H. A method of void fraction calculation for vapor or gas- liquid flow conditions. *Fizika nizkikh temperatur*, 1990, v.16, No 4, pp.428-433
8. Mandhane J.M., Gregory G.A., Aziz K. A flow pattern map for gas-liquid flow in horizontal pipes. *Int. J. Multiphase Flow*, 1974, v.1, pp.537-553
9. Bar-Cohen A. Ruder Z., Griffith P. (1986) Development and validation of boundaries for circumferential isothermality in horizontal boiler tubes. *Int. J. Multiphase Flow*, 1986, v.12, No 1, pp.63-77
10. Bar-Cohen A., Ruder Z., Griffith P. Thermal and hydrodynamic phenomena in a horizontal, uniformly heated steam-generating pipe. *Journal of Heat Transfer*, 1987, v.109, No 3, pp.739-745
11. Lin P.Y., Hanratty T.J. Prediction of the initiation of slugs with linear stability theory. *Int. J. Multiphase Flow*, 1986, v.12, No 1, pp.79-98
12. Brauner N., Maron D.M. Analysis of stratified/nonstratified transitional boundaries in horizontal gas-liquid flows. *Chem. Engng. Sci.*, 1991, v.46, No 7, pp.1849-1859
13. Barnea D. A unified model for predicting flow-pattern transitions for the whole range of pipe inclinations. *Int. J. Multiphase Flow*, 1987, v.13, No 1, pp.1-12
14. Rouhani S.Z., Sohal M.S. Two-phase flow patterns: a review of research results. *Progress in Nuclear Energy*, 1983, v.11, No 3, pp.219-259
15. Levitan L.L., Borevski L.Ja. Holography of steam-water flows. 1989, Moscow: Energoatomizdat (in Russian)
16. Styrikovich M.A., Miropolski Z.L. O temperaturnom regime raboti gorizontalnyh i naklonnyh parogeneriruyustchyh trub pri vysokih davleniyah. // V sb. *Gidrodinamika i teploobmen pri kipenii v kotlah vysokogo davleniya*. M., 1955, pp.229-254 (in Russian)
17. Ding Y., Kakac S., Chen X.J. Stratification of boiling two-phase flow in a single horizontal channel. *Heat and Mass Transfer*, 1995, v.30, No 3, pp.187-195
18. Flores A.G., Crowe K.E., Griffith P. Gas phase secondary flow in horizontal stratified and annular-mist two-phase flow. *Int. J. Multiphase Flow*, 1995, v.21, No 2, pp.207-222
19. Methodical instructions "Thermohydraulic calculation of the heat exchange equipment of atomic power stations", RD 24.035.05-89, Leningrad, 1991, 212 p.

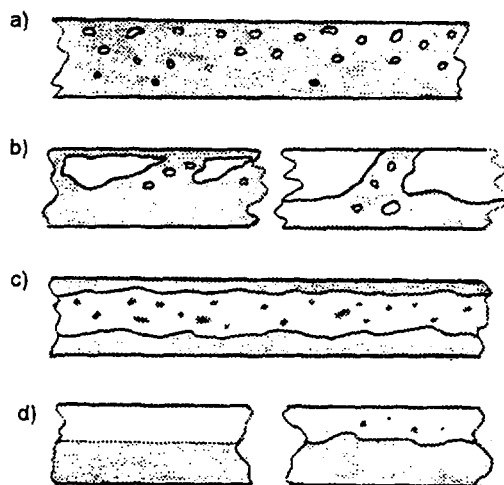


Fig.1. Flow regimes in horizontal tubes

a) bubbly; b) intermittent (plug and slug);
c) annular-mist; d) stratified (with smooth
and wavy surface)

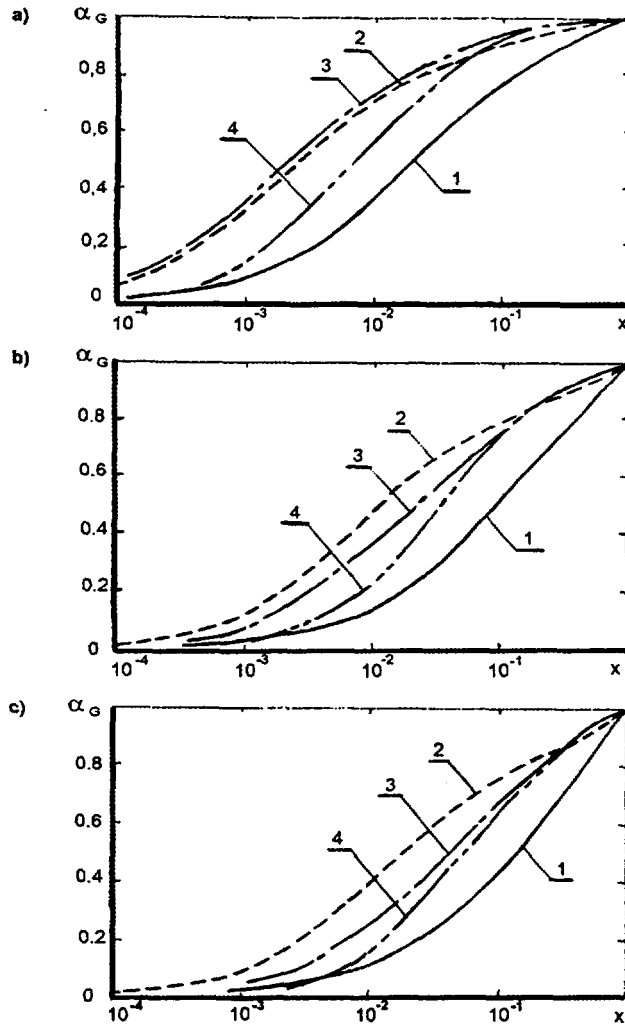


Fig.2. Void fraction as function of quality

a) P=0.1 MPa; b) P=2.0 MPa; c) P=4.0 MPa

$$1 - \alpha_G = \frac{1}{1 + X^{1/(1-n)}}; X = \left(\frac{1-x}{x}\right)^{0.9} \cdot \left(\frac{\rho_G}{\rho_L}\right)^{0.5} \cdot \left(\frac{\mu_G}{\mu_L}\right)^{-0.1}; n = 0.2 \quad [4];$$

$$2 - \alpha_G = 1 - \left(1 + \frac{21}{X} + \frac{1}{X^2}\right)^{-0.5} \quad [5]; \quad 3 - \alpha_G = \left\{1 + \frac{\rho_G}{\rho_L} \frac{1-x}{x} \left[0.4 + 0.6 \sqrt{\frac{(\rho_L/\rho_G) + 0.4(1-x)/x}{1 + 0.4(1-x)/x}}\right]\right\}^{-1} \quad [6]$$

$$4 - \alpha_G = \left(1 + S \frac{1-x}{x} \frac{\rho_G}{\rho_L}\right)^{-1}; S = \left(\frac{\rho_L}{\rho_G}\right)^k + \frac{x^{0.05} \cdot (1-x)^{0.05}}{Fr_{Lo} + 0.063 \cdot (\rho_G/\rho_L)^{0.5}};$$

$$k = \frac{0.57 \cdot (1-x)^{0.05} \cdot x^{0.25} \cdot (1 - \mu_G/\mu_L)}{1 + 6 \cdot (\mu_G/\mu_L)}; Fr_{Lo} = \frac{\rho W}{[\rho_L \cdot g \cdot d \cdot (\rho_L - \rho_G)]^{0.5}}; d = 0.013 m; \rho W = 1000 \frac{kg}{m^2 \cdot s} \quad [7]$$

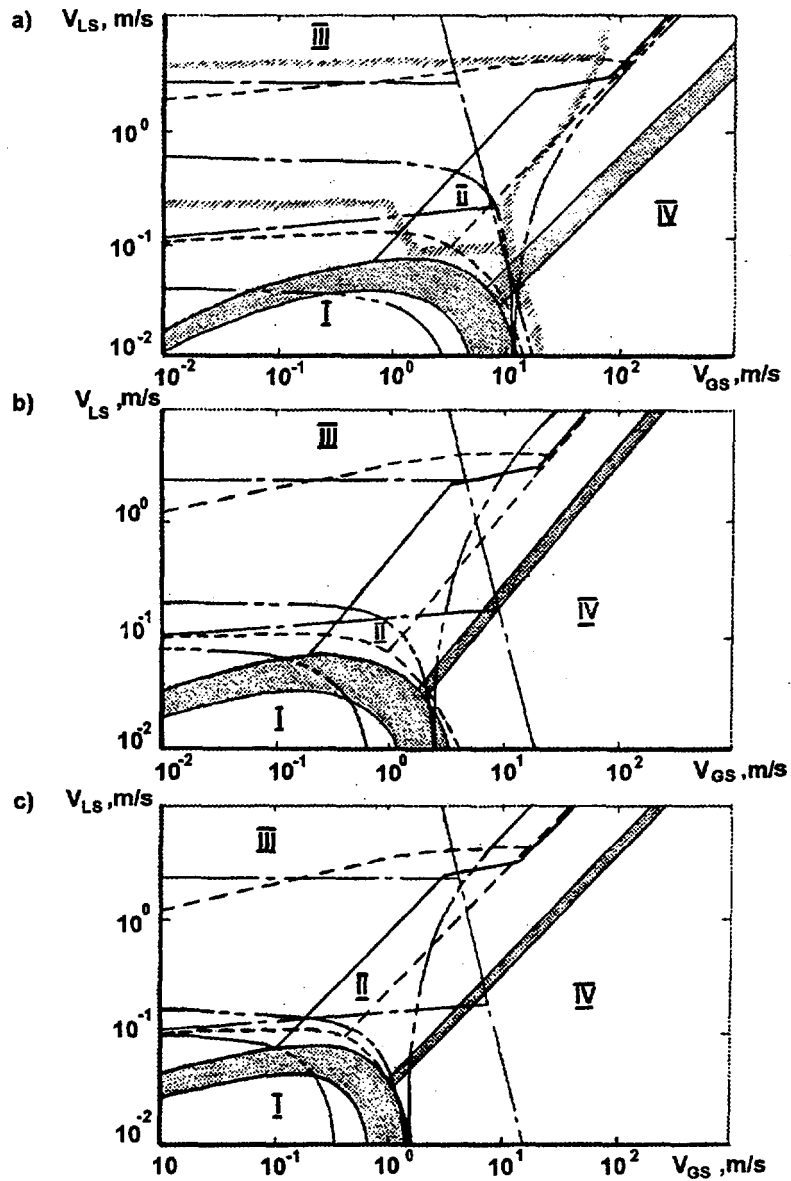


Fig.3. Comparison of different flow regime maps for adiabatic flow

a) $P=0.1 \text{ MPa}$; b) $P=2.0 \text{ MPa}$; c) $P=4.0 \text{ MPa}$

— RELAP5/MOD3, transition region [1];
 Mandhane et al [4]; — Weisman et al [3];
 - - - Taitel & Dukler [2]; - - - Budrik et al [7]
 Flow regimes: I - stratified, II - intermittent, III - bubbly,
 IV - annular-mist

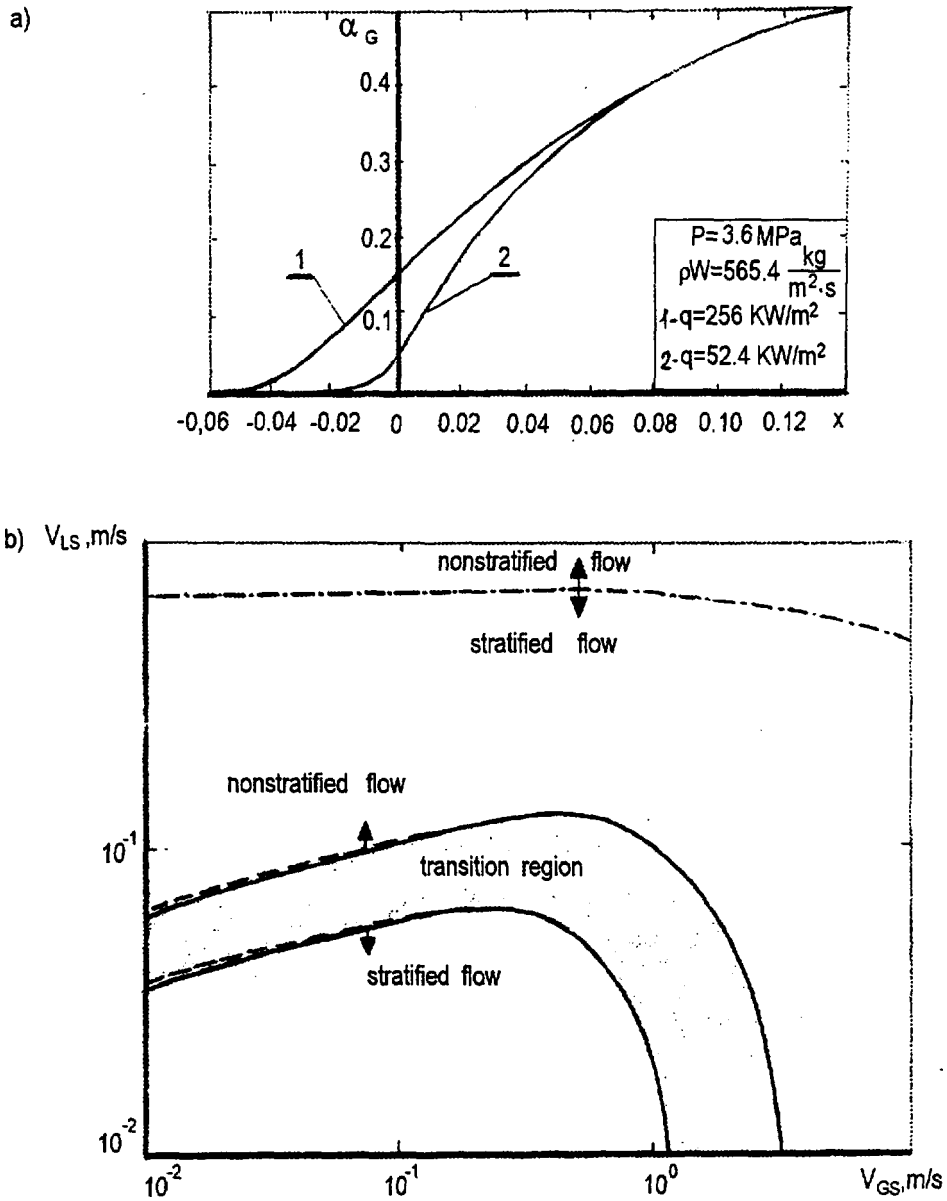


Fig.4. Comparison of RELAP5/MOD3 stratified flow boundary with experimental data [16] for horizontal heated tube ($d=0.04 \text{ m}$)

- a) correlation $\alpha_G = \alpha_G(x)$, calculated with [19];
- b) ——— RELAP5/MOD3, $q=52.4 \text{ KW/m}^2$;
 --- RELAP5/MOD3, $q=256 \text{ KW/m}^2$;
 - - - - - experimental boundary of stratified flow ($q=52.4 - 256 \text{ KW/m}^2$) [16]

a)

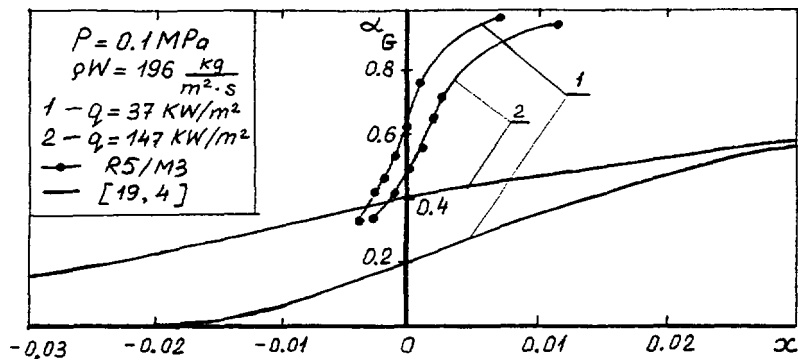
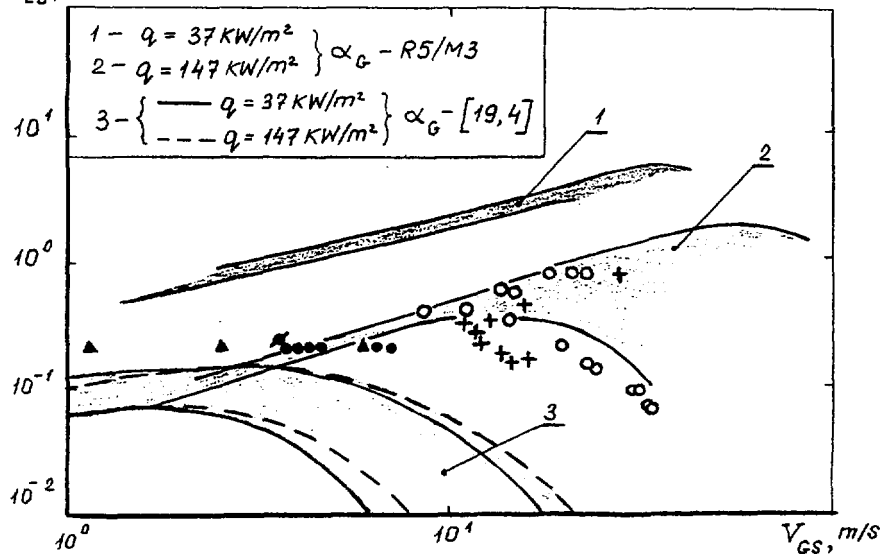
b) $V_{LS}, m/s$ 

Fig.5. Comparison of RELAP5/MOD3 stratified flow boundary with experimental data [18] for horizontal tube ($d=0.057m$)

a) correlations $\alpha_G = \alpha_G(x)$;

b) $\circ - q = 37 \text{ kW/m}^2$ } experimental points from [18];
 $+ - q = 147 \text{ kW/m}^2$ }

calculations with RELAP5/MOD3: $\bullet - \text{stratified flow}$ } $q = 147 \text{ kW/m}^2$;
 $\times - \text{bubbly flow}$ }
 $\triangle - \text{stratified flow}; q = 37 \text{ kW/m}^2$



FI9800030

Coolant rate distribution in horizontal steam generator under natural circulation

A. Blagovechtchenski, V. Leontieva, A. Mitrioukhin

St. Petersburg State Technical University

1 Introduction

Last some decades since the beginning of atomic energetics are characterized by formation and realization of conceptual rules for decision of reliability and safety problem for nuclear power plant (NPP). Necessity of decay heat removal without damages of the fuel elements at the extreme accidents (in particular, at complete blackout) has caused the wide scope of the researches for the introduction of use of natural circulation coolant (NCC) in atomic engineering. The topicality of these researches greatly increased after Chernobyl catastrophe. It is possible to state that in the Russian NPP with VVER (VVER-440 and VVER-1000) when the emergency stops of the main coolant circulating pumps (MCP) has happened the decay heat removal is provided by NCC. However, not all questions, concerning to the use of NCC, are possible to consider decided. The performances, basing on NCC, claim the comprehensive researches of the heat-hydraulodynamic features, which can play a determining role for the practical realization. It concerns to both the operative NPP and the new projects of NPP (for example with VVER-640), in which NCC is the main component of the reliability and safety guarantee. On the base of NCC there are the projects of the emergency passive core cooling systems (EPCCS). One of the features of Russian NPP in comparison with foreign NPP is the use of horizontal steam generators (SG). There is large scientific and practical interest to researches of coolant rate distribution in horizontal steam generator tubes under NCC. There are the several scientific works in this area. Among last the researches, distinguished by analysis depth, it is necessity to note [1,2]. However, these researches are basically directed on study of heat-hydraulodynamic processes directly in SG without the other factors, which concern to the NCC conditions in the primary circuit as a whole and also render determinative influence on coolant rate distribution in the horizontal tubes SG. In submitted report these factors are considered.

2 Main dependences

Proceeding from the present problem, we shall consider major factors, determining the conditions of NCC in the primary circuit. On the Fig. 1 the primary circuit of NPP with VVER and horizontal SG is schematically shown, where H_{SG}^{TB} is the height of the tube bundle (m) and ΔH is the distance on vertical between the middle of core and the middle of H_{SG}^{TB} (m). The natural circulation pressure head P_{NPH} can be determined with sufficient accuracy as

$$p_{NPH} = g\Delta\rho\Delta H \text{ (Pa)}, \quad (1)$$

where $g = 9.81 \text{ m/s}^2$ is the gravity and $\Delta\rho = \rho_c - \rho_h \text{ (kg/m}^3\text{)}$ is the density change of the coolant in the core, when its temperature change is $\Delta T \text{ (K)}$ between entrance and exit of the core. In the steady state

$$P_{NPH} = \Delta p_c, \quad (2)$$

where Δp_c is the hydraulic resistance of the primary circuit (Pa). The condition (2) defines the coolant rate ($G \text{ kg/s}$) in the primary circuit, as $\Delta p_c = f(G)$. Using linear approach of changes ρ from T and also accepting the average specific heat of the coolant is constant ($C_p = \text{const j/kg}\cdot\text{K}$) and $\Delta p_c \sim G^2$, it is easy to receive [3]:

$$Q \sim \Delta T^{3/2}; \quad G \sim Q^{1/3} \quad (3)$$

where Q is the heat power of the reactor under NCC. Conditions of the coolant rate distribution in horizontal tube rows have essential differences in the cases of compulsory coolant circulation and NCC. It is explained by determining influence of a gravity pressure heads in "hot" and "cold" vertical collectors SG on pressure drops of the tubes depending on coordinate z under NCC. The hydraulic losses on friction are negligible in comparison with a gravity pressure head. Also the mutual conversions of dynamic head in static pressure head are negligible in comparison with the same and the II-form collectors permit completely to exclude consideration of this factor in the conditions of NCC.

The simple scheme of SG is shown on the Fig. 2. The vertical coordinate $z = 0$ corresponds to the average tube row. The upper rows have $z > 0$, the lower rows have $z < 0$. Thus $|z| \leq H_{SG}^{TB}/2$.

The pressure difference between the entrance and the exit of the average row tube is equal to

$$\Delta p_T^{z=0} = p_1 - p_2. \quad (4)$$

Thus for tubes with coordinate z the pressure difference will be equal to

$$\Delta p_T^z = (p_1 - g\rho_h z) - (p_2 - g\rho_c z) = p_1 - p_2 + gz(\rho_c - \rho_h). \quad (5)$$

Let m be the share of the hydraulic resistance of the average tube in the complete resistance of primary circuit, then

$$m = \frac{\Delta p_T^{z=0}}{\Delta p_c} = \frac{\Delta p_T^{z=0}}{p_{NPH}}. \quad (6)$$

Hence $\Delta p_T^{z=0} = mp_{NPH}$. Using (1) we have

$$\Delta p_T^{z=0} = p_1 - p_2 = mg(\varrho_c - \varrho_h)\Delta H \quad (7)$$

and using (5) we receive

$$\Delta p_T^z = mg(\varrho_c - \varrho_h)\Delta H + gz(\varrho_c - \varrho_h). \quad (8)$$

Then the relation of the pressure difference in the tube with coordinate z to the pressure difference in the tube of the average rows is equal to

$$\frac{\Delta p_T^z}{\Delta p_T^{z=0}} = \frac{mg(\varrho_c - \varrho_h)\Delta H + gz(\varrho_c - \varrho_h)}{mg(\varrho_c - \varrho_h)\Delta H} = 1 + \frac{z}{m\Delta H}. \quad (9)$$

Having accepted

$$\Delta p_T^z \sim (G_T^z)^2, \quad (10)$$

where G_T^z (kg/s) is the coolant rate in the tube with coordinate z , we receive the hydraulic non-uniformity in the tubes of SG under NCC:

$$\frac{G_T^z}{G_T^{z=0}} = \sqrt{1 + \frac{z}{m\Delta H}}. \quad (11)$$

From (11) it is evident that the tube coolant rate increases if the tube row level rise (and vice versa). Thus the hydraulic non-uniformity will be larger or smaller depending on the combination of the geometrical and hydraulic characteristics of the primary coolant elements.

Moreover, from (11) we receive the condition

$$1 + \frac{-|z|}{m\Delta H} = 0; \quad |z| = m\Delta H \quad (12)$$

of flow stoppage in the tubes, located $m\Delta H$ lower than the average tube and the condition

$$1 + \frac{-|z|}{m\Delta H} < 0; \quad |z| > m\Delta H. \quad (13)$$

of flow reversal in the tubes, located more than $m\Delta H$ lower than the same.

As

$$|z|_{\max} = H_{SG}^{TB}/2, \quad (14)$$

we receive the criterion

$$\frac{H_{SG}^{TB}}{m\Delta H} < 2. \quad (15)$$

If the condition (15) is fulfilled, the flow stoppage and the flow reversal (in the lower tubes) are excluded.

3 Conditions of coolant rate distribution in the tubes of SG PGV-1000 under natural circulation

We shall consider a particular conditions of coolant rate distribution on the horizontal tubes of PGV-1000 in NPP with VVER-1000 under NCC. In this NPP $\Delta H = 9.2$ m. Primary pressure is equal to 16 MPa, secondary pressure is equal to 6.4 MPa.

PGV-1000 has the tube bundle of height $H_{SG}^{TB} = 2.1$ m, which contains 11000 tubes with diameter $d = 16 \times 1.5$ and average length $l = 11.1$ m, located with step 13.8×19 . The internal diameter of the "cold" and "hot" collectors is equal to 0.834 m and the internal diameter of the main pipelines of the primary circuit is equal to 0.85 m. In NPP there are 4 SG and 4 MCP (there are 4 parallel loops of the primary circuit).

For analysis we use the heat-hydraulic characteristics and parameters NPP with VVER-1000 from [4]. The hydraulic resistance multipliers (HRM) of the primary circuit and the stopped MCP are equal correspondently $\zeta_i = 16.7$ and $\zeta_{MCP} = 25.3$. These HRM are concerned to the coolant velocity in the "cold" pipeline ($d = 0.85$ m). Thus, the complete HRM is equal to $\zeta_{comp} = 42$; HRM of SG is equal to $\zeta_{SG} = 3.3$. From these data m is evaluated as

$$m = \frac{\zeta_{SG}}{\zeta_{comp}} = \frac{3.3}{42} = 0.0785. \quad (16)$$

That is under NCC the share of the hydraulic resistance SG in the common resistance of the primary circuit is very small. For getting of more correct value of m we use the experimental data of the work VVER-1000 on 10% capacity under NCC [4] (Table 1).

The calculation of the primary circuit hydraulic resistance is made by formula

$$\Delta p_c = \zeta_{comp} \frac{(G/4)^2}{2F^2 \varrho_c} \text{ (Pa)}. \quad (17)$$

Here

$$\frac{G}{4} = \frac{4427 \cdot 10^3}{3600 \cdot 4} = 307.4 \text{ (kg/s)}$$

is the primary coolant mass flow through one loop; $F = 0.785 \cdot 0.85^2 = 0.567 \text{ m}^2$ is the flow area of "cold" pipeline. Then

$$\Delta p_c = 8193 \text{ (Pa)}. \quad (18)$$

Comparison of Δp_c (18) and p_{NPH} (8345 Pa, Table 1) testifies about their satisfactory convergence (the error does not exceed 2%). The estimation of the average value of hydraulic resistance of SG shows that it is equal to

$$\Delta p_{SG} = \Delta p_c \frac{\zeta_{SG}}{\zeta_{comp}} = 8193 \frac{3.3}{42} = 644 \text{ (Pa)}. \quad (19)$$

The calculation of the average tube hydraulic resistance gives the close result

$$\Delta p_T^{z=0} = \left(\zeta_{in} + \xi \frac{l}{d} + \zeta_{out} \right) \frac{\bar{w}^2}{2} \bar{\varrho} = 699 \text{ (Pa)}. \quad (20)$$

Here

$\bar{w} = G/4n_{\text{TB}}f_{\text{TB}}\bar{\rho} = 0.297$ (m/s) is the average coolant velocity in the tubes of SG;

$\xi = 0.025$ is the wall friction multiplier (Re=30400, absolute wall rough $\bar{\Delta} = 0.01$ mm, $d/\bar{\Delta} = 1300$) [5];

$\zeta_{\text{in}} = 0.4$ and $\zeta_{\text{out}} = 0.6$ is correspondently the local resistance multipliers of “entrance” and “exit” [5];

$\bar{\rho} = (\rho_c + \rho_h)/2$ is the average coolant density in the tube.

The received value of $\Delta p_{\text{T}}^{z=0}$ is equal to the pressure difference between the points of entrance and exit for the average (on height) tubes row (see the Fig. 2). Consideration of change of the coolant rate in the horizontal tubes has meaning in the diapason $|z| \leq 1.05$ (m), because $H_{\text{SG}}^{\text{TB}}/2 = 1.05$ (m). Having $\Delta p_{\text{T}}^{z=0} = p_1 - p_2 = 699$ Pa (20), we receive

$$m = \frac{\Delta p_{\text{T}}^{z=0}}{p_{\text{NPH}}} = \frac{699}{8345} = 0.084. \quad (21)$$

It is a little bit more, than the previous estimation (16).

As

$$\frac{H_{\text{SG}}^{\text{TB}}}{m\Delta H} = \frac{2.1}{0.084 \cdot 9.2} = 2.72 > 2, \quad (22)$$

the criterion (15) is not fulfilled and in the lower tube rows with $|z| \geq 0.084 \cdot 9.2 = 0.773$ (m) the flow stoppage and flow reversal will take place.

Using (11), we receive $G_{\text{T}}^z/G_{\text{T}}^{z=0} = F(z)$. However, strictly speaking, this dependence is fair for the automodel mode of current (for number Re) in the tubes. Actually under the small coolant velocities some distinctions in the friction multipliers ξ will take place for the tubes of various rows. In particular, ξ can grow if the coolant velocity (and correspondently the number Re) reduces and it can decrease in tubes with larger coolant velocities. The results of calculations $G_{\text{T}}^z/G_{\text{T}}^{z=0} = F(z)$, received both on the simple dependence (11) and with consideration of change $\xi = \varphi(\text{Re}, d/\bar{\Delta})$ are given in the Table 2 and on the Fig. 3 for the considering variant. In the Table 2 these data are submitted correspondently in numerator and denominator. Their comparison testifies about an insignificant distinctions of the received numerical data.

Characteristically, that under NCC reactor power change will not render appreciable influence on the relative coolant rate distribution $G_{\text{T}}^z/G_{\text{T}}^{z=0}$ in horizontal tubes of SG. This influence can only indirectly affect on the distribution conditions by the possible small changes of the parameter m , connected with some changes of the velocities (correspondently Re and ξ) in the different parts of the primary circuit. A weak dependence of the coolant mass flow from the reactor power (3) also confirms the truth of the above-made consideration.

4 Conclusion

Under NCC large coolant hydraulic non-uniformity in the tubes of SG results to definite decrease of an overall heat transfer surface performance in emergency modes of residual heat removal and also limits perspectives of the operational opportunities expansion, in particular, in the direction of NCC use at the reactor partial power levels, when the MCP are break-down. It is obvious, that the coolant flow reversal in the tubes can harmfully influence on the work conditions of the metal of some constructive elements of SG, due to arising additional temperature stresses.

As it is visible from (15), at the stage of designing of NPP the opportunities of the coolant rate distribution improvement in the tubes of SG are available. In particular, it can be achieved by both a choice of the ratio $H_{SG}^{TB}/\Delta H$ and a choice of hydraulic characteristics of all primary circuit parts, determining numerical value of the internal parameter m . That is the designer of the primary circuit project has the ways of the optimum decisions search in this problem. Substantively that it is necessary to take into account the above-stated considerations at a physical modelling of the coolant rate distribution in the horizontal steam generator on a special heat-hydrodynamics facilities.

- [1] *Juhani Hyvärinen*. Heat transfer characteristics of horisontal steam generators under natural circulation conditions, Nuclear Engineering and Design **166** (1996), 191–223.
- [2] *Juhani Hyvärinen*. Horisontal steam generator primary side scaling. Appendix 4 Dissertation for degree of Doctor of Technology STUK-A135, December 1996.
- [3] *Б. Д. Гусев, Р. И. Калинин, А. Я. Благовещенский*. Гидродинамические аспекты надёжности современных энергетических установок, Л.: Энергоатомиздат, 1989.
- [4] Реакторная установка В-302. Расчёт теплогидравлический. ОКБ “Гидропресс” 302.00.00.00.000.РРО2.
- [5] *П. Л. Кириллов, Ю. С. Юрьев, В. П. Бобков*. Справочник по теплогидравлическим расчётам (ядерные реакторы, теплообменники, парогенераторы), М.: Энергоатомиздат, 1990.

Table 1.

Some characteristics of work NPP VVER-1000 on 10% capacity under NCC

Characteristics		Values
Heat power	MW	320
	%	10
Primary coolant pressure	MPa	16
Coolant temperature and enthalpy of entrance reactor T_{in}, h_{in}	$^{\circ}C$	280.6
	kJ/kg	1235.9
Coolant temperature and enthalpy of exit reactor T_{out}, h_{out}	$^{\circ}C$	326.7
	kJ/kg	1496.1
Primary coolant rate G и G/G_{nom}	t/h	4427
	%	7.2
Coolant density on the "cold" side of primary circuit ρ_c	kg/m ³	754.72
Coolant density on the "hot" side of primary circuit ρ_h	kg/m ³	662.25
NCC pressure head $p_{NPH} = g(\rho_c - \rho_h)\Delta H$, where $\Delta H = 9.2$ m	Pa	8345

Table 2.

Coolant rate distribution in the horizontal tubes of SG PGV-1000 on 10% power under NCC

Values	Coordinate of tube z										
z m	-1.05	-0.773	-0.65	-0.5	-0.3	0	0.3	0.5	0.65	0.773	1.05
$G_T^z/G_T^{z=0}$	< 0	0	0.4 0.594	0.594 0.587	0.782 0.767	1	1.178 1.2	1.283 1.323	1.36 1.41	1.41 1.475	1.536 1.605
w m/s	< 0	0	0.119 0.109	0.176 0.168	0.232 0.228	0.297	0.349 0.357	0.381 0.393	0.404 0.418	0.419 0.438	0.456 0.476
Δp_T^z Pa	< 0	0	109	246	427	699	971	1152	1289	1400	1659
Re	—	0	12000	18000	23800	30400	35800	39000	41300	42800	46700
ξ	—	—	0.025 0.029	0.025 0.0275	0.025 0.026	0.025 0.025	0.025 0.024	0.025 0.0235	0.025 0.0232	0.025 0.023	0.025 0.023

Here $G_T^z/G_T^{z=0}$ is the relative coolant rate; w is the coolant velocity in the tube; Δp_T^z is the pressure differences between the entrance and the exit of the tube; Re is Reynolds number; ξ is the friction multiplier.

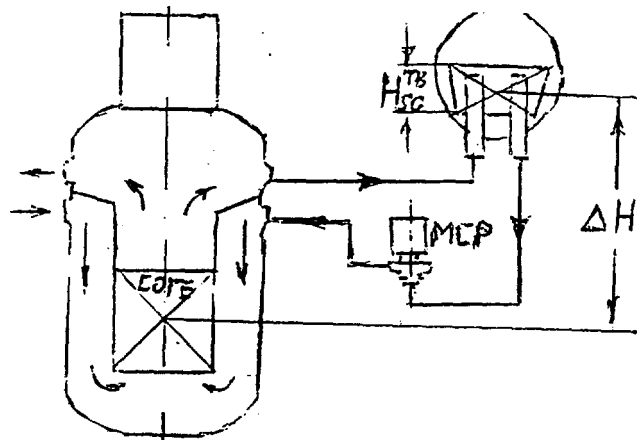


Fig. 1. The principle scheme of primary circuit of NPP with VVER and horizontal SG.

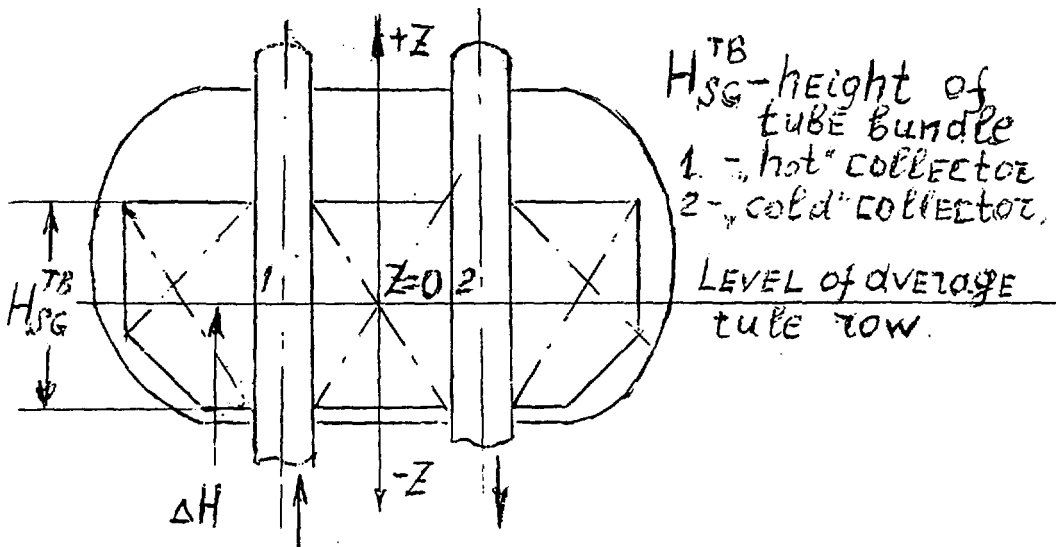


Fig. 2. The simple scheme of horizontal SG

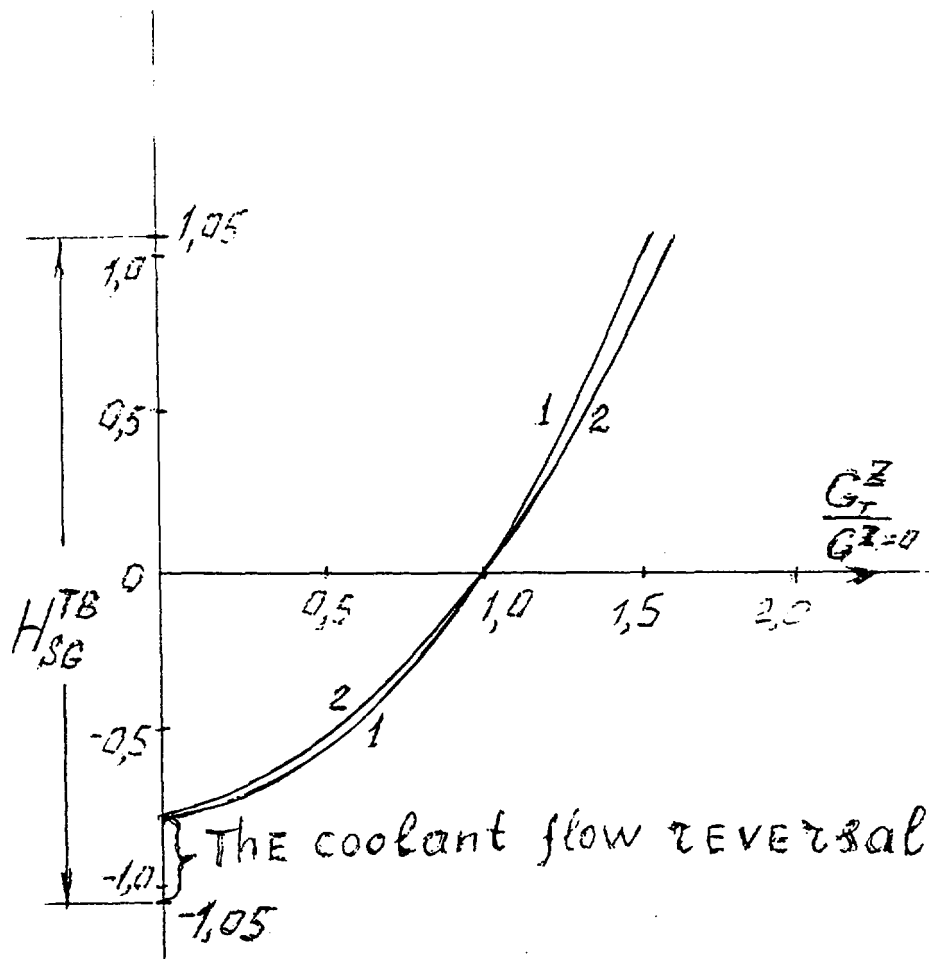


Fig 3. The results of calculation $\frac{G_T^Z}{G_T^{Z=0}} = F(Z)$, received:

- 1 on the simple dependence (11),
- 2 with consideration of change $\xi = \varphi\left(Re, \frac{d}{\Delta}\right)$.



POST TEST CALCULATION OF THE EXPERIMENT „SMALL BREAK LOSS-OF-COOLANT TEST“ SBL-22 AT THE FINNISH INTEGRAL TEST FACILITY PACTEL WITH THE THERMOHYDRAULIC CODE ATHLET

by W.Lischke, B.Vandreier

Institute of Process Technique, Process Automation and Measuring Technique
Dept. Nuclear Technology
at the University for Applied Sciences Zittau/Görlitz (FH)
D-02763 Zittau, Theodor-Körner-Allee 16
Tel: +49-(0)3583-61-1547, Fax: +49-(0)3583-61-1288
E-mail: vandreier@novell1.ipm.htw-zittau.de

1. Introduction

At the University for Applied Sciences Zittau/Görlitz (FH) calculations for the verification of the ATHLET-code for reactors of type VVER are carried out since 1991, sponsored by the German Ministry for Education, Science and Technology (BMBF). The special features of these reactors in comparison to reactors of western countries are characterized by the duct route of reactor coolant pipes and the horizontal steam generators. Because of these special features, a check of validity of the ATHLET-models is necessary. For further verification of the ATHLET-code the post test calculation of the experiment SBL-22 (Small break loss-of-coolant test) realized at the Finnish facility PACTEL was carried out. The experiment served for the examination of the natural circulation behaviour of the loop over a continuous range of primary side water inventory.

2. The integral facility PACTEL with a new steam generator model

The PACTEL facility (figure 1) is a volumetric scaled model (1:305) of a VVER 440 with three separate coolant loops. The facility has been designed to simulate the major systems and components of VVER - Pressurized Water Reactors during postulated small and medium size break loss of coolant accidents and other transients. The facility consists of primary system, secondary side (steam generators) and emergency core cooling systems. The design pressure are 8.0 MPa on the primary side and 4.6 MPa on the secondary side. The design power of reactor core is 1.0 MW. A new large diameter steam generator was used for this experiment (diameter increase from 0.376 m to 0.95 m). The new steam generator reflects better the behaviour of real steam

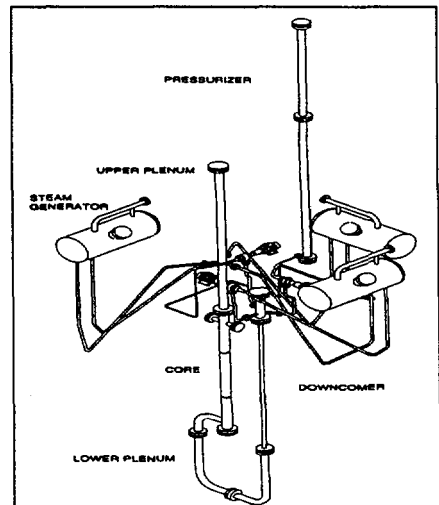


Figure 1: PACTEL Facility

generators, because of the greater geodatic difference between the lowest and uppermost u-tube.

3. Description of the experiment SBL-22

A small break loss-of-coolant experiment was performed using the PACTEL facility to examine the natural circulation behaviour of the loop over a continuous range of primary side mass inventory /1/. The effect of the new large diameter steam generator to the loop operation was of particular interest.

The experiment was started by establishing a 1000 s steady state with primary circulation pump running. At 1000 s the pump was stopped, pressurizer isolation valve closed and the break valve was opened. The pressurizer heaters were switched off as well. The break line was connected to a condensation tank. The level of the tank was measured and the primary side inventory and the break flow were determined using the level measurement. No actions were taken during the test other than maintaining the secondary side coolant level by periodic additions of feed water. The experiment was terminated when the cladding temperatures in the core rose over 300 °C.

Three natural circulation modes were observed during the test: single-phase, two-phase and boiler-condenser modes. The transition from single-phase flow to two-phase flow was not smooth. The loop flow stagnated when the level in the primary side reached the hot leg pipe entrance. The primary system pressure rose sharply during the flow stagnation. After the hot leg loop seal cleared the heat transfer from primary side to the secondary side changed into two-phase natural circulation. At about 5200 s the heat transfer mode changed into boiler-condenser natural circulation. The temperature measurements in the steam generator heat exchange tubes indicated internal circulation in the single-phase heat transfer mode.

4. Modelling of the facility with the ATHLET-code

The post test calculation was carried out with the ATHLET-code version cycle C Mod. 1.1. The basis of the simulation was the input deck, which was developed and verified for the participation within the international standard problem ISP-33 /2/ as well as for the post test calculation of the experiment LSR-10 (Loop Seal Refilling test) /3/.

The ATHLET-model describes the reactor vessel, the primary loop, the pressurizer and the steam generator. The u-tube cluster in the facility, which consists of 14 u-tube layers was modelled in the ATHLET-input deck by 7 u-tube layers. This detailed modelling was necessary to simulate the internal circulation in the u-tube cluster in a correct way. For the simulation of vertical temperature profile in the secondary side of the steam generator the two-dimensional model (figure 2), which was developed and verified within the post test calculation of the experiment LSR-10, was applied.

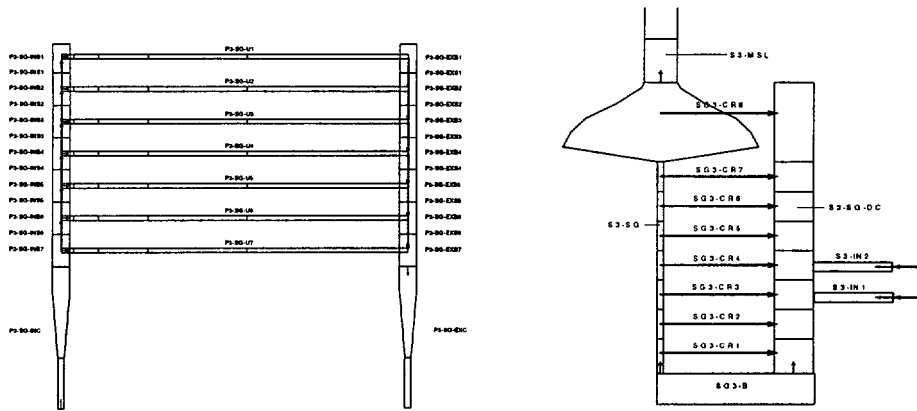


Figure 2: Nodalisation scheme of the primary and secondary side of the steam generator

The simulation of condensation in steam filled horizontal u-tubes was improved (analogous to the post test calculation of the experiment LSR-10), by using the correlation of Chato for the determination of the Nusselt-number. This correlation was included in the ATHLET-code /4/.

5. Comparison between experiment and post test calculation

As a result of the first test calculations the primary mass flow rate during the one-phase natural circulation mode (from $t=1100$ s to $t=3300$ s) was too high in comparison to the measured values. Therefore the calculated primary pressure was too small. During this period a steam filled region is located in the upper part of the hot leg P3-HL (figure 3).

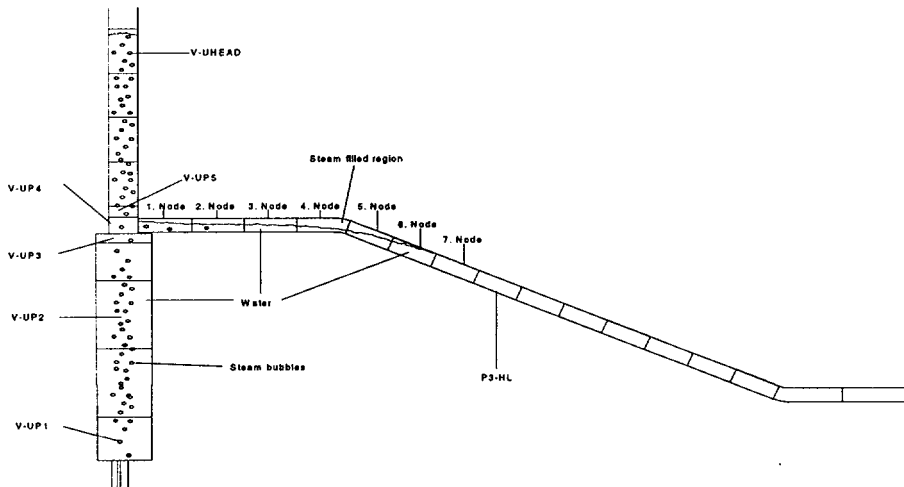


Figure 3: Location of the steam filled region in the upper part of the hot leg during the one-phase natural circulation mode

The primary mass flow rate is very sensitive depending on the value of this steam filled region in the upper part of the hot leg. Through the modification of two ATHLET-specific parameters for the hot leg (DEPO used for the calculation of the void gradient for the drift flux model and CMUC used for the condensation model) the value of calculated steam filled region could be expanded. The calculated primary mass flow rate corresponds to the measured mass flow rate (figure 4) by using the two modification.

Figure 5 shows the measured and calculated primary pressures. As a result of the modification of the two athlet-specific parameters for the hot leg, the experiment could better reproduced. The first pressure reduction caused by the leak, the primary pressure increase during the flow stagnation as well as the following value of the pressure during the two-phase flow natural circulation and the boiler-condenser natural circulation are reproduced very well by the modified calculation.

In figure 6 the measured and calculated water levels in the reactor are shown. A good agreement exists between these values. This means that the value of drained water as well as the distribution of the coolant inventory over the single components of the primary circuit during the different modes of heat transfer are correct.

Caused by the leak the water level sinks to the hot leg pipe entrance ($t=3900$ s). Then the level is nearly constant for the next 1400 s. This is the period of the two-phase circulation mode. If the level sinks below the hot leg entrance, the circulation mode change into the boiler-condenser mode. Then the mass flow in the downcomer

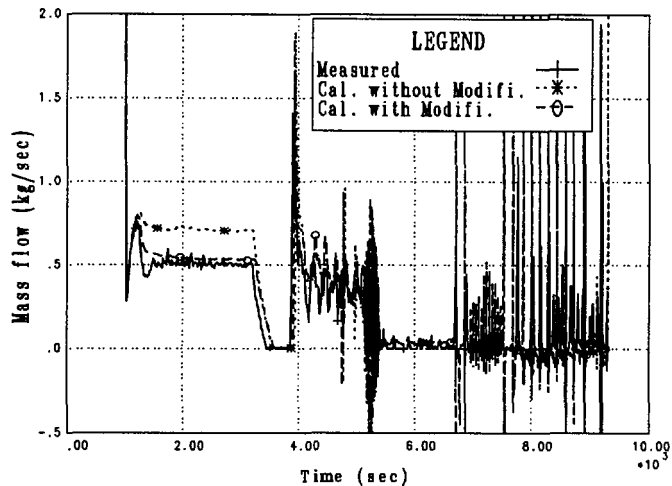


Figure 4: Measured and calculated mass flows in the downcomer

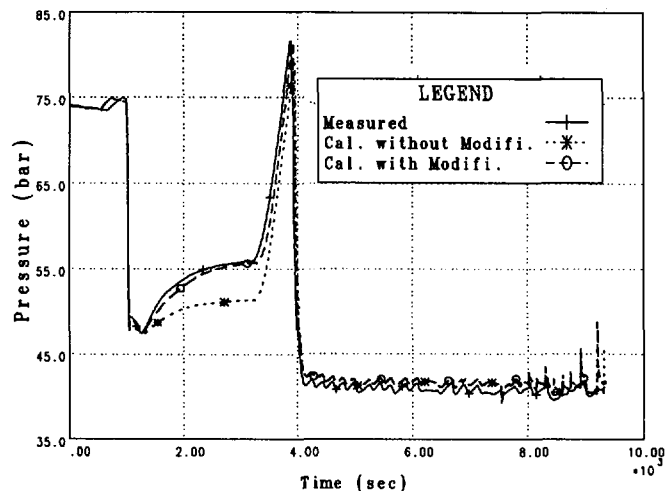


Figure 5: Measured and calculated primary pressures

(figure 4) sinks rapidly. The value of the measured mass flow during the different circulation modes are good reflected by the calculation. The points in time of the experiment and of the calculation, when the circulation modes change, are nearly identical.

Figure 7 shows measured and calculated water temperatures in the secondary side of the steam generator in the lower and upper part. As a result of the periodical addition of strong sub-cooled feed water, the temperature in the lower part sinks periodical up to 12 K under the saturation temperature. This effect is very good reflected by the calculation using the two-dimensional model for the secondary side.

The internal circulation in the u-tube cluster, characterized by water flow from the cold to the hot collector in the lower part and from the hot to the cold collector in the upper part, was reproduced by the post test calculation. This effect was also observed in the experiment LSR-10 /3/.

A good correspondence between the experiments and the post test calculations was obtained. All observed effects and phenomena are correctly reflected by the post test calculation. The good agreement between the experiment and the post test calculation demonstrate, that it is possible to simulate VVER typical NPP with the ATHLET- code.

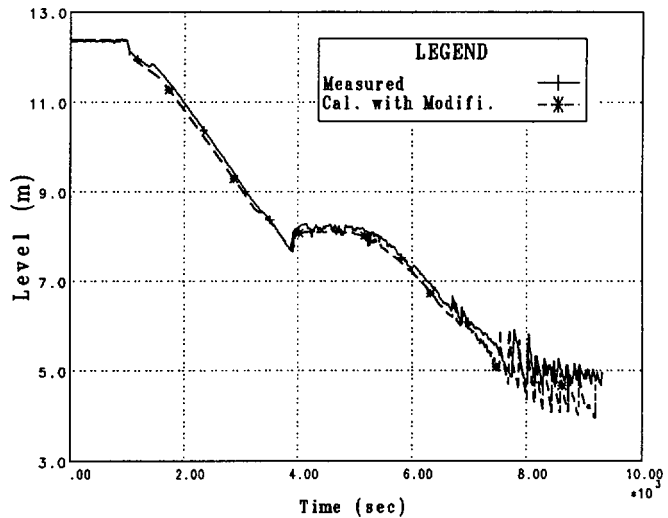


Figure 6: Measured and calculated water levels in the reactor

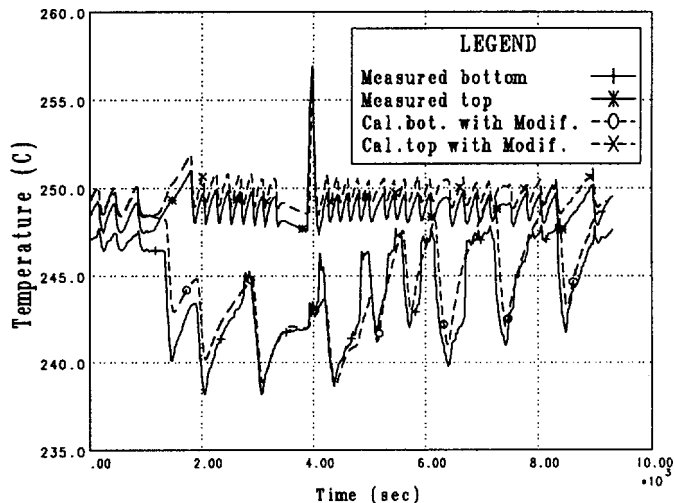


Figure 7: Measured and calculated temperatures in the secondary side of the steam generator

6. References

- /1/ Description of the experiment SBL-22; VTT Lappeenranta, Finland 1994
- /2/ Lischke, W.; Vandreier, B.
Rechnungen zum ISP 33 an der finnischen Versuchsanlage PACTEL
THZ-61205-11, Juli 1993, HTWS Zittau/Görlitz (FH)
- /3/ Lischke, W.; Vandreier, B.
Nachrechnung des Experimentes LSR-10 (Loop Seal Refilling test) an der finnischen
Versuchsanlage PACTEL mit dem Thermohydraulikcode ATHLET
THZ-61205-16, März 1996, HTWS Zittau/Görlitz (FH)
- /4/ Fjodorow, A.; Kraus, B.; Lischke, W.
Vorschlag für Modellerweiterung zum Kondensationswärmeübergang im Rechencode
ATHLET
THZ-61205-12, August 1994, HTWS Zittau/Görlitz (FH)
- /5/ Lischke, W.; Vandreier, B.
Nachrechnung des Experimentes SBL-22 (Small break loss-of-coolant test) an der
finnischen Versuchsanlage PACTEL mit dem Thermohydraulikcode ATHLET
HTWS Zittau/Görlitz (FH), Februar 97



Analysis of WWER 1000 Collector Cracking Mechanisms

K. Matocha , J. Wozniak

Institute of Material Engineering
Research and Development Division
Vítkovice , J.S.C., Ostrava , Czech Rep.

Introduction

In 1986 steam generator cold collector cracking was first detected at WWER 1000 units made and operated in the former Soviet Union. The causes of collector cracking have been identified as environmentally assisted cracking of low alloy bainitic steel of type 10NiMo8.5 (10GN2MFA) in secondary side water environment at about 290°C. A lot of steam generators under operation have not shown this type of cracking , hence the plant specific operational practices and or manufacturing procedures to be related to its occurrence.

Investigations over the last 15 years have indicated that in bainitic low alloy steel/high temperature water environment systems subcritical crack growth is significantly affected by sulphur content, MnS inclusion type, shape and orientation, dissolved oxygen content, stress/time pattern and temperature [1]. Very long term operation at about 300°C could result in thermal ageing of 10NiMo8.5 (10GN2MFA) steel because of its higher content of Ni. Due to the plastic deformation of ligaments between holes in perforated area of collector strain ageing could occur in these regions during operation of steam generator.

As a result of recommendations summarized in the final report of consultants' meetings on „Steam Generator Collector Integrity of WWER 1000 Reactors“ held in Vienna in 1993 [2] large experimental program was started in VÍTKOVICE focused on:

1. A detailed study of strain and thermal ageing, dissolved oxygen content and temperature on subcritical crack growth in 10NiMo8.5 (10GN2MFA) steel.
2. A detailed study of the effect of high temperature water and tube expansion technology on fracture behaviour of ligaments between holes for heat exchange tubes.
3. A detailed study of the effect of drilling, tube expansion technology and heat treatment on residual stresses on the surface of holes for heat exchange tubes.

The aim of all these investigations was to find a dominant damage mechanism responsible for collector cracking to be able to judge the efficiency of implemented modifications and suggested countermeasures and to answer a very important question wheather proper operation conditions (mainly water chemistry) make the operation of steam generators made in VÍTKOVICE safe throughout the planned lifetime.

Test material and experimental techniques

To study the effect of thermal and strain ageing, dissolved oxygen content and water temperature on subcritical crack growth, the 53x12x290 mm bars were cut from a collector forging. Its chemical composition is shown in Tab. I.

Table I. Chemical composition of studied heat of 10NiMo8.5 steel (wt.%)

C	Mn	Si	Ni	Cr	Mo	V	P	S	Cu	Ti
0,11	0,97	0,24	1,97	0,21	0,46	0,03	0,009	0,007	0,072	0,005

One third of the bars was deformed in tension at a deformation rate of $\dot{\epsilon}_a = 1.10^{-3} \text{ s}^{-1}$. When 5% plastic deformation was reached, the load was removed. Then the samples were aged for two hours at 250°C. The test specimens manufactured from the bars were oriented such that the fatigue crack propagation plane was perpendicular to the direction of plastic deformation. The second part of the bars was taken through a step cooling from 595°C used to simulate longterm service at operating temperature. Tensile properties of the studied structure states are summarized in Tab. II.

Table II. Summary of tensile properties at laboratory temperature.

	R_e [MPa]	$R_{p0,2}$ [MPa]	R_m [MPa]	A_5 [%]	Z [%]
as received condition	532		631	25,0	69
state after ageing 5% + 250°C/2h		742	742	12,4	66
after step cooling	547		647	25,2	74

It is evident from tab. II that step cooling had no detrimental effect on tensile properties at laboratory temperature. However severe loss of impact toughness and shift of transition temperature was observed after this heat treatment, see Fig. 1. This is due to significant occurrence of intergranular fracture mode, attributed to segregation of impurity elements, in our case mainly P, to prior austenite grain boundaries [3].

To determine the effect of a tube expansion technology and a water environment on a fracture behaviour of ligaments and to compare the effect of drilling and tube expansion technology on residual stresses on the holes surface the tubes were expanded into experimental blocks shown in Fig. 2a using both explosive and hydraulic expansion technology. Thickness of ligaments between adjacent holes has corresponded to that observed in a half of a collector wall thickness. Then the experimental blocks were cut, like schematically shown in Fig. 2a, and special C(T) specimens were manufactured (see Fig. 2b), and fatigue precracked in air. X-ray diffraction analysis was used to measure both axial and tangential residual stresses on holes surface.

Fracture mechanics tests in air were carried out at 290°C and 320°C an MTS 500 kN servohydraulic testing machine in stroke control at a displacement rate of 0,5 mm/min.

Slow strain rate tests of special C(T) specimens at 290 °C were performed at a displacement rate of 0,001 mm/min, to determine the effect of water environment on fracture behaviour. Both fatigue and fracture mechanics tests in high temperature water were

performed on an INOVA servohydraulic testing machine fitted with an 11 litre static autoclave at two significantly different dissolved oxygen contents:

1. oxygen content corresponding at the beginning of the test to aerated water (designated as $O_2 = 8\text{ppm}$) or oxygenated water.
2. oxygen content less than 15 ppb.

Results and Discussion

The effect of dissolved oxygen on subcritical crack growth in water environment at 290°C.

The results of fatigue crack growth rate measurements in air at room temperature are plotted against ΔK in Fig. 3 [4].

It could be reasoned that neither the threshold value for the fatigue crack propagation ΔK_{th} , nor the dependence of da/dN vers. ΔK are affected by strain aging in spite of the significant differences in mechanical properties of studied steel in as received condition and after strain aging.

Fractographic analyses of the fracture surfaces of failed specimens provide evidence that micromechanism of failure is not affected by strain ageing as well. Changing ΔK produced no significant change in micromorphology. Fields of striations and occurrence of transverse microcracks are considered to be typical microfractographic features.

Results of fatigue crack growth rate measurements in air and oxygenated water environment at 290°C as a function are ΔK of given in Fig.4 which shows a significant enhancement of fatigue crack growth rates compared with those in an air environment. Increasing the frequency of cyclic loading significantly lowered the kinetics of fatigue crack growth in water.

Experimental data fit very well with modified anodic dissolution/film rupture model [5]. Provided that the dissolved oxygen content was lowered significantly (see Fig. 5), no effect of the water environment was observed.

To determine the effect of corrosion potential (dissolved oxygen content) on susceptibility to stress corrosion cracking in water environment at 290°C, 1C(T) specimen was loaded at $ECP = -0,306 V_{SHE}$ up to $K = 105 \text{ MPa m}^{1/2}$. Under these conditions no subcritical crack growth was observed. The test was stopped and under conditions of constant displacement, increasing ECP by oxygen bubling, the stable crack was started to grow at $ECP = 0,012 V_{SHE}$ (see Fig.6). In a short time the crack growth rate reached the value of $da/dt = 4,6 \cdot 10^{-5} \text{ mm/s}$. Lowering ECP by nitrogen bubling crack growth began to decrease and at $ECP = -0,24 V_{SHE}$ the growing crack stopped. All these results demonstrate that anodic dissolution plays the leading role in environmentally assisted cracking in water environment at 290°C.

The effect of water temperature on subcritical crack growth behaviour.

Fig.7 summarizes the results of constant displacement tests ($K = 97 \text{ MPa m}^{1/2}$) carried out in oxygenated pure water at different temperatures ranging from 150°C to 290°C. Significant change in susceptibility to stress corrosion cracking in water environment was revealed at about 225°C.

The results of fatigue crack growth rate measurements in water environment at 60°C are illustrated in Fig.8 both for as received condition and for condition after strain ageing. The results obtained proved that for $\Delta K > 13 \text{ MPa m}^{1/2}$ the growth rates in water environment are significantly higher then those in air environment. Both the fields of fatigue striations and the areas of transgranular quasi-cleavage were found on the fracture surfaces of test specimens

tested in water environment. The degree of quasi-cleavage appeared to increase with increasing ΔK and at $\Delta K = 26 \text{ MPa}\cdot\text{m}^{1/2}$ is equal to approximately 50%. These facets could be produced by either hydrogen embrittlement or environmentally assisted cleavage. To decide which of the two mechanisms is more probable, the studied steel was tested in the state after step cooling in water both at 60°C and 290°C. The results obtained are shown in Fig.9. At 60°C the effect of water was found to be more pronounced at the lowest ΔK investigated. Besides the quasi-cleavage fracture mode, intergranular facets were observed on the fracture surfaces. The amount of intergranular fracture was observed to be the highest at the lowest ΔK investigated (11% IGF) and was seen to decrease with increasing ΔK . Due to the fact that the grain boundary is a trapping site for hydrogen and that hydrogen also lowers the grain boundary strength, the cooperative effect of impurity induced embrittlement and the hydrogen embrittlement can lower the grain boundary strength still more. Then crack growth can occur along these grain boundaries inducing fatigue crack growth enhancement at low ΔK values. As the ΔK value is increased the cooperative effect is less apparent. The concentration of hydrogen at the crack tip and hence at the grain boundaries as well will be lower causing the effect of step-cooling on fatigue crack behaviour in water environment at 60°C become to be less significant. However no quasi-cleavage and intergranular fracture mode was observed on fracture surfaces of test specimens made of 10NiMo8.5 steel after step cooling and tested in oxygenated water at 290°C. These experimental data fit also very well with anodic dissolution/film rupture model [5]. All these observations suggest that hydrogen embrittlement could be responsible for the environmental effect observed at 60°C. Thermodynamic calculations show that trapping sites like dislocation cores and grain boundaries should have little or no effect on the hydrogen solubility in iron at about 230°C for a trap density about 10^{17} cm^{-3} [6]. It means, this temperature could be the crossover point between the dominance of hydrogen embrittlement and anodic dissolution mechanisms for low alloy steel under investigation.

Besides the significant change in susceptibility to stress corrosion cracking observed at about 225°C this hypothesis can be supported by the results of fatigue crack growth rate measurements carried out in water at 100°C and 200°C [7]. In spite of the fact that no differences between fatigue crack growth behaviour in aerated water at 100°C and 200°C were observed, significant differences between fracture surface morphologies were seen. While the fractography showed brittle like fractures on fracture surfaces of test specimens cycled in water at 100°C, fracture surfaces of test specimens cycled at 200°C primarily showed large areas of striations over the whole range of ΔK investigated.

Fracture behaviour of ligaments between holes for heat exchange tubes.

To be able to judge the possibility of a catastrophic break of a collector in a quantitative manner the fracture behaviour of ligaments at operating temperature has to be known. For this reason fracture behaviour of ligaments was investigated in air and water environment at 290°C and 320°C. The aim of these experiments was to verify the effect of tube expansion technology and water environment on the fracture behaviour characteristics. As the characteristic feature of fracture behaviour of 10NiMo8.5 steel at temperatures from 20°C to 320°C was found to be a ductile stable crack growth the variation in J and δ with crack growth Δa (J -R, δ -R curves) was investigated using multiple specimen method [8]. Tests in air were carried out in a stroke control at the speed of 0,5 mm/min corresponding to the strain rate for dynamic strain ageing phenomenon [9]. The fracture mechanics tests in a high temperature both oxygenated and

de-aerated water were carried out at the speed of 0,001 mm/min. $J_{0,1}$ and $\delta_{0,1}$ were used to characterize the fracture behaviour of ligaments.

Fig. 10 and Fig. 11 show the J-R and δ -R curves obtained in air at 290°C and 320°C. No effect of tube expansion technology was found both at 290°C and 320°C. The values of $J_{0,1}$ and $\delta_{0,1}$ were expressed like stress intensity factors K_{CJ} , $K_{\delta C}$.

The values K_{CJ} and $K_{\delta C}$ calculated for both temperatures investigated are approximately the same like those obtained at laboratory temperature and at 250°C [10]. Therefore operating temperatures of collectors correspond to the upper shelf region of fracture behaviour of 10NiMo8.5 steel.

The effect of dissolved oxygen content on fracture behaviour of studied steel in water at 290°C is summarized in Fig. 12. In the case of testing in high temperature oxygenated water remarkably lower δ -R curve compared with that in air was received. Provided that the dissolved oxygen content was kept below 10 ppb no effect of water environment on fracture behaviour was found.

The effect of tube expansion technology on the residual stresses on the surfaces of holes.

X-ray diffraction analysis was used for measuring residual stresses on the surfaces of holes for heat exchange tubes. The test pieces were cutted from central parts of experimental blocks (see Fig. 2c). The results of axial and tangential residual stresses measurements are summarized in tab. III and tab. IV. The obtained results show that an appropriate drilling technology results in compressive stresses on the hole surface lowering the probability of crack initiation. While explosive expansion technology produces tensile residual stresses, protective compressive stresses are produced by hydraulic expansion technology. However these protective compressive stresses are lowered significantly by low temperature heat treatment (450°C/24h). On the other hand this heat treatment have little effect on the level of tangential tensile stresses produced by explosive expansion technology. But the level of tangential stresses is the driving force for environmentally assisted cracking of ligaments.

Tab. III The effect of drilling and expansion technology on the level of tangential residual stresses.

	as received/condition	after 290°C/24h	after 450°C/24h
after drilling	-204 MPa	-100 MPa	-37 MPa
after hydraulic expansion	-308 MPa	-262 MPa	-60 MPa
after explosive expansion	131 MPa	89 MPa	205 MPa

Tab. IV The effect of drilling and expansion technology on the level of axial residual stresses.

	as received/condition	after 290°C/24h	after 450°C/24h
after drilling	-204 MPa	-264 MPa	27 MPa
after hydraulic expansion	-658 MPa	-249 MPa	-54 MPa
after explosive expansion	164 MPa	152 MPa	-21 MPa

Conclusions

From the results obtained in this study it follows that:

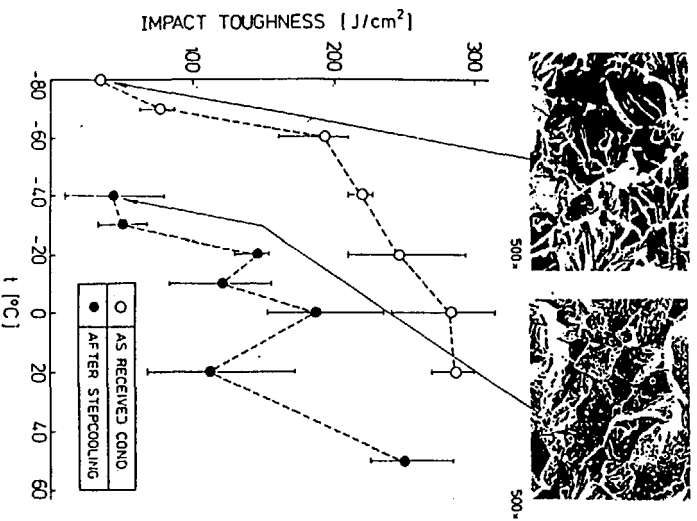
- 1) Strain ageing of 10NiMo8.5 steel affected neither the threshold value K_{th} nor the dependence of the fatigue crack growth rate on ΔK .
- 2) A reasonable agreement between anodic dissolution/film rupture model proposed by Ford and Andresen and experimental data obtained at 295°C was noted.
- 3) Oxygen content dissolved in water affects significantly the crack growth behaviour kinetics of fatigue.
- 4) Anodic dissolution at the crack tip and hydrogen embrittlement of material ahead of the crack tip are the main mechanisms responsible for fatigue crack growth rate enhancement in water. The temperature of 200°C seems to be the crossover point between the dominance of hydrogen embrittlement and anodic dissolution mechanisms for low alloy steels.
- 5) Corrosion potential and hence dissolved oxygen level affects significantly resistance of 10NiMo8.5 steel to stress corrosion cracking. It is possible to stop the growing crack by lowering the ECP to the level of -0,240 V_{SHE}.
- 6) Tube expansion technology doesn't affect fracture behaviour of ligaments both at 290°C and 320°C.
- 7) Operating temperature of collectors correspond to the upper shelf region of fracture behaviour of 10NiMo8.5 steel.
- 8) High temperature oxygenated water lower significantly δ -R curve compared with that in air.
- 9) Provided that the dissolved oxygen content was kept below 10 ppb no effect of water environment on fracture behaviour was found.
- 10) Appropriate drilling technology results in compressive stresses on the hole surface lowering the probability of crack initiation.
- 11) While explosive expansion technology produces tensile residual stresses, protective compressive stresses are produced by hydraulic expansion technology.

References

- [1] FORD, F.P.: 3 Mechanisms of Environmentally Assisted Cracking. Int. J. Pres. Ves. and Piping 40 (1989), p. 343.
- [2] IAEA extrabudgetary programme on the safety of WWER NPPs. Final report of the consultants' meetings on steam generator collector integrity of WWER-1000 reactors. Vienna, May 1993, WWER-RD-0057.
- [3] OHTANI, H.- McMAHON, C.J.: Modes of Fracture in Temper Embrittled Steels. Acta Metallurgica, Vol. 23, 1975, p. 377.
- [4] MATOCHA, K.- WOZNIAK, J.- SIEGL, J.: The Effect of Strain Aging on the Propagation of Fatigue Cracks in NiMoV Alloy Steel. In: Proc. of the IAEA Specialists Meeting on Thermal and Mechanical Degradation in Reactor Materials. Abington 19-21 November, (1991), p.167.

- [5] JAHNS, J.: The Corrosion Mechanical Damage of Low Alloy Steel of Type 10GN2MFA (10NiMo8.5) in Secondary Side Water Environment at 290°C, (in Czech). Research and Development Division Report, CZ-10/96, Vítkovice, J.S.C., March, (1996).
- [6] HIRT, J.P.: Metallurgical Transactions A, Vol.11A, (1980), p.86.
- [7] MATOCHA, K.- WOZNIAK, J.- JAHNS, J.- SIEGL, J.- NEDBAL, I.: Subcritical Crack Growth Behaviour of 10NiMo8.5 Steel Type a 508 Cl. 3a Steel in Air and High Temperature Water. In: Proc. of seventh Int.Symp. on Environmental Degradation of Materials in Nuclear Power Systems - Water Reactors. Breckenridge, Colorado, Vol.2, p.1169.
- [8] ESIS Procedure for determining the fracture behaviour of materials. ESIS P2-92, January 1992.
- [9] KIM, I.S.: Dynamic Strain Ageing Effect on Fracture Toughness of Vessel Steels. Presented at IAEA Technical Committee Meeting on Materials for advanced Water-cooled Reactors, Plzeň, 14-17 May 1991, Czech Rep.
- [10] MATOCHA, K.- WOZNIAK, J.: The Effect of Strain Ageing on Fracture Behaviour in Air and High Temperature Water at Operating Temperatures of Collectors, (in Czech), Report of Research and Development Div., VÍTKOVICE, J.S.C., CZ-50/95, June, 1995.

10NiMo8.5



10NiMo8.5

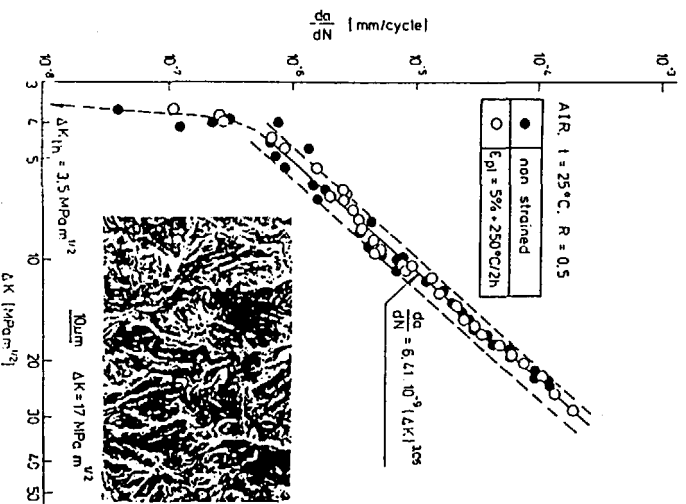


Fig. 1

Fig. 3

10NiMo8.5

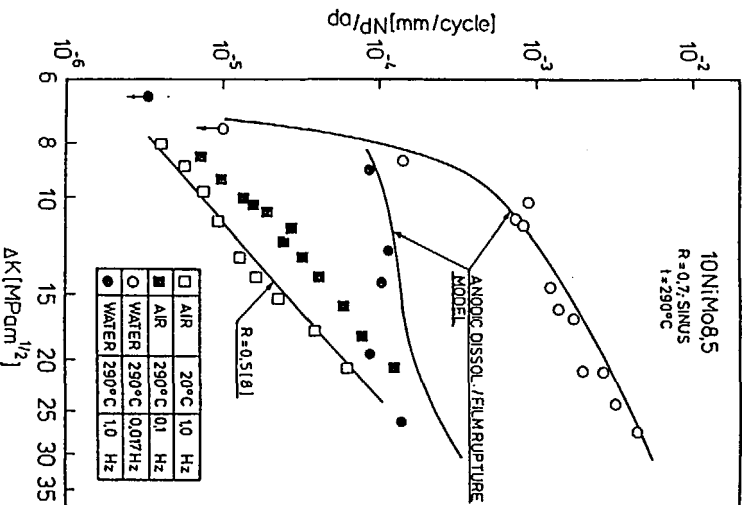


Fig. 4

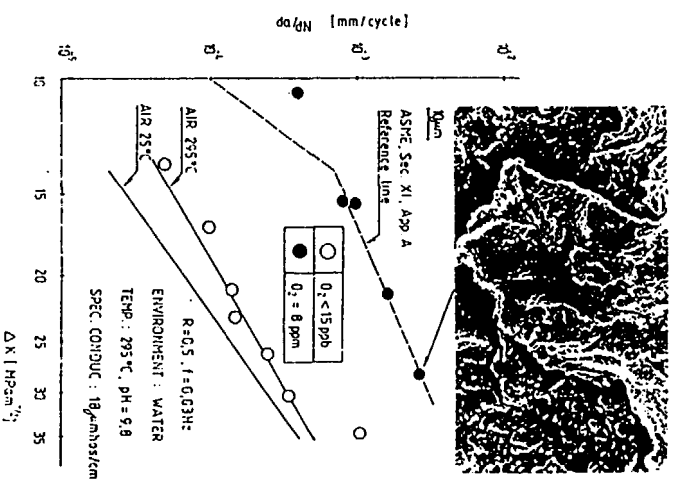


Fig. 5

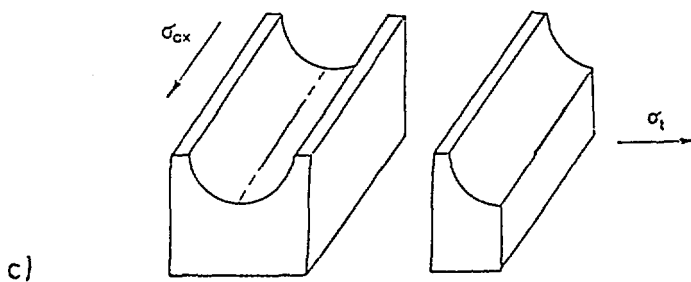
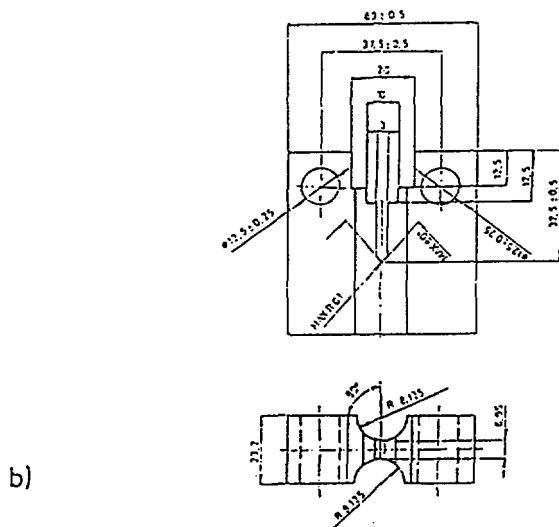
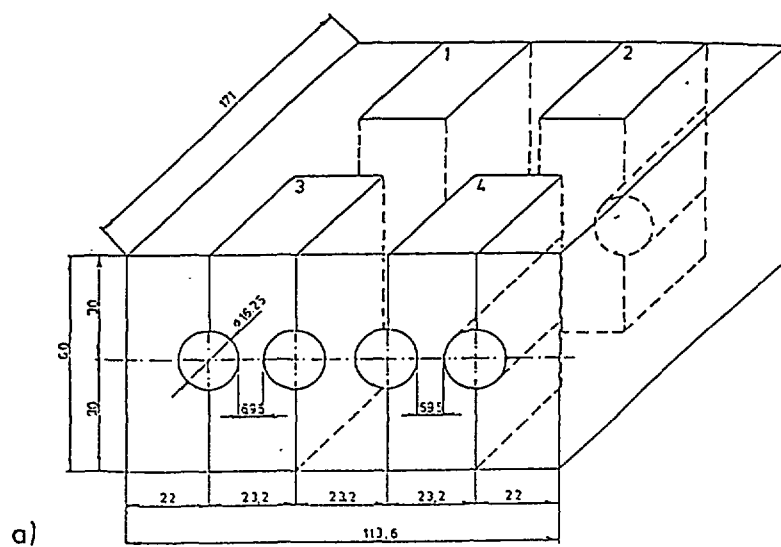


Fig. 2

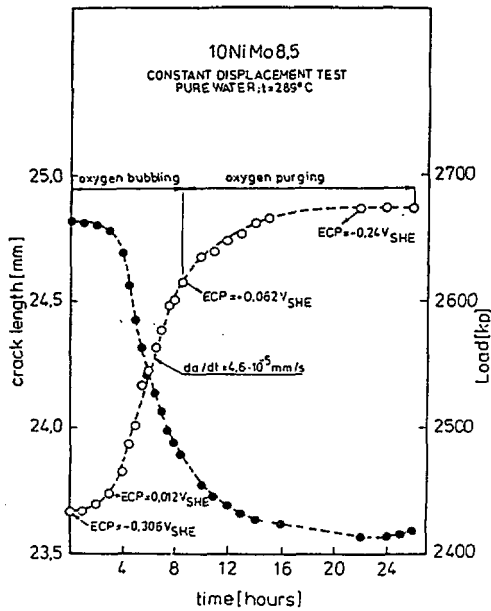


Fig. 6

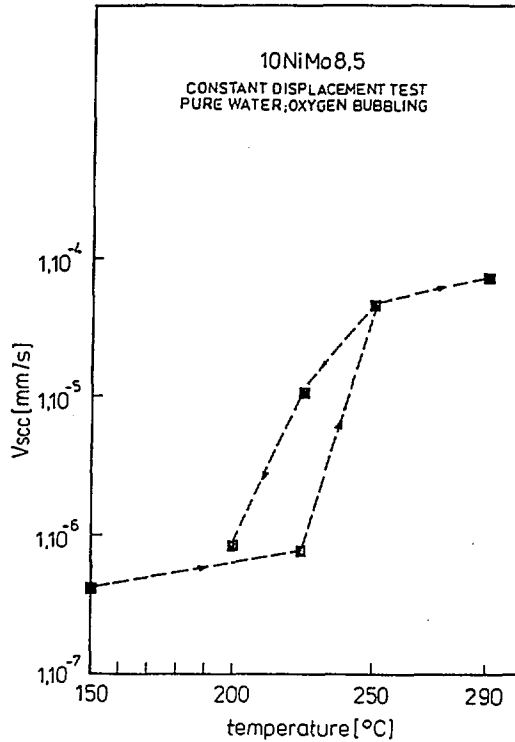


Fig. 7

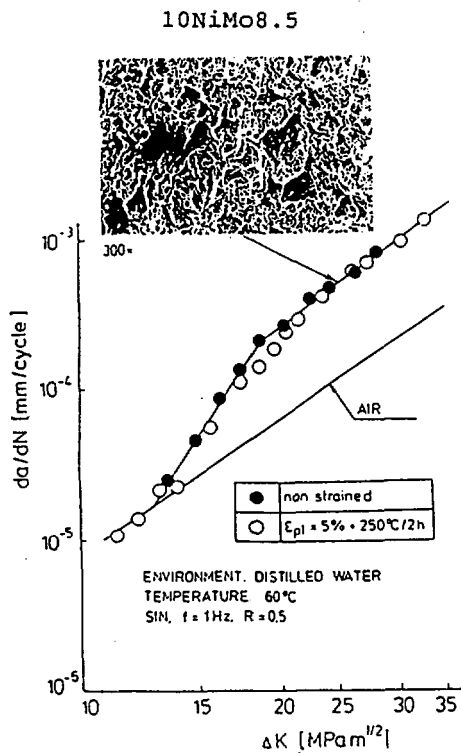


Fig. 8

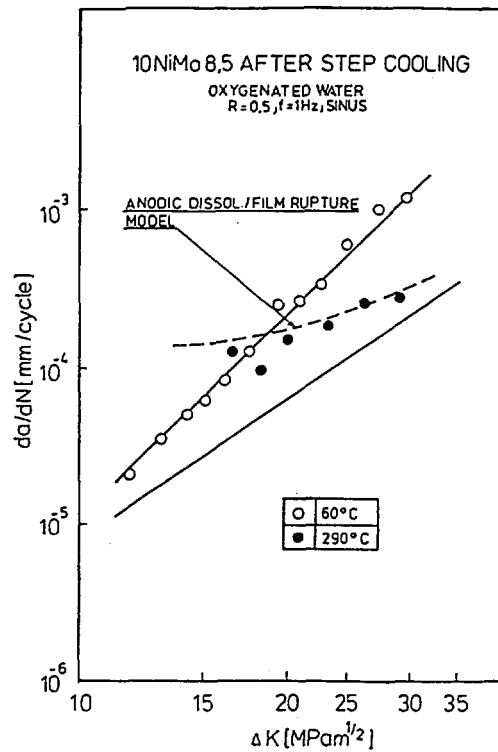


Fig. 9

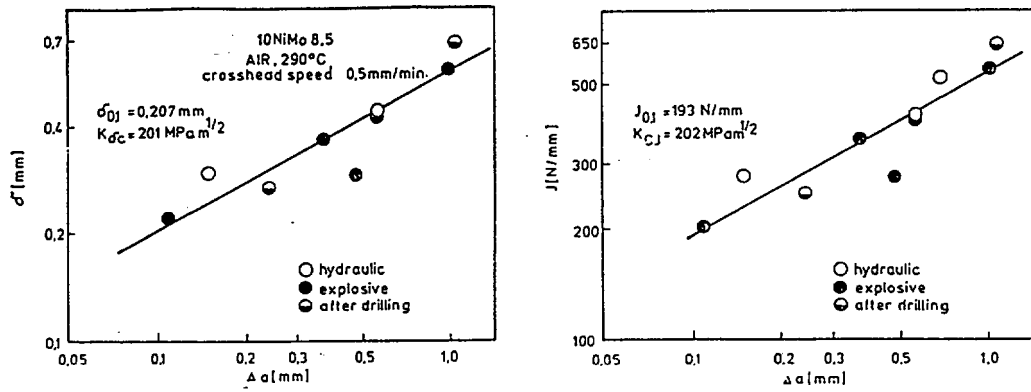


Fig. 10

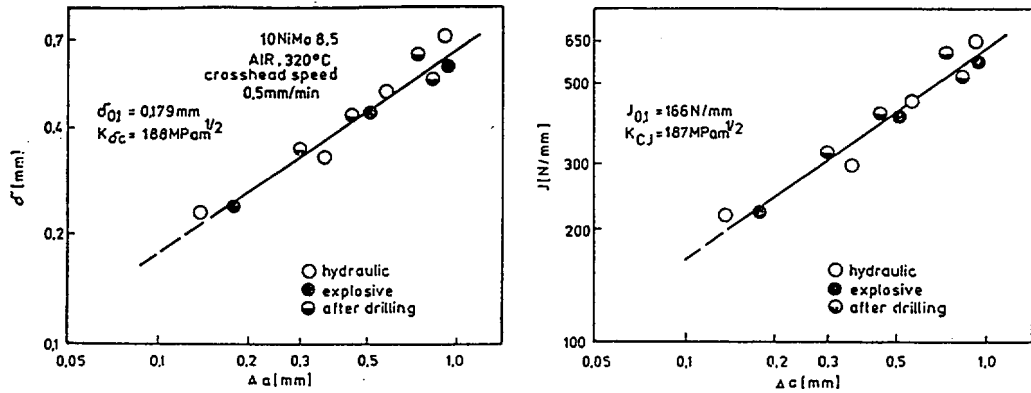


Fig. 11

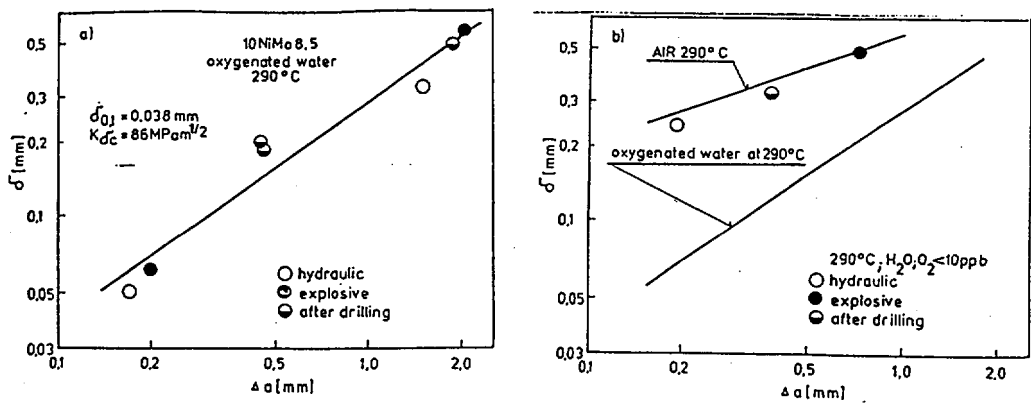


Fig. 12



Analysis of WWER 440 SG Primary Collector Bolted Joint Damage

K. Matocha* , J. Wozniak* , K. Pochman**

***Research and Development Division, Vítkovice , J.S.C., Ostrava , Czech Rep.**

**** NPP Dukovany, Czech Rep.**

Introduction

Bolted joint of a WWER 440 SG primary collector cover with a flange (see Fig. 1) was found to be the area of increased damage.

Cracking of bolts, made of type CHN35VT-VD stainless steel, is revealed from time to time by penetration test during in service inspections. Intergranular cracks are initiated from the thread roots and growth in thumb nail manner due to stress corrosion cracking.

In some cases cracks appeared also in threaded holes of the primary collector flange after some years of operation due to stress corrosion cracking of type 08CH18N10T (AISI 321) stainless steel. The replacement of the collector upper part had to be performed by cutting off the damaged portion with special equipment and welding a new upper part.

Stress corrosion cracking occurs when a susceptible alloy is exposed to a specific aggressive environment at a stress above a critical value. Crack propagation occurs when the parameters defining each of these conditions reach a critical value. If one of the parameters becomes non critical cracking may cease [1].

High level of bending stresses due to inconvenient method of bolt tightening and residual stresses in tension can raise the stress level above the critical value. The analysis of water solution withdrawn from the threaded holes and sediments on thread surfaces revealed high concentrations of Cl^- and SO_4^{2-} and the presence of copper ion, most likely from corrosion of brass condensers.

It is known that susceptibility of stainless steels to stress corrosion cracking is enhanced by chloride contamination of water in the presence of oxidant [2], [3]. The presence of SO_4^{2-} inhibits repassivation of steels, nickel base alloys and stainless steels. The presence of sulfide in excess of about 50 ppm can initiate accelerated EAC (environmentally assisted cracking) in the complete absence of any oxidant [4].

In this paper susceptibility of CHN35VT-VD and 08CH18N10T stainless steels to stress corrosion cracking in water environment, simulating water solution found in threaded holes, was investigated using rising load line displacement tests of precracked C(T) specimens. To judge the role of oxidant on stress corrosion cracking of both stainless steels, the effect of dissolved oxygen content (fully deaerated water, water aerated at the beginning of the test) was studied.

Experimental procedure

Rising load experiments were performed on type 08CH18N10T and type CHN35VT-VD stainless steels in air and high temperature water environment. The characteristic feature of fracture behaviour of both steels in air from 20°C to 300°C is a ductile stable crack growth. To be able to judge the effect of water environment on subcritical crack growth the variation in δ with Δa was investigated at load line displacement rate of 0,5 mm/min. using multiple specimen method [5].

Slow strain rate tests of C(T) precracked side grooved test specimens in high temperature water environment were used for investigating the susceptibility of the steels to stress corrosion

cracking [6]. The tests in both aerated and deaerated water solutions were carried out in an 11 litre static autoclave at the load line displacement rate of $5 \cdot 10^{-4}$ mm/min. δ -R curves obtained by multiple specimens method in water environment were compared with those gained in air environment.

SCC behaviour of type CHN35VT-VD steel was investigated at 280°C in secondary side water environment and water solution containing 10 ppm Cl^- and 30 ppm SO_4^{2-} (pH 10 treated by NaOH). Water solution containing 5 ppm Cl^- , 15 ppm SO_4^{2-} , 40 ppm Ca^{2+} , 40 ppm Al^{3+} and 300 ppm SiO_2 (pH 8,5 treated by NaOH) was used for tests on type 08CH18N10T steel at 275°C. The environmentally assisted crack growth rates and threshold values for SCC were determined for both steels from δ -R curves obtained.

Results and discussion

SCC behaviour of type CHN35VT-VD steel

1C(T) specimens (12 mm in thickness) were manufactured from forged bar (60 mm in diameter) used for manufacturing of bolts.

Fig. 2 shows δ -R curve obtained at 280°C in air together with results of slow strain rate tests carried out in WWER 440 secondary side water environment at 280°C. As the experimental data obtained in water fit very well with δ -R curve gained in air SCC is not induced in this environment. Fig. 3 summarizes results of tests carried out in water solution containing 15 ppm Cl^- and 30 ppm SO_4^{2-} at two significantly different dissolved oxygen contents. Provided that the dissolved oxygen content was less than 10 ppb no stress corrosion cracking was induced and tests resulted in fully ductile stable crack growth. However intergranular stress corrosion cracking was observed in aerated water solution. The threshold value K_{ISCC} calculated from δ -R curve for $\Delta a = 0,05$ mm is equal to $K_{\text{ISCC}} = 75 \text{ MPa}\cdot\text{m}^{1/2}$. The results obtained proved that in the absence of dissolved oxygen the alloy is not susceptible to stress corrosion cracking. Hence the presence of oxidant, most likely copper ion from corrosion of brass condensers, seems to be the main factor initiating SCC of bolts.

SCC behaviour of type 08CH18N10T

1C(T) specimens 25 mm in thickness were manufactured both from the upper part of not operated primary collector and from upper part of primary collector cutted off after 10 years of operation. To study the effect of grain size on susceptibility of 08CH18N10T steel to stress corrosion cracking testing material was cutted off from not operated collector and heat treated to obtain three significantly different grain sizes: $G = 6$ (0,044 mm in diameter), $G = 3$ (0,125 mm in diameter) and $G = -1$ (0,5 mm in diameter).

Fig. 4 shows δ -R curves in air at 280°C obtained for not operated steel and for the steel after ten years of operation at 275°C. Significantly lower δ -R curve was received for the steel after ten years of operation. However ductile dimples are, in both cases, the only characteristic fractographic feature of fracture surfaces created by stable crack growth.

The results of SSRT of precracked C(T) specimens in high temperature water environment are summarized in Fig. 5. Significant effect of water environment on δ -R curve was found in aerated water environment. On the other hand no effect of long term operation and grain size was found.

The threshold value K_{ISCC} and the average environmentally assisted crack growth rate calculated from δ -R curve by superposition based analysis method [7] are $K_{\text{ISCC}} = 43 \text{ MPa}\cdot\text{m}^{1/2}$ and $da/dt = 1,6 \cdot 10^{-6}$ mm/s respectively.

Fractographic analyses of fracture surfaces produced by stable crack growth in aerated water showed typical stress corrosion facets with crack arrest markings and some secondary

cracking in grain boundaries. Identical morphology was seen on fracture surfaces of damaged threaded holes of primary collector flange.

Testing in deaerated water environment did not induce stress corrosion cracking and resulted in ductile stable crack growth due to dimpled rupture as in the case of tests carried out in air at 275°C. These results confirmed that dissolved oxygen or another strong oxidizer must be present to induce SCC of 08CH18N10T steel in above mentioned environment.

Conclusions

- 1) Dissolved oxygen or another strong oxidizer must be present to induce SCC of both CHN35VT-VD and 08CH18N10T stainless steels in water environment containing less than 15 ppm Cl⁻ and 30 ppm SO₄²⁻.
- 2) Intergranular SCC was observed in CHN35VT-VD stainless steel similar in nature to SCC of stud bolts.
- 3) Transgranular SCC was induced in 08CH18N10T stainless steel. The same fractographic features like stress corrosion facets with crack arrest markings and some secondary cracking in grain boundaries was seen on fracture surfaces of damaged threaded holes of primary collector flange.
- 4) SCC of primary collector bolted joint is induced by simultaneous effect of high stress level mainly due to inconvenient method of bolt tightening and water environment containing oxidant most likely copper ion from corrosion of brass condensers. SCC of CHN35VT-VD and 08CH18N10T steels is enhanced by Cl⁻ and SO₄²⁻ contamination.

References

- [1] GABETTA, G.- COLE, I.: Fracture Control Guidelines for Environmentally Assisted Cracking of Low Alloy Steels. CISE 661. Presented at the 3rd ESIS Workshop on „Fracture Mechanics approach to corrosion assisted cracking“. NAL NLR, March 19, 1992.
- [2] ANDRESEN, P.A.- DUQUETTE, D.J.: Slow Strain Rate Stress Corrosion Testing at Elevated Temperatures and High Pressures. Corrosion Science, Vol. 20, 1980, p.211.
- [3] ANDRESEN, P.A.- DUQUETTE, D.J.: The Effect of Dissolved Oxygen, Chloride Ion and Applied Potential on the SCC Behaviour of Type 304 Stainless Steel in 290°C Water. CORROSION-NACE, Vol. 36, No. 8, August, 1980, p. 409.
- [4] ANDRESEN, P.L.- YOUNG, L.M.: Characterization of the Roles of Electro-chemistry, Convection and Crack Chemistry in SCC. In: Proc. of 7th Int. Symp. on Env. Degrad. of Materials in Nuclear Power Systems - Water Reactors, August 7-10, 1995, Breckenbridge, Colorado, Vol. 1, p. 579.
- [5] ESIS Procedure for determining the fracture behaviour of materials. ESIS P2-92, January 1992.
- [6] Recommendations for Stress Corrosion Testing Using Precracked Specimens Prepared for the Technical Committee 10 of ESIS, 1st Draft, March 1992.
- [7] TOIVONEN, A.- KARJALAINEN- ROIKONEN, P.: Evaluation of Environmentally Assisted Cracking Using Fracture Resistance Data. In: Proc. of EUROCORE '96, Corrosion Deformations Interactions, September 24-26, 1996, Nice, France.

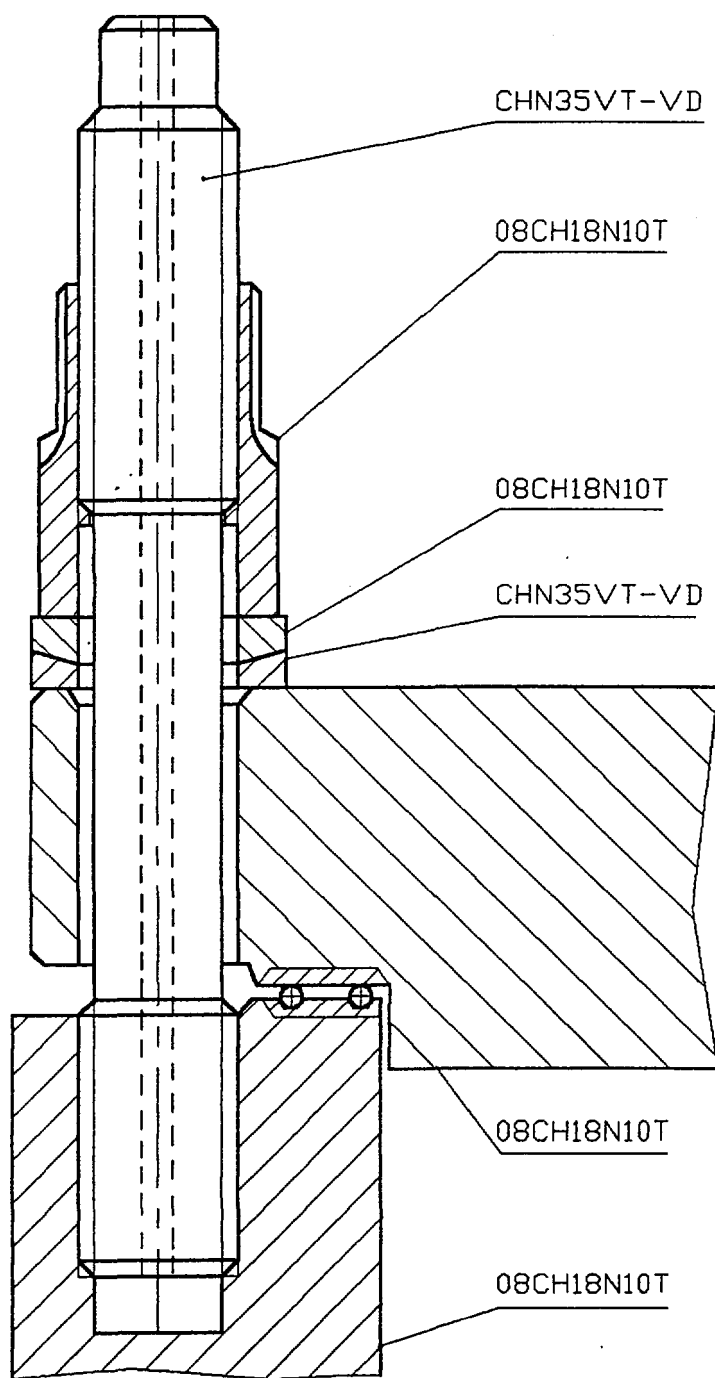


Fig. 1 Schematic drawing of WWER 440 SG primary collector bolted joint.

δ - Δa curve

Material: austenitic steel of type CHN35VT-VD

Test Temperature: 280°C

	ENVIRONMENT	DISPLACEMENT RATE
○	AIR	0,5 mm/min
●	SEC.SIDE WATER ENV.	$5 \cdot 10^{-4}$ mm/min

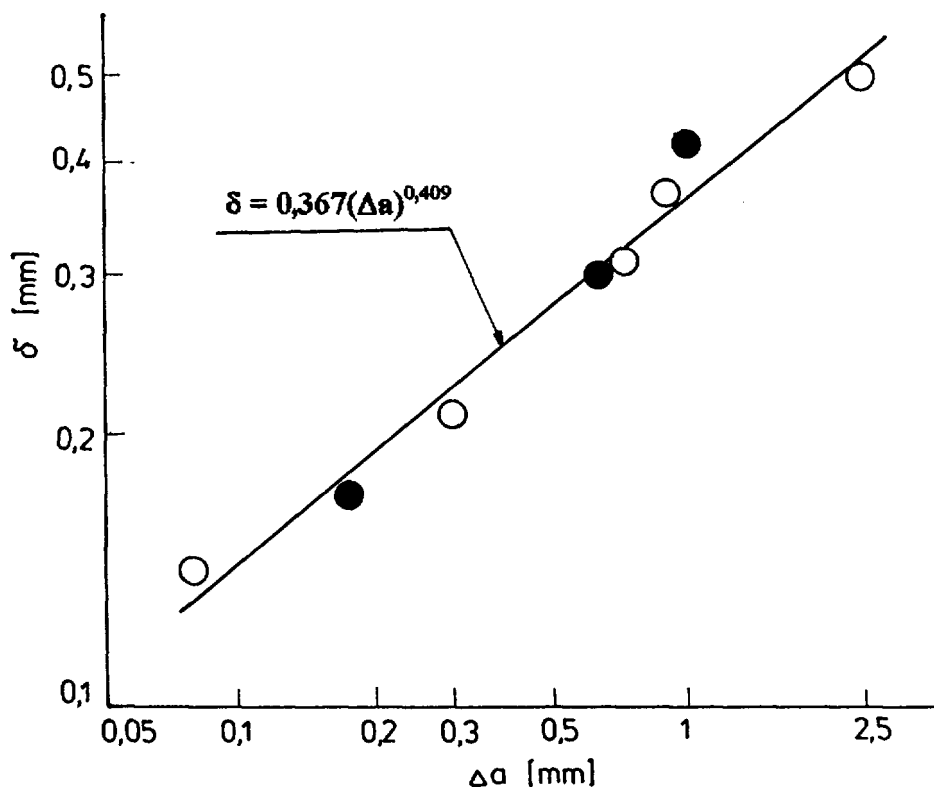


Fig. 2 The effect of secondary side water environment on δ - R curve of CHN35VT-VD stainless steel at 280°C

SSRT of precracked C(T) specimens

Material: austenitic steel of type CHN35VT-VD

Environment: H_2O containing 10 ppm Cl^- , 30 ppm SO_4^{2-}
pH 10 (treated by NaOH)

Test temperature: 280°C

Displacement rate: $5 \cdot 10^{-4}$ mm/min

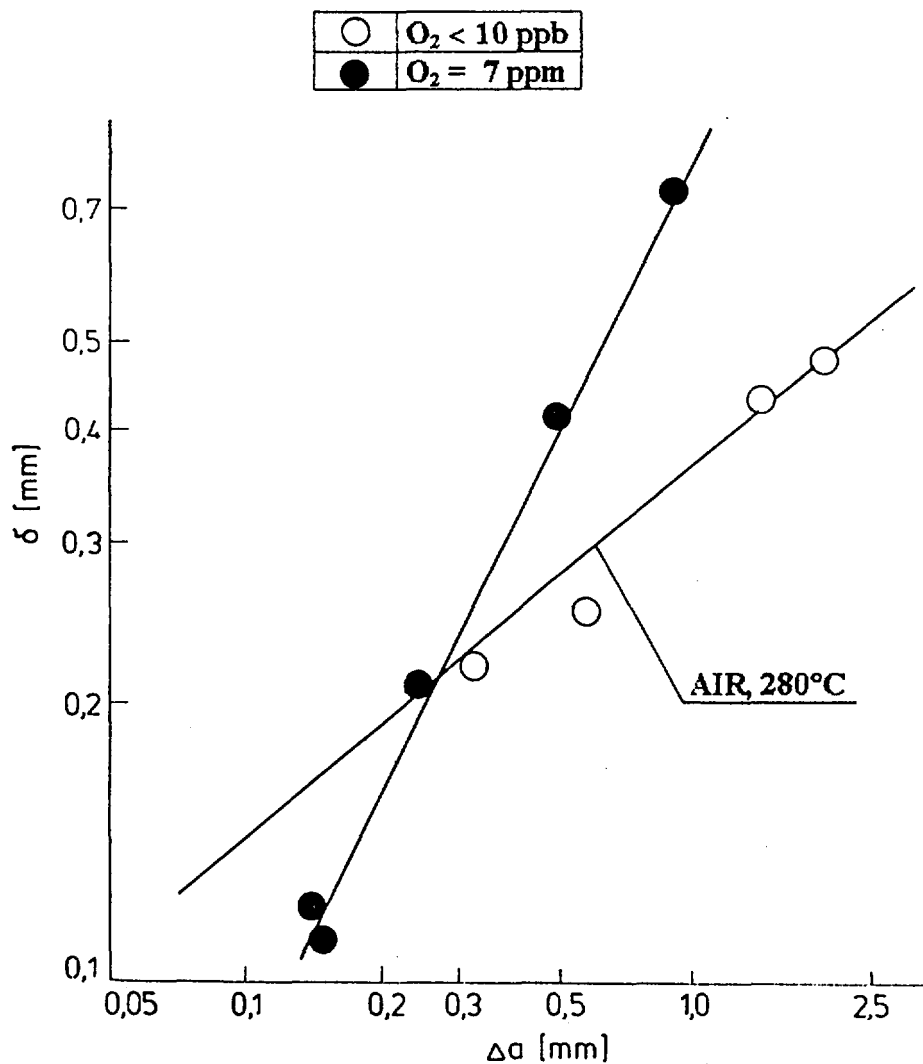


Fig. 3 The effect of dissolved oxygen content on $\delta - R$ curve of CHN35VT-VD stainless steel in water environment at 280°C .

Material: type 08CH18N10T stainless steel
 from upper part of primary collector
 Environment: air, 275°C
 Test specimens: 1C(T), orientation L-R
 Displacement rate: 0,5 mm/min

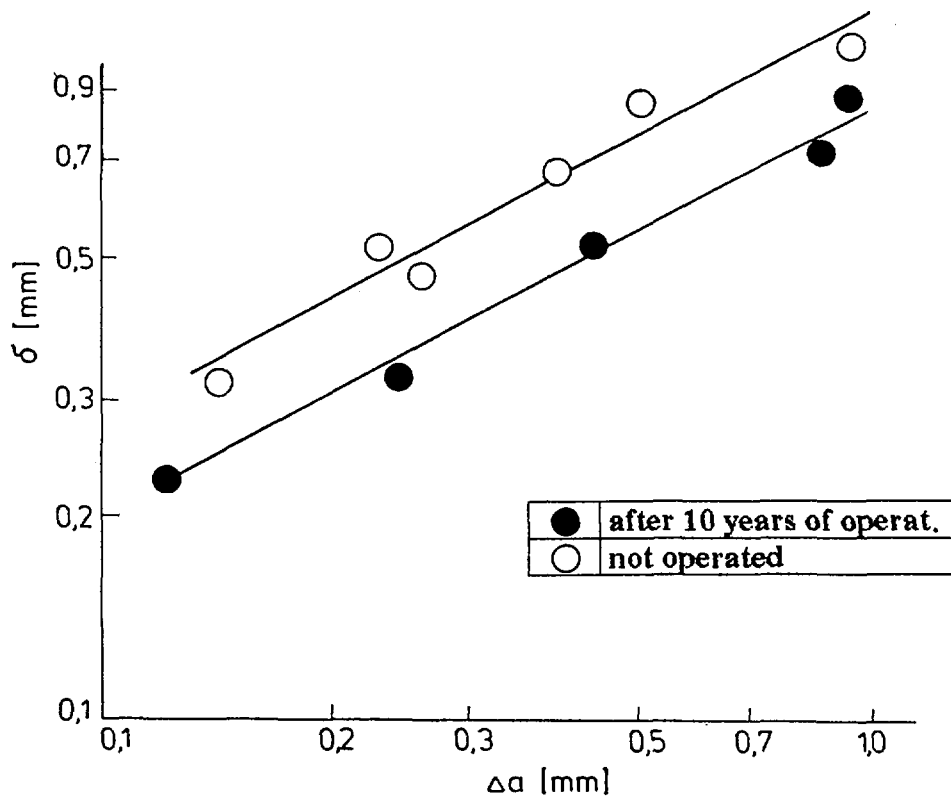


Fig. 4 The effect of long term operation on σ -R curve of 08CH18N10T stainless steel in air at 275°C.

SSRT of precracked C(T) specimens

Material: 08CH18N10T stainless steel

Environment: $\text{H}_2\text{O} + 5 \text{ ppm Cl}^- + 15 \text{ ppm SO}_4^{2-} + 40 \text{ ppm Ca}^{2+} + 40 \text{ ppm Al}^{3+} + 300 \text{ ppm SiO}_2$ pH 8,5 (treated by NaOH)

Test temperature: 275°C

Displacement rate: $5 \cdot 10^{-4} \text{ mm/min}$

	08CH18N10T	GRAIN SIZE	O ₂
○	after 10 years of op.	G = 6(7)	7 ppm
□	after 10 years of op.	G = 6(7)	< 10 ppb
●	not operated	G = -1	7 ppm
◐	not operated	G = 3	7 ppm
◑	not operated	G = 6(7)	7 ppm

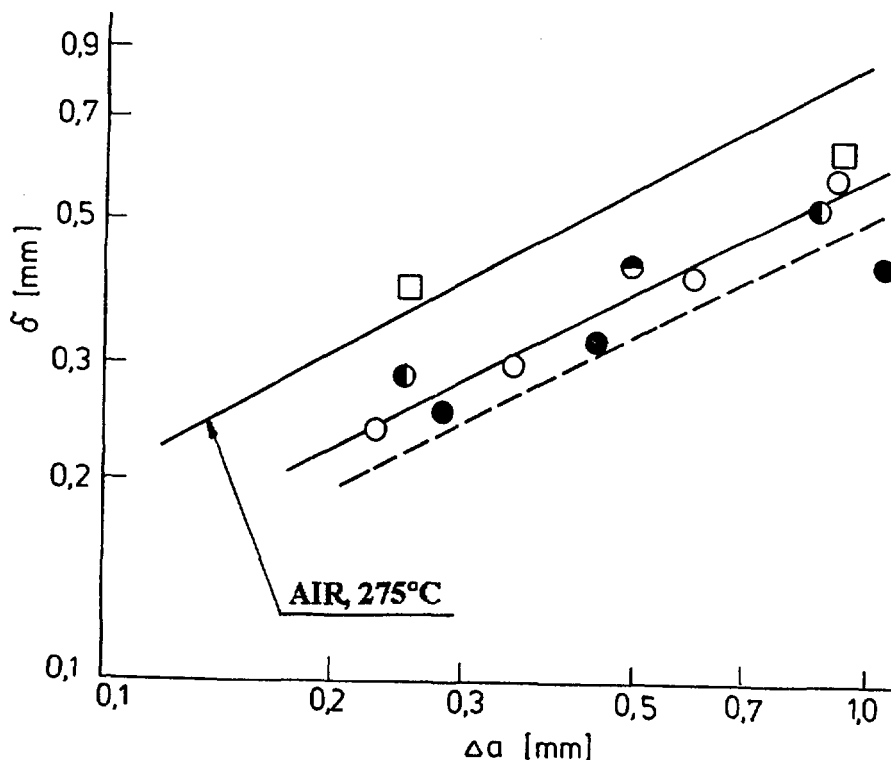


Fig. 5 Results of SSRT of precracked C(T) specimens of 08CH18N10T in aerated and deaerated water environment at 275°C. Effect of grain size.



COOLANT STRATIFICATION AND ITS THERMOHYDRODYNAMIC SPECIFICITY UNDER NATURAL CIRCULATION IN HORIZONTAL STEAM GENERATOR COLLECTORS

A.Blagovechtchenski, V.Leontieva, A.Mitriukhin

Saint-Petersburg Technical University, Russia.

The operation of existing nuclear reactor plants (NRP) requires special attention to guarantee the safety.

The maintenance of nuclear safety is a complex problem and it must be solved with help of some technical and organization measures, including creation of special safety system (SS).

One of the main safety principle used in creation of the safety system are the passive ways. Coolant natural circulation (NCC) is the basic mean used in those systems if pump circulation (PCC) has an accident stop. It can be used in other proceses, such as a normal core cooling, heating and so on. However, the wide using of NC demands to study its specificity.

There are some differences between natural and pump circulation. The coolant speed under natural circulation is much less then under pump circulation. The temperature stratification in the hot reactor plenum and in the upper part of horizontal steam generator collectors is the consequence of this difference.

Stratification is the peeling of coolant for "hot" and "cold" parts. There is a thin (~some cm.) layer containing large temperature drop between that parts. It leads to increased stresses in metal equipment. Therefore stratification is a dangerous and undesirable phenomenon. Moreover it may limit some other technological processes. There are some russian and foreign research devoted to this phenomenon in the reactor upper plenum, but there are no articles about the stratification in the upper part of horizontal steam generator collectors.

Hot and cold collectors are geoimetrically identical, and so we studied collectors proceses at the same facility changing the inlet and outlet of coolant water.

The facility (fig.1) is intending for research of the stratification phenomenon in the hot plenum of reactor and upper parts of the steam generator collectors. It is a flat facility with line scaling factor 1:10. It has the transparent walls and it makes possible to watch the process of stratification initiation under injection with a dye, to make pictures and to use a laser flowmeter. The coolant inlet was from

bellow and outlet was from the side of experimental plenum walls during research of the hot collector and inversely during research of the cold collector.

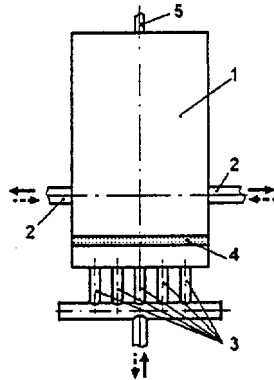


Fig.1.Experimental facility.

1 - plenum; 2 - side branch pipes; 3 - lower branch pipes;
4 - stabilizing plate; 5 - vapour pipe

—————→ coolant inlet-outlet in the hot collector

- - - - -→ coolant inlet-outlet in the cold collector

The aim of the experiments was to define the conditions of the stratification initiation, the researching of the temperature field in upper part, the definition of the characteristics in the stratification layer, the researching of the factors which cause the intensivity of the stagnant volume cooling.

The experimental model is not identical to the real object (it has no real inlet-outlet of coolant depending on the height), the results of this experiment do not give the real numbers but they show the whole picture, near identical to the real object. The main criterion for the stratification regimes is the ratio of Grashoff number to the square of Reynolds number which is called Richardson number:

$$Ri = \frac{Gr}{Re^2} = \frac{g\beta L\Delta T}{w^2},$$

β - the volume expansion coefficient, L - characteristic size, ΔT - temperature drop, w - coolant speed. Ri number was counted for the drainage part of experimental facility (hydraulic diameter of the plenum and the speed in it).

The experiments showed the following rules: in both cases (coolant injection from beneath (hot collector) and when coolant injection was from the side walls (cold collector)) beginning with some limit of Richardson number there begins the stratification, the volume above the stratification layer becomes stagnant and cooling goes slowly, the temperature picture for the both cases are identical (fig. 2).

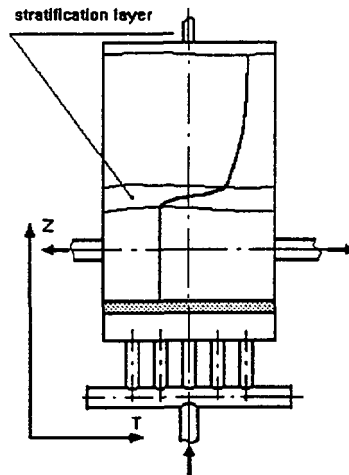


Fig.2. The temperature profil

The reducing of the coolant temperature in a stagnant volume depends on two processes. One of them - the heat transference through the stratification layer. The temperature, depending on the height, may be described with help of nonstationary heat transfer equation under definite border and initial conditions. The other process is the removing of the stagnant volume when the stratification layer has a contact with the coolant in a drainage part and that is why the stratification layer moves slowly up.

On fig.2 one can see a big temperature drop in stratification layer and, therefore, big density drop. This density drop prevents the penetration of the flows from the drainage part into the stagnant part, lowers the turbulence, which causes the wave generation in the stratification layer with frequencies under 1 Hz.

In the hot collector (fig.3) the coolant flow hits the stratification layer and moves a part of it, turns back and leaves the facility. This situation is stable enough, the stratification layer goes up, it keeps its horizontal orientation. The cooling of the stagnant volume goes mainly because of heat transference. The stratification may be initiated under condition $Ri > 2,5$.

It is necessary to count the temperature field properly to solve the durability problems.

We offer to use one-dimension heat transfer equation with effective coefficient of thermal diffusivity, which is unknown. It leads to the necessity of solving the inversed heat transfer problem. To solve this problem we need to have the dependence of temperature on time in some inner point of volume, which may be obtained experimentally. The processes which we have in a stratification layer and in stagnant volume are very different, so it is necessary to count temperature for these processes separately obtaining different numerical effective thermal diffusivity coefficient.

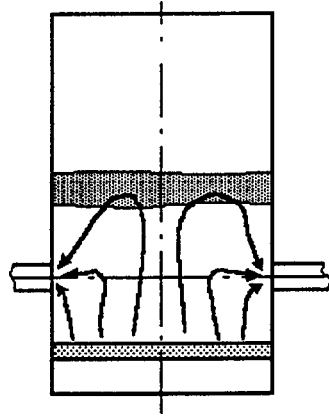



Fig.3. Flow picture in the hot collector.

 stratification layer.

Mathematical model will be:

$$\frac{\partial T_1}{\partial t} = a_1 \frac{\partial^2 T_1}{\partial z^2}, \quad z_{b1}(t) < z < z_{b2}(t) \quad t > 0 \quad (1)$$

$$T_1|_{z=0} = T_0(z) \quad T_1|_{z=z_{b1}} = g_1(t) \quad T_1|_{z=z_{b2}} = g_2(t) \quad (2)$$

$$\dot{Q}_{exp}|_{z=d} = f(t) \quad z_{b1}(t) < d < z_{b2}(t) \quad (3)$$

$$\frac{\partial T_2}{\partial t} = a_2 \frac{\partial^2 T_2}{\partial z^2}, \quad z_{b1}(t) < z < l \quad t > 0 \quad (4)$$

$$T_2|_{z=0}=T_0(z) \quad T_2|_{z=z_{b1}}=T_1|_{z=z_{b2}} \quad (5)$$

The second border condition for the volume with stratification may be regarded in two cases and depends on the conditions of experiments.

$$T_2|_{z=H}=g_3(t) \quad \text{ore} \quad \left. \frac{\partial T_2}{\partial t} \right|_{z=H} = 0 \quad (6)$$

$$\dot{O}_{exp}|_{z=d}=\varphi(t) \quad z_{b1}(t)<d_i<H \quad (7)$$

z_{b1} - the lower border coordinate of the layer, z_{b2} - the upper border coordinate of the layer.

Here index "1" is used for the stratification layer and index "2" - for the stratification volume.

T - the temperature, t - time, z - the coordinate, T_{exp} - the experimental temperature function, H - the height of volume, a - effective thermal diffusivity coefficient.

To define the thermal diffusivity coefficient (the solving of the inversed propleme) it is used the extreme method, based on the finding of the minimum, of functional of the difference with help of gradient descent.

$$J = \frac{1}{2} \sum_{i=1}^N \int_0^{t_m} \rho_i [T(d_i, t, a) - f_i(t)]^2 dt \rightarrow \min, \quad (8)$$

t_m - the maximum calculating time.

To find the effective thermal diffusivity coefficient we use the iteration procedure with help of gradient descent method.

$$\dot{a}_{n+1}=a_n+\Delta a_n \quad (9)$$

$$\Delta a_n = - \frac{\int_0^{t_m} [T(d_i, t, a_n) - f_i(t)] \vartheta(d_i, t, a_n) dt}{\int_0^{t_m} [\vartheta(d_i, t, a_n)]^2 dt}, \quad (10)$$

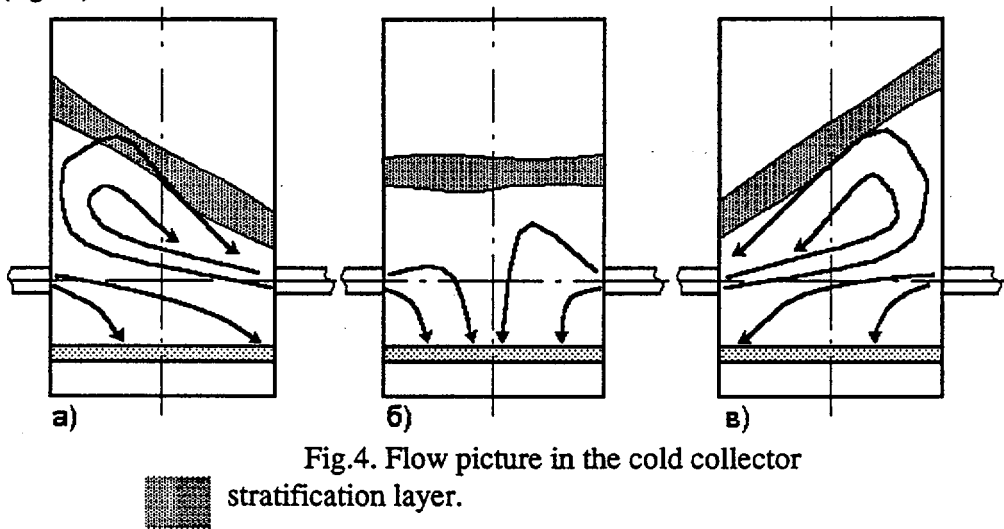
n - the number of iteration, i - the number of the point, where the temperature is used as an additional information.

$\vartheta = \frac{\partial T}{\partial a}$ - is a function of sensivity of the researched system to small variation of the a parameter.

Our calculations showed that the effective thermal diffusivity coefficient in a stratification layer has order of magnitude $10^{-2} \text{ m}^2/\text{s}$, this is by a factor of 10^3 more than in stratificated volume. This was an expected result. The main part of cooling there gives the stratificated layer. The wavering of the layer have an influence on the stagnant volume, therefore the effective thermal diffusivity coefficient in it is higher then thermal diffusivity coefficient in water more then by a factor of 10^2 .

The coolant current in a cold collector has big difference to a hot collector. The coolant in a cold collector goes from the sides and the streams have the contact with the layer along a tangent and, therefore, the stratifications begins earlear ($Ri > 1,5$). However, the futher process depends on the interaction of the contrary streams. The streams enters the plenum with high initial speed, they meets in the center of the plenum and one stream sink another and this process has an equal probability.

When one of the stream appears above, it goes up along the wall, it lift the stratification layer, then the stream turns around and sink itself (fig.4a). After this it happens an equilibrium (fig.4â) and then the streams change each other (fig.4â).



So, in a "cold" collector besides smallwavering of the stratification layer there are big wavering in a scale of plenum. This leads to the more intensive removing of

the stagnant volume. Such the processes with high speeds of a coolant makes the cooling of a stagnant volume more intensive then in a hot collector.

The flow is more stable under low coolant outlet. The macro wavering of the stratification layer is decreasing to the full stop. The experiments in wich there were used imitation plates (fig. 5) wich lower the inlet speed confirmed this. Besides it, this experiments showed that the inlet coolant speed influences on the stratification regime very much. It may be seen at a fig.6, where the left curve was obtained without the inlet imitation plates and the right curve - with them. These two curves compose one dependence.

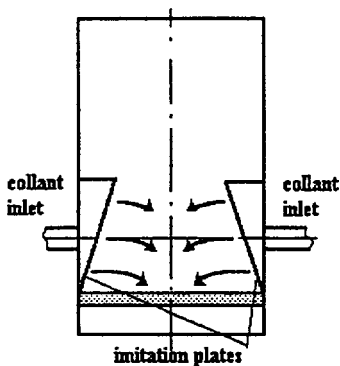


Fig. 5

The facility with imitation plates

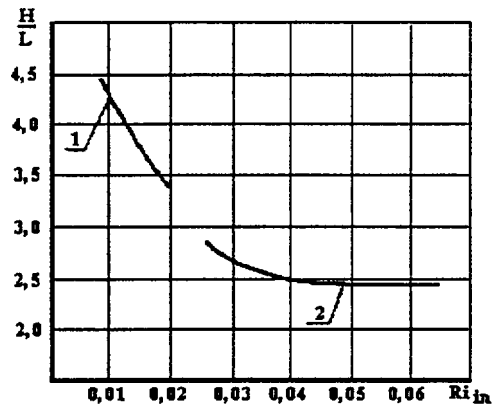


Fig.6

The stratification layer coordinate in Richardson number

- 1 - The facility without plates
- 2 - The facility with plates



ABOUT TECHNICAL POSSIBILITY TO USE VEERA FACILITY FOR INVESTIGATION OF COOLANT STRATIFICATION PHENOMENON IN HORIZONTAL STEAM GENERATORS

Valeri Mitioukov, Andrei Mitrioukhine
St. Petersburg State Technical University, Russia

Virpi Kortenieniemi
Lappeenranta University of Technology, Finland

1. Introduction

Coolant natural circulation provides a basic means of reactor core cooling during incidents and accidents where the main circulation pumps stop. Natural circulation is a passive mechanism: the driving hydrostatic head for natural circulation is created by coolant temperature differences (hence, by density differences) in the primary loops.

There are several aspects which must be considered when the effect of thermal stratification to the reactor safety is studied. The main points are effects to thermal stress, to the loop flow and to the reactivity. The temperature gradient can be sharp and it can occur in short distance (in fact only few centimeters) which increase the thermal stress of the structures. Thermal stratification can have very significant effect to the loop flow during natural circulation. In natural circulation the mass flow rate in the loop is so low that coolant can stratify according to the temperatures.

Thermal stratification can occur in almost any part of the reactor cooling system. Most obvious locations are upper plenum, primary loops and top of steam generator collectors. During accidents cold emergency core cooling water can cause stratification to these locations.

This paper gives a brief insight on possibility of using the VEERA facility in studying the stratification phenomenon. The idea for such experiments is to use the facility upper plenum part to simulate the conditions in upper part of horizontal steam generator hot collector. The upper part of steam generator hot collector is one of the locations where the stratification can take part during natural circulation mode.

2. VEERA facility /1/

The VEERA facility was built in 1987 in cooperation of Technical Research Centre of Finland (VTT), Lappeenranta University of Technology and Imatran Voima Oy. The facility is located at Lappeenranta University of Technology in the nuclear engineering research laboratory. The reference reactor for VEERA is the modified Soviet VVER-440 design of the

Loviisa nuclear power plant. The main design principle is the accurate simulation of the rod bundle geometry and the geometry of the structures above the rod bundle. The VEERA facility was originally built as part of a joint research program of the three partners in the studying the mixing and concentration of aqueous boric acid solution during pressurized water reactor loss-of-coolant accident.

There has been three different versions of VEERA facility. The first two versions were constructed for performing the boric acid experiments. Total three series of this type experiments have been carried out with VEERA. The last and present version of VEERA was adopted in order to use the facility for studies of the reflooding phenomenon. The objective of the experiments was to collect data for the improvement and verification of reflood models in different computer codes. The test matrix includes experiments with different emergency core cooling modes, power levels, initial rod surface temperatures and emergency core cooling water subcooling. Also, some boil-off experiments were carried out with the facility, /1/, /2/.

The reactor vessel in the VEERA facility is simulated by a stainless steel U-tube structure consisting of a downcomer, lower plenum, core, core outlet throttle and upper plenum, Fig. 1. The primary circuit loops with horizontal steam generators are not simulated in the VEERA facility. The exhaust steam line consists of a moisture separator and condenser. The major design characters of the VEERA facility are given in Table 1.

All elevations in the reactor vessel simulator below the hot leg connection are scaled 1:1. The scale of volumes and flow areas is 1:349 referring to the number of fuel rod simulators in the facility and the number of the fuel rods in the reference reactor.

The test section includes one full-scale copy of a VVER-440 reactor rod bundle. It consists of 126 electrically heated rod simulators and an unheated cold centre rod, which replaces the support tube of the actual fuel bundle. The bundle is enclosed in a thermally insulated hexagonal shroud. The inside distance of the opposite walls of the hexagonal shroud is 139 mm and the wall thickness 4 mm. Viewing windows on the side walls of the channel box can be used in visual observing of different phenomena in core part.

The heating coils are inside stainless steel cladding in a magnesium oxide insulation. The heated length, the outer diameter and the lattice pitch of the fuel rod simulators, as well as the number and construction of the rod bundle spacers, are the same as in the reference reactor. In order to simulate better the actual power profile of the reference reactor a nine-step chopped cosine axial power distribution is adopted.

The structures near the core top, i.e. the core outlet nozzles, are accurately simulated. The flow area of the perforated plate inside the core outlet nozzle corresponds to that of the upper tie plate of the reference reactor. The structures below the core are not simulated exactly due to the electric connections to the rod simulators. Surface heaters are installed on the side walls in different parts of the facility. The whole facility housing, except the viewing windows, is thermally insulated with mineral wool.

The main measurements in the earlier VEERA experiments have been coolant and cladding temperatures, system pressure, pressure differences and heating power. Thermocouples are used for temperature measurements. Most of them are in the rod bundle in different radial and axial locations. Thermocouples measuring coolant and cladding temperatures are of the NiCr-

Ni type with a 0,5 mm diameter. Wall temperatures are measured with 1,0 mm or 1,5 mm diameter thermocouples. System pressure is measured with a sensor in the upper plenum. Pressure taps and transducers are used for pressure difference measurements. The total number of temperature measurements and pressure and differential pressure transducers is 55 and 8 respectively. The general instrumentation of the VEERA facility is shown in Fig. 2.

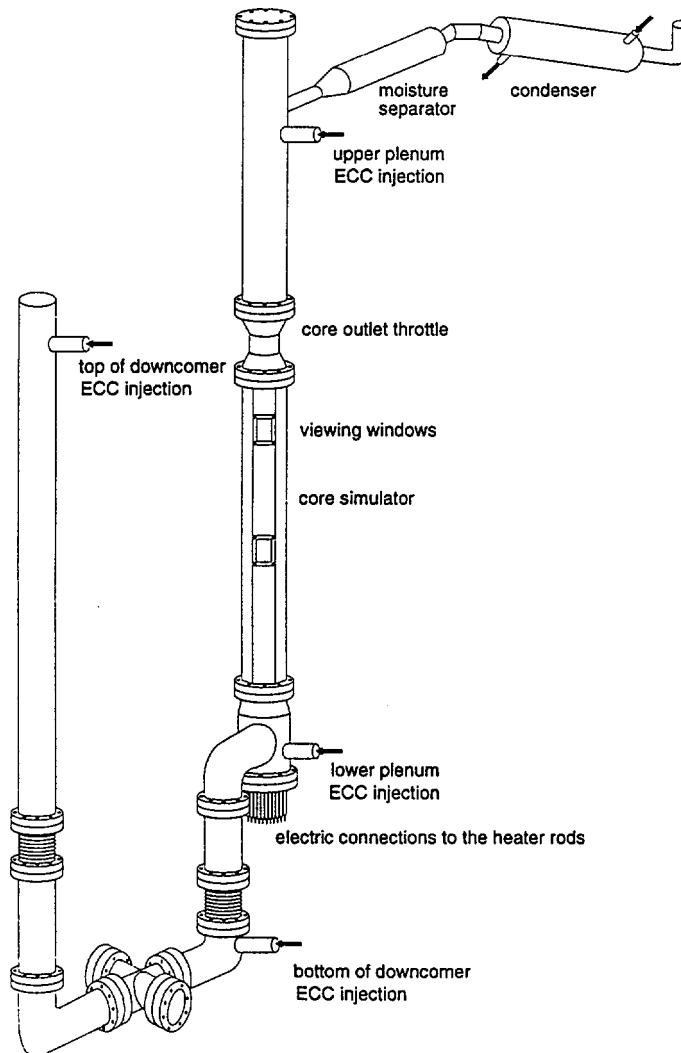


Fig. 1. VEERA facility, /1/.

Table. 1. VEERA facility characteristics, /1/.

Reference reactor	VVER-440
System desing pressure	0.5 MPa
Rod bundle	
number of rods in bundle	126
rod arrangement	triangular
bundle geometry	hexagonal
lattice pitch	12.2 mm
flow area in bundle	86.0 cm ²
heating power of fuel rod simulators	0 - 120 kW
linear heating power	0 - 20 W/cm
shroud tube geometry	hexagonal
shroud tube wall thickness	4 mm
number of axial spacer grids in bundle	11
Fuel rod simulators (Loval 9,1 mm)	
heated length	2420 mm
top unheated section	120 mm
bottom unheated section	1100 mm
outer diameter	9.1 mm
cladding thickness	1 mm
axial peaking factor	1.4
axial power distribution	nine-step chopped cosine
maximum clad temperature	900 °C
cladding material	stainless steel
insulator material	MgO
heating coil material	NiCr

3. Stratification studies using VEERA

It is possible to use the VEERA facility in investigations of the stratification phenomenon during natural circulation. Experiments should define some conditions of temperature stratification and help in estimation of temperature distribution of stratified volumes. The facility is suitable for investigation of the stratification phenomenon in horizontal steam generator hot collector. Some modifications are needed to VEERA in order to obtain useful data for stratification studies.

The upper plenum of the VEERA facility is suitable in simulation of the conditions of coolant flow in upper part of horizontal steam generator hot collector. To create such conditions several additional short tubes with control valves should be welded into the upper plenum of the facility. These tubes are simulating the steam generator heat exchange tubes of the steam generator. These tubes are further joined with the moisture separator and condenser to ensure coolant circulation in the test loop. The original outlet of the upper plenum would not be used.

Several thermocouples must be installed to the upper plenum to measure the temperature distribution.

Previous investigations on stratification phenomenon at the St.Petersburg State Technical University have shown that during natural circulation stagnant volume is at the distance of 10 diameters above the outlet nozzle. In VEERA the height of the upper plenum is 2400 mm whereas the diameter is 163 mm, /3/, /4/.

The experimental procedure for stratification experiments with VEERA in reaching stratified conditions and regimes goes as follows. To initialize needed conditions, the coolant in the facility is first heated up using the heater rods in core part and circulated through the facility. After the heating process, to reach the stratified conditions cold water ($t \approx 20^\circ\text{C}$) is injected into the facility. The flow rate of the cold coolant has to be chosen in accordance with the calculated coolant flow rate during reference regimes of cooling down processes, /3/, /4/.

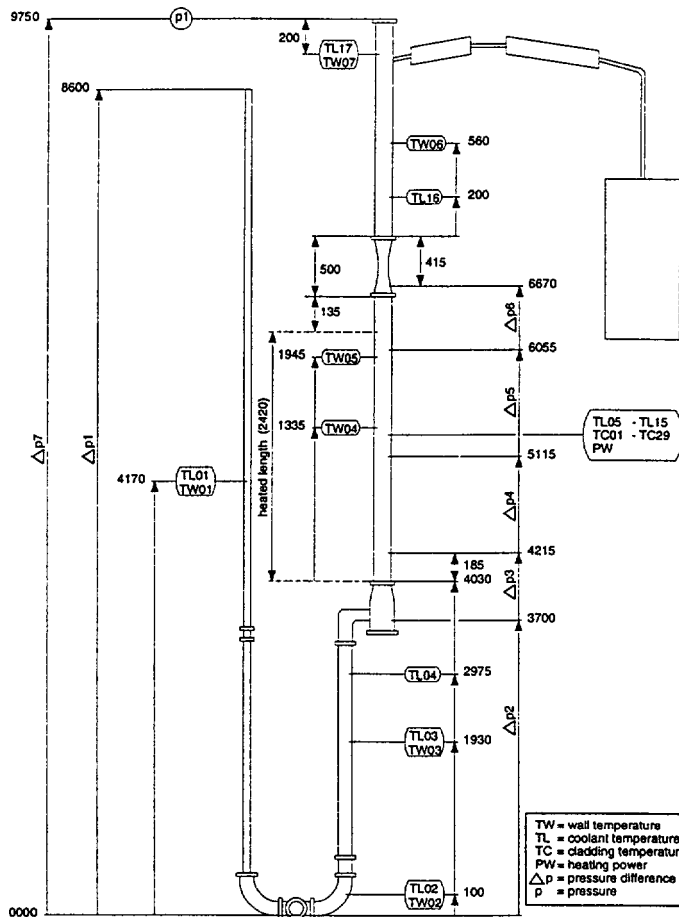


Fig. 2. Instrumentation of VEERA facility /1/.

Now, the cold coolant flows through the facility and through the added tubes simulating the heat exchange tubes of a steam generator. At the same time a stagnant volume of hotter coolant should stabilize into the upper plenum of the facility. At this point the stratification phenomenon and the temperature distribution can be studied. Fig. 3. presents a principle idea of a stratification experiment using the VEERA facility.

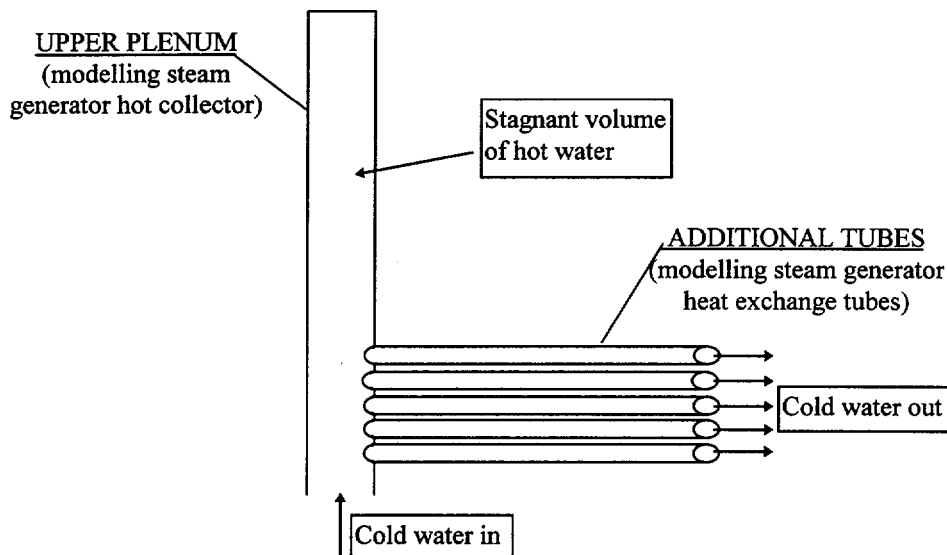


Fig. 3. Principles of stratification experiment with VEERA facility.

References

- /1/ Puustinen, M., Tuunanen, J., Raussi, P., *VEERA facility for studies of nuclear safety in VVER type reactors*. VTT Research Notes, 1618. VTT Offsetpaino, Espoo, 1994.
- /2/ Kortenien, V., *Analysis of emergency cooling tests of pressurized water reactor rod bundle*. Diploma Thesis, Lappeenranta University of Technology, Department of Energy Technology, Lappeenranta, 1994. (in Finnish)
- /3/ Blagovechtchenski, A., Kutuzov, A., Mitriukhine, A., Paramonov, A., *Coolant natural circulation in primary circuit and its role in ensurance of the reactor installations reliability and safety*. The report at the Second International conference on problems of NPP safety and personal training. St. Petersburg. October 8-11, 1991.
- /4/ Gusev, B., Kalinin, R., Blagovechtchenski, A., *Hydrodynamic aspects of modern power installations reliability Leningrad*. Energoatomizdat. 1989.



**FOURTH INTERNATIONAL SEMINAR
ON
HORIZONTAL STEAM GENERATORS
11 - 13 March 1997, Lappeenranta, Finland**

**CONDENSATION DRIVEN WATER HAMMER STUDIES
FOR**

FEED WATER DISTRIBUTION PIPE

**S. Savolainen, S. Katajala, B. Elsing, P. Nurkkala, J. Hoikkanen
Imatran Voima Oy**

**J. Pullinen
IVO Pover Engineering Ltd.**

**S.A. Logvinov, N.B. Trunov, J.K. Sitnik
EDO Hidropress**

1. ABSTRACT

Imatran Voima Oy, IVO, operates two VVER 440 reactors. Unit 1 has been operating since 1977 and unit 2 since 1981. First damages of the feed water distribution (FWD) pipes were observed in 1989. In closer examinations FWD-pipe T-connection turned out to suffer from severe erosion corrosion damages. Similar damages have been found also in other VVER 440 type NPPs. In 1994 the first new FWD-pipe was replaced and in 1996 extensive water hammer experiments were carried out together with EDO Hidropress in Podolsk. After the first phase of the experiments some fundamental changes were made to the construction of the FWD-pipe. The object of this paper is to give short insight to the design of the new FWD-pipe concentrating on water hammer experiments.

2. INTRODUCTION

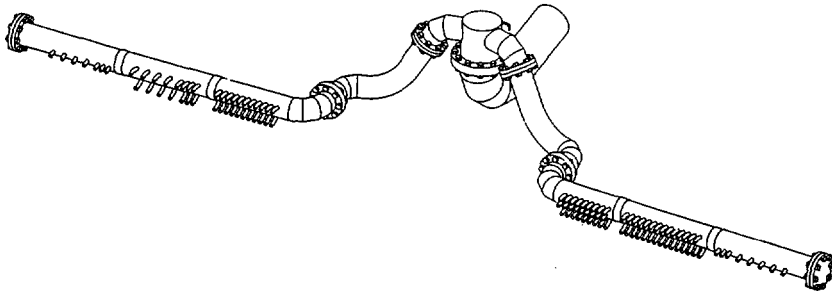
The first damages of the feed water distribution (FWD) pipes were observed in 1989. The FWD-pipe T-connection had suffered from severe erosion corrosion failures. Similar damages have been found also in other VVER-440 NPPs. Additionally the nozzles of the steam generator YB11 were inspected, but no signs of damages or signs of erosion were detected. The first damaged nozzles were found in 1992 in steam generators at both units.

In autumn 1992 different possibilities to repair the damaged FWD-pipes were studied. Since the old distributor is situated inside the tube bundle it was turned out to be more preferable to replace it with a new construction. In 1991 two new feed water distributors, designed by Vitckovice company, had been assembled at Dukovany NPP. Additionally, OKB Hidropress had presented their design for a new FWD-pipe.

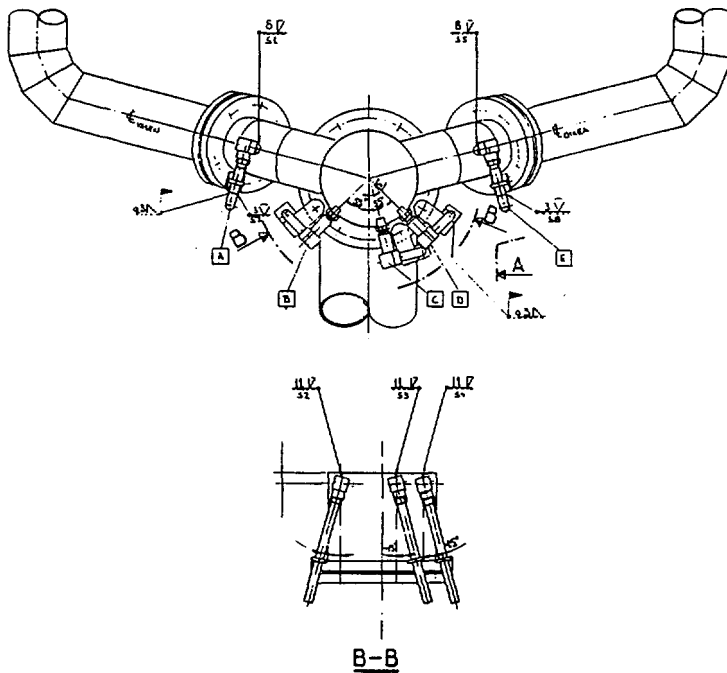
In spring 1994 all the six steam generators of Rovno NPP unit 1 were replaced with FWD-pipes designed by OKB Hidropress. After the assemblage of the new FWD-pipes an experimental program was carried out. After the successful experiments at Rovno NPP Unit 1, a decision was made to install OKB Hidropress designed FWD-pipe the steam generator YB52 at Loviisa Unit 2 in 1994 refueling outage. The collector is illustrated in Picture 1.

The FWD-pipe was instrumented to measure possible water hammer. The Finnish regulatory body, STUK, gave conditional permission for the FWD-pipe of new design requiring IVO to study water hammer phenomenon inside the FWD-pipe and the heat transfer tube's response to cold emergency feed water injection. The heat transfer tube response to cold emergency feed water was studied in spring 1995 together with Lappeenranta Technical University using the Pactel test facility.

In the refueling outage 1995 the cover of the T-piece was reinforced against possible hammering during the start-up phase. Additionally 5 venting pipes in the T-piece were assembled. The venting pipes were aimed to balance pressure difference between steam dome and T-piece. However, in the start-up phase it was deduced that the influence of the assembled venting pipes was almost insignificant. The intensity of pressure peaks seemed to be only slightly smaller than before the modifications. The modified design of the T-piece is illustrated in Picture 2. After these observations large scale experiments on condensation induced water hammers were decided to be carried out.



Picture 1. FWD-pipe assembled into YB52 in Loviisa Unit 2 in 1994.



Picture 2. Redesigned T-piece assembled in YB52 in 1995.

Finally in the early spring and summer 1996 extensive experiments were carried out together with Gidropress. For the first stage of the experiments the model of YB52 FWD-pipe was used and added with 5 venting pipes in the descending part. For the second stage experiments the original design was changed decreasing the maximum pressure pulses significantly. Furthermore by redesigning the T-piece cover the stress levels will remain below the critical fatigue fracture level also in accident conditions. In 1996 in the annual refueling outage of Loviisa Unit 2 a redesigned FWD-pipe was assembled into the steam generator unit YB56.

3. DESCRIPTION OF THE TEST FACILITY

In late summer of 1995 the first negotiations with Gidropress were held on water hammer experiments. It was foreseen that thermal-hydraulic analyses will need reliable validation methods, and experiments could not be avoided. A full scale model of one half of the FWD-pipe was to be used to avoid uncertainties related to scaling and interpreting down scaled results. The size of the model was limited by the size of the pressure vessel of the test facility.

The experiments were to be carried out in the Gidropress's thermal-hydraulic laboratory in Podolsk, Russia. Gidropress was responsible for manufacturing the model of the FWD-pipe, measuring the main process parameters and operating the facility. IVO was responsible for designing and assembling of the instrumentation of the FWD-pipe model and determining the test matrix.

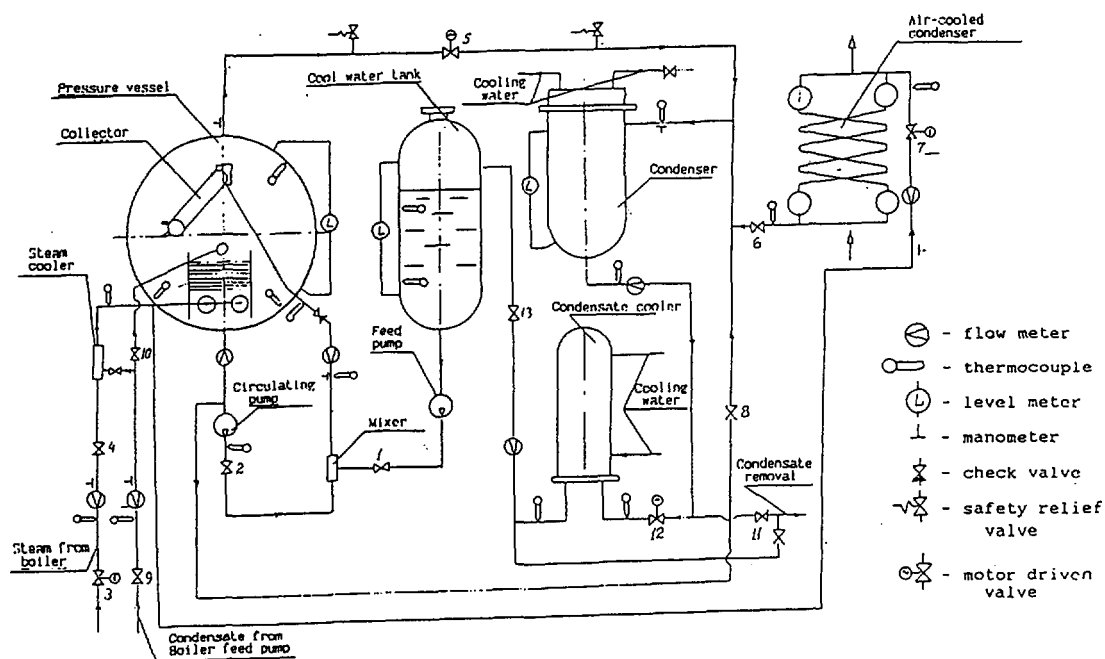
The thermal-hydraulic laboratory of Gidropress was built in 1971. The facility has been used for several thermal-hydraulic large scale experiments. It has been successfully applied for VVER-1000 steam separation experiments and steam drum experiments of RBMK reactors. Lately the facility has been used for researching the residual heat removal system of VVER-1000 type reactors.

The facility has been designed to provide full range parameters for the need of large scale experiments. The schematic diagram of the test facility is illustrated in Picture 3. The model of the FWD-pipe is shown in Picture 4. Feed water is injected using the pump 4P5-8A from the atmospheric tank. Maximum volume of the tank is 10 m³. Minimum temperature of the tank is 20 °C. To provide higher temperatures, saturated water is injected from the vessel using pump CEN148 and mixed with cold feed water in the mixing device. The required feed water mass flow rate and the temperature are controlled with manually operated valves 1 and 2. For controlling the pressure in the vessel superheated steam is injected through valves 3 and 4 and mixed with boiler condensate. The mixture is injected into the vessel under water level through the steam distributing device (Picture 4).

In most experiments a large amount of steam is required for balancing the pressure. Additionally, a relatively small volume of the system requires quick response from the boiler. The approximated demand for steam flow rates was defined by simple hand calculations before experiments. The system pressure as well as other main system parameters were controlled manually. In initial conditions valve 5 is open. In order to limit the pressure drop in vessel valve 5 is closed before the initiation of feed water injection. In some extreme experiments when cold feed water was injected into the vessel with maximum flow rates, the air cooled heat exchanger was operated parallel to the condensers.

To check the effect of the water level to water hammering the level of the vessel could be controlled by either draining the vessel or injecting additional water. The vessel is drained by opening valve 8. In order to speed up the water level rise velocity inside the vessel additional condensate can be injected into the vessel by opening valves 9 and 10 with a boiler feed pump.

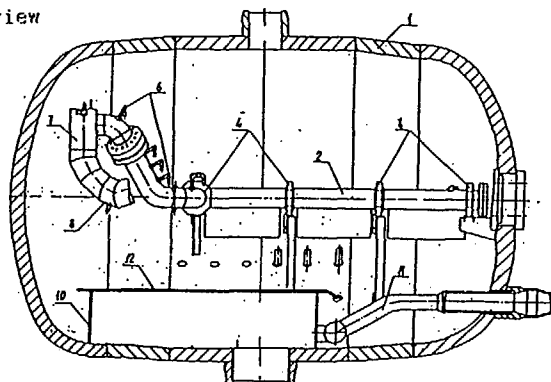
For the operation and for controlling the facility five persons were needed. All the controlling was carried out by manually operating valves. The main parameters as pressure in the vessel, feed water mass flow rate and feed water temperature were recorded in 2 Hz frequency.



Picture 3. Schematic diagram of the test facility.

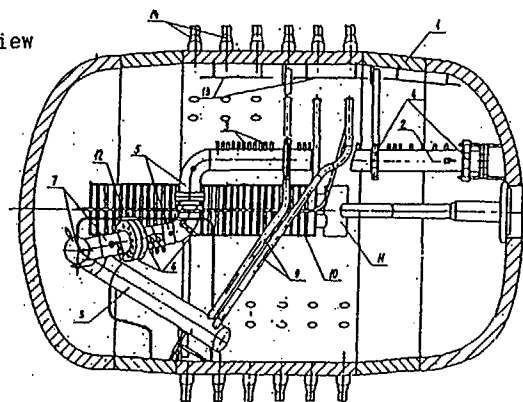
Picture 4. FWD-pipe model.

side view



- 1 - pressure vessel
- 2 - distributing pipe
- 3 - distributing nozzles
- 4 - supporting rings
- 5 - downcomer
- 6 - venting pipes
- 7 - T-piece
- 8 - supplying pipe
- 9 - feed water supply
- 10 - box with tube bundle
- 11 - steam supply to collector
- 12 - condensate supply to collector
- 13 - thermal shield of pressure vessel
- 14 - penetrations for transducers

top view



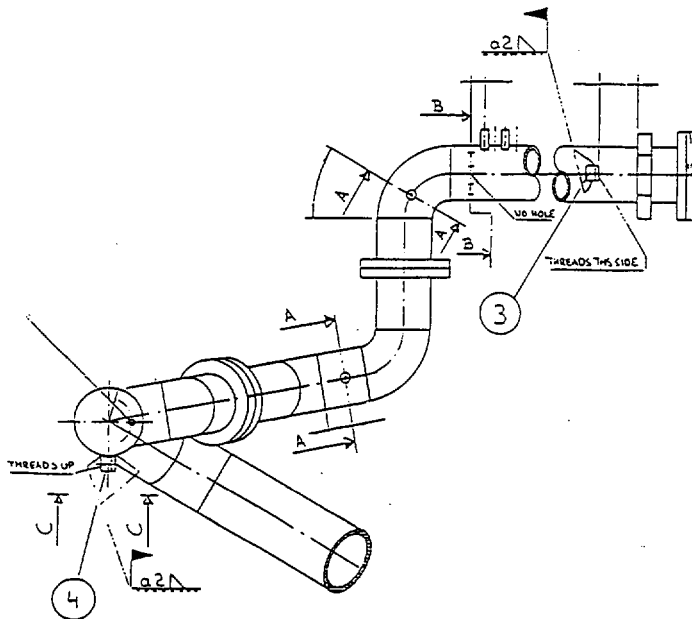
4. INSTRUMENTATION OF MODELLED FEED WATER DISTRIBUTION PIPE

The main objectives of the water hammer experiments were to find out the prevailing parameters leading to water hammers as well as the sensitivity of hammering to boundary conditions. Additionally, the measured feed water heat-up rate substantiated the earlier analyses of the heat transfer tube lifetime.

The design basis for the instrumentation was determined by hand calculations. Due to the high pressure wave velocity a high measuring frequency was required for all measurements. The high frequency noise components in every channel were removed using a low-pass filter.

Both the thermal hydraulic behavior and the FWD-pipe model response due to the water hammering were to be measured. The instrumentation of the facility is shown in Picture 5. The model of the FWD-pipe was instrumented with:

- 2 piezoelectric pressure transducers
- 21 thermocouples
- 4 strain gauges
- 4 accelerometers
- 1 pressure difference transducer for level measurements at T-piece.



Picture 5. Instrumentation FWD-pipe model.

The piezoelectric pressure transducers were mounted at the cover of the T-piece and in the end plate of the FWD-pipe. After the first phase experiments the pressure transducer in the end plate was replaced in the T-piece. The pressure pulses were measured with high 16 kHz frequency sampling rate to detect actual pressure behavior. This recorded pressure information has been later applied as the imposed loads for structural integrity and lifetime analyses of the T-piece.

The thermocouples were to measure the water level and its heat-up inside the distributor. The sampling rate of all 21 thermocouples was 50 Hz. The temperature distribution was measured at three different locations with one circular and 2 vertical matrixes. For the second phase experiments one thermocouple from the circular matrix was replaced to measure feed water heat-up rate in the feed water line inside the pressure vessel.

Four strain gages were mounted at locations where their signals would indicate global structural response due to excitation by water hammer pressure pulses. The sampling rate of the strain gages was 2 kHz. The experiments demonstrated that the global structural modes were excited by water hammering. The strain response, however, was not of high magnitude due to the short duration of pressure pulses (i.e. wide excitation band).

Three out of the four unidirectional accelerometers were mounted at the T-piece to measure its response in the three orthogonal axes. The fourth accelerometer was placed at the horizontal part of the FWD-model to measure the structure's axial response. The sampling frequency of the accelerometers was 2 kHz.

5. WATER HAMMER EXPERIMENTS IN LOVIISA NPP AND IN PODOLSK

In the refueling outage of 1994 the first new FWD-pipe was assembled into the steam generator YB52 in Unit 2 of Loviisa power station. The distributor was instrumented to measure possible water hammers. In the experiments during start-up phase indications of possible water hammers were observed.

Unfortunately the number of instrumentations was limited by the allowed penetrations in the manhole. Therefore, the measurements did not fully reveal the prevailing conditions during water hammers. However, it seemed obvious that the feed water mass flow rate and the temperature are the most important parameters influencing the intensity of hammering.

The experiments demonstrated that **water hammers may occur when the mass flow rate into the steam generator is more than 6 kg/s and the temperature difference between steam generator and feed water more than 100 °C**. Yet, some anomaly was detected. **In some experiments water hammering occurred when the temperature difference was relatively low, 40 °C**. Later it was deduced that a cold water plug in the feed water line initiated the hammering, and the phenomenon was upheld regardless of warmer feed water. The hysteresis feature of water hammering was later demonstrated in the experiments.

In summer 1996 extensive water hammer experiments were carried out together with Gidropress. Imatran Voima Oy was responsible for designing the instrumentation, measuring the water hammers and determining the test matrix. Gidropress was responsible for assembling the model of the FWD-pipe, operating the facility and measuring the main process parameters.

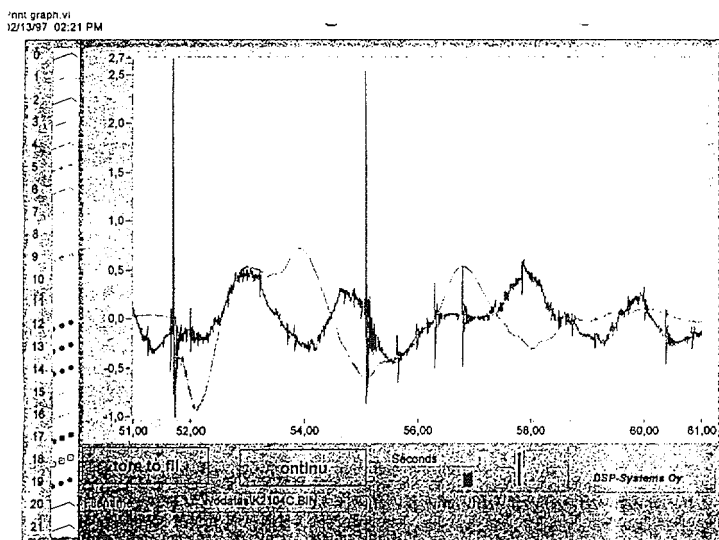
The experiment was carried out in three phases. In the first phase a modified model was studied and in the second phase a redesigned version was studied. In the third phase visual experiments were carried out. In the first two phases the experiments were carried out with actual secondary parameters $P_{sg} = 2\text{--}45$ bar and $T_{fw} = 20\text{--}160$ °C. One half of the actual FWD-pipe was used for water hammer studies. In the first phase experiments five venting pipes were assembled in the descending part of the model. The test matrix of the first phase is illustrated in Table 1. One should note that the mass flow rate corresponds to half of the initial mass flow rate of the actual FWD-pipe.

Table 1. Test matrix in the first stage.

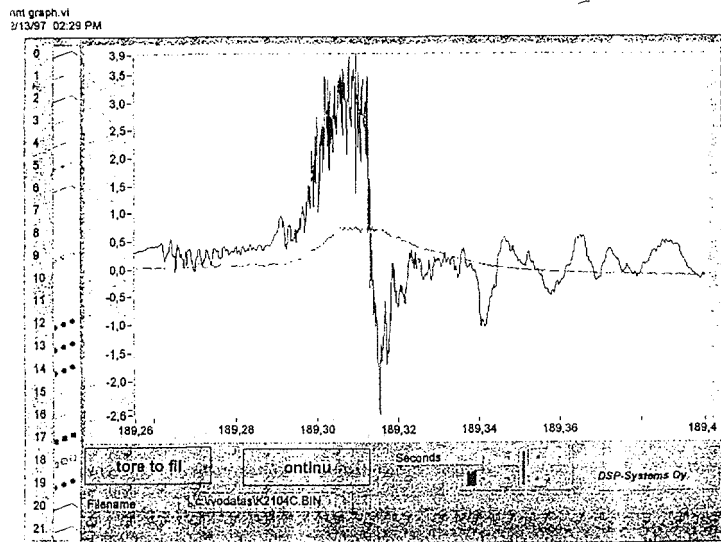
pressure [bar]	mass flow rate [kg/s]	temperature [°C]
45	3,6,9,12,15	20,100,164
7	3,6,9,12,15	100,164
2	3,6,9,12,15	20

The first experiments demonstrated that water hammers are strongly dependent on the combination of prevailing mass flow rate and temperature difference between water and steam. Maximum pressure peaks were found out to be about **65 bar** at mass flow rate 6 kg/s (12 kg in the actual steam generator). Additionally, it was found out that the behavior of hammering included hysteresis features. Furthermore, the hammering faded away always when the horizontal part of the distributor was flooded.

Picture 6 illustrates typical pressure peak behavior in both T-piece and in the end-plate and in Picture 7 a single pulse is shown in more detail. The data is taken directly from the recorded files. One should note that positive values mean underpressure and negative values overpressure. Prior to the pressure peak condensation of the steam exists leading to accelerating pressure drop. Simultaneously in the horizontal part water waves prevents the steam flow from



Picture 6. Typical water hammering ($m=6$ kg/s and $T=20$ °C)

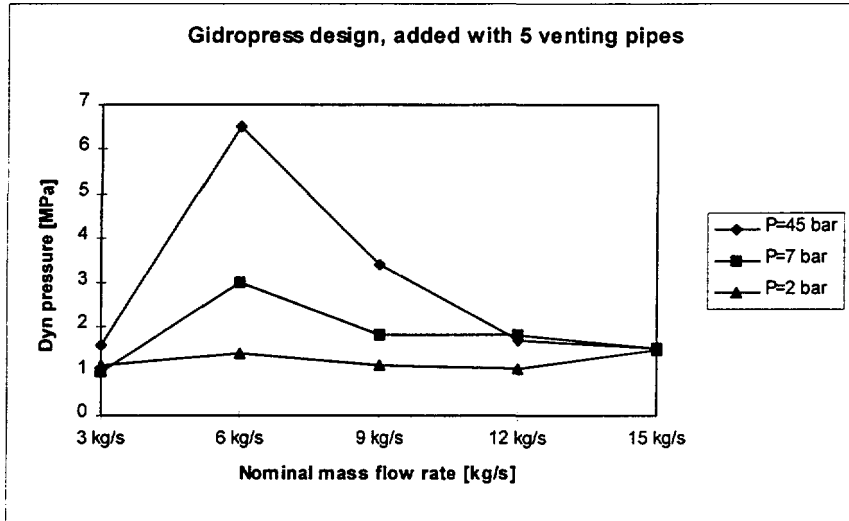


Picture 7. Single water hammer ($m=6$ kg/s and $T=20$ °C)

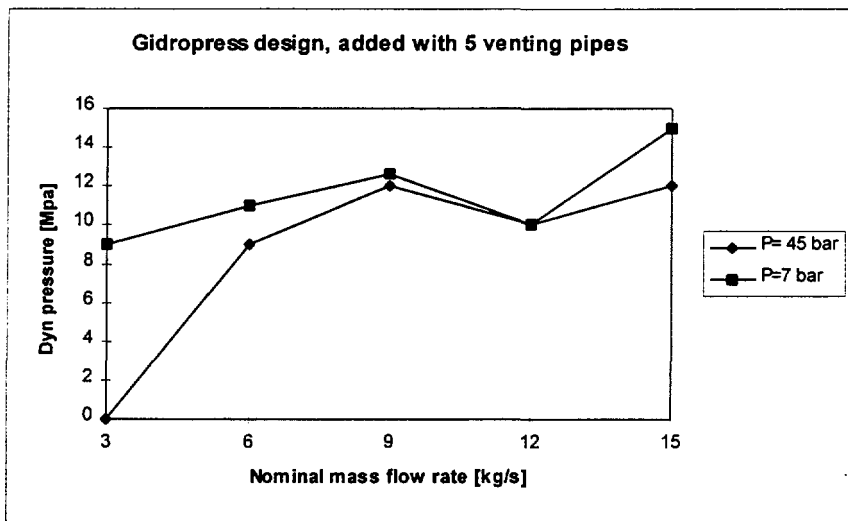
compensating the condensation. The strings of water plugs start to penetrate upwards leading to series of rapid pressure pulses. The whole duration of the peak from condensation till a stabilised phase takes roughly 50 milliseconds. Single pressure peak consists of series of minor pulses. The duration time of single pulse is typically about one millisecond.

The maximum pressure peaks of the experiments are presented in Picture 8 and Picture 9. It can be observed that the pressure peaks are strongly dependent on both feed water mass flow rate and its temperature. It should be noted that the temperature is measured outside the test facility.

After the first stage experiments, stress analysis for the FWD-pipe was carried out. According to those calculations the weakest part, the T-joint, may hold against such water hammers only a limited time, order of few minutes.



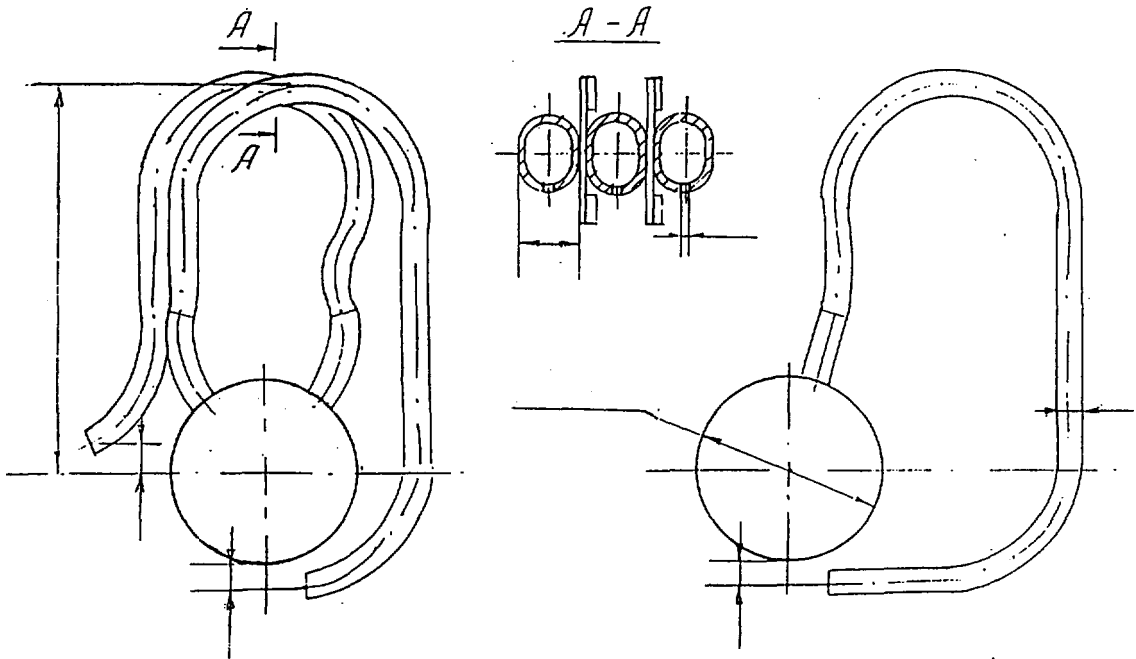
Picture 8. Maximum pressure peaks $T_{fw} = 20\text{ }^{\circ}\text{C}$.



Picture 9. Maximum pressure peaks $T_{fw} = 100\text{ }^{\circ}\text{C}$

For the second stage experiments the design of the FWD-pipe was changed. The principle of the new design is shown in Picture 10. The most important change was the new construction of the feed water nozzles and the removal of the venting pipes in the descending part.

With the new design the horizontal part of the pipe remains filled with water limiting the heat transfer area between water and steam. In addition, in the new distributing nozzles small holes were drilled to equalize the distribution between nozzles at low mass flow rates. In turn these siphon cutting holes prevent the level in the descending part from oscillating. In the T-piece flange a throttling device was assembled to choke down the kinetic energy of possible slugs. Additionally, a slug breaker was assembled in the T-joint. However, this device did not influence much the peak intensity. The test matrix of the second stage is presented in Table 2. The design the FWD-pipe slightly changed assemblage purposes.



Picture 10. Principle of the new construction.

Table 2. Test matrix in the second stage.

pressure [bar]	mass flow rate [kg/s]	temperature [°C]
50*	3,6,9,12,15	20,40,104,164
30	3,6,9,12,15	30
7	3,6,9,12,15	30,50,70,100

*Note the following experiments were not carried out:

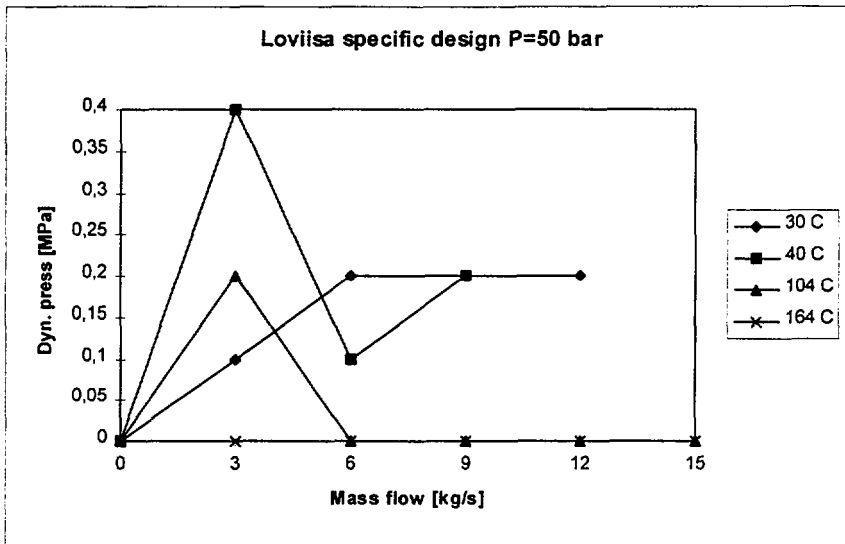
T=30 °C, m=15 kg/s and

T=40 °C, m=12 kg/s and 15 kg/s

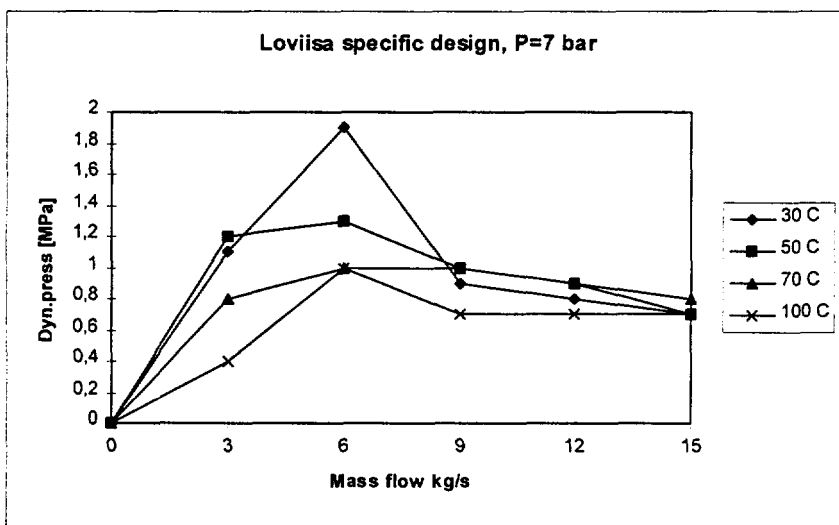
The redesign of the FWD-pipe proved to be successful. Maximum pressure peaks at $P_{sg}=45$ bar were limited to correspond to 4 bar. The maximum pressure peak at $P_{sg}=7$ bar was reduced from 30 bar down to 19 bar. The main result of the second stage experiments is presented in the Pictures 11 and 12.

In the third stage of the experiments the FWD-pipe behavior was visually inspected at atmospheric pressure. In the T-piece 15 holes ($d=2$ mm) were drilled to reveal the level behavior. Furthermore 5 holes ($d=2$ mm) were drilled in the descending part for revealing level behavior. The Final visual experiments have been carried out in Loviisa NPP. For this purpose a transparent plastic model was manufactured. The object of this study is to research phenomenon inside descending and horizontal parts of the model. The placing of the drilled holes is presented in Picture 13 and Table 3 illustrates the main results and observations. With low mass flow rates only nozzles were operating and the level in the descending part remained stable.

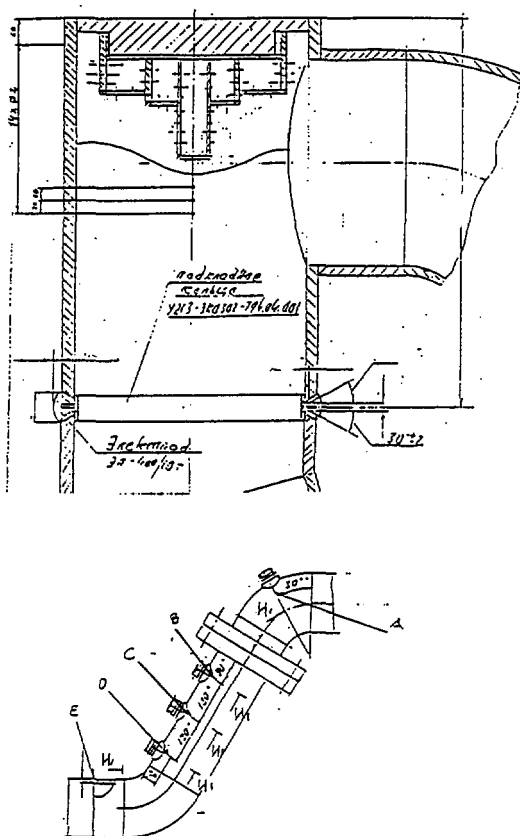
In autumn 1996 the last set of the experiments with transparent PVC model was carried out. The study dealt with both YB52 and redesigned construction. The T-piece, descending part and the 10 first nozzles of the redesigned construction were modelled. Picture 14 illustrates the used PVC-model of the FWD-pipe. The object of this study was to research visually the phenomenon inside the pipeline at atmospheric pressure.



Picture 11. Maximum pressure peaks $P_{sg}=50$ bar.



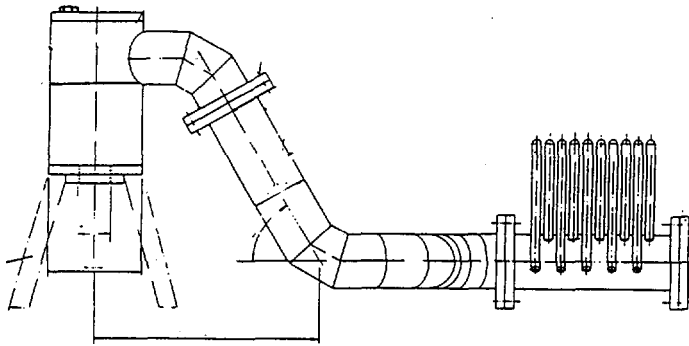
Picture 12. Maximum pressure peaks $P_{sg}=7$ bar.



Picture 13. Placing of the holes in the visual experiments.

Table 3. Major results of the visual experiments in Podolsk

Mass flow rate [kg/s]	Observations		
	T-Piece level [mm]	Descending part level	Functioning nozzles [%]
3	62	C	50
6	82	C, (B fluctuating)	70
9	112	C, (B fluctuating)	100
12	full	C, (A fluctuating) (B no flow)	100
15	level hitting the top	all but not B	100



Picture 14. PVC-model used in visual experiments.

6. WATER HAMMER PHENOMENON INSIDE THE FWD-PIPE

In industrial applications water hammers are usually a consequence of abrupt flow rate changes. A rapid closure of a valve or a flow perturbation influencing promptly fluid velocity may lead to extensive pressure peaks. With simple hand calculations the water hammer magnitude can be easily predicted. The maximum pressure peak and its duration time can be calculated from the well known equations (1) and (2), respectively:

$$\Delta P = c \cdot \rho \cdot \Delta v \quad (1)$$

$$\Delta t = \frac{2 \cdot \Delta l}{c} \quad (2)$$

where

ΔP = pressure peak magnitude

c = modified sound velocity, typically 1000 m/s -1500 m/s (includes both fluid and structure)

ρ = density of the fluid

Δl = length of the water slug.

In condensation induced water hammers the water plug is accelerated by pressure difference due to the condensation between water and steam. A typical feature in condensation driven water hammers is the flow perturbation leading to rapid condensation. The condensation, in turn, promptly increased by flow mode change from stratified to wavy mode. The velocity for a frictionless water slug can be determined from the equation (3).

$$v = \sqrt{\frac{2 \cdot S \cdot dp}{\Delta l \cdot \rho}} \quad (3)$$

where

v = end velocity for the slug

S = acceleration length

dp = driving pressure difference over the water slug

Δl = length of the water slug

ρ = density of the fluid

The equations (1) and (3) show that sufficient pressure peaks are generated with low pressure difference and in short distance. The duration time is only order of few milliseconds and the frequency of the hammers round 1 Hz.

The experiments in Podolsk demonstrated that the maximum pressure peaks occur with maximum subcooling. Further more the pressure peaks are strongly dependent on the mass flow rate. Maximum water hammers were observed when the mass flow rate into the test facility was round 5-6 kg/s. Undoubtedly the predominant factor in hammering is the condensation heat transfer coefficient which, in turn, is dependent on the flow mode and the subcooling rate of the water. The first stage experiments revealed the most important initiating mechanisms to water hammering:

- water mass flow rate
- temperature difference between steam and water
- water level in the vessel

Later the visual experiments with PVC-model confirmed the earlier observations deduced with actual parameters. The water hammers seem to be initiated with three different mechanisms:

- the flow mode transition in the distribution part from stratified flow to wavy or stratified wavy
- flow rate perturbation
- collapse of an annular vortex in the horizontal part
- condensation in the T-piece.

The preliminary hand calculations predicted that the transition from stratified mode to wavy flow mode may exist with the SG mass flow rate round 6 kg/s. Furthermore, it was assumed that the hammering is decreased when the horizontal part is flooded as a consequence of the decreased heat transfer area between phases. The flooding criteria can be calculated from the equation (4).

$$\dot{m} = \pi \cdot \rho \sqrt{g \cdot R^5} \quad (4)$$

where

\dot{m} = mass flow rate

ρ = fluid density

g = gravitational acceleration

R = radius of the pipe

When the mass flow rate into the facility is about 13 kg/s, the water almost fills the T-piece and the horizontal part of the tube before distribution nozzles. This feature limits the heat transfer reducing the condensation. However, the condensation in the descending part occurs, but it can be compensated with the venting pipes. The capacity of the venting pipes is enough for compensating relatively low condensation at. The condensation heat transfer in the descending part is limited due to the stabile stratified flow mode.

Some hammering was detected with mass flow rates of 13-14 kg/s. The T-piece is not fully filled with water and some condensation may take place in this small steam volume. Initiating mechanism for the hammering is normal flow oscillation. The disappearance of the hammering was observed also when the level raised above the collector level. This feature is an indication of decreased heat transfer area like in the case of higher mass flow rates.

In some additional experiments the effect of the flow perturbation was clearly demonstrated. Abrupt shut off of 6 kg/s mass flow rate generated maximum water hammer order of 70 bar. Additionally if the mass flow rate was promptly increased an intense water hammer response could be seen. With low pressures the hammering frequency seemed to increase. On the other hand the magnitude of the hammering was limited due to the lower subcooling of the feed water. The wavy flow mode is a consequence of lower steam density. With a vessel pressure of 2 bar the controlling of the facility was extremely difficult.

In the PVC-facility the annular vortex in the horizontal part was demonstrated. To study the phenomena in YB52 construction the end plate was removed. The observed flow modes as function of mass flow rates are presented in Picture 15. At relatively slow velocities, up to 0.5 kg/s, the phases are well separated and flow remains stratified. The level becomes unstable and wavy if the mass flow rate is increased. When the mass flow rate is roughly 1 kg/s the annular vortex flow exist in the horizontal part between two bends. In this flow mode flow dispersion can be detected.

When the mass flow rate is further increased, the stratified flow becomes wavy after the second bend. The flow mode between the bends include the mode of the annular vortex flow and wavy

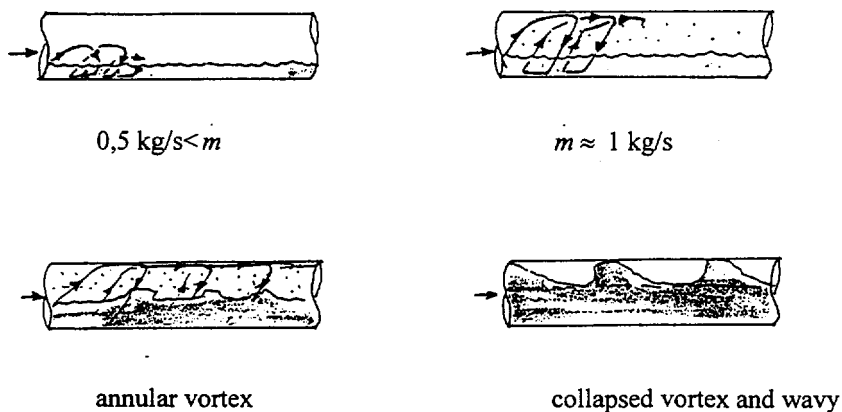
flow. In this mode the annular vortex may collapse forming water slugs. Different flow modes are illustrated in Picture 16. These observations are valid only if steam flow rates remains low.

In YB52 construction the water level inside the collector is depending on the mass flow rate and the capacity of the distribution nozzles. With higher mass flow rates the water hammers may be consequences of the condensation in the T-piece. With higher mass flow rates, about 13-15 kg/s, the T-piece is almost filled with water as can be seen from Table (3). However, stagnated steam bubbles will be formed under the T-piece cover and in the descending part. If the condensation is effective enough the underpressure is capable of accelerating water slugs from horizontal part leading to water hammering. With smaller feed water subcooling the hammering is less dependent on mass flow rate.

For the Loviisa specific design (YB56) the new nozzles were designed to limit the condensation heat transfer area. Additionally the 5 venting nozzles in the T-piece are balancing the possible condensation. Furthermore throttling device was assembled in the T-joint flanges to choke down kinetic energy of the slugs.

It was remarked that with certain low mass flow rates the water level in the descending part may start to oscillate provoking water hammering. Additionally, it was pointed out that a possible siphon pipe effect may occur in the case of abrupt decrease or disconnection of feed water flow. To avoid both these phenomena small holes in the upmost part of the inner curve of the nozzles were drilled. The effect of the holes was demonstrated in visual experiments both in Podolsk and with PVC-facility.

The venting pipes in the T-piece were needed for two reasons. When injecting cold feed water the at high pressures the 5 venting pipes are capable enough of compensating the condensation and the possibility of a steam bubble in the T-piece can not be excluded. If feed water flow into the collector is disconnected, underpressure in the T-piece is formed leading to steam flow from the steam dome. When cold feed water is injected injection of the cold feed water steam bubble is collapsed sucking new steam into the T-piece leading to continuous hammering. At lower pressure the capacity of the venting pipes seems to be inadequate but the water hammer magnitude is tolerable.



Picture 15. Different flow modes in YB52 FWD-pipe construction.

7. CONCLUSIONS

The first damages of the feed water distribution (FWD) pipes were observed in 1989. The FWD-pipe T-connection had suffered from severe erosion corrosion failures. Similar damages have been found also in other VVER 440 NPPs.

In spring 1994 all six steam generators of Rovno NPP unit 1 were replaced with FWD-pipes designed by OKB Gidropress. Later in summer 1994 an OKB Gidropress designed FWD-pipe was assembled into steam generator YB52 at Loviisa Unit 2. The Finnish regulatory body, STUK, gave conditional permission for the FWD-pipe of new design requiring IVO to study water hammer phenomena inside the FWD-pipe and the heat transfer tube's response to cold emergency feed water injection. During the first years operation several water hammerings were detected in start-up conditions.

In the refueling outage 1995 the cover of the T-piece was reinforced against possible hammering during the start-up phase. Additionally 5 venting pipes in the T-piece were assembled. However, in the start-up phase water hammering was clearly observed. The influence of the assembled venting pipes was almost insignificant. After these observations large scale experiments on condensation induced water hammers were decided to carry out.

In summer 1996 extensive water hammer experiments were carried out together with Gidropress. The experiment was carried out in three phases. In the first phase a modified model was studied and in the second phase a Loviisa specific FWD-pipe version was studied. In the third phase visual experiments were carried out. In the first two phases the experiment was carried out with actual secondary parameters and one half of the actual FWD-pipe was used for water hammer studies. The third stage experiments were carried out in atmospheric pressure for visualising the phenomenon.

In the first stage experiments the model of the YB52 FWD-pipe was used. The maximum pressure peak was found to be about 65 bar. According to strength calculation the life-time for the T-piece was analyzed to be order of few minutes. For the second stage experiments the construction of the FWD-pipe was redesigned. The changes proved to be successful. The maximum pressure peak was decreased down to 19 bars. However, the construction of the T-piece was redesigned to better tolerate better possible water hammers. In 1996 in the annual refueling outage of Loviisa Unit 2 a redesigned FWD-pipe was assembled into the steam generator unit YB56. The remaining FWD-pipes of old design and the FWD-pipe in the YB52 will be changed during the next 4 years.



F19800037

INTEGRATED EXPERIMENTAL TEST PROGRAM ON WATERHAMMER PRESSURE PULSES AND ASSOCIATED STRUCTURAL RESPONSES WITHIN A FEEDWATER SPARGER

Pekka Nurkkala, Juhani Hoikkanen

ABSTRACT

This paper describes the methods and systems as utilized in an integrated experimental thermohydraulic/mechanics analysis test program on waterhammer pressure pulses within a revised feedwater sparger of a Loviisa generation VVER-440-type reactor.

This program was carried out in two stages:

- measurements with a strictly limited set of operating parameters at Loviisa NPS
- measurements with the full set of operating parameters on a test article simulating the revised feedwater sparger.

The experiments at Loviisa NPS served as an invaluable source of information on the nature of waterhammer pressure pulses and structural responses. These tests thus helped to set the objectives and formulate the concept for series of tests on a test article to study the water hammer phenomena.

The heavily instrumented full size test article of a steam generator feedwater sparger was placed within a pressure vessel simulating the steamgenerator. The feedwater sparger was subjected to the full range of operating parameters which were to result in waterhammer pressure pulse trains of various magnitudes and duration. Two different designs of revised feedwater sparger were investigated (i.e. "grounded" and "with goose neck").

The following objects were to be met within this program: 1) establish the thermohydraulic parameters that facilitate the occurrence of water hammer pressure pulses, 2) provide a database for further analysis of the pressure pulse phenomena, 3) establish location and severity of these water hammer pressure pulses, 4) establish the structural response due to these pressure pulses, 5) provide input data for structural integrity analysis.

1 INTRODUCTION

1.1 Revised feedwater sparger

One feedwater sparger (i.e. or a collector as it is better known in the CIS-countries) of the original design has been replaced with a feedwater sparger of a revised design at Loviisa 2 NPS. This feedwater sparger comprises of two horizontal distribution tubes (or legs)

connected with series of elbows to the incoming feedwater tube. These two distribution tubes have a large number of nozzles for ready path for the feedwater to enter the steamgenerator. These holes also provide a path for the steam to enter the feedwater sparger

A question was raised whether injection of cold emergency cooling water into the revised feedwater sparger of steamgenerator in a Loviisa-generation of VVER-440-reactor involves a risk for occurrence of waterhammer pressure pulses.

These highly dynamic waterhammer pressure pulses originate when pockets of steam are trapped within the incoming cold emergency coolant water. Rapid condensation of the trapped steam takes place resulting in these pockets collapsing. The collapse of a steam pockets creates a local vacuum for a short period of time.

This local vacuum in turn results in a slug of water being accelerated by the pressure difference between this local vacuum and the prevailing pressure in the steam generator. It is when these slugs hit parts of the feedwater they create local but highly dynamic pressure pulses.

These pressure pulses posses great potential for creating damage due to their highly dynamic nature and due to the high pressures involved.

Loss of integrity of a feedwater sparger involves considerable risks to the integrity of the primary collectors of a VVER-440 plant.

A range of experiments was carried out at the Loviisa-plant to find out if there is any risk of occurrence of waterhammer pressure pulses. It was established through these experiments that the occurrence of these waterhammer pressure pulses within a revised feedwater sparger can not be ruled out with a certain set of operating parameters.

1.2 Parameters unknown

Any attempt to carry out analytical or numerical analysis with any accuracy for the occurrence of waterhammer pressure pulses within a feedwater sparger is quite difficult. This is because the various parameters or correlations governing the themohydraulic phenomena are extremely ill-known or at best have extremely large margins of uncertainty (for example: condensation heat-transfer).

Thermohydraulic behaviour of the incoming feedwater is also difficult to predict although some general ideas of the behaviour of the feedwater can be presented. It is therefore impossible to determine the exact operating parameters (i.e. the combination of prevailing pressure, feedwater flow rates & temperatures, water level within steamgenerator, etc.) which will result in water hammer phenomena.

Although it is possible to make more than an academic estimation of the location where these pressure pulses might occur it is difficult to predict the exact direction of these pulses within a complex structure like the feedwater sparger.

Due to the ill-known nature of the initiation mechanisms it is difficult to estimate the magnitudes and frequency of occurrence of these pressure pulses.

Structural analysis of a feedwater sparger therefore becomes a task where most of the input parameters needed are either known with insufficient accuracy or totally unknown. These problems become particularly acute when carrying out fatigue life estimation for structural integrity analysis.

2 PRELIMINARY TESTS AT LOVIISA NPS

As indicated in the introduction preliminary measurements were carried out at Loviisa power plant. These measurements consisted of experimental modal analysis and operating tests to monitor structural response with a strictly limited set of operating parameters. Due to reasons easy to understand these operating tests were not carried out with full range of operating parameters (i.e. as covered by the full test matrix on the test article).

The experimental modal analysis measurements involved analysis of the actual feedwater sparger structure in-situ. The modal analysis results indicated the frequency band of the major global flexural modes. This established the bandwidth for the measurement of structural responses. The responses were to be measured with strain gauges and accelerometers during operating conditions at Loviisa NPS.

The measurements under operating conditions served to confirm the frequency range of interest for various structural responses as well as established the very possibility for the occurrence of waterhammer pressure pulsation.

The instrumentation mounted on the feedwater sparger included thermocouples, accelerometers strain gauges and a LVDT-type displacement transducer. All transducers were of the hostile environment type with specifications meeting the operating environment within the steamgenerator.

The specifications called for transducers to operate reliably at temperature of 250 C, pressure 50 bars and operation media steam or immersion in water. The accelerometers were of piezoelectric type and the strain gauges were of weldable resistive type. All instrumentation was with integral MI-cable.

It was established that a certain set of operating parameters was necessary to initiate the waterhammer phenomena. Initiation required that there was a considerable thermal imbalance between the prevailing temperature within the steamgenerator and the temperature of the emergency feedwater being injected.

The occurrence of waterhammer pressure pulsation was unambiguously detected by the accelerometer and strain gauge. The existence of waterhammer was also detected by Loose Part Monitoring system (i.e. LPM). The highly dynamic nature of water hammer phenomena also became evident.

These preliminary measurements covered a period of two operating years. The arrangement for accelerometer measurements (direction of measurement) was modified after the first year. This was due to experience and insight gained during the first operational year on the location

and the direction of waterhammer pressure pulsation. It was also established that thermocouples, strain gauges and accelerometers provided reliable and long-term operation under hostile operating conditions.

These measurements strongly pointed out that two likely locations existed for the occurrence of waterhammer pulsation. The likely locations for water hammer pressure pulses were:

- the top of the T-piece and
- the end of the distribution tube.

These operational tests also pointed out the directions where these waterhammer pulses were likely to take place. These directions were the vertical direction of the T-piece and the axial direction at the distribution tube.

These operational experiments at Loviisa NPS therefore served as an invaluable source of information on the nature of waterhammer pressure pulses and subsequent structural responses. These tests also greatly enhanced confidence in the instrumentation to operate in hostile environment and to detect occurrence of waterhammer pressure pulses.

The data acquisition methods also gradually evolved from the somewhat conventional plotter & tape recorder type of equipment with off-line data analysis into a PC-based measurement system with capability to analyse monitored signals immediately after each test has been run. Some data was however still monitored and recorded with the conventional plant process instrumentation.

These tests pointed out and emphasised the necessity and ability to analyse the test results with an integrated system monitoring all pertinent parameters. The integrated data-acquisition system greatly enhances learning and the understanding of the phenomena and reduces the number of unnecessary tests.

3 TEST PROGRAM OBJECTIVES AND CONCEPT

Only a limited set of operating parameters could be studied at Loviisa NPS. It is for this reason that a comprehensive experimental test program was necessary for understanding and analysis of waterhammer phenomena and subsequent structural responses.

The first step in this test program was to establish clearly defined objectives. It is only after these objectives have been defined the measurement concept can be formulated /1/.

As the objectives and the concept of the measurement are highly interrelated one has to assess carefully all the implications of various arrangements within any measurement concept so as not to rule out or interfere with any important objectives of the test.

It is in this stage that the experts from analysis groups (i.e. various disciplines of engineering science or thermohydraulic and analytical/numerical/experimental structural mechanics) must put forward their objectives/views concerning the test program under consideration. It is important that all goals/objectives are expressed in this stage as it is extremely difficult if not impossible, to accommodate any additional measurement objectives once the test concept has been formulated.

This is an iterative stage where one considers how the various test concepts as put forward meet the objectives of the test program under consideration. One also has to pay attention to the overall financial considerations as they play a major role when the concept is being finalized.

3.1 Test objectives

With the large number of parameters of unknown magnitude and mechanisms not fully understood as presented above the following were set as the objectives of the this experimental program:

- 1) establish the thermohydraulic parameters that facilitate the occurrence of water hammer pressure pulses,
- 2) provide empirical database for understanding and further analysis of the thermohydraulics of waterhammer phenomena within the feedwater sparger,
- 3) establish location and severity of the water hammer pressure pulses,
- 4) establish actual structural response due to pressure pulses,
- 5) provide experimental input data for structural analysis and structural analysis model correlation.

3.2 Test concept

In view of the highly complex phenomena associated with waterhammer phenomena it was decided that only a full scale experiment will be able to meet the objectives of this experimental program. Therefore a full scale model of the revised feedwater sparger was to be studied.

It was also decided that the objectives of the test were to be met with a single integrated test/measurement arrangement. This was due to financial considerations as individual test arrangements to study each of the unknown aspects would have resulted in a prohibitively lengthy and costly test program.

Definition of the final test/measurement concept therefore required some consultation. This was because the needs and objectives of the various groups interested in the analysis of diverse aspects (thermohydraulic and structural) of the waterhammer phenomena had to be met. The resulting measurement arrangement was to be such that it did not interfere with or distort any of the very problems one was investigating.

The final test/measurement concept called for the full scale model of the feedwater sparger to be placed within a pressure vessel simulating a steam generator. The boundary conditions for the feedwater sparger were to simulate the actual conditions within an actual steam generator.

The specifications for the pressure and the temperature within the vessel were to meet the full operating parameters of a steam generator. Emergency coolant water of various temperatures and at various flow rates was to be injected into the full-scale model of the feedwater sparger. The operating parameters that were to be varied were the following:

- pressure within the pressure vessel simulating the steam generator
- flow rate of feedwater
- temperature of feedwater
- water level within the steam generator (feedwater sparger submerged in water vs. above water level)

Due to the saturation conditions within the pressure vessel the temperature is subsequently determined by the prevailing pressure.

A set of parameters (latter known as the test matrix) covering a wide range of operating conditions was agreed on. It was through running tests as set by this test matrix and detecting occurrence of waterhammer pressure pulses that one established the regions(s) (i.e. combination of operating parameters) which facilitated the occurrence of waterhammer pressure pulsation.

The instrumentation mounted on the feedwater sparger monitored various thermohydraulic parameters, occurrence/magnitude of waterhammer pressure pulses and subsequent structural responses.

The thermohydraulic parameters to be measured were to yield experimental data and insight on the various unknown parameters/phenomena. This thermohydraulic data subsequently served also as a database for interpolation of behaviour of feedwater under operating parameters not studied within the test matrix.

The occurrence, magnitude and location of waterhammer pressure pulses were to be measured. The magnitude of the resulting pressure was to be measured at locations where one expected the water hammer pressure pulses to take place. The time-series of waterhammer pressure pulses thus measured and recorded were to be used as input load-data for structural integrity analysis (i.e. FEM-analysis) of the feedwater sparger.

The data measured and recorded during these tests would also have to cover subsequent structural responses so as to give indication of the severity of these waterhammer pressure pulses. The structural responses were to be monitored with accelerometers and strain gauges. The structural responses monitored were to be due to global responses.

It was not only the phenomena after incipient pressure pulsation that would be of interest but it was also extremely important to establish the hydrodynamic parameters that prevailed some time prior to the incipient pressure pulses. This was a particularly crucial requirement for understanding the initiation mechanism of waterhammer pulsation.

It was also decided that all the data measured were to be recorded by an integrated PC-based measurement system. This was because preliminary analysis of each test was to be carried out immediately after the test was run. This placed considerable demands on the system. Additional back-up recording system was also to be provided. Limited number of pertinent measurement channels were to be displayed and plotted real-time for detection of water hammer pressure pulses.

Structural response of the test article is due to its inherent dynamic properties. The analysis of the structural response thus becomes more comprehensive when the actual structural properties are established by experimental means. Experimental modal analysis was therefore

to be carried out to establish the modal parameters (i.e. natural frequency, mode shape and associated damping value) of the structure. These parameters can be used for FEM-correlation.

3.2.1 Test article

With highly limited number of locations available to accommodate the full scale model of revised feedwater sparger with two legs it was decided that the experimental model of feedwater sparger will consist of only half of the feedwater sparger. This is to be called the test article hereafter.

The test article consists of the following items (Figure 1):

- incoming section with elbow
- T-piece
- downcomer section with elbow
- horizontal section with two elbows
- one horizontal distribution tube with large number of exit holes

The diameter of the elbow and T-piece was scaled down accordingly to simulate actual velocities within the actual two-legged feedwater sparger. The nozzles in the distribution tube were of the straight/short type.

The test article was originally placed within the pressure vessel in a configuration where the free end of the incoming section was restrained only to a limited degree. The first modal analysis was carried out in this “floating” configuration.

It was thereafter decided that the free end would have be restrained in manner simulating actual boundary conditions in the steamgenerator. The free end was subsequently welded to a bracket to add restraint. This configuration was called the “grounded” configuration. Second modal analysis was carried out in this “grounded” configuration prior to the first waterhammer tests. The first series of waterhammer tests was carried out in this “grounded” configuration.

Subsequently the nozzles were modified with long looping “goose necks”. The incoming section remained welded to the bracket. The third modal analysis was carried out in this “goose neck” configurations prior to the second waterhammer tests. The second series of waterhammer tests was carried in this “goose neck” configuration.

4 DEFINITION OF THE TASKS TO MEET THE OBJECTIVES

There were numerous unknown parameters required by the theoretical analysis of the waterhammer phenomena and associated structural integrity & structural mechanics analysis as indicated above. One has to define specific tasks which are to be met/established through experimental methods.

The specific tasks of this test range were as follows:

- 1.1) establish the combination of operating parameters (flow rate and temperature of feedwater & pressure and influence water level within the pressure vessel) that will

facilitate the occurrence of water hammer pressure pulses,

- 2.1) provide insight to the mechanisms that contribute to the initiation waterhammer pulses and termination these pressure pulses,
- 2.2) provide comprehensive empirical thermohydraulic database to facilitate further consideration and semi-empirical analysis of the various other operating parameters as not studied by this range of tests.
- 3.1) establish the location/direction within the feedwater sparger where the waterhammer pressure pulses take place at various operating parameters,
- 3.2) establish the magnitudes and frequency of occurrence of these pressure pulses at various operating parameters,
- 4.) monitor structural responses due these pressure pulses
- 5) derivation of experimental modal parameters (natural frequencies and mode shapes & associated damping) of major global flexural vibration modes to be used for FEM-correlation.

4.1 Parameters to be measured

4.1.1 Thermodynamic parameters

There were numerous unknowns as far as the behaviour of the incoming feedwater was concerned. Heat transfer to feedwater (from steam) along the collector and the feedwater level within the sparger were totally unknown. Determination of the behaviour of these parameters was of paramount importance.

To establish the heat transfer (due to condensing) the temperatures of the feedwater were measured at several locations along the sparger. The temperature of the feedwater was measured at the inlet of the sparger, T-piece and at three cross sections at horizontal section of the sparger. The cross sections monitored were as follows:

- right after the downcomer section before the first horizontal elbow (one straight array of five thermocouples at five different elevations),
- at the second horizontal elbow (one straight array of five thermocouples at five different elevations) and
- after the second horizontal elbow at the beginning of the straight part of the distribution tube (nine or ten thermocouples arranged into a circular array).

Initiation of the waterhammer phenomena required that there was a significant difference between the prevailing temperature within the simulated steam generator (steam at saturation temperature) and the cold (emergency) feedwater. This temperature difference could be as high as 220 °C.

This significant temperature difference could therefore be used as an indication of water level within the feedwater sparger. The three temperature arrays (two straight and one circular) thus also served as indicators of water level (or presence of steam or water) at their respective mounting locations.

The feedwater level within the T-piece was to be monitored by a conventional pressure differential measurements system.

4.1.2 Pressure pulses

The magnitude of waterhammer pressure pulses were to be measured with pressure transducers at the two locations where one expected them to take place. These locations were as follows:

- top of the T-piece
- end of the distribution tube

4.1.3 Structural responses

Global structural response due to water hammer pressure pulses were to be measured with strain gauges and accelerometers. It was decided that that the structural responses to be recorded were to be due to global responses.

This was based on the experience gained with data acquired at Loviisa 2 NPS. This was also partly because monitoring and recording of response data with local responses would be quite confusing to analyze. High local responses sometimes almost totally mask global responses. Local responses are also quite sensitive to boundary conditions which further also adds confusion. Recording of the data that included local responses would also result in excessive amount of response data.

Global structural responses were measured with four accelerometers and four strain gauges.

Three piezoelectric accelerometers were to be placed at the top of the T-piece to measure structural response in the three orthogonal axes. The remaining accelerometer would monitor axial response at the distribution tube.

The strain gauges were to be mounted at locations as determined by the experimental modal test and analysis. This analysis would yield global structural modes. The modal analysis would be carried out prior to the waterhammer tests.

5 INSTRUMENTATION IN DETAIL

5.1 Specific tasks

There were additional specific tasks that had to be considered when addressing the broader tasks above. These specific tasks were directly related to transducers and data-acquisition system specifications and parameters.

The tasks related to instrumentation or transducers included:

- specifications of transducers considering the hostile operating environment,

- consideration of the dynamic operating environment,
- determination of precise mounting location of transducers,
- specifications for associated transducer electronics,
- acquisition/calibration and testing of transducers and associated electronics.

All transducers were to be with integral MI-cable. As all the transducer were to be located within the pressure vessel penetrations for signal cables were to be utilized. This involved the following tasks:

- specifications of the penetrations for MI-cables through the pressure boundary
- acquisition and testing of penetrations for the various transducer MI-cables

5.2 General environmental specifications

All transducer, their integral MI-cabling and associated penetrations were specified to provide reliable operation within the full steamgenerator operating envelope. This included the following:

- temperature range 20...265 °C
- pressure 1...46 bars
- media: condensing steam and/or immersion in water

5.2.1 Temperature measurement task

In addition to the above environmental specifications the thermocouples would have to meet some additional requirements. One of the specific requirements was rapid response to abrupt temperature changes involved with detection of level of cold feedwater injected.

This called for a thermocouple with minimal thermal mass and high thermal diffusion. Still requirements structural integrity of the thermocouples would have to be met with high degree of confidence. Additionally there was a requirement for some structural rigidity.

5.2.2 Waterhammer pressure pulse measurement task

One of the particular problems of this project was finding a pressure transducer to meet the particular and complex requirements as placed by the curious nature of waterhammer phenomena.

The very objects of this project called for a transducer to be able to measure the waterhammer pressure fluctuations with extremely rapid rise times. Rise times were referred to be as short as 0.5 msec /2/.

This resulted that significant frequency components of the waterhammer pressure pulse extended well into the kHz-region.

Another specific feature of the pressure measurement system was that the transducer would be placed at a location/detail of the structure which would possess global and local natural frequencies in the frequency band excited by the waterhammer pressure pulse.

This resulted in a requirement that the pressure transducer should be capable to accommodate also the dynamics of the mounting location.

5.2.4 Global acceleration response measurement task

Somewhat similar requirements as discussed in conjunction with the pressure transducer were also placed on the choice of accelerometers.

An accelerometer with high overload capacity would also be highly preferred.

5.2.5 Global strain response measurement task

The weldable encapsulated strain gauges provided reliable operation at Loviisa NPS for a period of more than two years. It was therefore decided that similar type of strain gauges were specified for the waterhammer tests with the test article.

5.3 Penetrations

As all the transducers were to be placed within the pressure vessel simulating a steam generator penetrations for the integral MI-cables were to be devised. The penetrations through the pressure boundary were to meet same environmental specifications as the transducers.

An additional requirement for the penetrations was that one has to be able to dismantle the penetrations in order to evacuate all the transducers from the pressure vessel after the tests.

A patented design of screw-type was utilized throughout these tests. These penetrations offered reliable operation.

5.4 Signal conditioning

Piezoelectric pressure transducers and accelerometers were to utilize individual and conventional charge amplifiers for signal conversion/conditioning into high-level voltage signal.

Resistive strain gauges also utilized conventional strain gauge amplifiers for signal conditioning/ conversion into high-level voltage signal.

Frequency band of each of the signal conditioning equipment was matched with that of the required frequency band of the particular signal being measured.

6 DATA ACQUISITION SYSTEM

It was absolutely necessary high degree of integrity was provided by the data-acquisition/analysis system. This was due to the unique nature of these experiments and the high costs involved with running of these tests

Primary data-acquisition and analysis was to be carried with an integrated PC-based system. Definition of specifications for data acquisition system was of paramount importance. An additional back-up data acquisition system was to be utilized in case of primary system malfunction.

Although extensive experience was gained during operational measurements at Loviisa NPS considerable attention had to be given to the following tasks:

- specification for the data acquisition front-end equipment and parameters
- determination of data acquisition sampling rates for the various measurement channels.

Due to the highly different character of the phenomena to be monitored (i.e. pressure pulse vs. temperature measurements) highly diverse requirements were placed for data acquisition parameters for the various measurement channels. The front-end and actual data acquisition parameters of the PC-based system had to be flexible enough to accommodate these requirements as well as any further requirements as might arise in the future.

6.1 Front-end

One of the first requirement for the front-end was that all measurement channels were isolated. This will guarantee acquisition of data with high degree of integrity in case of spurious signals and ground loops.

As there was a considerable number of thermocouple channels (21 channels) to be measured this required that the data acquisition system should accommodate thermocouple signals directly without any additional instrumentation.

All other signals were of high-level voltage type and were thus directly connected to the front-end.

Primary data-acquisition and subsequent analysis was to be based on digitized time-serie of the signals. Thus meaningful and reliable analysis required that the AD-conversion rate for various channels was set properly and that the front-end included lowpass filters to remove unwanted spurious signal components.

The of AD-conversion rate is highly related to the frequency content of the phenomena under consideration (i.e. pressure vs. acceleration vs. temperature). The choice of lowpass filter frequency is related to the significant frequency content of the signal as well as to the AD-conversion-rate for that particular measurement channel.

The choice of lowpass filter frequency will therefore be discussed in conjunction with choice of AD-rate for each type of signal.

6.2 Data-acquisition

6.21 Pre-trigger

As indicated above it was not feasible to predict the exact time for the initiation of the pressure pulsation. Subsequently it was not possible to predict the exact time when one would start or trigger data acquisition. There however was a need to establish the prevailing thermohydraulic conditions and structural behaviour some time prior to the initiation of waterhammer pressure pulses. This data would provide great insight into the initiation

mechanism of water hammer phenomena. This led to the requirement for a pre-trigger data-acquisition arrangement. This particular feature of data-acquisition system allows one to record data some time prior to the trigger pulse given by the user.

It was decided that one would have to be able to recover 60 seconds of events prior to the trigger pulse.

6.2.1 Data-acquisition parameters

6.2.1.1 Thermocouples

One was primarily interested in the warm-up of feedwater due to various heat-transfer mechanisms and the dynamic behaviour of the two-phase flow of steam and water.

6.2.1.2 Pressure pulse

As indicated above the waterhammer pulse possesses extremely rapid risetimes. It was imperative that no significant signal components were lost through an insufficiently high A/D-conversion rate or by an inappropriately set lowpass filter.

6.2.1.4 Structural responses

Based on the experience gained at Loviisa NPS it was decided to monitor structural responses only due to global responses.

7 MODAL ANALYSIS

Experimental modal analysis of the feedwater sparger was carried out after it was installed into the test vessel. The boundary conditions were thus same as during the waterhammer tests excluding the influence of thermal expansion and the added mass of water within/outside the sparger. Three separate experimental modal analyses were carried out corresponding to the various configurations (i.e. "floating", "grounded" and "with goose neck").

The experimental modal analysis was based on experimental determination of frequency response functions (FRF's) between response and excitation location. These FRF's were derived between all desired response locations and the selected excitation location(s). The FRF's determined were of type acceleration/Force.

The FRF-data-base can be analyzed to extract the modal parameters. These parameters consist of natural frequency, associated damping value and the associated mode shape. The mode shapes extracted can be animated for visualisation.

7.1 Determination of strain/Force FRF

After the first modal analysis was carried out it was decided to mount strain gauges at locations which exhibited greatest local flexibility with consideration given to rigidity of the structure at the location.

Frequency response functions (FRF's) strain/Force were measured. The strains responses were measured by the hostile environment strain gauges. The excitation force was provided by the instrumented impact hammer. The excitation locations were the locations where one expected the waterhammer to take place.

Contribution of the same structural modes (natural frequencies and mode shapes) which were detected by modal analysis was also detected when analyzing these FRF's (i.e. strain responses over Force).

The contribution of these same modes was also detected when studying the spectrums of strain responses due to waterhammer pulses.

8 EXPERIMENTS

Several dozens of waterhammer experiments were carried out in two phases i.e. in "grounded" and "goose-neck" configurations. The PC-based measurement system provided reliable operation during these waterhammer tests.

9 RESULTS

Comprehensive analysis of thermohydraulic test results is given by Mr Samuli Savolainen. et. al /3/.

Summary

Injection of cold emergency cooling water into a the revised feedwater sparger (i.e. collector as it is better known in the CIS-countries) of the steamgenerator involves risk of occurrence of waterhammer pressure pulses in a Loviisa-generation of VVER-reactor.

A series of tests was carried out at Loviisa to find out the risk for the occurrence of waterhammer pressure pulses. The number of operating parameters tested was limited. These tests established that waterhammer does take place under certain combination of parameters.

A integrated experimental thermohydraulic/experimental mechanics analysis program was therefore carried out with model of a revised feedwater sparger. One half of a feedwater sparger was placed within pressure vessel simulating the steam generator. The full range of operating parameters were studied within this program. Two different designs of the revised feedwater sparger were studied within this program.

An integrated data acquisition system was used to acquire data on the parameters/events taking place within the feedwater sparger. The system accommodates signals from the following transducers located within the pressure vessel:

- 1) twenty one thermocouple temperature channels
- 2) four piezoelectric accelerometers
- 3) four resistive strain gauges
- 4) two piezoelectric, dynamic pressure transducers

All instrumentation (i.e. transducers) was of hostile environment type specified for the full operating parameters of the steamgenerator. Patented screw-type penetrations were used for routing the integral MI- (Mineral Insulated) cables through the pressure boundary (i.e. from within the pressure vessel).

The following objectives were met for the two design of collectors:

- 1) establish the thermohydraulic parameters that facilitate the occurrence of water hammer pressure pulses,
- 2) provide database for further analysis of waterhammer pressure pulses,
- 3) establish the location and severity of these pressure pulses,
- 4) establish structural response due to these pressure pulses
- 5) provide input parameters for structural mechanics FEM-analysis.

Conclusion

An integrated experimental thermohydraulic/experimental mechanics test program was carried out for the analysis of waterhammer phenomena within a revised Loviisa generation of VVER-440-reactor feedwater sparger.

The following objectives of this experimental program were met: 1) the range and combination of operating parameters that facilitate the occurrence of water hammer pressure pulses was conclusively established, 2) experimental database was established for further analysis of waterhammer phenomena, 3) the range of parameters was established for two different designs of feed water sparger, 4) the locations/directions within the feedwater sparger where these pulses take place were pinpointed, 5) the magnitudes and frequency of occurrence of these pressure pulses were established, 6) modal parameters for the feedwater sparger were derived based on experimental modal analysis, 7) the magnitudes of structural responses (acceleration and strain histories) due to water hammer were established at various locations.

References

- 1 Ryan, S, "Practices in Adequate Structural Design", Transactions of ASME, Journal of Pressure Vessel Technology, Vol. 114, August 1992, pp 300-307.
2. Rothe P.H, Wallis G.B, Crowlwy C.J. "Water in the Feedwater Systems of PWR Steam Generators", Fluid Transients and Acoustics in the Power Industry. 1978 Winter annual Meeting; pp 75-85.
3. Savolainen S., Katajala S., Elsing B., Nurkkala P., Hoikkanen J., Pullinen J., Logvinov S.A., Trunov N.B., Sitnik J.K., "Condensation Driven Water Hammer Studies for Feedwater Distribution Pipe. FOURTH INTERNATIONAL SEMINAR ON HORIZONTAL STEAM GENERATORS; 11 - 13 March 1997, Lappeenranta, Finland



F19800038

EBO FEED WATER DISTRIBUTION SYSTEM, EXPERIENCE GAINED FROM OPERATION

Oldřich MATAL, ENERGOVÝZKUM s.r.o.
Božetěchova 17, 612 00 Brno
Czech Republik

Štefan SCHMIDT, Milan MIHÁLIK, Slovenské elektrárne, a.s.
Atómové elektrárne Bohunice
Jaslovské Bohunice,
Slovak Republic

Abstract:

Advanced feed water distribution systems of the EBO design have been installed in to steam generators at Units 3 and 4 of the NPP Jaslovské Bohunice (VVER 440). Experiences gained from the operation of steam generators with the advanced feed water distribution systems are discussed in the paper.

1. Introduction

The first advanced feed water distribution system (FWDS) of the EBO design was installed in the steam generators Nr 35 in 1994 (VVER 440). The first stage period of FWDS testing was finalized to the end of 1995 [Ref.1,2].

Nevertheless, distribution and concentration values of sodium chlorides and sulphates (generally of impurities) in the SG 35 secondary water have been measured and analyzed since 1994.

2. Blow down water standard requirements

Blow down water samples taken from the blow down pipeline of each steam generator shall be analyzed three times in 24 hours (each 8 hours). Acceptable values of the blow down water quality sampled in blow down pipeline are in Table 1:

Table 1: Acceptable upper values of blow down water characteristics

pH	8,0 to 9,0
conductivity (after catex)	5,0 $\mu\text{S} / \text{cm}$
sodium	300 $\mu\text{g} / \text{kg}$
chlorides	150 $\mu\text{g} / \text{kg}$

3. Distribution of impurities in the water along the tube bundle [Ref. 3]

3.1 Sodium concentrations

Averaged values of sodium concentrations in steam generator secondary water derived from results of analyses of water samples for four periods of Unit 3 operation from 1994 to the January 1997 are in bar diagrams in Fig 1.

3.2 Chlorides concentrations

Averaged values of chlorides concentrations ($\mu\text{g} / \text{kg}$) in the secondary water along the tube bundle are in bar diagrams in Fig.2. Numerical values are averaged chlorides concentrations in SG blow down water.

3.3 Sulphates concentrations

Averaged values of sulphates concentrations ($\mu\text{g} / \text{kg}$) in the secondary water along the tube bundle are in bar diagrams in Fig.3. Numerical values are averaged sulphates concentrations in SG blow down water.

4. Discussion

The distribution of sodium in the water at secondary side of the steam generator with EBO designed feed water distribution system is uniform along the tube bundle. Measured local sodium concentration values have been typically in an interval of 25 to 50 $\mu\text{g} / \text{kg}$. Furthermore these values are five to twelve times lower than acceptable upper values in blow down water, see Tab.1 and Fig.1.

Similar results have been obtained for chlorides and sulphates distribution in secondary water along the tube bundle.

Measured local chlorides concentration values along tube bundle have been typically in an interval of 4,5 up to 30 $\mu\text{g} / \text{kg}$ and in blow down water typically 12 $\mu\text{g} / \text{kg}$ in the period 1996 / 1997.

Nevertheless, all these values are minimum five times lower than acceptable upper value for chlorides concentration in the blow down water, see Tab.1 and Fig.2.

Of interest are also obtained values of local sulphates concentrations along the tube bundle, Fig 3. Registered maximum local sulphates concentrations averaged in evaluated period have been below 25 $\mu\text{g} / \text{kg}$.

Results mentioned above support one of the expected good features of the EBO - FWDS namely positive contribution to a water flow redistribution in the steam generator and to defined environmental conditions for SG tube bundle. Selected results of water flow versus in water impurities distribution analysis at SG secondary side are presented in [Ref.4].

5. Conclusions

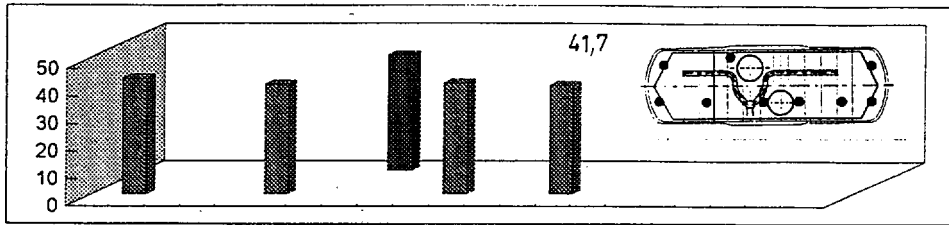
Advanced feed water distribution system of the EBO design is in operation in SG Nr.35 since 1994. Positive experience gained from the operation, namely

- uniform distribution of impurities (sodium, chlorides, sulphates) in water along the tube bundle and
- very low values of impurities concentrations in SG secondary water and blow down water consequently, supported the NPP owner decision approved by authorities to install EBO - FWDS in to all steam generators of Unit 3 and 4 in Jaslovské Bohunice.

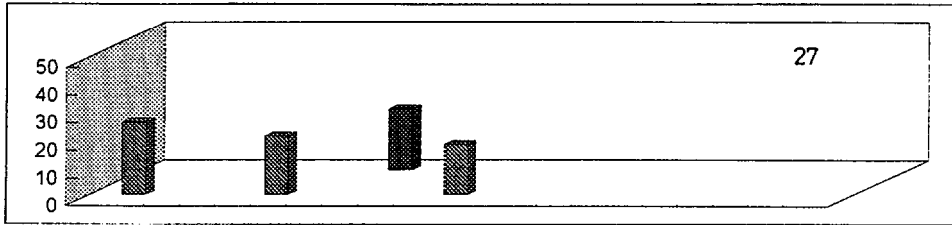
References:

- [1] Matal,O.et.al: Advanced Feed Water Distribution System for WWER 440 Steam Generators, paper presented at the Third International Seminar on Horizontal Steam Generators, Lappeenranta, 18 - 29 October 1994, Finland.
- [2] Matal,O., Klinga, J., Šimo, T.: EBO Feed Water Distribution System Performance Evaluation at Steam Generator Nr. 35 and Comparison with Steam Generator Nr.33, Energovýzkum Report QR-EM-016-95, March 1995.
- [3] Šimo, T., Matal,O.: Evaluation of EBO Unit 3 Blow Down and Sludge System Characteristics and Chemical Environment at the SG 35 Secondary Side, Energovýzkum Report QR-EM-003-97, 1997.
- [4] Matal,O., Šimo,T., Kučák, L., Urban, F.: Modelling of Soluble Impurities Distribution in the Steam generator Secondary Water, Fourth International Seminar on Horizontal Steam Generators, 11.-13.3.1997 Lappeenranta

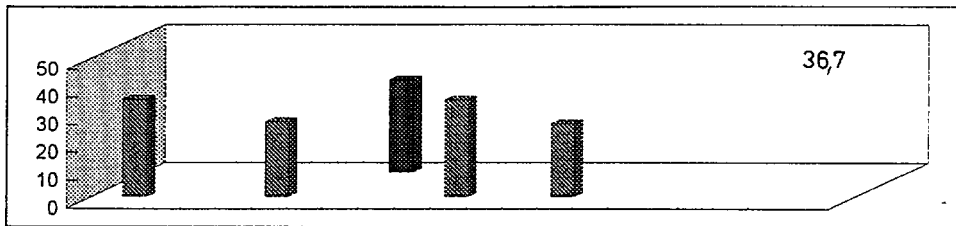
Period 1994 / 1995



Period 1995 / 1996 - October 1995



Period 1995 / 1996 - February 1996



Period 1996 / 1997 - January 1997

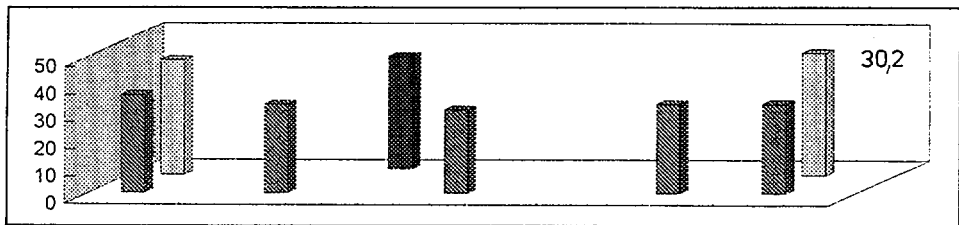
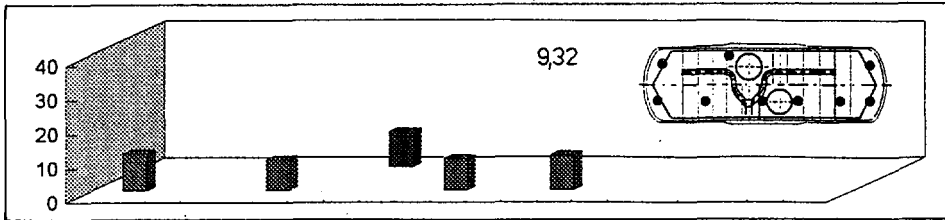
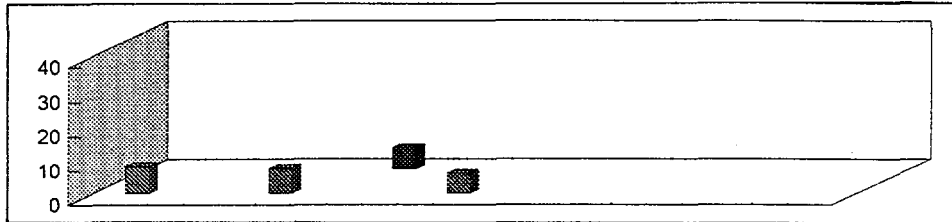


Fig.1: Averaged values of sodium concentrations ($\mu\text{g} / \text{kg}$) in steam generator secondary water along the tube bundle (bars), in blow down water (numerical values) for four periods of SG operation from 1994 to 1997

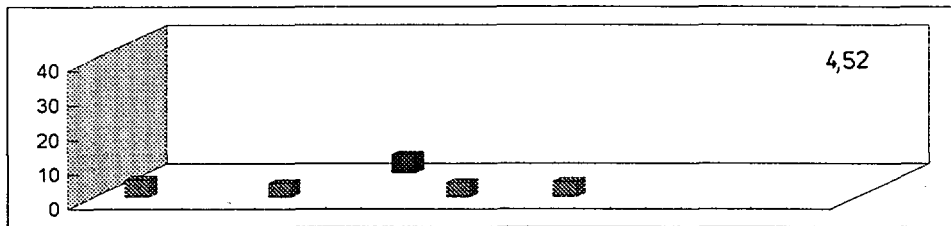
Period 1994 / 1995



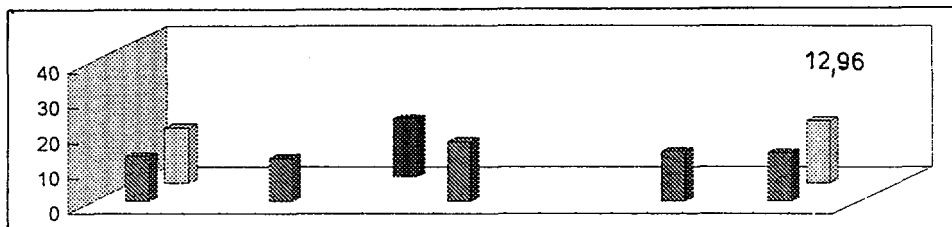
Period 1995 / 1996 - October 1995



Period 1995 / 1996 - February 1996



Period 1995 / 1996 - November 1996



Period 1996 / 1997 - January 1997

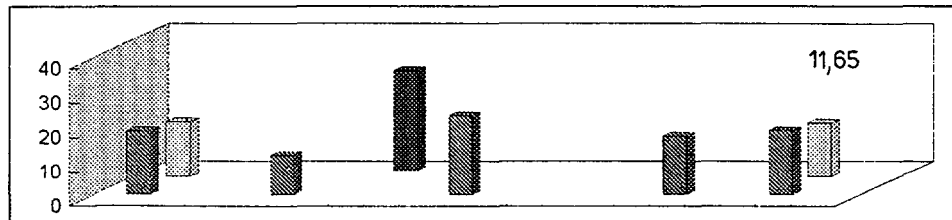
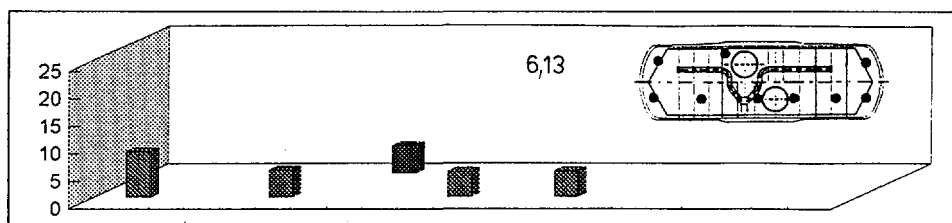
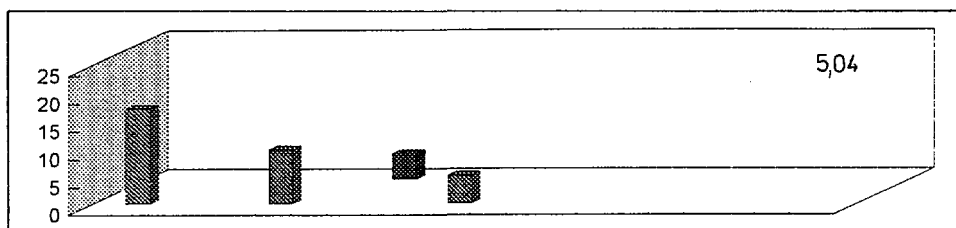


Fig 2: Averaged values of chlorides concentrations ($\mu\text{g} / \text{kg}$) in steam generator secondary water along the tube bundle (bars), in blow down water (numerical values) for four periods of SG operation from 1994 to 1997

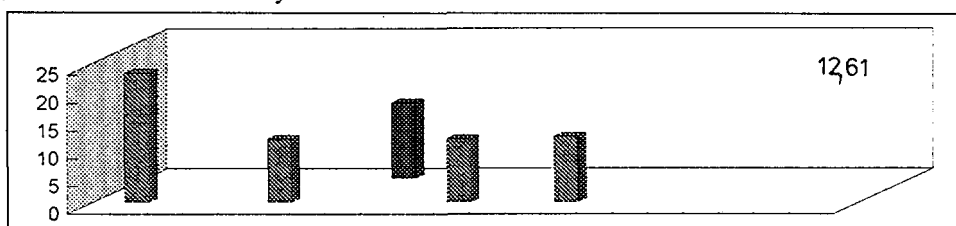
Period 1994 / 1995



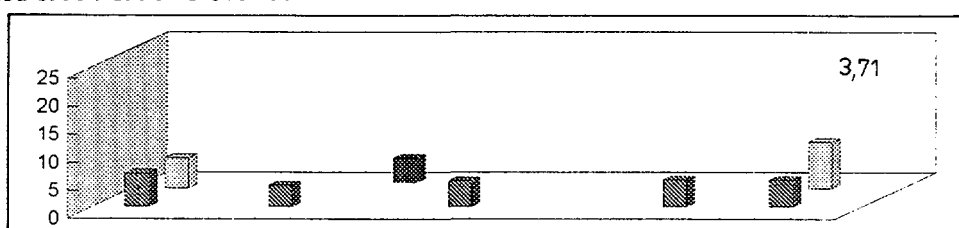
Period 1995 / 1996 - October 1995



Period 1995 / 1996 - February 1996



Period 1995 / 1996 - November 1996



Period 1996 / 1997 - January 1997

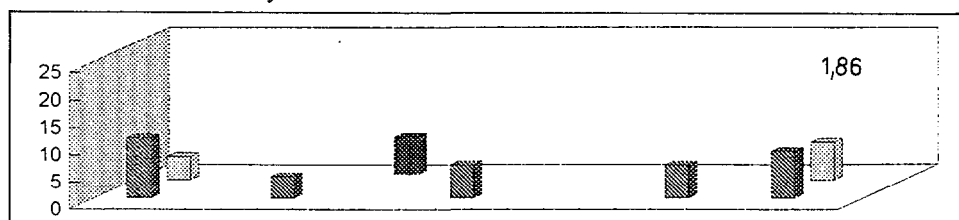


Fig.3: Averaged values of sulphates concentrations ($\mu\text{g} / \text{kg}$) in steam generator secondary water along the tube bundle (bars), in blow down water (numerical values) for four periods of SG operation from 1994 to 1997



Feedwater Flow-in to Steam Generators Tube Bundle

Ludovít Papp, VÍTKOVICE NPP Services

1. Introduction

To enhance the WWER 1000 steam generators reliability, the feedwater distribution and blowdown systems were modified at many operated steam generators. The basic idea of these modifications is to create a „ salt corner “ in steam generator and consequently to provide the blowdown of SG from this place. To fill this target, the asymmetric feedwater distribution is used. As follows from measurements of OKB GIDROPRESS, the concentration of impurities around the collectors dramatically decreased after this corrective measures. The same results we have obtain at Dukovany WWER 440 NPP.

Nevertheless, the system of feedwater distribution can be used for the modification of hydraulic characteristics of SG. This possibility was studied during the design of Temelin NPP steam generators modification.

2. Calculation of flow rate along the tube bundle

We will assume the tube bundle with height H and length L . The feedwater is flowing downstream along the margin column of bundle. The width of feedwater channel is d_{fc} . The zero point of the coordinate system is at the bottom of tube bundle. The total flow rate of feedwater in the feedwater channel as well as of two-phase mixture in the tube bundle in the interval $0-h$ is given by equation

$$M(h) = L \cdot \int_0^h G \cdot dh \quad [\text{kg} \cdot \text{s}^{-1}] \quad (1)$$

where $G(h)$ $[\text{kg} \cdot \text{m}^{-2} \cdot \text{s}^{-1}]$ is density of mass flux which is generally the function of hight h . Quality of two-phase mixture will be

$$x = (q \cdot h) / (r \cdot j) \quad (2)$$

where q $[\text{kW} \cdot \text{m}^{-2}]$ is heat flow density, r $[\text{kJ} \cdot \text{kg}^{-1}]$ is evaporation heat and j $[\text{kg} \cdot \text{m}^{-1} \cdot \text{s}^{-1}]$ given by the integral on the right side of eq. (1) is the sought flow rate.

The following equation of equilibrium must by filled for any coordinate h :

$$g \cdot \int_0^h (\rho_{fc} - \rho_{TP}) dh = \int_0^h dp_{fc} + \int_0^h dp_{TPF} \quad (3)$$

where ρ_{fc} resp. ρ_{TP} are density of medium in the feedwater channel, resp. density of two-phase mixture in the bundle, dp_{fc} resp. dp_{TPF} are the pressure drop on the feedwater channel, resp. on the tube bundle (we have neglected the local pressure drops) and g is the constant of gravitation. Assuming the linear function of density of mixture in the feedwater channel, density of medium in this channel is given by equation

$$\rho_{fc} = \rho' - k \cdot h \quad (4)$$

where k can be calculated from outlet void fraction α_{out} using the following equation

$$k = \alpha_{out} \cdot (\rho' - \rho'') / H \quad (5)$$

where ρ' resp. ρ'' are density of water, resp. vapor for given pressure.

Using homogenous model of two-phase flow, density of two-phase mixture is given by equation

$$\rho_{TP} = (\rho' \cdot \rho'') / (x(\rho' - \rho'') + \rho'') \quad (6)$$

where x is the two-phase mixture quality.

In case of homogenous model of two-phase flow across the tube bundle the two-phase pressure drop can be written as

$$\int_0^h dp_{TPF} = (\zeta / d_{eq}) \cdot K_1 \cdot \int_0^h j^2 \cdot dh + (\zeta / d_{eq}) \cdot K_2 \cdot \int_0^h (h \cdot j) dh \quad (7)$$

where ζ is the pressure drop coefficient for the given tube row, d_{eq} is the equivalent hydraulic diameter of tube bundle and the coefficients K_1 resp. K_2 are given by equations

$$K_1 = L^2 / (2 \cdot \rho' \cdot F_v^2) \quad (8)$$

where F_v is the total gap area of the tube row, and

$$K_2 = K_1 \cdot (q / r) \cdot (\rho' / \rho'' - 1) \quad (9)$$

The pressure drop on the feedwater channel can be expressed as

$$\int_0^h dp_{fc} = \xi_{fc} \cdot K_3 \cdot \int_0^h j^2 dh \quad (10)$$

where ξ_{fc} is the feedwater channel friction factor and the coefficient K_3 is given as

$$K_3 = 1 / (2 \cdot \rho' \cdot d_{fc,h} \cdot d_{fc}^2) \quad (11)$$

Using the equations described above we obtain from eq. (3) the final equation for calculation of flow rate distribution along the bundle $j(h)$ as

$$\begin{aligned} g(\rho' - \rho'') = & ((\zeta / d_{eq}) K_1 + \xi_{fc} K_3) \cdot ((\rho'' \cdot r) / (\rho' \cdot q h)) \cdot j^3 + \\ & + ((1 - (\rho'' / \rho')) (K_1 \zeta / d_{eq} + \xi_{fc} K_3) + K_2 \zeta \cdot \rho'' \cdot r / (d_{eq} \rho' \cdot q)) \cdot j^2 + \\ & + ((1 - (\rho'' / \rho')) K_2 h \zeta / d_{eq} + kg \rho'' \cdot r / (\rho' \cdot q)) \cdot j + \\ & + kgh(1 - \rho' / \rho'') \end{aligned} \quad (12)$$

Using eq. 12, the influence of heat flux, tube bundle geometry and feedwater characteristics on distribution of flow rate along the tube bundle was investigated.

3. Conclusions

1. The influence of heat flow is evident from Fig.1 and Fig.2. According to results of flow models with bottom feeded bundles the influence of heat flow on flow-in rate across the bundle is minimal.
2. The influence of void fraction in the feedwater channel is more significant - see Fig.3 and Fig.4. In case of $\alpha_{out} = 0.7$, which is the realistic value for the first 1m of the tube length, the total mass flux in the tube bundle decrease from $50 \text{ kg.m}^{-1}.\text{s}^{-1}$ to $34 \text{ kg.m}^{-1}.\text{s}^{-1}$.
3. The most important result of our calculations is the fact that in the upper part of the tube bundle the two-phase mixture flows from tube bundle to feedwater channel - this flow pattern appears for $h > 0.7 \text{ m}$ in case of $\alpha_{out} = 0$, resp. $h > 0.2 \text{ m}$ in case of outlet void fraction $\alpha_{out} = 0.7$.
4. With the aim to support the circulation in the hot leg of the tube bundle, the partially submersed feedwater distribution is investigated for Temelin NPP. This system is a modification of OKB GIDROPRESS solution for the reconstruction of SG feedwater system.

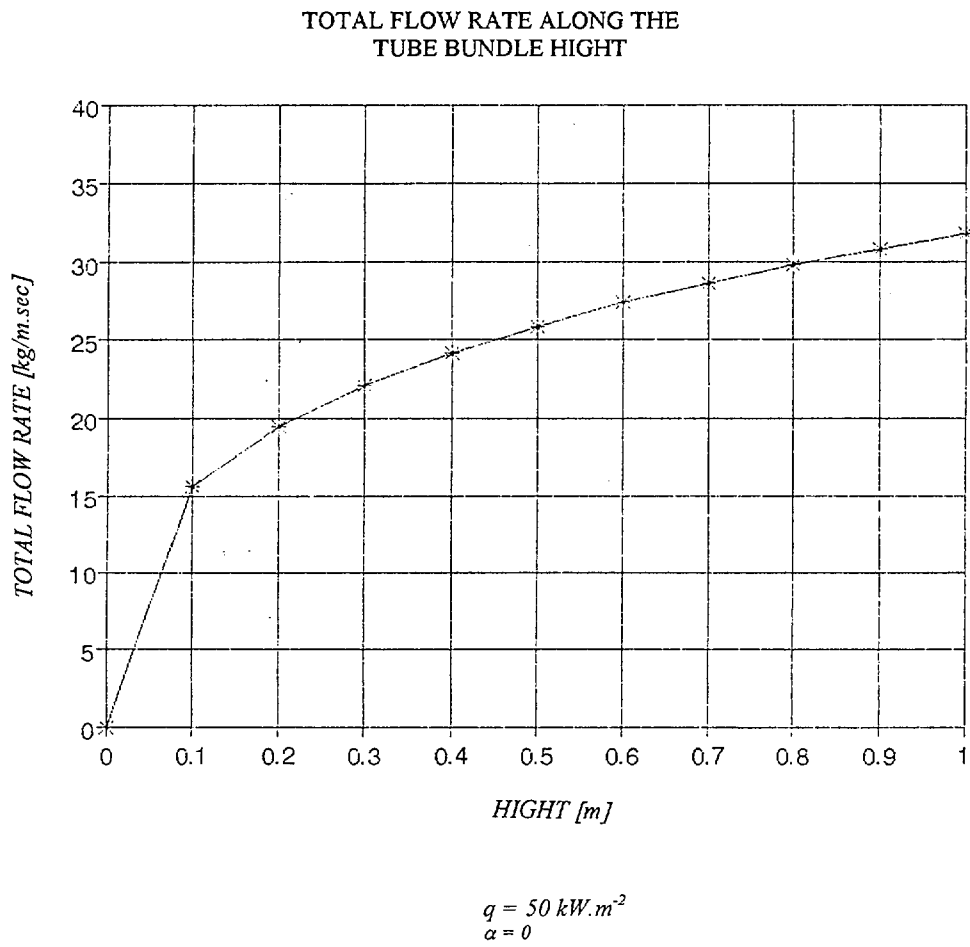


Fig. 1

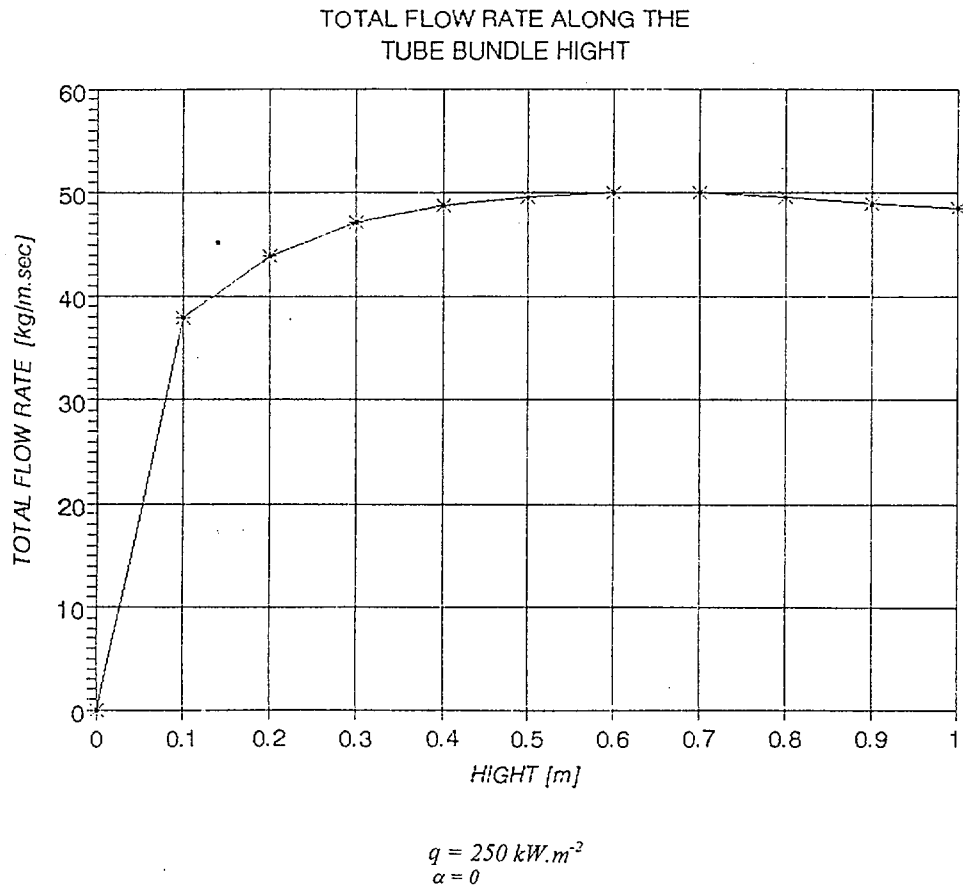


Fig. 2

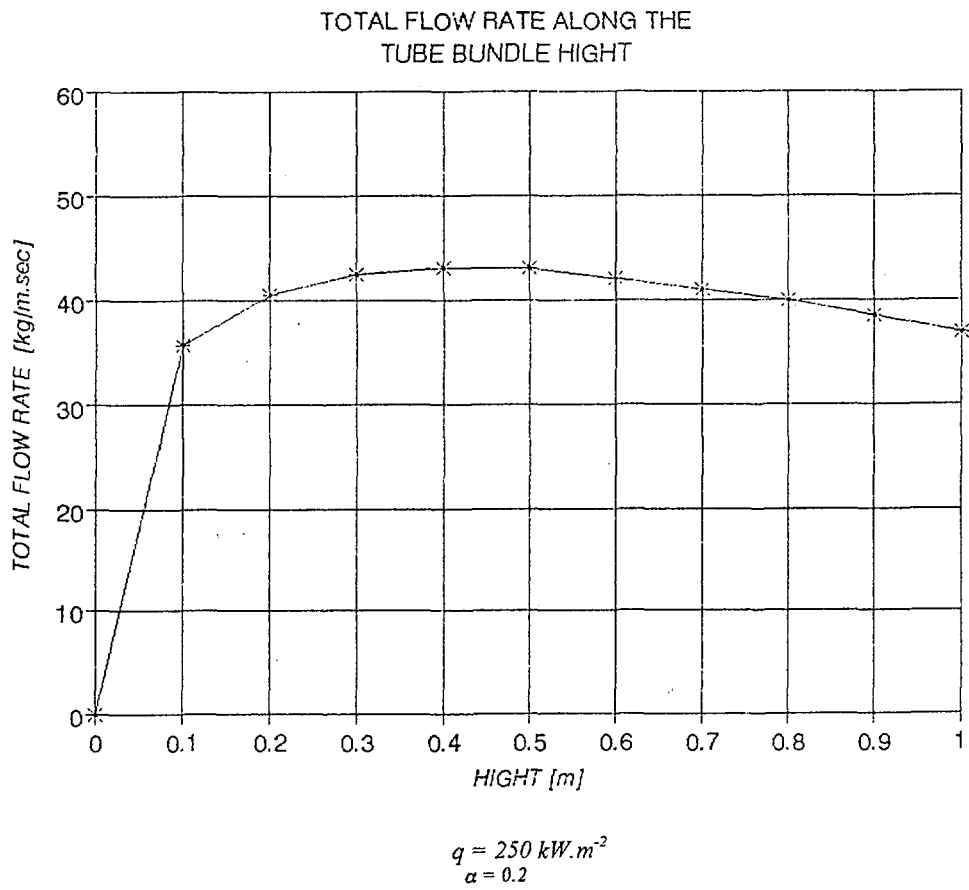
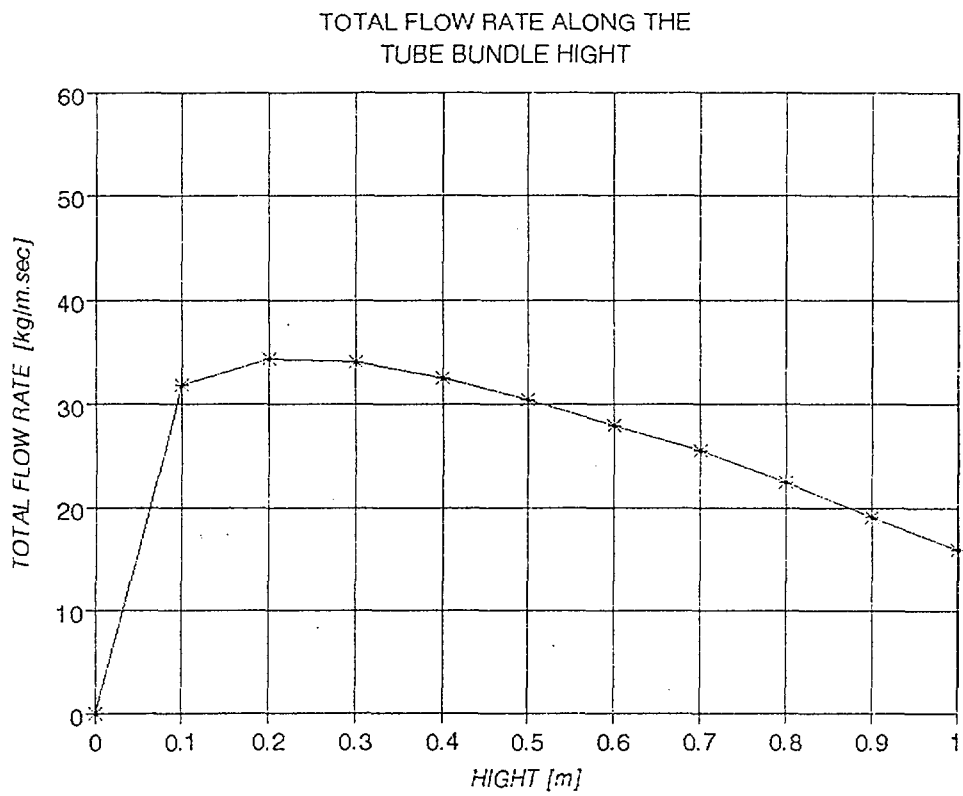


Fig. 3



$$q = 250 \text{ kW.m}^{-2}$$
$$\alpha = 0.7$$

Fig.4



MODELING OF SOLUBLE IMPURITIES DISTRIBUTION IN THE STEAM GENERATOR SECONDARY WATER

Oldřich MATAL, Tomáš ŠIMO, ENERGOVÝZKUM s.r.o.
Božetěchova 17, 612 00 Brno
Czech Republic

Lubor KUČÁK, František URBAN, SLOVAK TECHNICAL UNIVERSITY
Bratislava , Slovak Republic

Abstract:

A model was developed to compute concentration of impurities in the VVER 440 steam generator (SG) secondary water along the tube bundle. Calculated values were verified by concentration values obtained from secondary water sample chemical analysis.

1. Introduction

A computer code PG EN BS was developed to calculate soluble impurities (sodium etc) distribution in steam generator secondary water along the tube bundle as a function of water distribution, blow down flow rates, sludge flow rate, SG power level and time. Measured impurities concentration values [Ref 1] provided a tool for PG EN BS code verification.

2. Steam generator simplifications for simulating purposes

The fundamental computation procedure is based on thermal analysis of processes in the SG. To compute heat transfer coefficients at the primary as well as secondary side well known formulas were used, namely

$$\alpha_1 = 0,021 \cdot \frac{\lambda}{d} \cdot \text{Re}^{0,8} \cdot \text{Pr}^{0,43}$$

and

$$\alpha_2 = 1,18 \cdot p^{0,176} \cdot q^{0,7}$$

Thermal analysis take in to consideration different lengths of individual tubes in tube bundle, different flow rates of primary water in tubes due to different pressure loss and also different heat flow rates in individual sections.

To simulate soluble impurities distribution in the secondary water the steam generator was subdivided in to sections with boundaries more or less identical with tube bundle supports and pressure vessel wall, Fig 1.

In each section mass balance is calculated, where a given water mass flow rate from an adjacent section in to the section is possible, Fig 2. Relative values of the feed water rate transported in to each section by the feed water system can be selected. Selected values depend on the design characteristics of the feed water distribution system used in the steam generator.

On the other hand the water mass value in the section decreases by evaporation, water flowing in to adjacent sections and blow down if applicable for the given section.

It is also assumed the impurities flow rate with the steam flow is negligible.

The impurity concentration value in the section is a time dependent function.

The model was developed for steady operational state of the steam generator, that means no changes in power level, temperatures and pressures are supposed. The impurities ballance is done in time periode $\Delta\tau$ balancing the impurities amount transported into steam generator in the feed water.

3. Sodium distribution in the secondary water

3.1 Former feed water distributing system

Distribution of water flow rates in to sections along the tube bundle is not uniform as also reported in [Ref 2] .

One of the concequencies is sodium distribution in secondary water shown in Fig 3. Very similar values as calculated in Fig 3 were obtained also from chemical analysis of water samples sampled from steam generator secondary side under steady state conditions at nominal power level. Maximum of sodium concentrations between 200 and 250 $\mu\text{g} / \text{kg}$ at one end of the steam generator is typical.

3.2 EBO design feed water distributing system

Calculated distribution and concentration values of sodium are Fig 4. Distribution and concentration values are very similar to that obtained from chemical analyses of secondary water samples [Ref 1].

4. Conclusion

Developed model provides values of sodium concentrations in secondary water very closed to that obtained from chemical analysis of secondary water samples.

Calculations demonstrated that the EBO design feed water distributing system contributes to more intensive water redistribution in the steam generator VVER 440 than the former feed water distribution system. Concenquently impurities distribution in the water along the tube bundle is more or less uniform. Absolute concentration values depend on feed water quality at the inlet of the steam generator.

References

- [1] Matal,O., Schmidt,Š., Mihálik, M.: EBO Feed Water Distribution System, Experience gained from Operation, Fourth International Seminar on Horizontal Steam Generators, 11 - 13 March 1997, Lappeenranta

- [2] Longvinov, S.A et al: Thermohydraulics of PGV - 4 Water Volume during Damage of the Feedwater Collector Nozzles, paper presented at the Third International Seminar on Horizontal Steam Generators, 18 - 20 October 1994, Lappeenranta

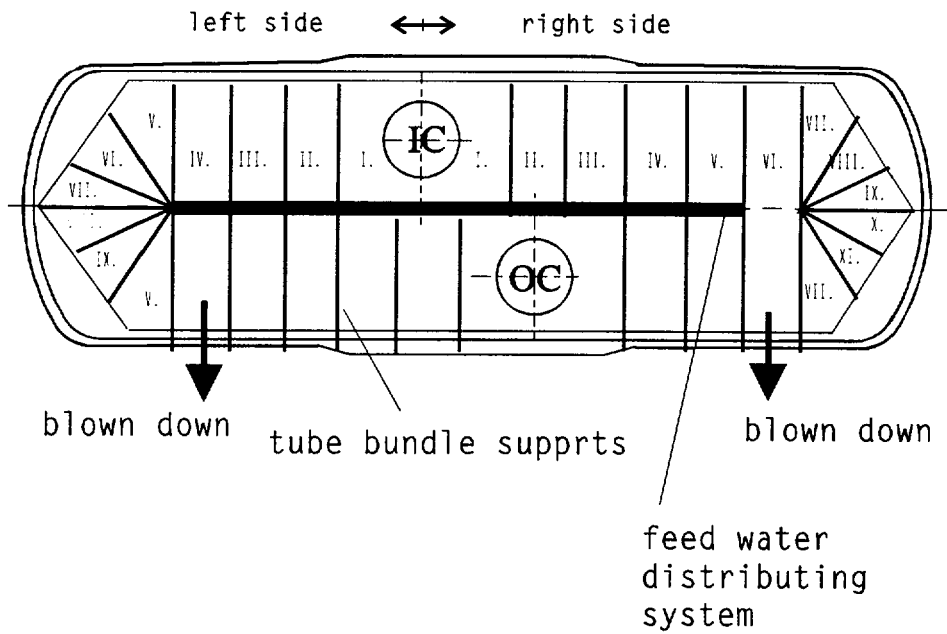


Fig.1 Schematic diagram of the steam generator distribution into sections in order to simulate soluble impurities distribution in the secondary water

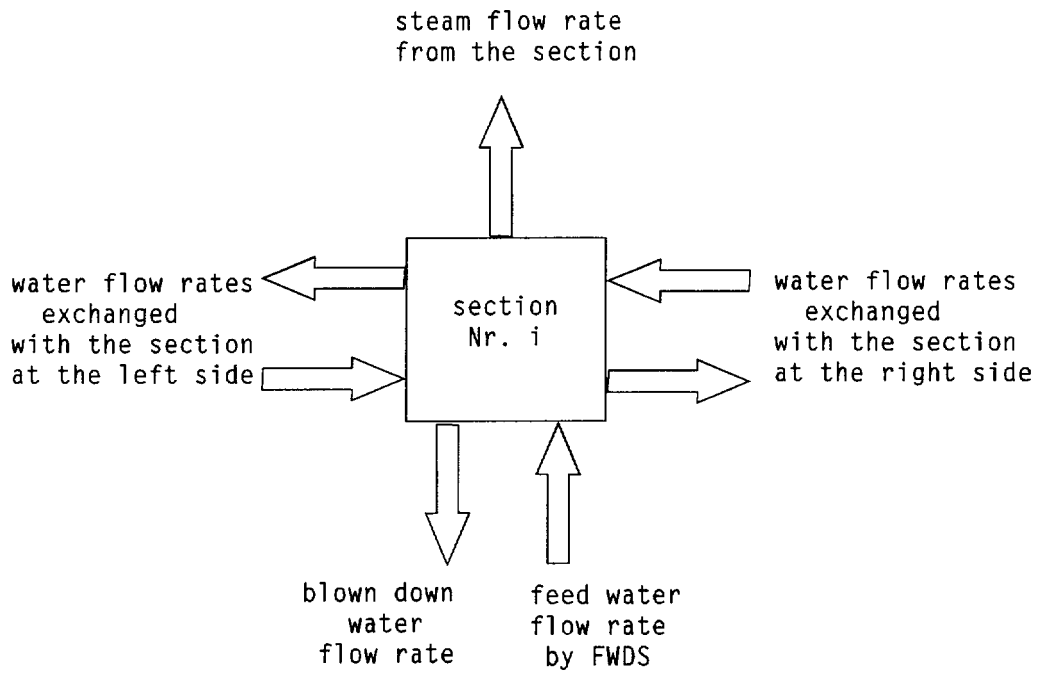


Fig.2 Schematic diagram of the mass balance in the section

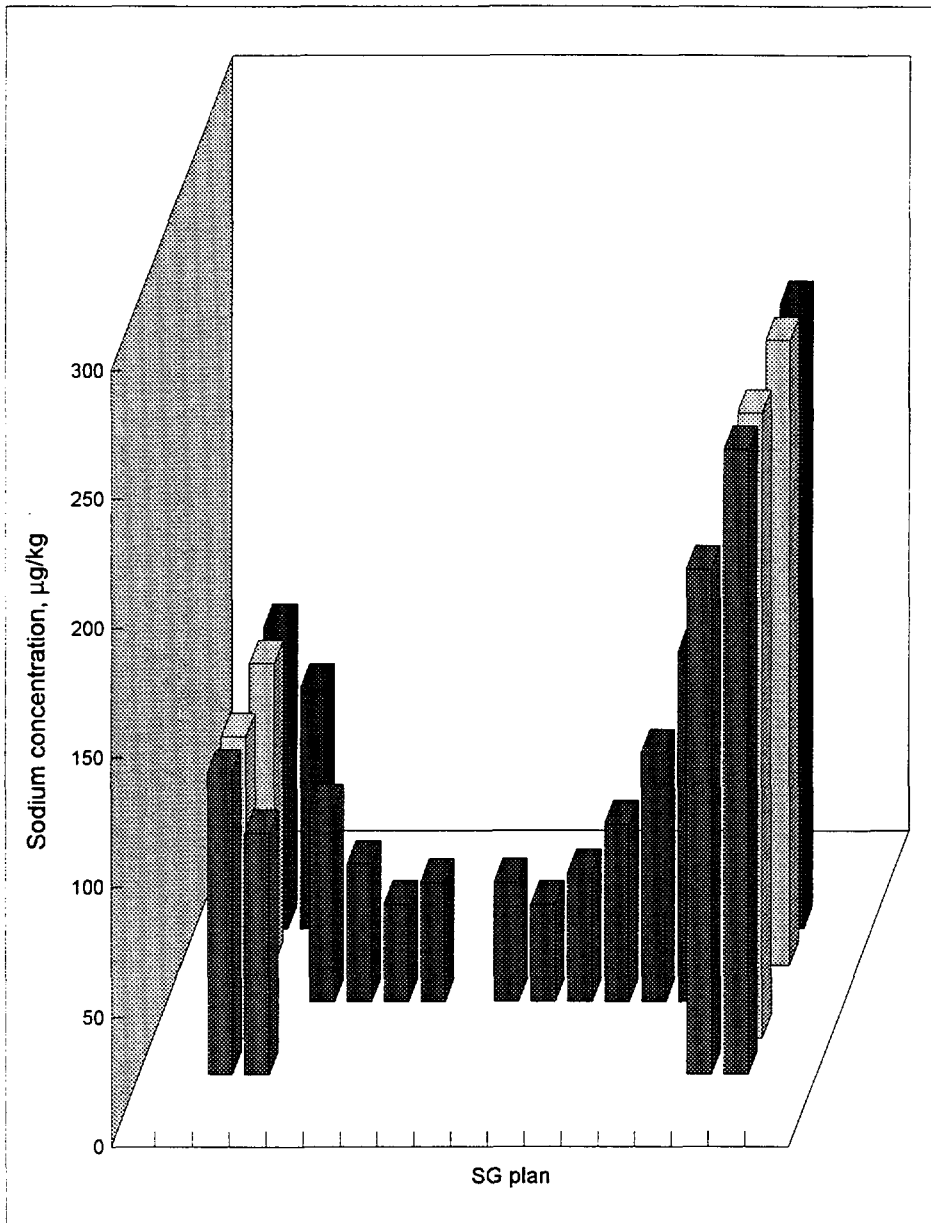


Fig.3 Sodium concentrations calculated in secondary water for the former feed water distributing system

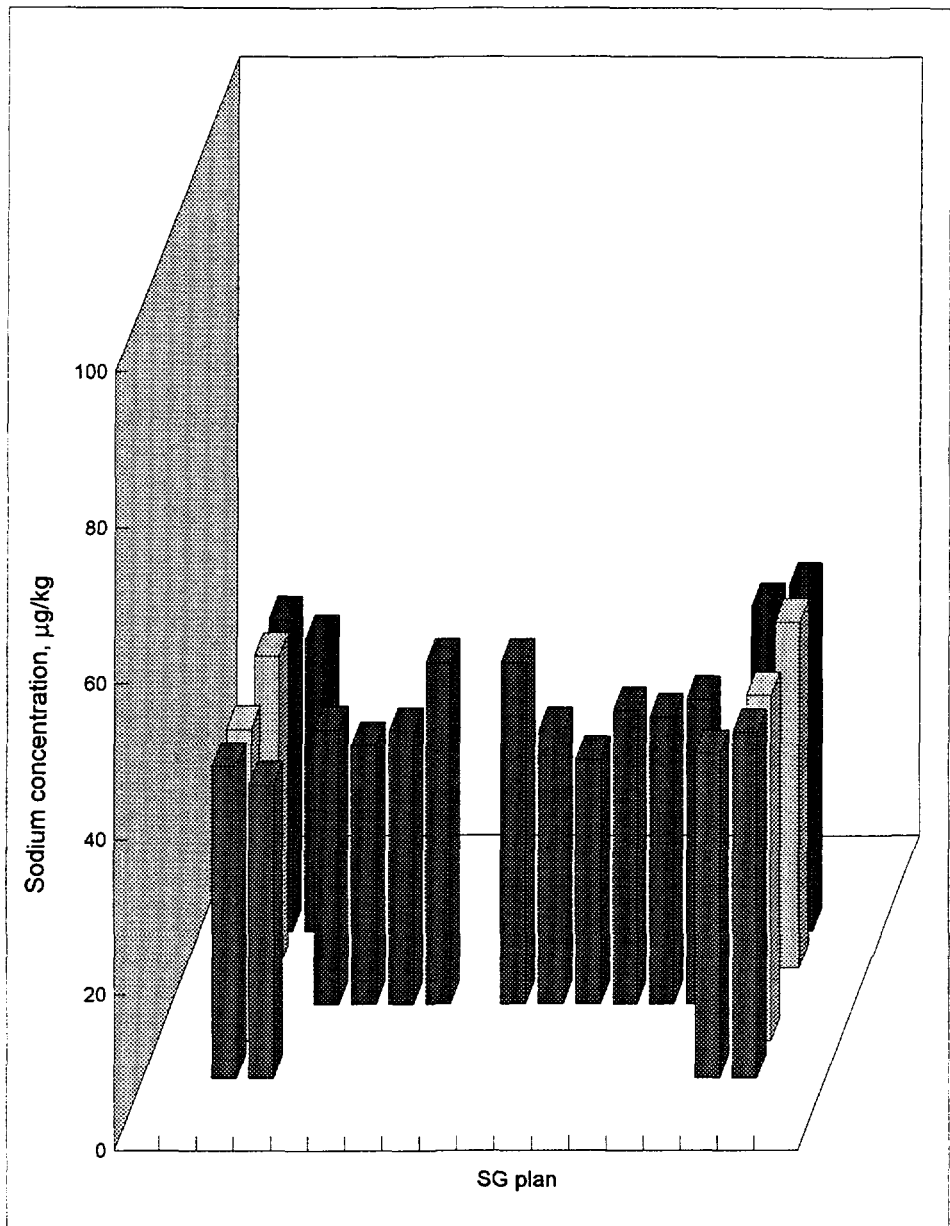


Fig.4 Sodium concentrations calculated in secondary water for the EBO design feed water distributing system



FI9800041

Plugging Criteria for WWER SG Tubes

Ludovít Papp, Martin Wilam, VÍTKOVICE NPP Services

Miroslav Herman, VÚJE Trnava

1. Introduction

At operated Czech and Slovak nuclear power plants the 80 % criteria for crack or other bulk defect depth is used for steam generator heat exchanging tubes plugging. This criteria was accepted as the recommendation of designer of WWER steam generators. Verification of this criteria was the objective of experimental program performed by VÍTKOVICE, J.S.C. , ÚJV Řež , J.S.C. and VÚJE Trnava , J.S.C.. Within this program the following factors were studied.

1. Influence of secondary water chemistry on defects initiation and propagation.
2. Statistical evaluation of corrosion defects progression at operated SG.
3. Determination of critical pressure for tube rupture as a function of eddy current indications.

In this paper , the items 2. and 3. are presented..

2. Crack propagation

To predict a crack growth rate the statistical evaluation of prior eddy current inspection data has been performed. This analysis involved data measured within 1990 - 1995 on NPP Dukovany (WWER 440). Most of these indications were located at the hot legs in tube - tube support regions with restricted flow.

The progression of signals depending on time has been evaluated from this data set - see Fig.1. The indication growth rate is $v_{EC} = 1.16$ % of wall thickness per month in this case. This result is strongly influenced by the fact , that the crack propagation rate is probably much higher in the initial phase of defect growth then in the phase of „developed“ corrosion crack or pitting. Taking into account this phenomena, forty six defects with the first EC indication higher then 20 % of wall thickness have been selected. Such case is shown in Fig.2. The crack propagation rate calculated from these data set is $v_{EC} = 0.58$ % of wall thickness per month. To validate the anticipation mentioned above , the dependence of the EC indication progression on the initial defect size has been analyzed. The result is shown in Fig.3.. The slope of regression line is -0.515 and for indications about 80 % of wall thickness the crack propagation rate reaches zero. This result validates the hypothesis concerning the decrease of the indication progression rate with the defect size increasing. Therefore, for further calculations the corrosion defects propagation rate, we will use the value $v_{EC} = 0.58\%$ EC/month.

Statistical meaning of this value is evident from data shown in Tab.1, too. This table shows the history of SG tubes plugged due to leakage during SG operation.

Tab. 1

	Date of inspection	EC indication
1.	11.11.1992	0
	09.04.1994	56, 30, 97 (three indic.)
2.	09.07.1992	0
	12.04.1994	88

3.	28.07.1990	38
	04.08.1991	79
4.	20.11.1990	0
	09.11.1992	61
	12.01.1994	99
5.	06.08.1991	0
	01.10.1994	91

Notice: As follows from these data, not even 100% inspection of SG tubes in 4-year period can't ensure leakage-free operation of SG.

3. Burst tests

Steam generator tube burst tests were performed on tubes with artificially prepared stress corrosion cracks. The tests were performed at operating temperature on free length of the tube.

The correlation between the burst pressure and the eddy current size of defect is shown in Fig.4. The burst pressure has never dropped under the value 0.2 of normalized burst pressure even for the tubes with indications between 80 - 100 % of wall thickness. A bulging effect has occurred in the area of the defect up to 70 % indication while the tube rupture is realized without any plastic deformation in the case of indications higher than 70 % of wall thickness.

Burst testing of damaged tubes has shown that the limiting factor of the tube integrity is the thickness of the tube wall under the flaw. Regarding the burst test results and SG tube material behavior we can conclude that failure probability of the WWER SG tubes with longitudinal defects under the operating conditions is extremely low.

4. Plugging criteria

As an example, the burst tests results including regression line for WWER 440 MW SG are plotted in Fig.5. The regression line is given by equation:

$$P_{CRIT} = 95.226 - 0.72.\%EC \quad /1/$$

P_{CRIT} critical pressure
 $\%EC$ eddy current indication

For determination of plugging criteria the probabilistic approach was used. It means that the limit lines for chosen probabilities have to be calculated. For limit line calculation we have used the Little and Jebe, 1975 approach. The limit line for 0.97 probability that 96 % of future burst test results will lie above the limit line is shown in Fig.5. Besides the choice of the probability level it is necessary to define the pressure conditions for plugging criteria evaluation. For our calculations, we have assumed following pressure conditions:

- | | |
|--|----------------------------|
| 1. Operating pressure | $dp = p_p - p_s$ |
| 2. Steam line break pressure | $dp = p_p$ |
| 3. 3 times operating pressure difference | $dp = 3 \cdot (p_p - p_s)$ |

Δp pressure differential
 P_p primary side pressure
 P_s secondary side pressure

This pressure conditions are sketched in Fig.5 as a horizontal lines. The intersection of chosen pressure condition and the limit line determines the basic point for plugging criteria calculation. From this basic value is necessary to subtract progression of crack size within the requested time period. It means that the following factors influence the final value of the plugging criteria:

1. Requested level of probability
2. Requested pressure conditions
3. Requested time period between two SG tubes inspections

For example , for limit line resp. pressure conditions shown in Fig.5 we obtain for 48 month inspection period the following plugging criteria : 60 % for pressure cond.1., 54 % for pressure cond.2. and 39 % for pressure conditions 3.

Similar calculations were performed for other probability levels.

5.Conclusions

1. Plugging criteria are complex phenomena . Determination of this criteria needs to define the boundary conditions as well as requested levels of confidence.
2. The progression rate of particular defects depends on individual conditions in SG. The plugging criteria should be specific for each utility.
3. Improvement of the plugging criteria demand future defect progression monitoring on NPPs under operation..

References

Little,R.,E.,Jebe,E.H.,“Statistical design of Fatigue Experiments“,J.Wiley and sons,New York,1975

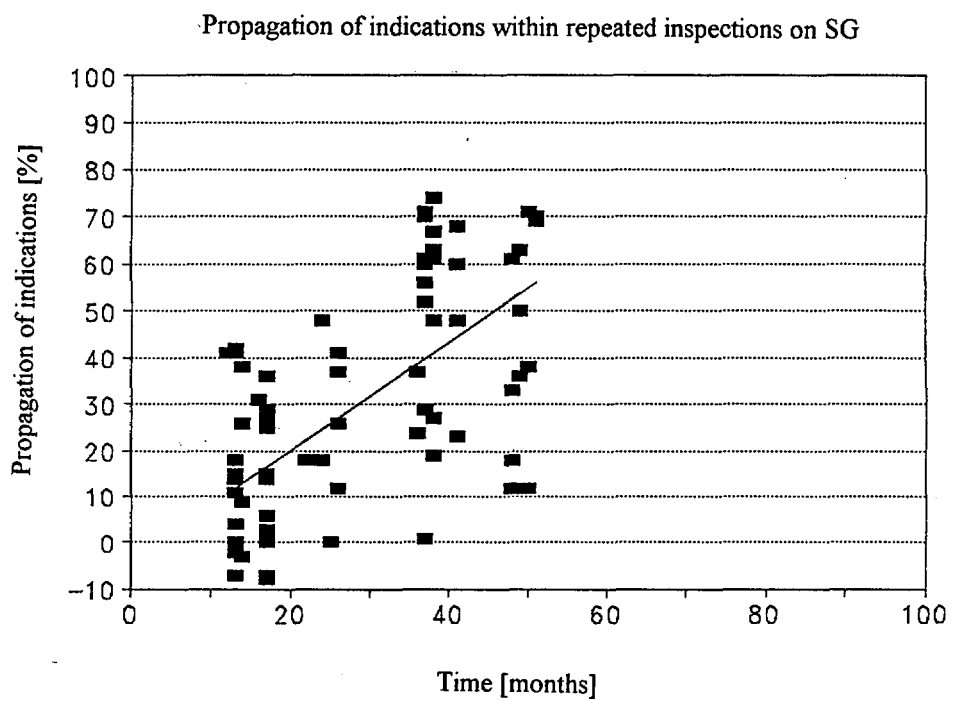


Fig. 1

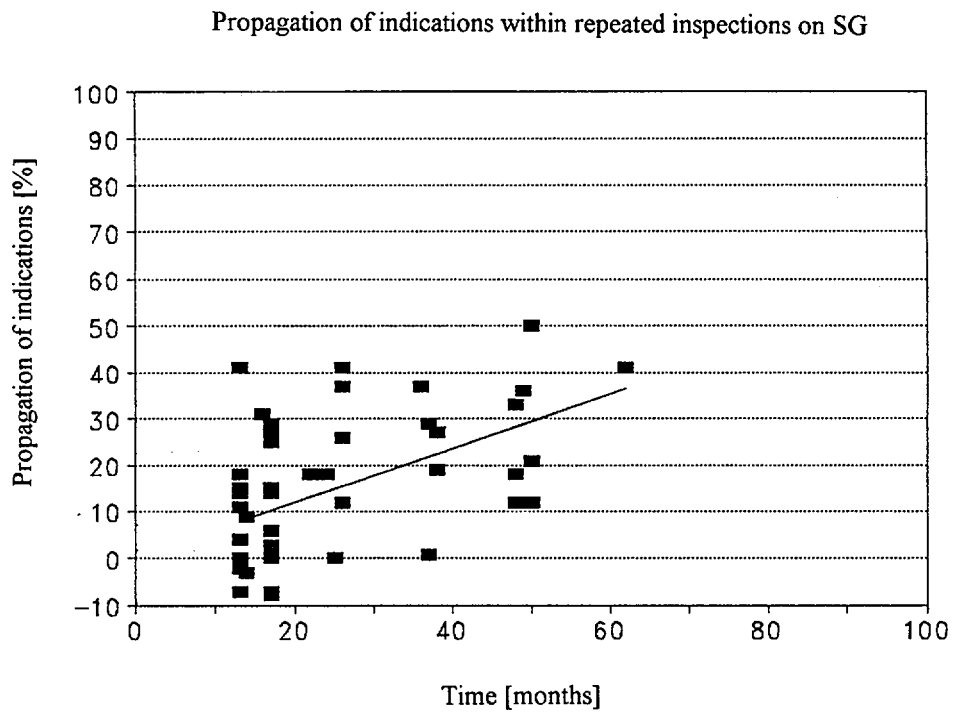


Fig.2

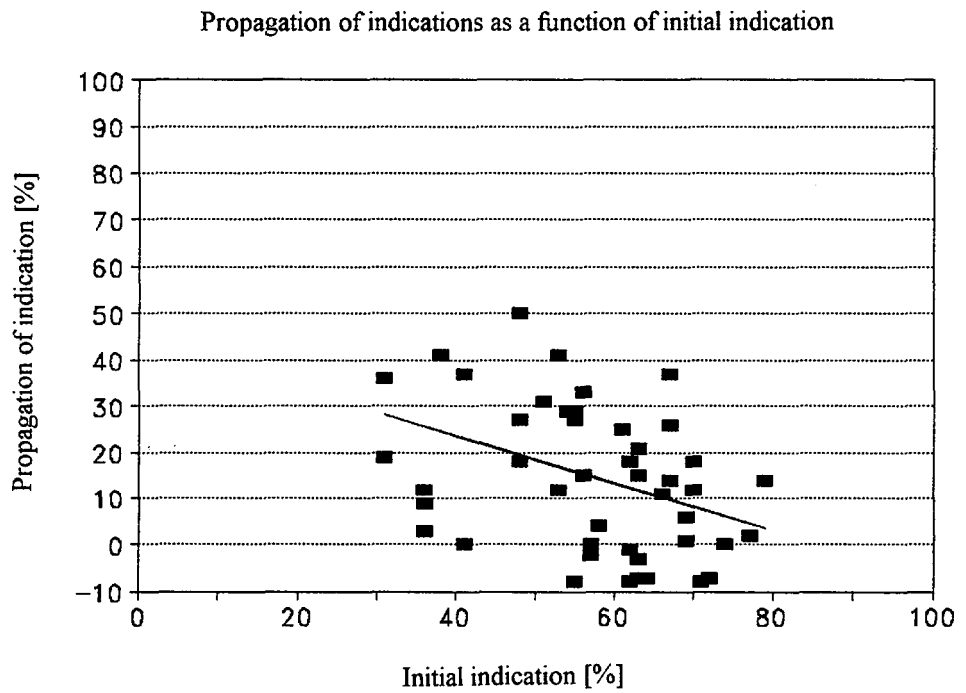


Fig.3

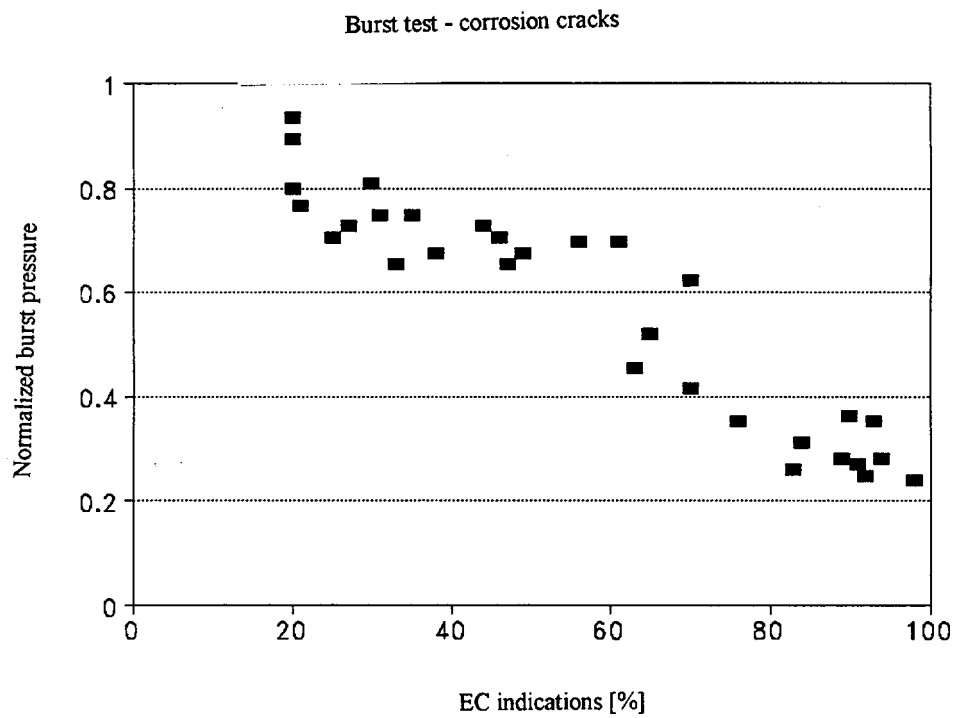


Fig.4

Limit line for probability 96 % that at least 0.96 proportion of future burst tests will lie above the limit line

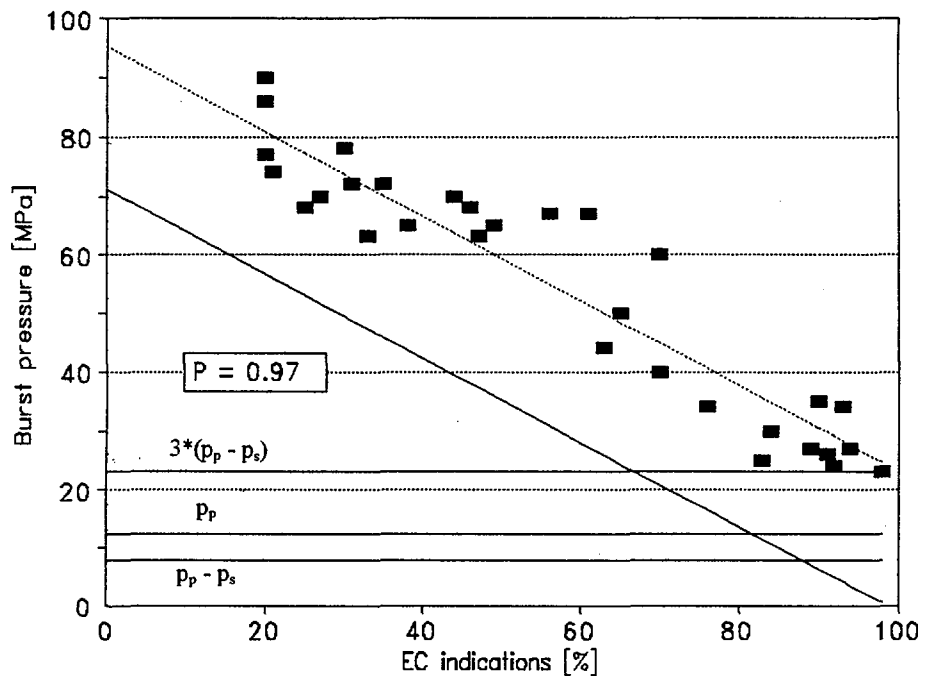
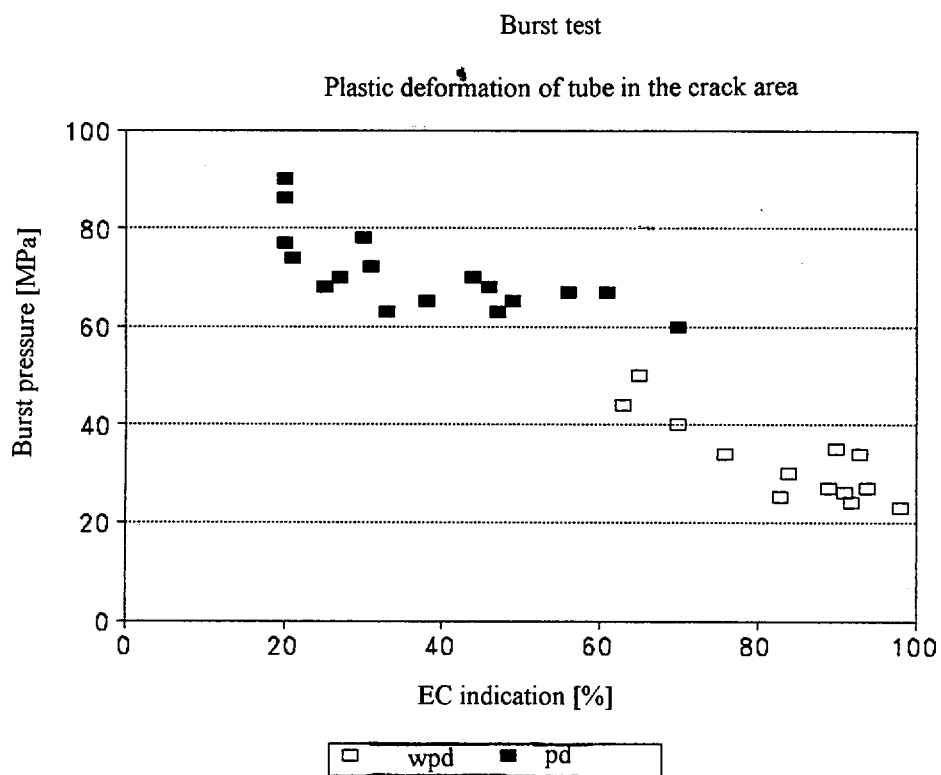


Fig.5





FI9800042

STRUCTURAL AND LEAKAGE INTEGRITY ASSESSMENT OF WWER STEAM GENERATOR TUBES

KAREL ŠPLÍCHAL, JOSEF OTRUBA

Nuclear Research Institute plc. Řež, 250 68 Řež, Czech Republic

*4th International Seminar on Horizontal Steam Generators
11-13 March 1997, Lappeenranta, Finland*

1. INTRODUCTION

The integrity of heat exchange tubes may influence the life-time of WWER steam generators and appears to be an important criterion for the evaluation of their safety and operational reliability. The basic requirement is to assure a very low probability of radioactive water leakage, preventing unstable crack growth and sudden tube rupture. These requirements led to development of permissible limits for primary to secondary leak evaluation and heat exchange tubes plugging based on eddy current test inspection.

The stress corrosion cracking and pitting are the main corrosion damage of WWER heat exchange tubes and are initiated from the outer surface. They are influenced by water chemistry, temperature and tube wall stress level. They take place under crevice corrosion condition and are indicated especially:

- under the tube support plates, where up to 90 - 95 % of defects detected by the ECT method occur
- on free spans under tube deposit layers.

Both the initiation and crack growth cause thinning of the tube wall and lead to part thickness cracks and through-wall cracks, oriented above all in the axial direction.

2. LEAK RATE LIMITS

The basic approach to the determination of primary-to-secondary leak permissible limits follows from Fig. 1 and is based on the measurement on tubes with through-wall cracks. The evaluation should be comprised of location of defects in the tube free spans, the region of the tube support plate, and the tube to collector expansion zones. In our work the limits have been derived only for the tube free spans. The tests were carried out on equipment which enabled simulation of the primary and secondary circuit temperatures and pressures of WWER 440 and 1000 steam generators. The leakage of medium through the crack was measured in time dependence of exposure to the pressure during pressurization of inside of the tube by primary water from the experimental reactor water loop. Resulting relationships between the leak rate and the inner crack length or the inner crack cross-section are shown in Fig. 2 and 3, respectively [1,2]. The smaller scatter of measured values in the leak rate crack cross-section

relationship, is due to a measured parameter involving the crack width, which is decisive for clogging of cracks with primary water particles.

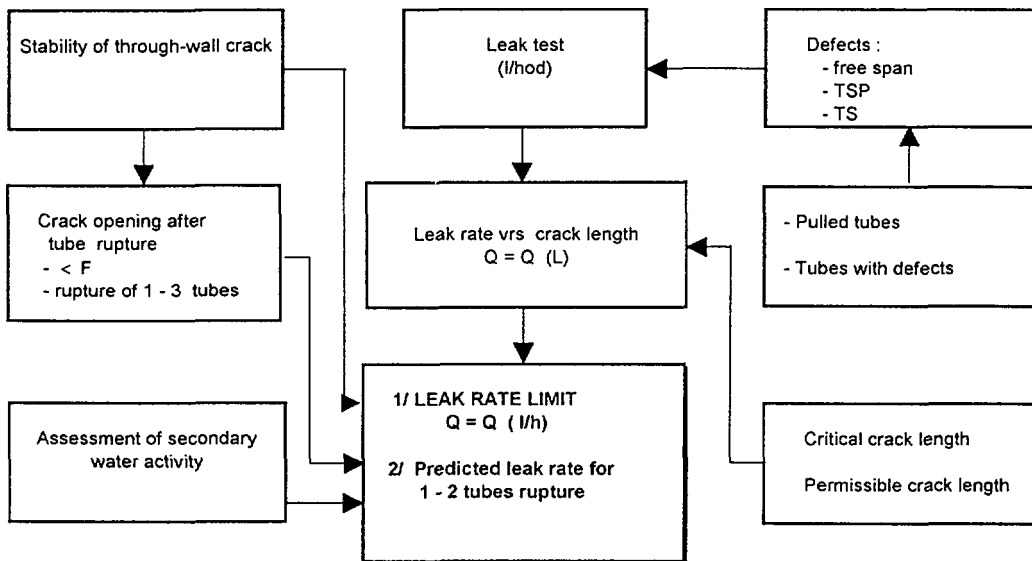


Fig.1. SG tube leak assessment

The permissible leak rate value was determined using following assumptions :

(1) The leak occurs under normal conditons. The permissible crack lengths were calculated under loads which are defined as a threefold value of the primary-to-secondary pressure difference, i.e. $\Delta P = 3 \times 7.8 = 23.4$ MPa for WWER 440, resp. $\Delta P = 3 \times 9.4 = 28.2$ MPa for WWER 1000 steam generators.

(2) The leak rate can occur at the primary circuit pressure of 12.5 MPa (WWER 440), resp. 15.7 MPa (WWER 1000) attained under accident conditions, such as secondary side depressurization resulting from a main steam line or feedwater line break. Under these conditions the permissible crack length were evaluated, using a safety factor of $\sqrt{2}$.

On the basis of graphical evaluation using lower bound curve, as shown in Fig. 2a, 3a the permissible leak rates have been determined, as 8 l.h^{-1} for crack length of 11.3 mm (WWER 440) and 10.2 mm (WWER 1000). Permissible crack lengths were determined by means of the instability criterion for given pressures using the conservative σ_f value and a relation taken from [3]. The obtained results are sumarized in Table 1. The evaluation of results by means of a lower bound curve has been used in other works, e.g.[4]. The leak rate value of 5 l.h^{-1} is recommended to keep secondary water radioactivity under sufficient low level.

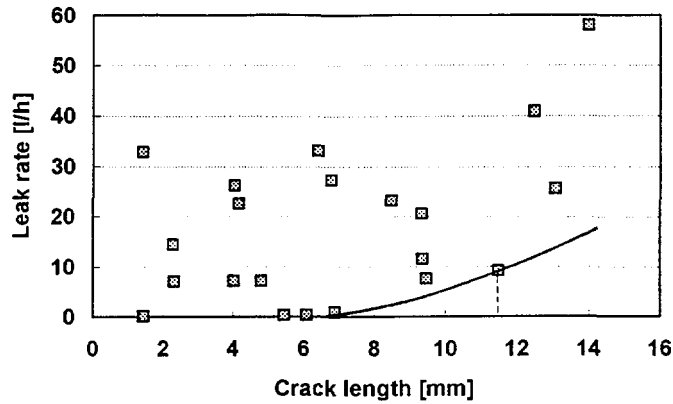


Fig. 2a. Relationship between leak rate and crack length on the tube inner surface for WWER 440 steam generator tubes

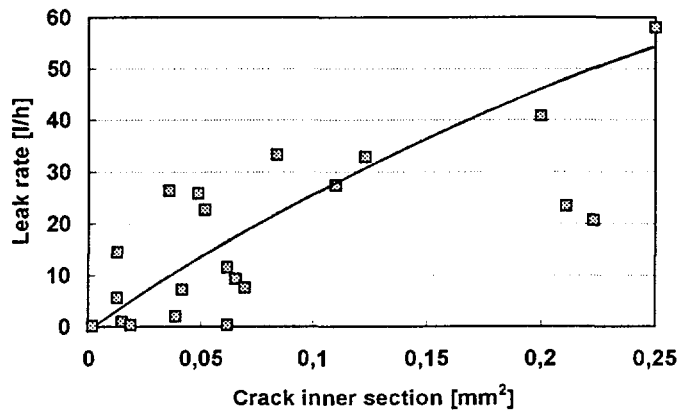


Fig. 2b. Relationship between leak rate and crack section on the tube inner surface for WWER 400 steam generator tubes

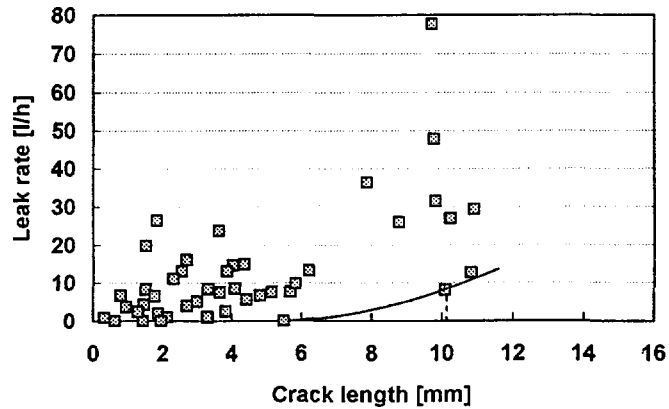


Fig. 3a. Relationship between leak rate and crack length on the tube inner surface for WWER 1000 steam generator tubes

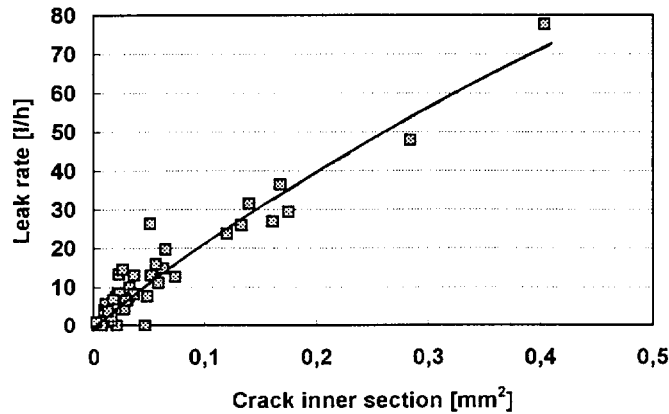


Fig.3b. Relationship between leak rate and crack section on the tube inner surface for WWER 1000 steam generator tubes

Table 1. Permissible leak rates

Power plant	Loading [MPa]	Coefficient of safety	Permissible crack length [mm]	Leak rate [$l \cdot h^{-1}$]
WWER 440	$P_{ID} - P_{OD}$	3	11.3	8
	$P_{ID} = 12.5$	$\sqrt{2}$	20.3	$\gg 10$
WWER 1000	$P_{ID} - P_{OD}$	3	10.2	8
	$P_{ID} = 15.7$	$\sqrt{2}$	20.1	$\gg 10$

3. INTEGRITY OF HEAT EXCHANGE TUBES WITH THROUGH-WALL DEFECTS

As Hahn et al. [5] showed, the instability criterion of a straight tube with longitudinal through-wall defects is given by relation:

$$\sigma_f = M\sigma_N \quad (1)$$

where : $\sigma_f = k(\sigma_y + \sigma_u)$; σ_f , σ_y , σ_u are flow, yield and ultimate stress; σ_N is nominal hoop stress; M is stress magnification factor (bulging factor); k is constant.

For the evaluation of burst tests of heat exchange tubes with longitudinal defects this criterion has been used in following form:

$$P^* = \frac{P_a}{\sigma_f} \cdot \frac{R}{t} = \frac{1}{M} \quad (2)$$

where: P^* is normalized burst pressure, P_a is measured burst pressure, R , t are mean radius and wall thickness of tube.

The dependence of the bulging factor on the normalized length of an axial through-wall defect λ has been derived by Folias [3] (relation 3 in Table 2) and Erdogan [6] (relation 4) respectively.

The normalized through-wall defect length λ is given by relation

$$\lambda = \frac{2a}{\sqrt{Rt}} \quad (6)$$

where $2a$ is the through-wall defect length.

The heat exchange tube integrity was evaluated by means of a burst test. Through-wall axial defects were prepared by electro-spark machining and the SCC method. For the burst test purposes the tubes were lined with a plastic bladder of 2 mm thickness. In Fig.4 the normalized burst pressure values obtained on tubes with electro-spark defects are compared with $1/M$ criteria (for M see Table 2). The value of the "k" constant in the expression for σ_f was determined as $k = 0,522$. The results show a relatively small scatter and correspond best with the criterion, where M is given by the Erdogan's relation (4).

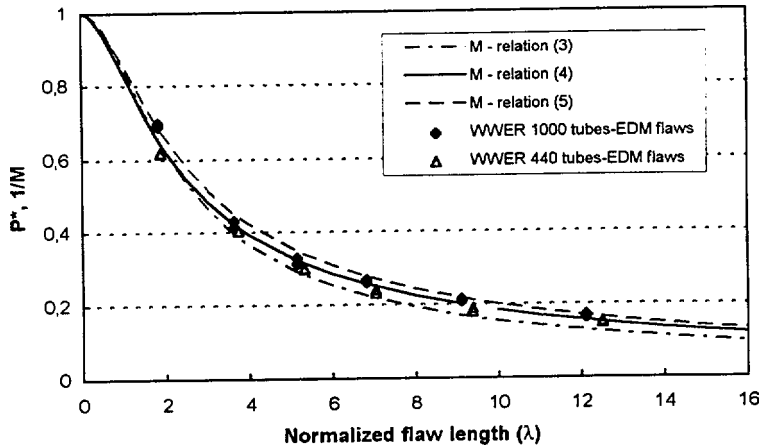


Fig. 4. Burst test results on WWER tubes with EDM axial through-wall defects in free span

Table 2. Bulging factors M and constants k

Relation	M	k	Material	References
(3)	$(1 + 1.61a^2/Rt)^{1/2}$	0.58	Inconel	Cochet [7]
(4)	$0.614 + 0.386^{(-1.25\lambda)} + 0.481 \lambda$			
(5)	$0.614 + 0.386^{(-1.15\lambda)} + 0.436 \lambda$	0.55	Inconel	Hernalsteen [8]
	relation (3), (4)	0.522	08Kh18N10T	this paper

The Folias' relation (3) represents rather a lower bound curve of the test results. This fact is also confirmed by the Fig.5 showing the burst test results obtained on WWER 1000 tubes with artificial SCC cracks. All the normalized burst pressure values lie above the curve determined by the Folias' relation. The larger scatter is caused probably by the uncertainty of the through-wall crack length. In fact the crack usually does not represent a single defect, but rather a system of multiple cracks mutually separated on the tube outer surface by strips of material, their failure occurring only when the unstable crack propagation takes place during the burst test. Individual cracks have a trapezoidal shape, rather than a rectangular one, with a longer side on the tube outer surface. In our evaluation the crack length was taken as the maximum length of the crack system, measured on the tube outer surface.

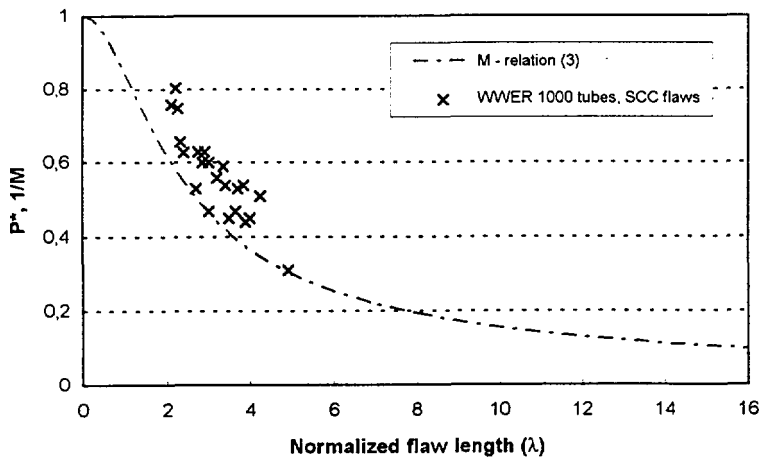


Fig. 5. Burst test results on WWER tubes with SCC axial through-wall defects in free span

The relations (3) and (4) were used for the determination of the length of axial through-wall cracks on WWER 440 and 1000 steam generator tubes, permissible from the point of view of a controllable crack development under normal operation conditions, accident conditions (e.g. secondary circuit depressurization), as well as under conditions of a threefold of the normal operating pressure value. The results are summarized in Table 3.

Table 3. Critical lengths of axial through-wall crack

pressure conditions	WWER 440		WWER 1000	
	ΔP [MPa]	L [mm]	Δ [MPa]	L [mm]
normal operation	7.8	41.9	9.4	36.6
accident	12.5	26.1	15.7	21.9
threefold pressure value difference	23.4	13.8	28.2	12.0

4. CONDITIONS FOR THE THROUGH-WALL CRACK FORMATION

The probability of the through-wall flaws rise is proportional to the number and the depth of partly through-wall flaws during the steam generator operation. Application of the 80 % wall thinning (Figure 6) limit in combination with the ECT in-service inspections can assure safe continuous operation of the tube, i.e. operation excluding uncontrolled unstable crack growth accompanied by the radioactivity leakage [2].

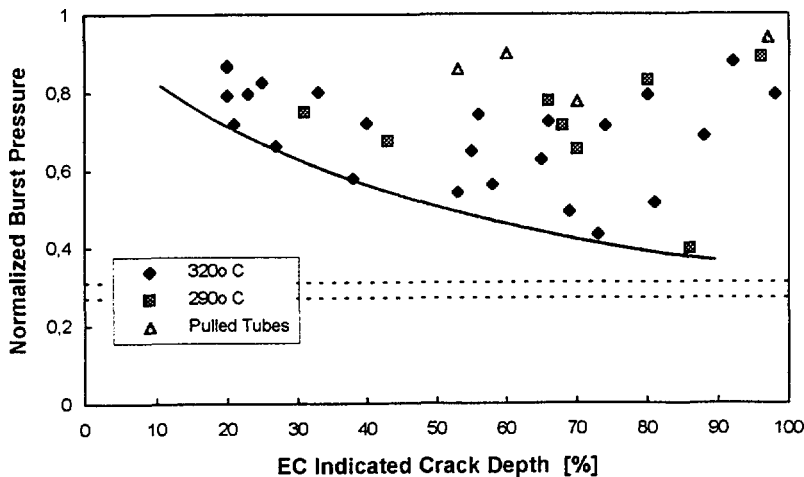


Fig. 6. Normalized burst pressure vs. SCC - slot depth

The acceptance of the 80 % allowable wall thinning criteria for tube plugging is supported by a number of factors:

1. The flow through narrow cracks is limited. In the first period of the growth the defects propagate through the tube wall in the form of narrow cracks and their widening takes place in the course of further exposure to the secondary environment.

The formation of narrow through-wall cracks in the initial period does not necessarily lead to a primary-to-secondary leak because the leakage is determined primarily by the crack width on the tubes inner surface. In the experiments performed on leak test equipment under primary and secondary circuit operating conditions WWER 440 and 1000 (primary-to-secondary pressure difference of 7.8 and 9.4 MPa), tube samples with axial cracks of 3 - 45 μm inner width and 1.3 - 14 mm inner length were investigated. No primary-to-secondary leak was determined at cracks of inner width 3 - 5 μm , whereas in 5 - 20 μm wide cracks the leakage was restricted. The leakage was blocked by clogging of cracks with particles either from the corrosion products or other compounds precipitating during expansion of primary water through the cracks. The average primary water particle size was 7.5 μm for the research reactor water loop and in the range 1 - 5 μm for three WWER nuclear power plants conditions [1].

2. The statistical evaluation of the ECT in-service inspection results from the eight units have shown, that about 15 % of damaged tubes were contained defects deeper than 80 % of the wall thickness. In operation conditions it makes one or few heat exchange tubes in one steam generator.
3. The defected tubes with wall thinning above 80 % are ruptured under burst test condition with the critical pressure of 35 MPa, which is higher than the threefold value of primary to secondary pressure difference 23.4 MPa for WWER 440 and 28.2 MPa for WWER 1000. The critical pressure is also higher than the primary pressure i.e. 17.8 MPa for WWER 440 and 22.2 MPa for WWER 1000.
4. Primary water leakage is monitored by nitrogen N^{16} measurement or other similar sensitive methods, able to identify immediately the formation of through-wall cracks.

5. PRIMARY WATER LEAKAGE CALCULATIONS

Evaluation of leakage was performed for a postulated rupture of one or two tubes and for predicted defects. The programme LEAKH [9] was used, which describes the relation between the geometrical dimensions of an axial crack and the amount of leaking coolant.

In dependence on the crack geometry the model takes into account the pressure drop at the entrance into the crack, friction effects at the crack surface and changes of the through-wall crack cross-section from the inner to the outer tube surface. The calculations have been performed under simplified assumptions, where the flow was taken as one-dimensional, in the two-phase zone the flow was considered to be homogeneous (i.e. the slip between the phases was neglected), the heat exchange between the flow and the surroundings was neglected, the passage cross-section along the flow direction was changing linearly, the input parameters were not time-dependent.

The size of through-wall cracks or defects was determined by means of following data:

1. Cracks with extreme defect size found on operated tubes from NPPs, where the ECT method was not used upon in-service inspections and the tube tightness measurement was performed only by pressurizing of the tube secondary side by water.
2. Failure corresponding to a rupture of one (2 F) or two (4 F) tubes. The postulated defects for the failure extent of 0,05 to 0,3 F, where F is the tube inner cross-section.

Table 4. Calculated primary to secondary leaks

Defects	Inner surface defect size			Calculated leak [l.h ⁻¹]
	Width [mm]	Length [mm]	Cross section [F]	
Pulled tubes	0.100	4.5	0.0027	22.32
	0.085	31.0	0.016	35.28
Postulated defects			0.1	2 912.0
			0.2	5 849.6
			0.3	8 784.00
			2	34 416.0
			4	658 832.0

As follows from the obtained values shown in Table 4, the leakage amounting up to about 35 l.h⁻¹ at defect cross-sections up to 0,016 F was larger by an order of magnitude than suggested limits for the primary coolant leakage. This was the exceptional case of extreme defects from a nuclear power plant. Now the presence and size of such defects during operation of existing NPPs is virtually excluded, thanks to the use of the ECT method. The leakage values determined for the rupture of one or two tubes are by two orders of magnitude higher than that for the postulated extreme defects.

6. CONCLUSIONS

1. The permissible value of primary to secondary leak rate 8 l.h⁻¹ was evaluated with respect to permissible through-wall defect size of WWER 440 and 1000 steam generator tubes.
2. Blocking of the tube cracks by corrosion product particles and other compounds reduces the primary to secondary leak rate.
3. The rate of a crack penetration through the tube wall is higher than the crack widening.
4. The validity of the criterion of instability for tubes with through-wall cracks has been experimentally confirmed. The permissible size of axial through-wall cracks is 13,8 and 12,0 mm respectively for the threefold value of the primary-to-secondary pressure difference in WWER 440 and 1000 steam generators.
5. The calculated leakage for rupture of one tube is by two orders of magnitude higher and for assumed extreme defects by one order of magnitude higher than the suggested primary water leakage limit value of 8 l.h⁻¹.
6. The crack lengths observed on pulled tubes were in all cases lower than the established critical crack lengths. The preliminary statistical evaluation ECT in-service inspection data proved that the crack growth is also sufficiently low [10]. Thus the leakage can be

monitored for a long period under operating conditions. Therefore the leak before break approach could be applied with a sufficient margin of safety.

7. As shown by experimental studies, the use of permissible thinning value of 80 % for the heat exchange tube plugging does not lead to an uncontrollable radioactive leakage or to an unstable crack growth. This corresponds to experience hitherto obtained at WWER 440 NPPs.

LITERATURE

- [1] Šplíchal K. et al.: Evaluation of Steam Generator WWER 440 Tube Integrity Criteria, CNRA/CSNI Int. Workshop on Steam Generator Tubing Integrity in Nuclear Power Plants, Chicago, Illinois, 1995
- [2] Šplíchal K. et al.: Evaluation of Steam Generator WWER 1000 Tube Integrity Criteria, IAEA Topical Meeting on WWER 1000 Steam Generator Integrity, Tokyo, Japan 1995
- [3] Folias E.S.: On the effect of initial curvature on cracked sheets, UTEC CE 69-002, January, 1969
- [4] Esposito J.N.: Use of ECD Data to Assess the Progression of Steam Generator Tubing Degradation, IAEA Specialists Meeting on Steam Generator Problems and Replacement, Madrid, 1993
- [5] Hahn G.T. et al.: Criteria for crack extension in cylindrical pressure vessels, Int. J. Fracture Mechanics, 5 (1969), pp. 187-210
- [6] Erdogan F.: Ductile-fracture theories for pressurized pipes and containers. Int. J. Pres. Ves. Piping 4,(1976), 253-83
- [7] Cochet B: Steam generator tube integrity flaw acceptance criteria, *ibid* 1
- [8] Hernalsteen P.: The influence of condition on burst pressure assessment for inconel tubing, Int. J. Pres. Ves. Piping 5 (1992), pp. 41-57
- [9] Krhounek Vl.: Programme LEAKH (in Czech), Report ÚJV 9919-A, Nuclear Research Institute, Řež, 1993
- [10] Papp L.: Hodnocení integrity teplosměnných trubek PG 440, Vítkovice 1/96, Ostrava, 1996



Support Calculations for Management of PRISE Leakage Accidents

vúje

Peter Matejovič, Ľubomír Vranka

***Nuclear Power Plants Research Institute (VÚJE)
SLOVAKIA***

1. INTRODUCTION

Accidents involving primary-to-secondary leakage (PRISE) caused by rupture of one or a few tubes are well known design basis events in both, western and VVER NPPs. Operating experience and in-service inspections of VVER-440 units have demonstrated also the potential for large PRISE leaks in the case of the steam generator (SG) primary collector cover lift-up (Rovno NPP). Without performing any countermeasure for limitation of SG collector cover lift-up, a full opening results in PRISE leak with an equivalent diameter 107 mm. Although this accident was not considered in the original design, this event is usually analysed as DBA too.

Different means are available for detection and mitigation of PRISE leakage in NPPs which are currently in Slovakia in operation (J.Bohunice V-1 and V-2) or under construction (Mochovce).

2. POSSIBLE HAZARDS

The main feature of large PRISE leakage is confinement bypass. If at least a minimum emergency core cooling system (ECCS) configuration is available during the accident, the core cooling is assured. The possible hazards associated with this kind of accidents are:

- radioactivity release to the environment via BRU-A and SG safety valves;
- long-term loss of ECCS water inventory;
- pressurised thermal shock of reactor pressure vessel after break isolation (cooldown and subsequent repressurisation);
- boron concentration dilution and reactivity increase due to reverse flow (secondary to primary side) through the break;

- core cooling (short and medium term).

The results of the PRISE leaks strongly depend on the assumptions of the analysis. For example, in the first three of the above mentioned points the full ECCS configuration is a pessimistic assumption. In addition, the loss of off/site power and the application of the single failure criterion make the process more dangerous because only limited means are available for mitigation of the accident. In the following, only the first two points are discussed.

3. RADIOLOGICAL CONSEQUENCES

The main safety concern associated with PRISE is the radioactivity release into plant environment. The primary water during the reactor operation gets radioactive due to induced activity. In addition the corrosion products and the fission products increase the activity of the primary inventory. The water in the secondary system contains also some radioactivity, which is due to leaks from the primary to the secondary side, but at normal operating conditions the concentrations of radioactive substances in the secondary coolant are very low. The secondary activity is at least a few orders of magnitude less than the primary activity. Therefore it does not influence the radioactive releases to the environment in the case of a PRISE leaks.

4. LONG TERM ECCS WATER RESOURCES

One of the most dangerous features of PRISE leaks is irreversible loss of primary coolant leaking to the secondary side and via BRU-As and SG safety valves (SV) to environment. The following failures in accordance with [1] should be assumed:

- failure of main reactor circulation loop isolation valves
- depending on the plant configuration, stuck in open position of one BRU-A or SG SV in affected SG.

Since the loop isolation valves are not safety graded system, their failure in affected loop does not mean that the single failure criterion was fulfilled. Besides the initiation event (break opening), loop isolation valve failure, an additional failure of safety related system during break isolation should be considered. Depending on the plant configuration it should be assessed whether the application of single failure criterion may lead to un-isolable leak from secondary side to environment. The full ECCS configuration is a pessimistic assumption. This kind of analysis should be performed until the final safe condition of the plant is reached. This means that the primary pressure drops below the setpoints of the BRU-As and SG SVs in the case of their proper operation or the primary system is depressurised nearly to atmospheric pressure, respectively.

5. SYMPTOMS OF PRISE

Characteristic symptoms of primary to secondary leaks are:

- LOCA symptoms in primary without increasing pressure in confinement;
- rising of water level in affected SG and decreasing feedwater mass flow-rate;

- activity on the secondary side (steam, drainage of SG).

6. ACTIVITY TRANSPORT FROM PRIMARY TO SECONDARY

One of the recommendations given in IAEA documentation "Safety Issues and their Ranking for WWER-440/V213 NPPs" [3] is installation of the primary to secondary leakage system based on N^{16} activity monitoring system for reliable detection of damaged SG in the early phase of crack opening. A PRISE leak detection system can improve plant safety significantly by giving early indications and alarms on developing leaks and thus allowing for countermeasures. Taking into account very short half time $T_{1/2}$ of isotope N^{16} ($T_{1/2} = 7.14$ s), there is a need to verify correlation of the N^{16} activity measurement with leakage rate, leakage crack size and critical crack size. Correlations should be available for operators and should include various operational conditions.

French computer code CATHARE 2 seems to be convenient tool for the modelling of the transport of N^{16} from the place of the activation (core) to detector location (steam line) taking into account radioactive decay of N^{16} . The goal of work performed up to now [6] was to develop a correlation between leak size and measured activity. Besides its main purpose (non-equilibrium two-phase flow modelling), the CATHARE code is able to model transport of one radioactive isotope. The activity is transported by both, liquid and gas phase using the phase velocities v_L and v_G as transport velocities. They are treated as passive scalars for the thermal-hydraulics (i.e. no influence upon the thermal-hydraulic equations). No diffusion is modelled.

The activity transport is described by following equations:

$$A \frac{\delta \alpha \rho_G X_G}{\delta t} + \frac{\delta A \alpha \rho_G X_G v_G}{\delta z} = A f X^* \Gamma + S_G \quad (1)$$

$$A \frac{\delta (1 - \alpha) \rho_L X_L}{\delta t} + \frac{\delta A (1 - \alpha) \rho_L X_L v_L}{\delta z} = - A f X^* \Gamma + S_G \quad (2)$$

where:

A	cross section area of the pipe
α	void fraction
ρ_L, ρ_G	density of water and steam
X_L, X_G	activity in liquid and gas
S_L, S_G	activity source term in water and steam
f	fraction of activity changing phases in case of vaporisation or

condensation
 Γ interfacial steam flux per unit volume ($\Gamma < 0$ for steam condensation)

Specific constitutive laws are as follows:

$$\begin{aligned} X^* &= X_L && \text{for vaporisation} \\ X^* &= X_G && \text{for condensation} \\ f &= f_{GL} && \text{for condensation } (0 < f_{GL} < 1) \\ f &= f_{LG} && \text{for vaporisation } (0 < f_{LG} < 1) \end{aligned}$$

Radioactive decay with prescribed $T_{1/2}$ is considered simultaneously with the solution of above mentioned equations. There are two major difficulties when modelling transport of isotope N^{16} in the case of small primary to secondary leaks.

The first difficulty is low value of half life time. It means, that the results are very sensitive to the accurate estimation of transport delay from core to steam lines. As a consequence, the activity measured in steam lines depends strongly on the operational conditions (reactor power, reactor coolant pumps...).

The second difficulty is in estimation of the interfacial activity transfer coefficient f , which describes the transport of activity from one phase to another in the case of phase changes (evaporation and condensation). Since in the case analysed the evaporation in the secondary side of affected SG is the only one important phenomena, it is sufficient to know the value of coefficient f_{LG} . Taking into account, that the isotope N^{16} is gas soluble in water and during evaporation behaves in the same way, it was assumed that $f_{LG} = 1$.

Three loop nodalization of the primary side was used in the analyses. Simplified nodalization of the secondary side was prepared using average lengths of steam lines. Three layers of heat exchange tubes were used to model the primary side of SGs. The secondary side of SGs was modelled using recirculation model [7]. Nominal operation of the unit was assumed. Source of activity (water phase) with intensity corresponding to nominal power was located at the core outlet. Different primary to secondary leakage rates from 0.5 to 100 litres per hour were considered. A leak location with the corresponding diameter was considered on a heat exchange tube. Sensitivity studies were performed varying the break location from hot to cold collector and from lower to upper tube row. As outputs, stationary values of activity in the steam lines were investigated.

The activity transport from core to detector is closely tied with transport of coolant. The flow path in the primary side is from core to affected SG. Through the leaking tube, primary (active) coolant flows to the secondary side. Taking into account the leak position below the secondary SG water level and the low value of leak, it was assumed that the hot primary water mixes ideally with slightly subcooled secondary water. Here active secondary water is evaporated and transported to the detector. Obviously, this mechanism is able to model only average behaviour of the SG secondary side.

Typical transport velocities in nominal conditions are as follows:

- primary side (hot leg) $v_L = 10.7 \text{ m/s}$
- primary side (SG tubes) $v_L = 2.5 \text{ m/s}$
- secondary side (steam lines) $v_G = 38 \text{ m/s}$

The main transport delay arises on the secondary side of the affected SG due to the thermal-hydraulic mechanism described above. Final results can be summarised as follows:

- Within the analysed leak size range (0.5 - 100 l/h) the activity in the steam line depends linearly on leak size.
- Significant increase in transport delay (i.e. decrease in the activity in the steam line) is caused due to mixing of active primary water with slightly subcooled secondary water.
- The position of the leak on the damaged heat exchange tube has only minor influence on the primary side transport delay. The secondary side effect is much more important; it can be expected that the secondary side transport delay near the hot collector will be much shorter than near cold collector due to intensive steam production.
- In the case of leaks above the SG secondary side water level direct evaporation of active primary coolant can be expected (leaks from SG collector). Therefore the transport delay will be significantly shorter and, consequently, the measured activity in the steam line will be higher in comparison to leaks with the same size from SG tube.

Further calculations are planned for several values of reactor power and different modes of plant operation.

7. SUPPORT ANALYSES FOR EOP

Depending on the plant, different means are available for identification of PRISE leak and mitigation of the consequences. Basic information important for PRISE accidents for NPPs in Slovakia is summarised in Table I..

Emergency operating procedures (EOP) define the actions of the operation staff in abnormal or accident conditions. The main feature of the accident analyses performed for the EOP preparation is consideration of the operator interventions, which affect the course of the process. Analyses of this kind were (and still are) being performed for the joint effort of Dukovany and J.Bohunice V-2 NPPs in the frame of symptom oriented EOP preparation using RELAP 5/Mod3 code. Similar calculations are in preparation for Mochovce NPP.

Best estimate analyses were performed for Dukovany and J.Bohunice V-2 NPPs in order to find the proper strategy for mitigation of primary to secondary leaks. As initiating event, double ended break of one and three SG tubes was considered. It was assumed, that the main gate valves are not available for the isolation of affected SG on the primary side. Significant effort was put in with the aim of finding the optimal strategy for mitigation of primary to secondary leaks. Therefore various operator interventions were considered. The main goal was to prevent the radioactivity release from the affected SG into plant

surroundings. A necessary task is therefore to reduce primary pressure below the setpoints of the secondary side steam dumps to the atmosphere. There are two major obstacles which make this task difficult:

- the pressure in hydroaccumulators (about 6 MPa) is higher than setpoints of steam dumps into atmosphere (about 5.2 MPa);
- it is not possible to switch off the high pressure (HP) pumps by operator action before signals "small break" or "large break" disappear. Definition of these signals in V-2 NPP is as follows:
 - * small leak : $h_{prz} < h_{nom} - 3.2 \text{ m}$ and $T_{hot \text{ leg}} > 180 \text{ }^{\circ}\text{C}$ at least in 2 loops
 - * large leak : $p_{prim} < 8.3 \text{ MPa}$ and $T_{hot \text{ leg}} > 240 \text{ }^{\circ}\text{C}$ at least in 2 loops.

The basic idea for mitigation of the consequences of PRISE consists of isolation of the hydroaccumulators (HA) and cooling down the primary with the aim of cancelling signals for ECCS actuation. Then the depressurization of the primary to below the setpoints of steam dumps to the atmosphere can be initiated. Depending on the off-site power availability and plant configuration, various means are available for these tasks.

An effective means for primary cooldown is using the secondary side of non affected SGs. For this purpose, isolation of the affected SG from the part of the secondary side used for heat removal, is necessary. This can be done in two ways:

- i) isolation of the affected SG using steam line isolation valve;
- ii) splitting secondary side into two parts using the isolation valve on the main steam header.

In the first case, the pressure increase in affected SG is faster due to limited volume available to cope with leakage of primary coolant. On the other hand, five SGs (and both BRU-A and both BRU-K) are available for heat removal from primary side. In the second case, much larger volume (more than three times) is available and the pressure increase is therefore slower. On the other hand, only three SGs and one BRU-A and one BRU-K are available for heat removal.

Availability or non-availability of off-site power is an important point for the selection of optimal strategy. In the case when off-site power is available, the following means are available:

- i) heat removal from primary to secondary side (using non affected SGs) and from secondary side to plant surroundings:
 - reactor coolant pumps (i.e. forced circulation)
 - BRU-K, BRU-A, SG safety valves
- ii) depressurization of primary:
 - pressurizer (PRZ) spray (RCPs are working)
 - PRZ safety (relief) valves

In the case when off-site power is not available, only limited tools are available:

- i) heat removal from primary to secondary (natural circulation) and from secondary side to plant surroundings:
 - BRU-A, SG safety valves
- ii) depressurization of primary:
 - PRZ safety valves

All the above cases were analysed. First, the strategy with isolation of the affected SG on the secondary side was applied. In this case it was not possible to prevent opening of the SG safety valve. Therefore this approach was abandoned and, later, splitting the secondary side into two parts using the isolation valve on the main steam header was found to be a more appropriate strategy. Totally over 30 different variants were analysed [4],[5].

Application of the strategy with divided main steam header was possible without any significant difficulties in the cases where off-site power was available and BRU-K was used to cooldown primary side. The basic idea is illustrated for the case of three SG tubes rupture:

$t_0 = 0\text{ s}$	break of 3 SG tubes
t_1	first order scram (drop of PRZ water level by 2.7 m and primary pressure drop to 11.3 MPa)
t_2	signal "small break", start of 3 HP pumps
$t_3 = 600\text{ s}$	splitting main steam header into two parts, switch the BRU-A on isolated part to manual mode operation (opening setpoint 5.4 MPa instead of 5.2 MPa in automatic operation), interruption of FW supply to isolated SGs
t_4	start of cooldown of primary (using BRU-K or BRU-A on non-affected SGs)
t_5	isolation of HA
t_6	switch off HP pumps as soon as the primary temperature drops to below required value, start of depressurization of primary (PRZ spray, PRZ safety valve)
t_7	end of depressurization (primary pressure equal to secondary)
t_8	end of calculation

Application of the strategy with divided main steam header is much more difficult in the case where the initial event is combined with loss of off-site power. Similar scenario like in previous case was used. However, in this case only natural circulation in primary side and BRU-As on the secondary side are available to decrease primary temperature. Furthermore, PRZ spray is not available.

These results are illustrated on the Figs 1.3, 1.4, 1.7, 1.8, 1.9 and 1.10. Main difficulties are caused due to low capacity of BRU-A in V-2 NPP and low mass flow-rate in primary. However, the main reason is that the operator is not allowed to switch off HP pumps before the temperatures in hot legs of five loops drop to below required value (necessary condition for depressurization). In the analysis where the HP pumps were switched off by operator at 1000 s of the transient (regardless to the existence of signal "small" or "large" break), it was much easier to fulfil required criteria.

TABLE I: Comparison of J.Bohunice V-1, V-2 and Mochovce NPPs from the PRISE leakage point of view

means for :	Bohunice V1	Bohunice V2	Mochovce	Remarks :
limitation of SG collector cover lift-up (max. leak diameter)	no (107 mm)	no (107 mm)	yes (42 mm)	* available in the case of loss of off-site power **there are differences between 3rd and 4th unit ***an additional spray line available supplied from DG
N ¹⁶ activity measurement	planned	planned	N ¹⁶ in each steam line	
depressurization of primary	PRZ spray 1 RV 2 SVs	PRZ spray 1 RV 2 SVs	PRZ spray *** 1 RV 2 SVs	
heat removal from primary	6 RCPs 2 BRU-Ks 2 BRU-As (MSH) 6 x 1 BRU-A (steamline) 6 x 3 SG SVs	6 RCPs 2 BRU-Ks 2 BRU-As (MSH) 6 x 3(4) **SG SVs	6 RCPs 2 BRU-Ks 6 x 2 BRU-As (steamline) 6 x 3 SG SVs	
isolation of steamlines	FAV* motor valve	FAV* motor valve	2 FAVs* check valve	

REFERENCES

- [1] Guidelines for Accident Analysis of WWER Nuclear Power Plants, IAEA-EBP-WWER-01, IAEA Vienna, Austria, December 1995
- [2] Best Estimate Approach to Accident Analysis of WWER Nuclear Power Plants, WWER-SC-133, IAEA Vienna, Austria, Draft Report, Revision 1, April 1996
- [3] Safety Issues and their Ranking for WWER 440 Model 213 Nuclear Power Plants, WWER-SC-108, IAEA Vienna, Austria, March 1995
- [4] L.Vranka, P.Liška: Support Analyses for the Strategy for the SG Tube(s) Mitigation, Volume I, Report VÚJE 265/94, Trnava, Slovakia, December 1994
- [5] L.Vranka, P.Matejovič: Support Analyses for the Strategy for the SG Tube(s) Mitigation, Volume II, Report VÚJE 134/95, Trnava, Slovakia, August 1995
- [6] P.Matejovič, L.Vranka: Estimation of N^{16} Activity in the Steam Lines of J.Bohunice V-2 NPP During Nominal Operation, report VÚJE 133/95, Trnava, Slovakia, September 1995
- [7] P.Matejovič, L.Vranka, E.Václav: Application of the Thermal-hydraulic Codes in WWER-440 Steam Generators Modelling, Third International Seminar on Horizontal Steam Generators, Lappeenranta, Finland, October 1994
- [8] Primary to Secondary Cooling Circuit Leakages for VVER-1000 and VVER 440NPPs, WWER-SC-179, Draft report, IAEA Vienna, Austria, June 1996

3 SG tubes rupture with loss of off-site power

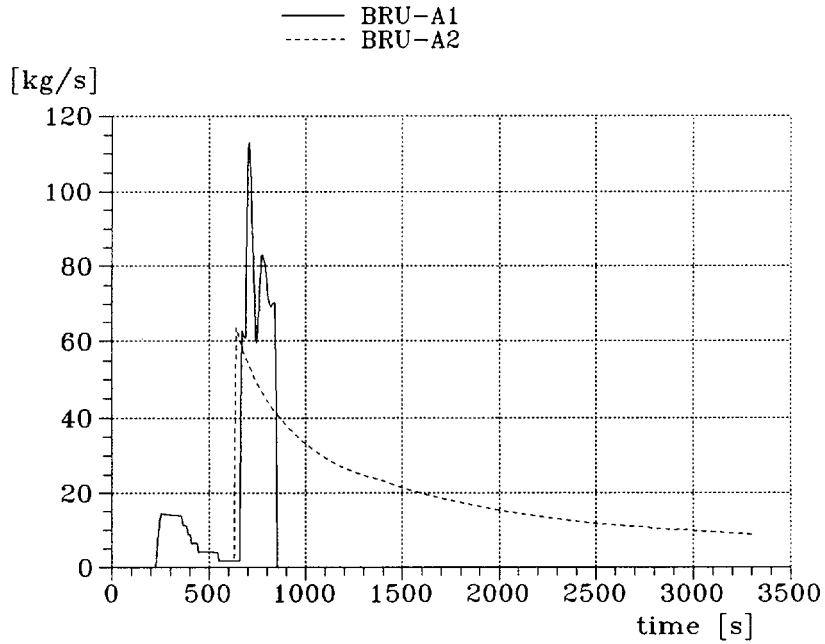


Fig.1.3. BRU-A mass flow.

3 SG tubes rupture with loss of off-site power

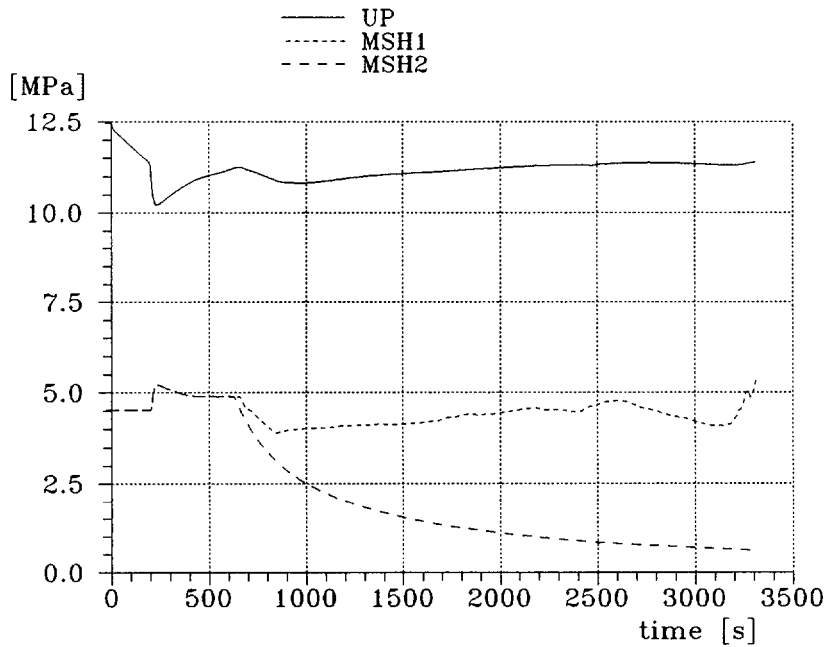


Fig.1.4. Primary and secondary pressure.

3 SG tubes rupture with loss of off-site power

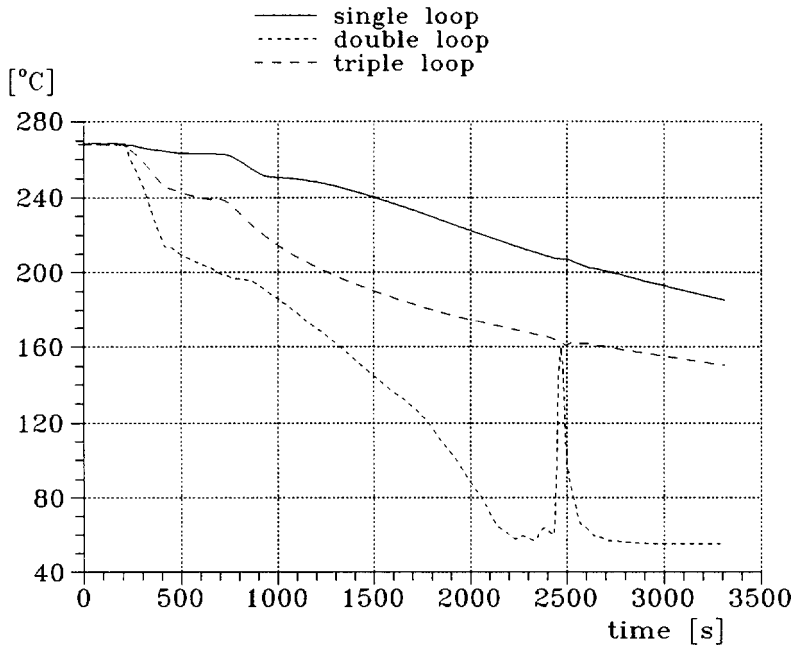


Fig.1.7. RV inlet nozzles water temperature.

3 SG tubes rupture with loss of off-site power

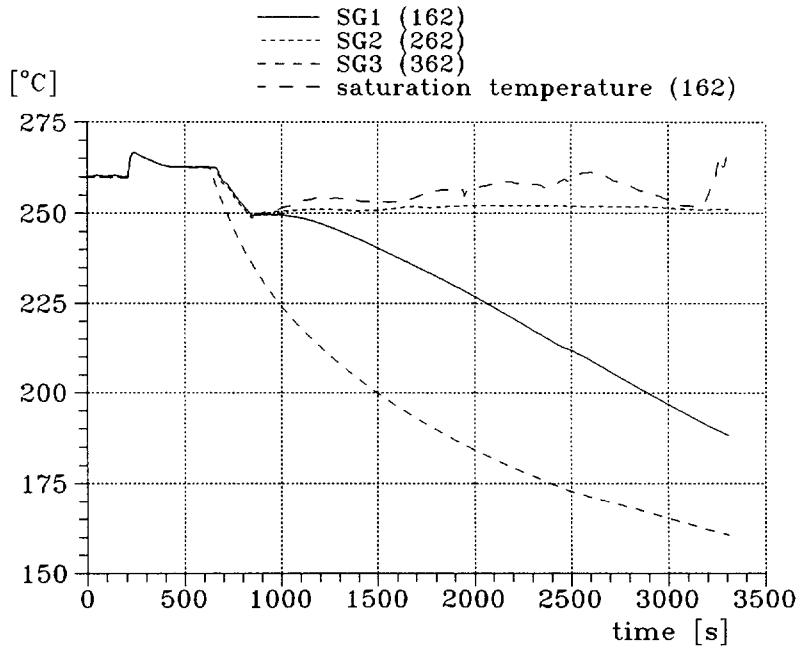


Fig.1.8. SG secondary side water temperature.

3 SG tubes rupture with loss of off-site power

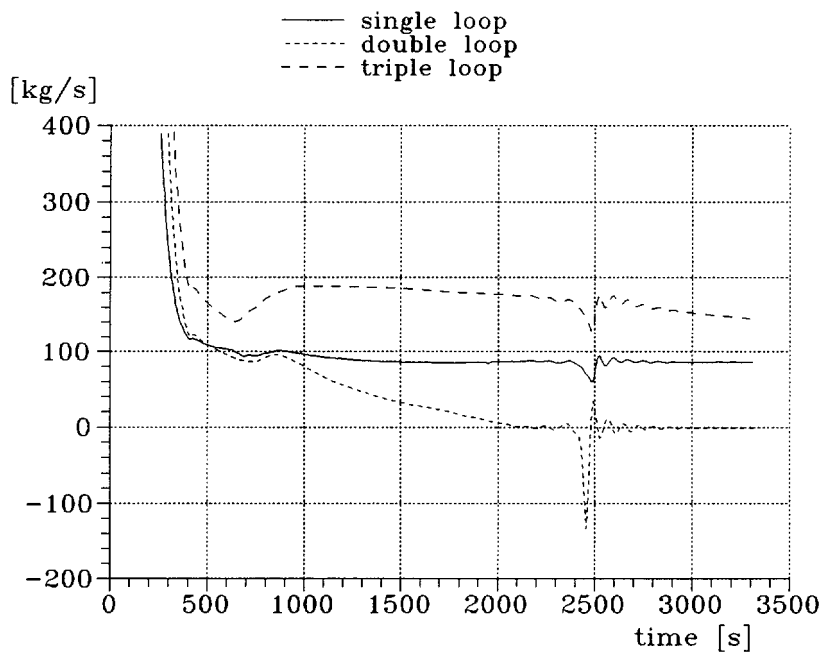


Fig.1.9. Mass flow in RV outlet nozzles.

3 SG tubes rupture with loss of off-site power

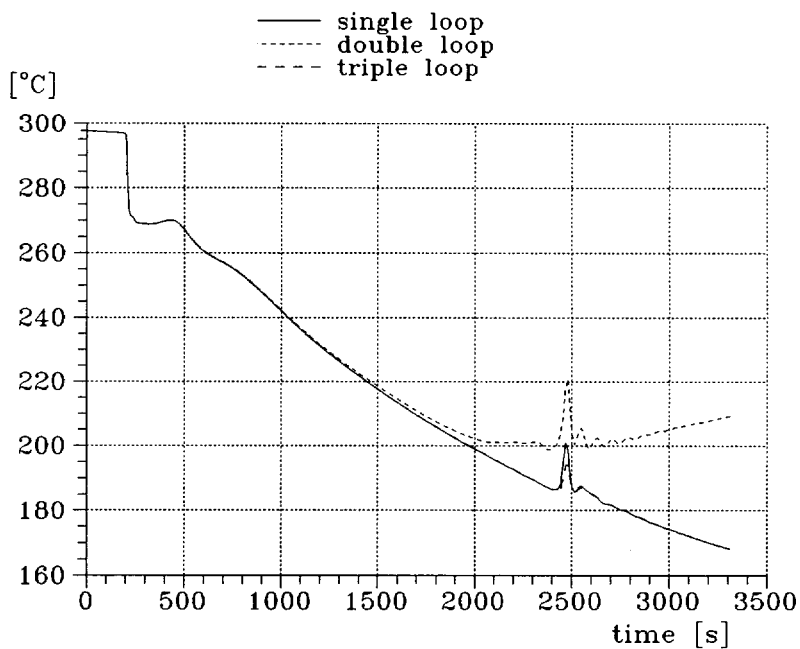


Fig.1.10. RV outlet nozzles water temperature.



**LARGE-SCALE EXPERIMENTAL FACILITY FOR EMERGENCY
CONDITION INVESTIGATION OF A NEW GENERATION
NPP WWER-640 REACTOR WITH PASSIVE SAFETY SYSTEMS**

**Yury N. Aniskevich, Viacheslav A. Vasilenko,
Vitaly K. Zasukha, Yury A. Migrov, Vladimir B. Khabensky**

Research Institute of Technology (NITI)

188537, Sosnovy Bor, Leningrad Region, Russia

Fax: +7 - (812-69) 636-72

ABSTRACT

The creation of the large - scale integral experimental facility (KMS) is specified by the programme of the experimental investigations to justify the engineering decisions on the safety of the design of the new generation NPP with the reactor WWER-640.

The construction of KMS in a full volume will allow to conduct experimental investigations of all physical phenomena and processes, practically, occurring during the accidents on the NPPs with the reactor of WWER type and including the heat - mass exchange processes with low rates of the coolant, which is typical during the utilization of the passive safety systems, process during the accidents with «a large leak», and also the complex intercommunicated processes in the reactor unit, passive safety systems and in the containment with the condition of long-term heat removal to the final absorber.

KMS is being constructed at the Research Institute of Technology (NITI), Sosnovy Bor, Leningrad region, Russia.

1. INTRODUCTION

The most significant improvements in NPP designs over the latest years have been related to the incorporating in reactor safety systems of passive principles (PCS) based on such physical phenomena as gravitation, convection, compressed gas energy.

Attractive and easy as these technical solutions may be, their implementation may turn out an inordinary job since passive systems functioning is based on significantly lower driving pressure as compared with active ones. Besides, there is no experience of PCS application at operating NPPs.

The aforementioned reasons justify a large amount of research and calculation for developing safety case for new NPP designs embodying PCS [1,2]. The said studies are to:

- demonstrate capacity of existing (or newly developed) computer codes to adequately describe thermohydraulic phenomena and processes in PCS at low values of the coolant velocity and pressure;
- confirm the PCS normal and efficient functioning, in particular, in their interaction with active systems, for various scenarios of design-basis accident development.

The internationally used method of new NPP design safety case based on calculation and experiments covers:

- simulation of individual thermohydraulic phenomena and processes at local (“fragmentary”) rigs, verification and validation of base computer codes describing these phenomena and processes;
- simulation of thermohydraulic processes at integral stands, as well as verification and validation of system computer codes describing the “through” heat removal processes from the reactor core to the ultimate sink.

2. DESIGNATION AND OBJECTIVES OF THE KMS CREATION

The large -scale integral experimental facility KMS is designed to simulate thermohydraulic processes in a reactor installation and PCS inside and outside the containment in order to justify the design and technological solutions on the new generation NPP WWER-640 reactor safety [3].

With this aim in view, the KMS serves to solve the following tasks:

- demonstration and justification of the PCS performance and efficiency under various scenarios of emergency situations and design-basis accidents;
- complex experimental study of interrelated thermohydraulic processes in the reactor installation, PCS and containment in “through” simulation of transients and design-basis accidents;
- study of the stress-strained state of the steel containment under design-basis accidents with the primary circuit depressurization and coolant leak to the containment;
- verification of base and system computer codes.

3. MAIN KMS TECHNICAL SOLUTIONS AND CHARACTERISTICS

3.1 Simulation principles

The KMS design embodies the following main simulation principles:

- the reproduction of the structure of the natural object, including a reactor installation model inside the containment, in as many detail as possible (Fig.1);
- the minimum allowable modelling scale which provides for reproduction of spatial in-circuit and containment processes characteristic of NPPs with passive systems.

In selecting the KMS parameters and equipment, the principle of volume-power simulation was used which is widely practised throughout the world [4,5].

In this case the geometric, kinematic and energetic parameters of models smaller than natural objects, are known to be selected out of real time conditions. At that, the scale of internal specific energy release is taken equal to one; vertical dimensions of model elements sections are taken equal to vertical dimensions of corresponding sections of a natural object and the rest dimensions are selected out of the equality of pressure losses and coolant transport delay in the model and nature elements.

There is a number of deviations from the above-mentioned simulation principle in the KMS design, specifically:

- different height scales for the reactor installation and containment are applied;
- the height of the natural circulation (NC) circuit in the passive containment cooling system (PCCS) is reduced as compared to the natural object;
- the pressurizer and the core makeup tanks (CMT) are outside the containment;
- the distance between the hot and cold nozzles in the reactor model is roughly half as long as that in the natural object.

The first of those solutions has been stipulated by the heat mass transfer process reproduction conditions in the containment, on the one hand, and in-circuit processes in the reactor installation, on the other. It is evident that retention of the natural height of the containment at the KMS could cause a 5.2-fold reduction in its cross-section (the scale being 1:27) as compared to the natural object. According to the calculations the aero- and hydrodynamics inside such a cigar-like containment would be significantly different from those in reality. Besides, there may occur difficulties with the reactor installation model equipment placement in such a containment. That is why it was decided to develop a containment model proceeding from the necessity to provide for a maximum similarity in terms of containment and in-containment premises. All the containment model dimensions, height inclusive, are selected on the basis of the geometrical similarity. The geometrical dimensions of PCCS and PSGCS models are selected proceeding from the maximum similarity of the systems static and dynamic properties as well as from the necessity to reproduce the characteristic heat exchange phenomena and two-phase flow in these systems channels.

The latter three solutions are determined by the first one, i.e. PCCS circuit height reduction as well as the pressurizer and CMT models relocation outside the containment are caused by the containment model limited height, and a closer arrangement of nozzles in the reactor model - by a smaller depth (in comparison to the natural object) of the emergency and fuel pools.

All the described departures from the precise simulation conditions do not significantly distort the dynamic changes in the main parameters for the characteristic scenarios of emergency situations development. This assumption was tested by system code comparative calculations with the facility parameters complying with the precise simulation conditions, the deviations being accepted.

3.2. Technical characteristics of the reactor installation model:

Rated electrical power of the core imitator 15 MW

Number of assembly imitators7

Number of fuel rod imitators in an assembly.....	312
Total number of fuel rod imitators.....	2184
Fuel rod imitator dimensions:	
outer diameter	9 mm
length	3770 mm
Electric heater type.....	indirect heating
Primary circuit pressure	18 MPa
Secondary circuit pressure	12 MPa
Primary circuit coolant temperature.....	350°C
Secondary circuit coolant temperature.....	300°C
Rated containment pressure	0.7 MPa
Number of heat exchange loops.....	4
Volume-power scale	1:27
Height scale.....	1:1

For collection and processing of the experimental data the Data Acquisition System “ANIS KMS” is used. DAS “ANIS KMS” was developed at NITI, Sosnovy Bor, on the basis of their own proven software.

The total number of experimental measuring channels is 1204, including 661 at the KMC first stage, the maximum polling speed is up to 10 Hz.

Besides, DAS “ANIS KMS” enables data acquisition from the Instrument and Control System (ICS KMS) via the high-level local network in order to complement the experimental data if need be. Thus, the total number of parameters (both analog and discrete) recorded at KMS is 2689.

4. STUDY PROGRAMME AT KMS

The experimental study programme at KMS was developed jointly by OKB “Gidropress”, Podolsk, “Atomenergoprojekt”, St. Petersburg, RCS “Kurchatov Institute”, Moscow, Physics and Energetics Institute, Obninsk and NITI, Sosnovy Bor. The programme encompasses step-by-step tests conducting, taking into account the stepwise manner of putting the facility into operation.

The first step is devoted to the experimental study of heat mass transfer inside the containment and in the heat transport system to the ultimate sink where steam is supplied from an external source. For this test rooms and building structures are modeled inside the containment but not the reactor installation equipment and systems.

At the second step the heat removal from the reactor in the natural circulation mode is simulated.

At the third stage the complex simulation of modes of abnormal operation, emergency situations and design-basis accidents is carried out.

At the second and third steps experiments are conducted at the reactor installation model with electric heated assemblies as a core simulator.

At the fourth step the complex try-out and optimization of the passive cooling principles and long-term decay heat transport to the ultimate sink are held with "through" simulation of design-basis accidents. The reactor installation model with B-407 RI full-scale fuel assembly simulators is used for the said experiments.

The construction of the KMS first stage is planned to be completed in 1998 and in the years 1999-2000 the first step experiments are to be conducted. The commissioning of the second stage is scheduled for 2001, and the second and third steps experiments - for 2002-2003. In 2004 the KMS construction shall be completed and the full-scale studies shall commence in compliance with the fourth step of the programme.

5. CONCLUSION

The decision on construction of a large-scale integral experimental facility KMS for investigation of interrelated thermohydraulic processes in a reactor installation, passive safety systems and containment of NPPs with WWER-640 complies with modern approaches to new design safety case.

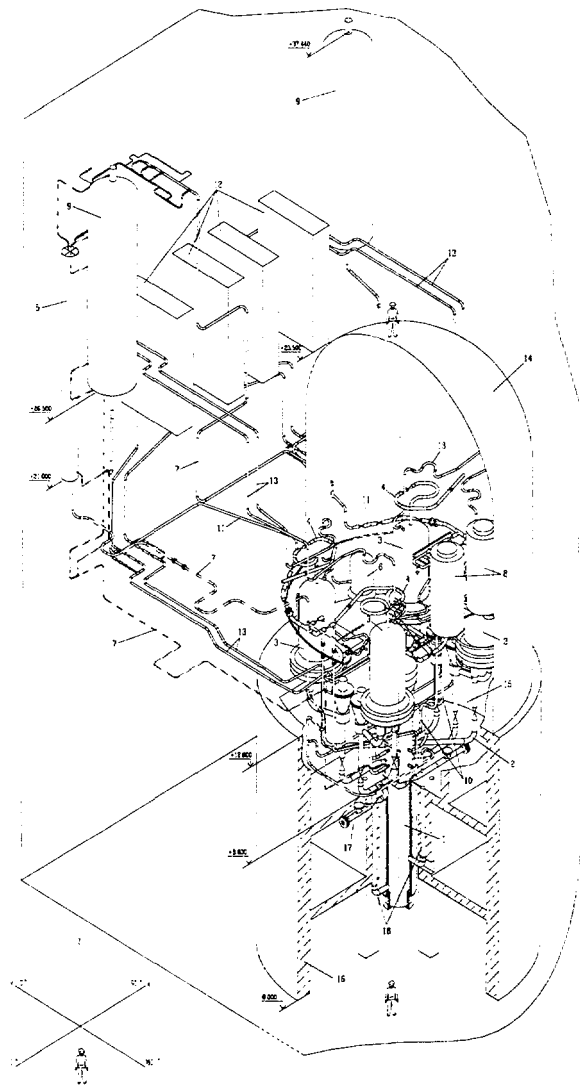
The necessity of analytical and/or experimental corroboration of all safety systems performance and efficiency in interaction under accidents in the mode of long-term heat removal from the reactor to the ultimate sink is acquiring a major importance in licensing new NPP designs.

In this connection the scale and principles of simulation embedded into the KMS design provide for complex experimenting and obtaining experimental data for system computer codes verification, the said codes being used for WWER-640 safety case.

The successful demonstration of the integral experiment with the primary circuit rupture at the large-scale experimental facility KMS will have a positive effect on all NPP designs using PCS.

REFERENCES

- [1] Brushi, H.J., 1996, «We're Ready if You're Ready: the Westinghouse AP600 is Tested and on its Way to Final Design Approval». *ICONE-4, New Orleans*, 10-14.03.96, V-2, p. 395.
- [2] Wilson, G.E., et al., 1996, «Use of Phenomena Identification and Ranking (PIRT) Process in Research Related to Design Certification of the AP600 Advanced Passive Light Water Reactor (LWR)». *ICONE-4, New Orleans*, 10-14.03.96, V-2, p. 581
- [3] Zasukha, B.K., et al., 1993, «Large-scale Facility for the Simulation of Accidents in New Generation NPPs with B-407 (KMS NP-500)». *The Fourth Annual Scientific Conference of the Nuclear Society, Nijni Novgorod, Russia*, 28.06-02.07.93.
- [4] Levin, A.E. and Mc Phersou, G.D., 1995, «A Practical View of the Insights from Scaling Thermal-Hydraulic Tests». *NURETH-7, V-2*, p. 1291.
- [5] Ishii, M., et al., 1995, «Scaling for Integral Simulation of Thermal-Hydraulic Phenomena in SBWR During LOCA». *NURETH-7, V-2*, p.1272.



- 1 - Reactor Model
- 2 - Main Coolant Circuit (MCC) Model
- 3 - Stem Generator (SG) Model
- 4 - Secondary Coolant Circuit (SCC)
- 5 - Pressurizer
- 6 - Bubble Condenser
- 7 - Pipelines of Pressure Suppresin
- 8 - Storage Tank of ECCS High Pressure (HP)
- 9 - Storage Tank of ECCS Low Pressure (LP)
- 10 - Pipelines of ECCS HP
- 11 - Pipelines of ECCS LP
- 12 - Chemical Pure Water Tank
- 13 - Pipelines of PCS SG
- 14 - Containment Model
- 15 - Emergency Pool
- 16 - Foundation
- 17 - Leak Imitation System
- 18 - Pipelines of Vault Reactor Model

NOTE

On this picture isn't show conditionally:

- metal constructions and floors;
- PCS of containment;
- pipelines and equipment of SCC out of containment;
- auxiliary systems and equipments.

Fig. 1. Reactor plant model. General View



F19800045

FOURTH INTERNATIONAL SEMINAR ON HORIZONTAL
STEAM GENERATORS
Lappeenranta, Finland
11 - 13 March 1997

**MODERNISATION AND POWER UPGRADING
OF THE LOVIISA NPP**

Aarno Keskinen
IVO Power Engineering Ltd, Vantaa, Finland

ABSTRACT

In 1995, Imatran Voima Oy (IVO) started a project for Modernisation and Power Upgrading of the Loviisa Nuclear Power Plant. The main objectives of the project are to ensure plant safety, to increase electricity production and to improve the expertise of the IVO staff.

The total electricity output of Loviisa 1 and 2 units is planned to be increased by about 100 MW. This will be achieved through renovation of the steam turbines and through gradual increase in the thermal reactor power up to 1,500 MW from the present level of 1,375 MW.

The Loviisa NPP Final Safety Analysis Report has been revised to a great extent in connection with the licensing process of the reactor power upgrading. The project also includes certain improvements in the primary and safety systems to ensure plant safety.

The total cost estimate of the project is around 200 million Finnish marks. The project implementation started in 1995 and in accordance with the plans in 2000 after several phases the last measures at power plant will be completed.

1. INTRODUCTION

Loviisa 1 and 2 Nuclear Power Units owned and operated by Imatran Voima Ltd (IVO) started commercial operation in 1977 (LO1) and in 1981 (LO2). During this time, a number of measures has been carried out to improve plant safety and reliable operation, in addition to better and better operational results.

IVO aims to continue the operation of the Loviisa NPPs for a long time to the future. The project for modernisation and power upgrading of the Loviisa NPPs gives an excellent possibility to take advantage of the latest developments in the nuclear power plant technology. The key aspects are to verify the plant safety, to improve production capacity and to give a good basis for extension of the plant's life.

In the long-term operation of an NPP, it is very important for the safety point of view to keep operation of the plants on an economically profitable level. In future, this viewpoint is becoming more and more important for the whole nuclear industry after competition with the other methods of producing electricity is becoming tougher. This is admitted extensively in the whole world, and we can see that a large number of NPP operators has corresponding projects under planning and implementation.

2. FEASIBILITY STUDY

In the first phase, before starting the project, the feasibility study was carried out applying to the reactor thermal power uprating in particular. The main result was briefly that no technical issues or issues relating to licensing could be found which would prevent the raising of the reactor thermal output up to 1,500 MW from the present level of 1,375 MW.

The feasibility study was divided into the following nine subtasks:

- Plant design and definition of new main process parameters
- Reactor core studies
- Reactor systems and main components
- Turbine plant systems and main components
- Fuel inspections
- Electrical, automation and ventilation systems
- Safety analyses and licensing
- Drafting of project plan and proposed decision
- Management, supervision and report of the feasibility study

In accordance with the feasibility study, there are certain modifications which was necessary to be carried out, including securing of the hp turbine and control valve steam flow capacity, enhancement of the generator cooling, modification of the main transformer and possible measures for reducing the HP preheater load.

In addition to the direct measures at the plant, a number of specific areas were found where additional studies will be necessary. RPV irradiation embrittlement, revision of major safety analyses, securing of the emergency heat transfer chain capacity during LOCA and steam generator moisture separation with increased mass flow were identified, for example.

3. PROJECT OBJECTIVES

The IVO Group intends to secure safe and economical operation of the Loviisa Nuclear Power Units 1 and 2 far into the future. This is the basis for setting the following objectives for the project:

- (1) Plant safety as a whole will be checked and, if needed, improvements will be made,
- (2) Plant units will be licensed for 1,500 MW reactor thermal output,
- (3) Gross electric output of plant units will be raised up to about 500 MW,
- (4) Assistance to extension of the life of the plant units,
- (5) Plant long-term availability not impaired
- (6) Increase in staff expert knowledge

4. TIME SCHEDULE

The feasibility study concerning the reactor power upgrading and turbine efficiency improvements was started in spring 1994. After one year and about 1,500 man-hours' extensive work, the base work for the project to modernise and upgrade power output of the Loviisa NPP was completed.

This project was established in summer 1995. The work to revise the Loviisa NPP Final Safety Analysis Report was started to a great extent at the same time as the whole project organisation was compiled and the project master plan was prepared. It was indicated already in the feasibility study that revision of the safety analysis reports in necessary extent is in the critical path of the time schedule.

Implementation of the modifications in the plant will be carried out in several phases from 1995 to the year 2000. The heaviest measures at the plant are made on turbine and electrical components related to power transmission from the generator to the national grid.

After extensive analysis, design and plant modification work the necessary test runs connected to the reactor thermal power upgrading was started in the beginning of 1997. These test runs are planned to be implemented gradually in several stages before starting the permanent operation of the plant with upgraded reactor power. IVO aims to receive a licence for the operation of the reactor with the thermal power of 1,500 MW in 1998.

The modernisation of the steam turbines including all the measures to improve efficiency of the turbines will be carried out within the annual maintenance outages and will be completed by the year 2000.

5. METHOD OF IMPLEMENTATION AND ORGANISATION

The implementation of the project is carried out in co-operation between the Loviisa NPP and IVO Power Engineering Ltd (IVO PE). In addition, many other organisations such as the Technical Research Centre of Finland (VTT) participate in the work. Special attention has been paid to co-ordination of the work in several directions. Particular subject-specific groups with many specialists have been established to ensure control of the entirety in essential sections such as nuclear safety and commissioning.

The project group is composed of about ten subprojects, including a responsible person from both the Loviisa NPP and IVO Power Engineering Ltd. organisations. One person is named as the main responsible person for the subproject, case by case. The subprojects are as follows:

- (1) Operating licences
- (2) Other licences
- (3) Safety analyses and basic data management
- (4) FSAR revisions and YVL guide comparison
- (5) PSA (including the level 2 PSA)
- (6) Modification of the turbines
- (7) Electricity systems
- (8) Reactor and fuel
- (9) Process systems and automation
- (10) Commissioning and revision of instructions

The instruction system including all the important activities in the project have been produced. There is also one person assigned to follow-up and develop quality assurance (QA) of the project. A project support / supervision group has been composed of the persons responsible for the personnel resources in the line organisations, which can support the responsible leader of the project and the project manager to arrange appropriate resources needed in the project.

6. SAFETY ANALYSES AND OTHER STUDIES

The starting point of the project has been to take advantage of the latest developments of technology, feedback of the operating experience, expertise in the ageing processes and safety reassessment coupled to the evolution of safety standards.

An extensive safety review and comparison of the plant with the latest national YVL guides has been carried out. This work was performed taking many international standards into account /1,2,3,4/, such as for example the IAEA standard "A Common Basis for Judging the Safety of Nuclear Power Plants Built to the Earlier Standards INSAG-8". As a result of the work, a particular safety review report has been completed.

The safety review together with the licensing process for the thermal reactor power of 1,500 MW includes renewal of the Final Safety Analyses Reports (FSAR) to a great extent. New accident analyses have been made concerning the containment pressure, LOCA and MSLB, for example. In addition to the accident analyses, there is a large number of transient situations which have been analysed too.

In addition, the operations of reactor, turbine and other systems as well as the main components in these systems have been considered. The necessary modifications in the plant were mainly considered already during the feasibility study. In the project, further plans for the implementation of the improvements have been prepared together with the implementation of these plans.

7. TECHNICAL IMPLEMENTATION

Increase in the plant power output is composed of reactor thermal power upgrading and improvements in the turbine efficiency. The final increment in electrical output will be around 50 MW per one plant unit. Approximately about 80 % is done through reactor power upgrading and the rest comes from the modernisation of the high-pressure and low-pressure steam turbines.

Temperature difference between the primary coolant into the reactor and the coolant out of the reactor will be increased in proportion to upgrading of the reactor thermal power. The primary system cooling water flow rate and the pressure in the primary system are intended to remain on the present level. The reactor power upgrading by 9.1% (up to 1,500 MW) means that the temperature rise of the primary coolant in reactor will be slightly less than 3 °C, compared with the present level.

The live steam flow rate to the hp turbine will increase in proportion to the thermal power, but the live steam pressure is not affected. HP turbines are to be modified according to the increased flow rate. In the main cooling sea water system, the flow rate will remain on the present level, which means that the temperature of cooling water after the main turbine condenser will rise about 1 °C before releasing to the sea with 1,500 MW reactor power compared to the original power level.

The reactor core fuel loading is considered on the basis of the present limits set for the maximum fuel linear power and fuel burn up. Increase in reactor thermal output will be carried out by optimising the power distribution in the core, so that the loading of one single fuel bundle will not be increased above the present maximum level. In parallel with this work, more advanced options have been investigated relating to the real mixing rate of the cooling water in the fuel subchannels and the increasing of the fuel enrichment. The most important purpose of these studies is to optimise fuel costs in the long term. The dummy elements installed on the side of fuel core in Loviisa 1 and 2 will be preserved to minimise irradiation embrittlement of the reactor pressure vessel.

The focus in the plant modifications is on the conventional side of the plant, and only minor modifications in the primary systems are necessary. Thermal efficiency and reliability of the steam turbines will be improved in consequence of the turbine modernisation. Certain modifications in the electrical generators and the main transformers are needed before continuous operation with upgraded power net output. The only remarkable measure on the primary side is the replacement of the pressuriser safety valves. The extensive studies concerning the functioning of the systems and equipment and review of the safety analyses have resulted some additional safety improvements. These are not necessary for the reactor power upgrading, but they are part of the continuing effort to maintain and raise the safety level of the plant.

Before starting continuous operation with the upgraded reactor power, a long-term trial operation with specific tests will be carried out in accordance with a separate test programme. Sequence programs are to be approved by the authorities, and the test results of each reactor power level shall also be approved before it is allowable to pass on to the next power level defined in the programme. The first phase of the plant trial operation with 103 % reactor power was started in the beginning of 1997. Preliminary results from the test run made at power plant seem to be equal with all analyses. After all phases of the trial operation has been completed successfully and the results have been considered, the authorities can make the final decision about the continuous operation of the reactor on the new power level.

8. ENVIRONMENTAL IMPACTS ASSESSMENT

The law on the Environmental Impact Assessment (EIA) came into force in Finland at the beginning of September 1994. Before, the environmental impact had been assessed within the framework of other environmental legislation, which was fragmented by its nature. This is the first time in Finland that the EIA Procedure has been applied to a nuclear power plant. At the same time with the assessment of the environmental impact of reactor power upgrading, other significant plans of the power plant have also been considered, such as extension of the storage for spent fuel and a solidification plant for the radioactive plant waste.

The EIA Procedure consists of three main elements: 1) the scope of application (screening), 2) the EIA programme (scoping) and 3) the EIA report (EIA statement). The law and the decree set certain procedures for these stages. The co-ordination authority is the Ministry of Trade and Industry.

The environmental impact has been assessed in the EIA Report, which was completed in December 1996. The main result concerning the reactor thermal power upgrading was that no other considerable environmental impact could be found than a slight increase in the cooling water outlet temperature. This means that the maximum temperature increase of the cooling water in the main condenser, before releasing back to the sea, is about 1 °C more than the present temperature increase, which is typically close to 10 °C.

9. SUMMARY

The project for modernisation and power upgrading of the Loviisa NPP utilizes the advancement of the nuclear plant technology and analysing methods. This makes it possible to verify safety of the plant, to improve production capacity and to give a good basis for extension of the Loviisa NPP's life.

The total electricity output of the Loviisa NPP is aimed to be increased by about 100 MW. This is done by improving the steam turbine efficiency and by uprating reactor thermal power gradually to 1,500 MW from the present level of 1,375 MW. The project is estimated to cost around MFIM 200, and the project will be completed in the year 2000.

An extensive safety review and comparison of the plant with the latest national YVL guides have been carried out. Certain improvements in the primary and safety systems are planned to be carried out. This is the first time in Finland that the environmental impact of a NPP have been assessed in accordance with an EIA Programme which provides a systematic procedure for the assessment of the environmental impact of the project.

REFERENCES

- /1/ INSAG-8, A Common Basis for Judging the Safety of NPP's built to Earlier Standards, IAEA, Vienna, 1994.
- /2/ NUSS-guide, 50-SG-012, Periodic Safety Review of Operational NPP's, IAEA, Vienna, 1994.
- /3/ CB-4, Safety Evaluation of Operating NPP's built to earlier standards, Draft, IAEA, Vienna, 1 June 1995.
- /4/ NUCLESUR, Safety Evaluations of Nuclear Power Plants Designed to earlier Standards, rev. 2, Arnhem, Marc 1996

DESIGN AND PRODUCTION UPGRADES OF STEAM GENERATORS WWER - 1000 OFFERED TO CHINA REPUBLIC (LIANYUNGANG PROJECT)

Dr. Miroslav KAWALEC, VITKOVICE, a.s., Ostrava, Czech Republic

INTRODUCTION

Due to the capability of our company in design and manufacturing of the WWER - 440 and WWER - 1000 steam generators and reasonable commercial credit, China Nuclear Energy Industry Corporation (Lianyungang Nuclear Power Plant Preparatory Department) asked VITKOVICE, a.s. to submit offer on WWER - 1000 steam generators with innovations fulfilling the IAEA recommendations.

Having analysed the failure of the primary collectors at the NPPs in Ukraine and Russia, a number of innovations have been implemented that principally increase the service life and operational reliability of the steam generators. These innovation elements fulfill entirely the recommendations following from the IAEA meeting of the consultants held in Vienna in May 17 - 21, 1993 devoted to the cracking causes of primary collectors.

The overall dimensions and basic operational parameters of the steam generators (SG) for Lianyungang NPP Project (LNPPP) are being planned to maintain the same as for WWER - 1000/320. The LNPPP steam generators meets the requirements:

- a) Rules for Erection and Safety Operation of the Nuclear Power Equipment and Piping. PN-AE-G-7-008-89
- b) Standards for Strength Calculations of the Equipment and Piping of Nuclear Plants. PN-AE-G-7-007-86
It is possible to provide strength calculations according to the ASME Code (Section III) if required by the customer.
- c) Welds and Cladding. Basic Conditions. Pn-AE-G-7-009-89
- d) Welds and Claddings. Inspection and Testing Program. PN-AE-G-7-010-89

The SG belongs to the 1st category of seismic resistance equipment. The SG structure and the way of its fixing assures:

- a) Maintaining of normal operation without break at the effect equal to the Project Earthquake (PE) up to 8 of MSK - 1964 scale.
- b) Reactor equipment cooling at the seismicity more than PE up to max. calculated earthquake 9 degrees.
- c) Parallel capturing of the load developed by max. calculated earthquake with complete breaking of the main circulation piping O.D. 850 mm.

To fasten the SG, there is a mechanical supporting system and a system of antiseismic snubbers that guarantee:

- a) Capturing of mass and seismic loads
- b) SG displacement at thermal dilatation of piping

- c) Capturing of vertical forces developed as resultants of the mass itself and reactive force at the piping O.D.850 complete breaking

INNOVATIONS

- a) Basic parts manufacture

The manufacture of primary collectors and other SG parts from steel 10GN2MFA in accordance with high quality steel production technology (double vacuum treatment, implementation of high quality forming technology and heat treatment assuring very low value of the harmful elements content, high homogeneity of the steel composition) allow to guarantee the following steel parameters in Technical Conditions on semi-products delivery:

content of P max. 0,008 %

content of S max. 0,008 %

critical temperature of brittleness T_{ko} max. - 10 C

This high quality steel 10GN2MFA is the answer to the first root cause of WWER-1000 SG collector cracking - high level of impurities content in 10GN2MFA steel.

- b) Production technology

- Hole boring technology assures compressive stress on the hole surface.
- Controlled hydraulic expansion of the tube to collector connection assuring minimum plastification of the ligaments of SG primary collectors.
- Manufacture of the elliptical head from one piece of plate (without weld) which increases the service life and costs effective with respect to removeable thermal insulation and in-service inspections.
- Manufacture of threads in threaded holes in the primary collector flange by precise milling operation.
- Using of submerged welding technology for seal claddings of the primary collector flange, secondary circuit heads and manholes.
- Using of controlled electric heating for preheating and postweld heat treatment of SG pressure vessel parts.

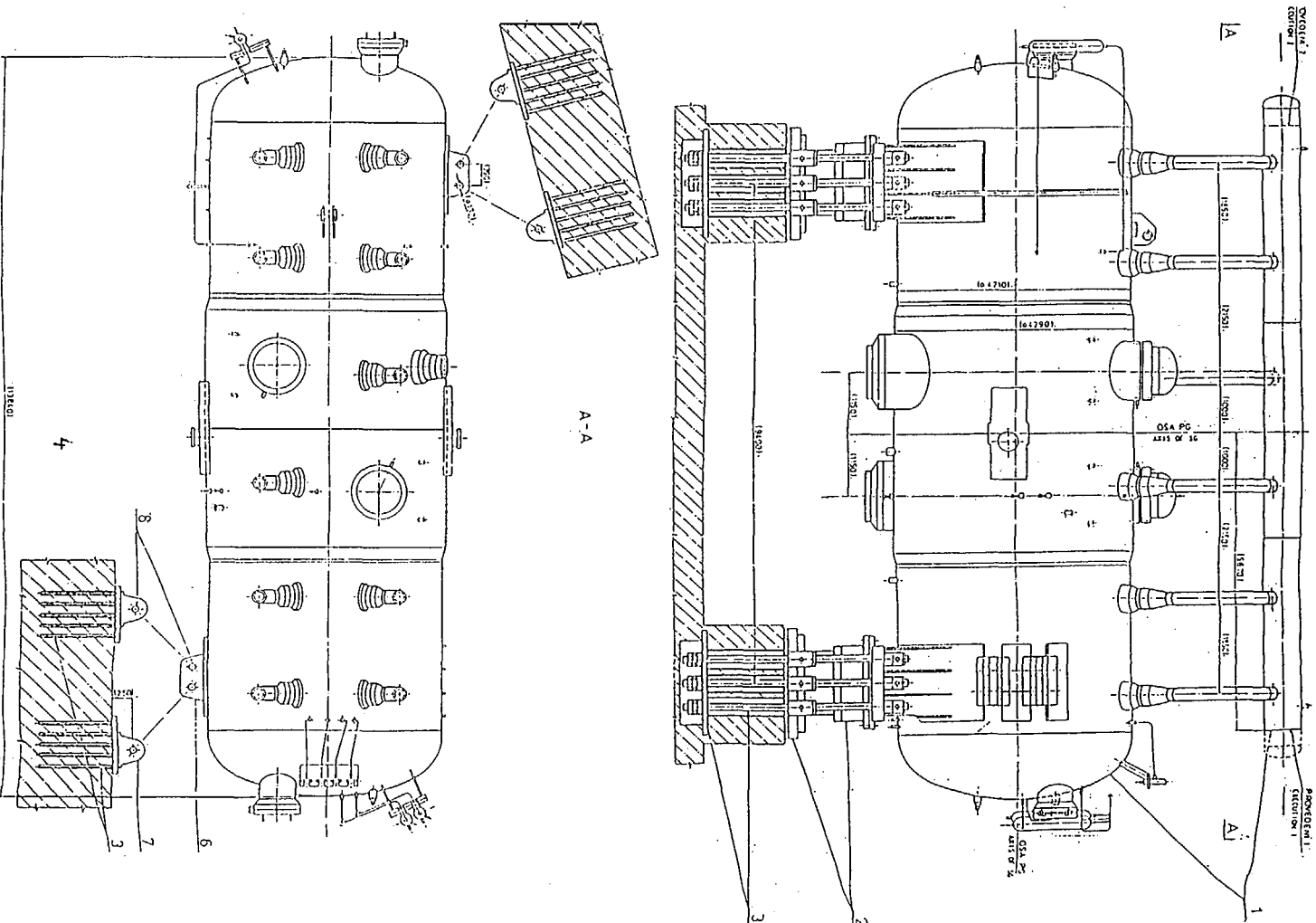
- c) Design

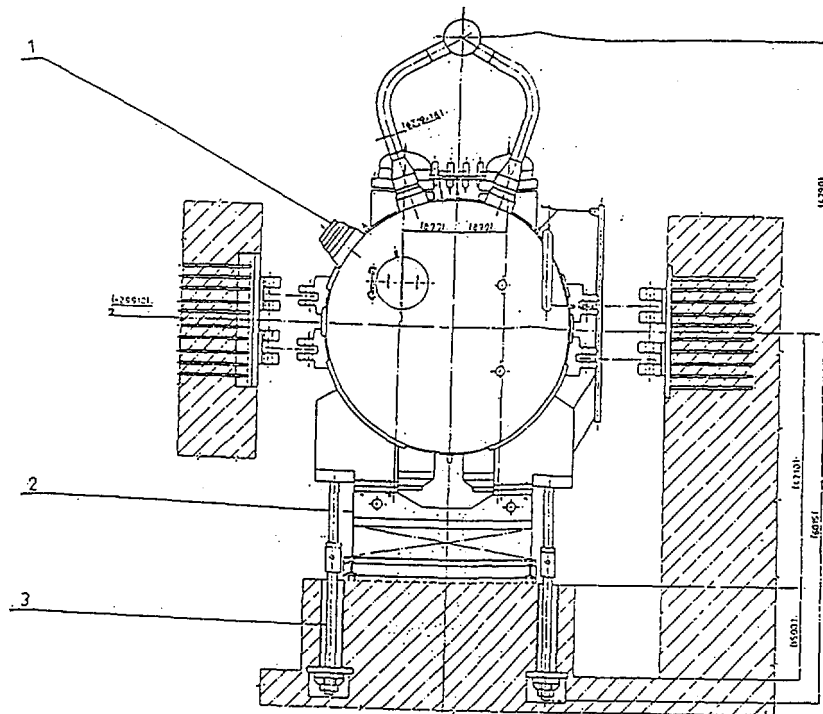
- Increased thickness of the primary collector from 171 mm to 182,5 mm (6,75 %) which enable to decrease ligament stress.
- Structural modification of the bundle (with the heat exchanging tubes manufactured from the steel 08CH18N10T) and the distance system assuring a considerable decrease of the ligament stress in the area co called "wegde".

The number of tubes is decreased from 11000 to 10450 (5 %), the tube dimensions are changed from 16 x 1,5 mm to 15,6 x 1,33 mm. This enables to ligament dimension from 8,45 mm to 9,42 mm (11,45 %). Thermal power of S6 does not change.

These above mentioned design measures are the answer to the second root cause of WWER - 1000 S6 collector cracking - high ligament stress. Structural modification of the tube bundle also improves flushing of heat exchanging tubes and enhances resistance against corrosion.

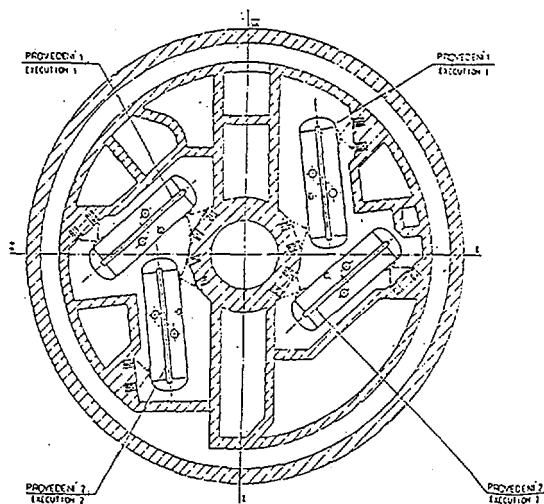
- Reconstruction of inside and outside blowdown lines and feedwater collector leading to a considerable reduction of the impurities concentration, first of all in the primary collectors area.
- Reconstruction of moisture separators leading to a moisture reduction of general steam.
- Enlargement of the bending radius of heat exchanging tubes that allows to increase the quality and the speed of eddy current inspection or non-destructive examinations.
- Design modification for the application of diagnostic systems and special measurements (cladding layers and special nozzles for fixing of sensors and for cable lines).
- Replacement of nickel sealing rings by expanded graphite sealing rings leading to a large reduction of stresses in the primary collector flange connection.





PŮDORYSNÉ ROZMÍSTĚNÍ PAROGENERÁTORŮ
GROUND ARRANGEMENT PLAN OF STEAM GENERATORS

M 1:300
SCALE



-ROZMĚRY ODČÍTAT DLE TP VĚ KOD 150
DIMENSION SCOPE ACCORDING TO TPV 1000/150

-V ROZMĚRE JSOU UVĚDĚNY POČTY KUSŮ PRO 1 PAROGENERÁTOR.
NUMBER OF PIECES IN SPECIFICATION IS FOR ONE SG

1	1-1220-510	12	12	32
2	2-1220-515	3	3	315
3	3-1220-510	2	2	315
4				
5				
6				
7	0-1220-1	1	1	315
8	0-1220-2	2	2	315
9	0-1220-3	3	3	315
10	0-1220-4	4	4	315
11	0-1220-5	5	5	315
12	0-1220-6	6	6	315
13	0-1220-7	7	7	315
14	0-1220-8	8	8	315
15	0-1220-9	9	9	315
16	0-1220-10	10	10	315
17	0-1220-11	11	11	315
18	0-1220-12	12	12	315
19	0-1220-13	13	13	315
20	0-1220-14	14	14	315
21	0-1220-15	15	15	315
22	0-1220-16	16	16	315
23	0-1220-17	17	17	315
24	0-1220-18	18	18	315
25	0-1220-19	19	19	315
26	0-1220-20	20	20	315
27	0-1220-21	21	21	315
28	0-1220-22	22	22	315
29	0-1220-23	23	23	315
30	0-1220-24	24	24	315
31	0-1220-25	25	25	315
32	0-1220-26	26	26	315
33	0-1220-27	27	27	315
34	0-1220-28	28	28	315
35	0-1220-29	29	29	315
36	0-1220-30	30	30	315
37	0-1220-31	31	31	315
38	0-1220-32	32	32	315
39	0-1220-33	33	33	315
40	0-1220-34	34	34	315
41	0-1220-35	35	35	315
42	0-1220-36	36	36	315
43	0-1220-37	37	37	315
44	0-1220-38	38	38	315
45	0-1220-39	39	39	315
46	0-1220-40	40	40	315
47	0-1220-41	41	41	315
48	0-1220-42	42	42	315
49	0-1220-43	43	43	315
50	0-1220-44	44	44	315
51	0-1220-45	45	45	315
52	0-1220-46	46	46	315
53	0-1220-47	47	47	315
54	0-1220-48	48	48	315
55	0-1220-49	49	49	315
56	0-1220-50	50	50	315
57	0-1220-51	51	51	315
58	0-1220-52	52	52	315
59	0-1220-53	53	53	315
60	0-1220-54	54	54	315
61	0-1220-55	55	55	315
62	0-1220-56	56	56	315
63	0-1220-57	57	57	315
64	0-1220-58	58	58	315
65	0-1220-59	59	59	315
66	0-1220-60	60	60	315
67	0-1220-61	61	61	315
68	0-1220-62	62	62	315
69	0-1220-63	63	63	315
70	0-1220-64	64	64	315
71	0-1220-65	65	65	315
72	0-1220-66	66	66	315
73	0-1220-67	67	67	315
74	0-1220-68	68	68	315
75	0-1220-69	69	69	315
76	0-1220-70	70	70	315
77	0-1220-71	71	71	315
78	0-1220-72	72	72	315
79	0-1220-73	73	73	315
80	0-1220-74	74	74	315
81	0-1220-75	75	75	315
82	0-1220-76	76	76	315
83	0-1220-77	77	77	315
84	0-1220-78	78	78	315
85	0-1220-79	79	79	315
86	0-1220-80	80	80	315
87	0-1220-81	81	81	315
88	0-1220-82	82	82	315
89	0-1220-83	83	83	315
90	0-1220-84	84	84	315
91	0-1220-85	85	85	315
92	0-1220-86	86	86	315
93	0-1220-87	87	87	315
94	0-1220-88	88	88	315
95	0-1220-89	89	89	315
96	0-1220-90	90	90	315
97	0-1220-91	91	91	315
98	0-1220-92	92	92	315
99	0-1220-93	93	93	315
100	0-1220-94	94	94	315
101	0-1220-95	95	95	315
102	0-1220-96	96	96	315
103	0-1220-97	97	97	315
104	0-1220-98	98	98	315
105	0-1220-99	99	99	315
106	0-1220-100	100	100	315
107	0-1220-101	101	101	315
108	0-1220-102	102	102	315
109	0-1220-103	103	103	315
110	0-1220-104	104	104	315
111	0-1220-105	105	105	315
112	0-1220-106	106	106	315
113	0-1220-107	107	107	315
114	0-1220-108	108	108	315
115	0-1220-109	109	109	315
116	0-1220-110	110	110	315
117	0-1220-111	111	111	315
118	0-1220-112	112	112	315
119	0-1220-113	113	113	315
120	0-1220-114	114	114	315
121	0-1220-115	115	115	315
122	0-1220-116	116	116	315
123	0-1220-117	117	117	315
124	0-1220-118	118	118	315
125	0-1220-119	119	119	315
126	0-1220-120	120	120	315
127	0-1220-121	121	121	315
128	0-1220-122	122	122	315
129	0-1220-123	123	123	315
130	0-1220-124	124	124	315
131	0-1220-125	125	125	315
132	0-1220-126	126	126	315
133	0-1220-127	127	127	315
134	0-1220-128	128	128	315
135	0-1220-129	129	129	315
136	0-1220-130	130	130	315
137	0-1220-131	131	131	315
138	0-1220-132	132	132	315
139	0-1220-133	133	133	315
140	0-1220-134	134	134	315
141	0-1220-135	135	135	315
142	0-1220-136	136	136	315
143	0-1220-137	137	137	315
144	0-1220-138	138	138	315
145	0-1220-139	139	139	315
146	0-1220-140	140	140	315
147	0-1220-141	141	141	315
148	0-1220-142	142	142	315
149	0-1220-143	143	143	315
150	0-1220-144	144	144	315
151	0-1220-145	145	145	315
152	0-1220-146	146	146	315
153	0-1220-147	147	147	315
154	0-1220-148	148	148	315
155	0-1220-149	149	149	315
156	0-1220-150	150	150	315
157	0-1220-151	151	151	315
158	0-1220-152	152	152	315
159	0-1220-153	153	153	315
160	0-1220-154	154	154	315
161	0-1220-155	155	155	315
162	0-1220-156	156	156	315
163	0-1220-157	157	157	315
164	0-1220-158	158	158	315
165	0-1220-159	159	159	315
166	0-1220-160	160	160	315
167	0-1220-161	161	161	315
168	0-1220-162	162	162	315
169	0-1220-163	163	163	315
170	0-1220-164	164	164	315
171	0-1220-165	165	165	315
172	0-1220-166	166	166	315
173	0-1220-167	167	167	315
174	0-1220-168	168	168	315
175	0-1220-169	169	169	315
176	0-1220-170	170	170	315
177	0-1220-171	171	171	315
178	0-1220-172	172	172	315
179	0-1220-173	173	173	315
180	0-1220-174	174	174	315
181	0-1220-175	175	175	315
182	0-1220-176	176	176	315
183	0-1220-177	177	177	315
184	0-1220-178	178	178	315
185	0-1220-179	179	179	315
186	0-1220-180	180	180	315
187	0-1220-181	181	181	315
188	0-1220-182	182	182	315
189	0-1220-183	183	183	315
190	0-1220-184	184	184	315
191	0-1220-185	185	185	315
192	0-1220-186	186	186	315
193	0-1220-187	187	187	315
194	0-1220-188	188	188	315
195	0-1220-189	189	189	315
196	0-1220-190	190	190	315
197	0-1220-191	191	191	315
198	0-1220-192	192	192	315
199	0-1220-193	193	193	315
200	0-1220-194	194	194	315
201	0-1220-195	195	195	315
202	0-1220-196	196	196	315
203	0-1220-197	197	197	315
204	0-1220-198	198	198	315
205	0-1220-199	199	199	315
206	0-1220-200	200	200	315
207	0-1220-201	201	201	315
208	0-1220-202	202	202	315
209	0-1220-203	203	203	315
210	0-1220-204	204	204	315
211	0-1220-205	205	205	315
212	0-1220-206	206	206	315
213	0-1220-207	207	207	315
214	0-1220-208	208	208	315
215	0-1220-209	209	209	315
216	0-1220-210	210	210	315
217	0-1220-211	211	211	315
218	0-1220-212	212	212	315
219	0-1220-213	213	213	315
220	0-1220-214	214	214	315
221	0-1220-215	215	215	315
222	0-1220-216	216	216	315
223	0-1220-217	217	217	315
224	0-1220-218	218	218	315
225	0-1220-219	219	219	315
226	0-1220-220	220	220	315
227	0-1220-221	221	221	315
228	0-1220-222	222	222	315
229	0-1220-223	223	223	315
230	0-1220-224	224	224	315
231	0-1220-225	225	225	315
232	0-1220-226	226	226	315
233	0-1220-227	227	227	315
234	0-1220-228	228	228	315
235	0-1220-229	229	229	315
236	0-1220-230	230	230	315
237	0-1220-231	231	231	315
238	0-1220-232	232	232	315
239	0-1220-233	233	233	315
240	0-1220-234	234	234	315
241	0-1220-235	235	235	315
242	0-1220-236	236	236	315
243	0-1220-237	237	237	315
244	0-1220-238	238	238	315
245	0-1220-239	239	239	315
246	0-1220-240	240	240	315
247	0-1220-241	241	241	315
248	0-1220-242	242	242	315
249	0-1220-243	243	243	315
250	0-1220-244	244	244	315
251	0-1220-245	245	245	315
252	0-1220-246	246	246	315
253	0-1220-247	247	247	



VÍTKOVICE - POWER SYSTEMS ENGINEERING 706 02 Ostrava, Czech Rep.

F. Cikryt, L. Bednárek, L. Kusýn

Replacement of Nickel Sealing Rings by Expanded Graphite Sealing Rings - Upgrading of SG Primary Collector Flange Connection

Introduction

One of the most loaded parts of a steam generator of VVER 440 MW type are the bolts and thread holes of the primary collector cover sealing set. The strength calculations and tensometric measurings performed during operation proved the high degree of a load on the bolts. The conditions of the stress limitation are not met in some cases according to the pertinent standards. The untightnesses at nickel rings occurred during putting the units of Jaslovské Bohunice and Dukovany nuclear power stations into operation. With regard to improve the reliability, the producer has taken measures to improve the quality of the rings and users have introduced more strict regulations for bolts tightening. Due to these measures the high reliability of the set has been obtained from point of view of the tightness, but substantial reduction of bolts and holes threads loading have not been obtained. Several years operation experience proved relatively low service of bolts, damage of thread holes and sealing grooves.

As the degree of mechanical load is one of the vital parameters influencing the damage of sealing set, in 1996 we started with the works aimed at a possibility of nickel sealing rings replacement for a more modern type of sealing which assure the higher reliability and service life of the individual part of sealing set under the reduced load.

Aims of the Solutions

The below given aims have been followed during this works:

- reduction of initial tightening force by 20% at minimum as a basic Precondition for improvement of bolts service life
- anticipation of damage of sealing surfaces
- improvement of sealing set reliability
- construction modifications minimization of sealing surfaces
- assurance of tightness in all -steam generator working mode--
- assurance of conclusive evidence of proposed solution for approval by supervisor bodies
- accetable price of new sealing elements

Technical parameters

A primary collector works under the following basic parameters:

Pressure:	operation	12,2 MPa
	calculation	12,7 MPa
	test	16,3 MPa for NPP Dukovariy
		17,2 MPa for NPP J. Bohunice

Temperature:	operation	300 °C
	calculation	325 °C

Medium: primary and secondary circuit water

Initial tightening force on one bolt during use of the nickel sealing rings: 272,2 kN

Scheme of sealing set is shown in Figures 1,2.

Evaluated types of sealing

The elastic steel sealing of circular section composed of three layers, plate metal sealing composed with a graphite layer, spiral sealing of rectangular section with a graphite sealing strip, sealing of expanded graphite of rectangular section pressed in distance rings and profiled sealing of expanded graphite pressed in the steel distance rings have been evaluated within a project solution.

Proposal for solution

Based on the evaluation of the individual types of sealing appropriateness according to criterion set-down in the beginning of the solution, the profiled sealing according to the shape of grooves have been chosen as the most suitable one, made of the expanded graphite and pressed in the -steel distance rings. It works in secondary force flow. The cover bears on the distance steel rings during assembly and in the same time compresses the graphite rings. The tightness is assured by holding of a minimum sealing pressure between the sealing graphite ring and sealing surfaces. The calculation of forces on the bolts has been prepared for proposed type of sealing and for all working modes. The results of calculation proved that the reduction of the initial tightening force on the bolts by almost 25% is possible compared with the primary value.

Scheme of sealing set with a new type of sealing is shown in the Figure 3.

Photos of new type of sealing complet - see Figure 4.

Properties of the new sealing complet

- a modern sealing material
- composed of two steel distance rings and a graphite sealing ring of nuclear grade ($C > 99,85\%$, $Cl < 0,005\%$ and ash)
- prepressed according to sealing groove shape
- it works in secondary force flow
- it is not so much sensitive to pressure and temprature changes and dilatation
- it is more reliable and safe than nickel
- it doesn't stick on a groove surface
- it reduces tightening force by 25% minimum

By its properties the graphite is predetermined as a substitution for the nickel sealing rings working in a main force flow within reconstruction of sealing aggregate of primary cover with a collector SG VVER 440 and 1000.

Technical specification

The graphite sealing completes consist partly of two Steel distance rings and partly of the own graphite sealing - see figure 4. The graphite is prepre.-zsed according to the shape of grooves on the collector. The distance rings prevent the graphite run out in a radial direction, make manipulation easy and particularly transfer all pressure, temperature and dilatation changes.

The input material used for production of sealing rings is an expanded graphite of nuclear grade, it means $C > 99,85\%$ and $Cl < 0,005\%$, ash is the remaining part of a content. The distance rings, are of austenitic steel.

Sealing consists in assembly of a flange connection and tightening of bolts to the pertinent extension. Considering the fact that the graphite is prepressed according to the shape of existing grooves and surface quality of grooves doesn't need to be as perfect as when the nickel sealing rings are used, the graphite doesn't require the machining of collector flange grooves. It needs, however, machining of primary cover sealing surface.

A rise of 0,4 mm on a sealing surface of the cover is necessary to be machined to the level of overlay as the sealing set works in secondary force flow. The work of sealing in secondary flow means that the primary cover will fit through the distance rings of sealing complete on the collector flange.

Compared with nickel sealing rings used till now and working in the main force flow, this arrangement has the advantage consisting in that all pressure and temperature changes and dilatations are transferred through the distance rings and the own sealing is stressed by a constant pressure. The nickel sealing rings transfer these changes themselves. For this reason the sealing working in the secondary force flow is more reliable and safe than the sealing working in the main force flow.

Application of a modern graphite sealing enables reduction of tightening forces in bolts by 25% which leads to considerable improvement of service life , reliability and nuclear safety of primary collector sealing aggregate.

Application suitability verification

Two programs of pressure tests were accomplished for purpose of verification of graphite sealing complete application in a primary cover bolted connection with a PG VVER 440 collector.

These were both pressure tests in cold state performed within Vítkovice a.s. including deformation characteristic investigation, and pressure tests with a full model of primary SG VVER 440 collector performed in OKB Hidropress, Podolsk, Russia with simulation of crucial stationary and nonstationary modes.

In the course of pressure tests in cold state performed in Vítkovice, among others the graphite properties were verified when untightness within impulse line at a model of primary cover bolted connection with the collector SG VVER 440 was indicated. It is necessary to state that after tightness failure the inside graphite sealing was ruptured in three places but, taking it out from the groove it remained together all the time, consequently there was no danger that pertinent parts of the graphite sealing could fall down in a primary circuit. The sealing showed distinct longitudinal cracks of 5 - 10 cm length. The inside sealing was not damaged.

The results have been proved also by tests done on fixture performed by OKB Hidropress. The tests Proved that the graphite will not be crushed and broken down under possible untightness and that there is no danger of contamination of primary collector by the graphite.

It is suitable to follow the below given principle during removal of sealing completes from the grooves:

First, move round a slight amount with the sealing complete in the grooves and then remove the distance rings with the graphite .from the grooves.

Conclusion

The experimental works performed with graphite sealing completes in Vítkovice, a.s. in the course of pressure tests in cold state and the experiment works performed with test equipment simulating operational load of sealing set, unambiguously confirmed appropriateness of proposed type of sealing application as a substitution for nickel sealing rings used by now. The experiments further confirmed the results of theoretical calculations showing that the initial tightening force on the bolts is possible to reduce by 22% approximately compared with the primary value under assurance of the joint tightness. The real initial tightening force will be set down based on detail evaluation of all experiments and carrying out of the detail calculation which will take into account the deformation characteristics of graphite complete.

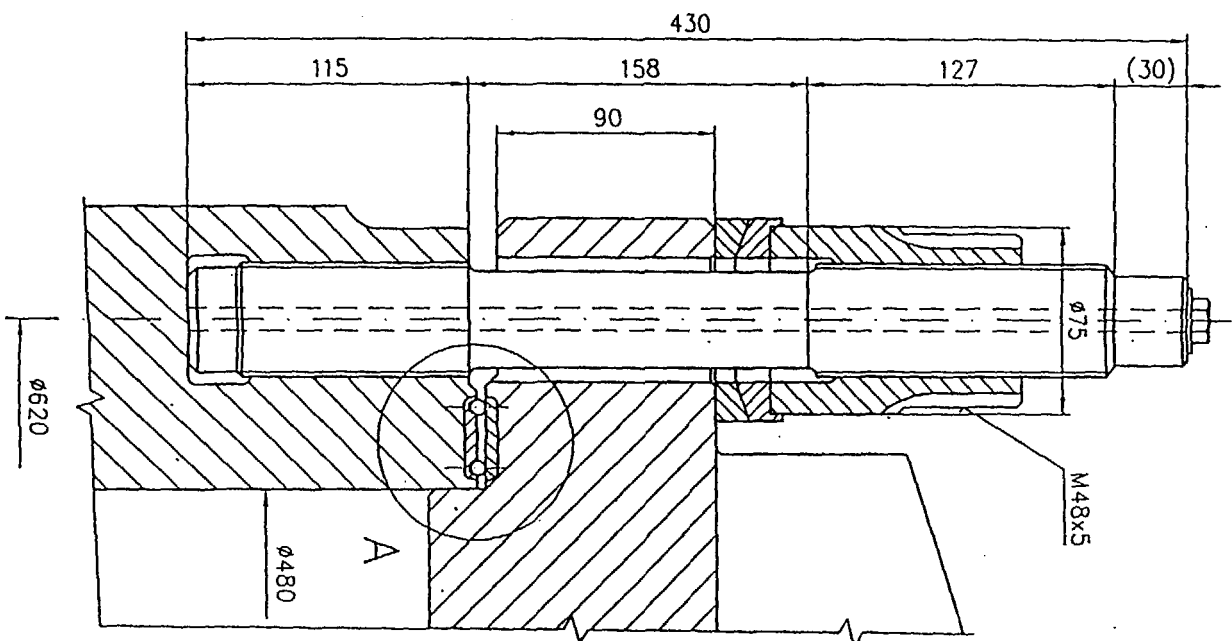


Fig 1.

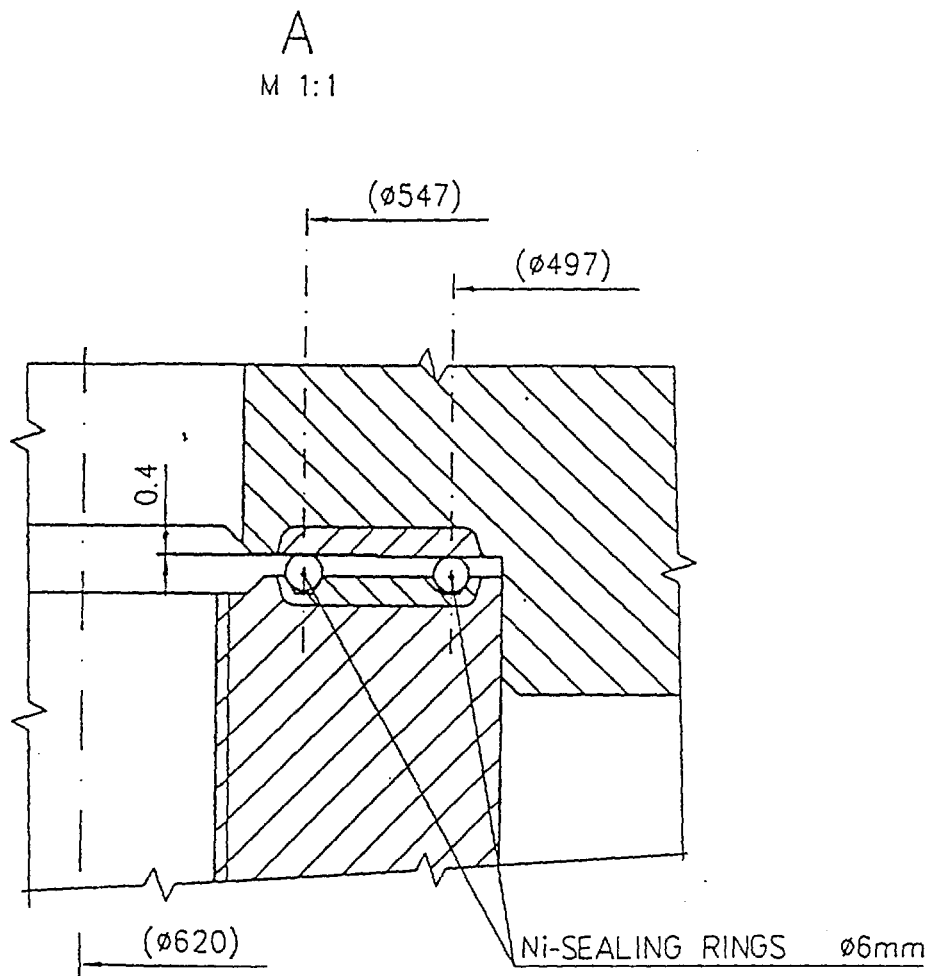


Fig. 2

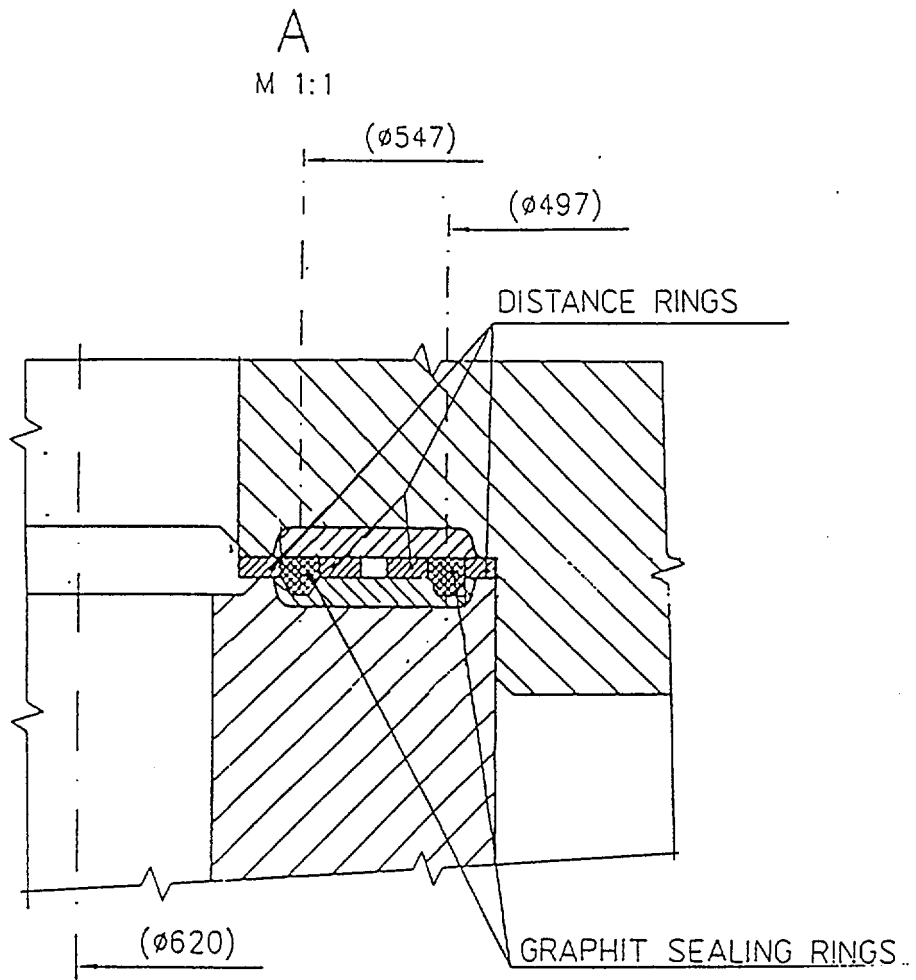


Fig. 3

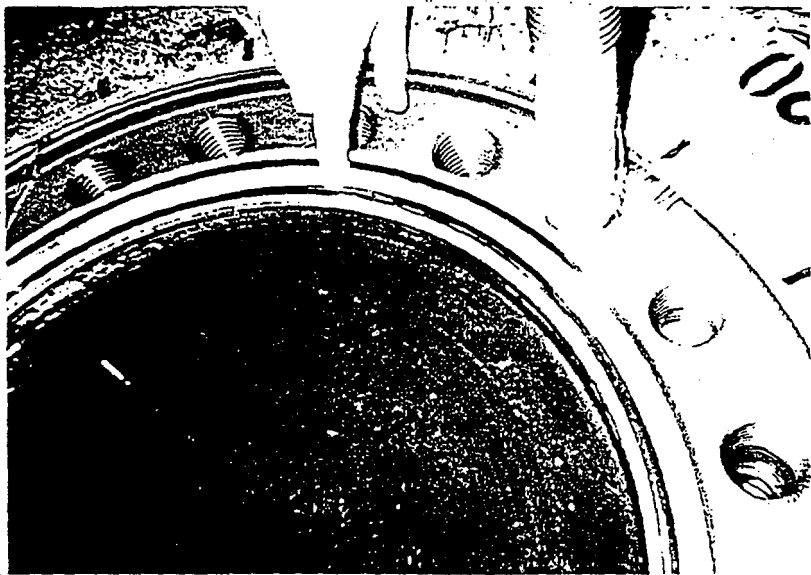
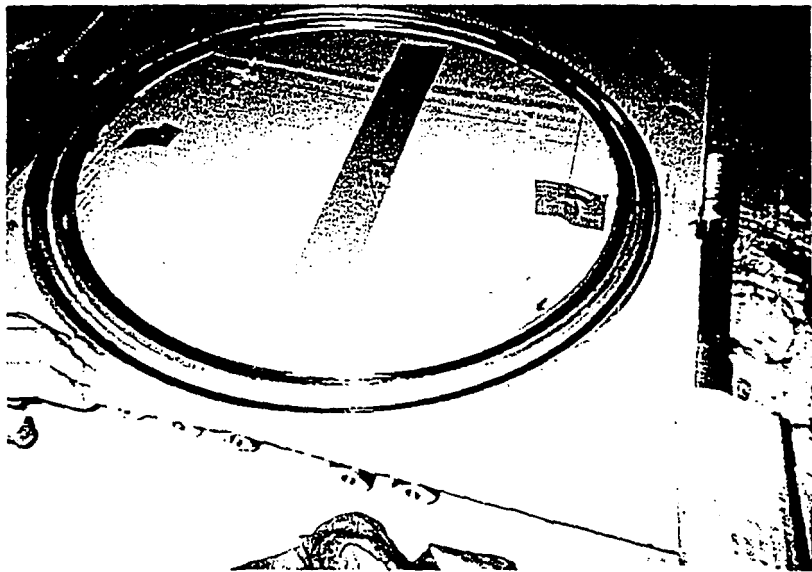


Fig. 4

REPORT

***prepared for the fourth international seminar for horizontal SGs
which will be held on 11–13 of March 1997, in Lappeenranta,
Finland.***

***Analysis of Kalinin NPP Steam Generator PGV–1000 thermophysical
characteristics.***

Messrs Aksyonov V.I., Bay V.F., Bogatchek L.N., Timofeyev A.E. (Russia).

1. Special features of Steam–Generator PGV–1000 design.

PGV–1000 is a steam–generator of horizontal type with U–type tube bundle, which consists of stainless steel (08x18H10T) tubes of 16 x 1,5 mm diameter and their total heat exchanger surface is 6115 sq.m. Tube bundle is situated in the bottom part of SG vessel and is separated from steam plenum by perforated sheet, sheet's perforation is 3.6 % for Unit 1 and 8 % for Unit 2.

Feedwater header is situated under perforated sheet over a tube bundle and provides stable natural boiler water multiple circulation mode in a tube bundle, when the operation level of boiler water is 1250–2250 mm from lowest generatrix of SG vessel. The diameter of SG vessel is 4000 mm. Perforated sheet, steam plenum and jalousie separator, situated in the top part of SG vessel, provide steam humidity less than 0.2 % at pressure $p=60$ bar for all stationary and transient modes of unit operation for the capacity not more, than 1470+103 ton/hour [1].

2. Changing of Kalinin NPP PGV–1000 thermophysical characteristics during operation.

Kalinin NPP Unit 1 and 2 PGV–1000 provided safe operation during 11 fuel campaigns at Unit 1 and 9 fuel campaigns at Unit 2.

In the table N1 there are shown relevant values of Unit 1,2 PGV–1000 heat transfer characteristics, obtained during Units operation in the begining and in the end of fuel campaigns.

On the figure 1 there are shown curves of relevant values of PGV–1000 heat transfer characteristics for 10 fuel campaigns of Unit 1 and 8 fuel campaigns of Unit 2.

The analysis of these data shows, that when design requirements for feedwater quality and water plenum blowdown conditions are provided, degradation of PGV–1000 thermophysical characteristics does not exceed 3–5 %.

Following water–chemical washings of the secondary side practically in full scope restore heat transfer characteristics of PGV–1000.

3. Ensuring of stable conditions of operation of reactor VVER-1000 cores in case of considerable changes of PGV-1000 operation conditions.

Big quantity of feedwater, boiler water natural multiple circulation self-regulation in water plenum, simple principle of steam separation foreseen in the PGV-1000 design allow to provide stable operation of core in the wide range of PGV-1000 operation modes. So, during reactor operation at rated power, coolant temperature in the SG outlet practically does not depend on changing of feedwater temperature from 164 °C to 224 °C (in different modes of high pressure feedwater heat-exchangers operation) and boiler water level from 2250 mm (rated value) to 1250 mm.

During reactor operation with not full quantity of working RCPs (3 or 2 RCPs of 4) SGs are operated at different power levels (from 10 % of full rated power at the loop with switched off RCP to 100 % at the loop, opposite to the loop with switched off RCP). In such situation the coolant temperature in all loops at reactor inlet is practically the same.

In modes of total deenergizing of reactor installation SGs provide stable transition to the coolant natural circulation mode in the primary side keeping similar temperature conditions in the reactor loops.

On the base of the analysis of SGs operation modes we see slight dependence of coolant outlet temperature on boiler water level and feedwater temperature and also on capacity and coolant flow rate and, that coolant outlet temperature mainly depends on steam pressure and SG heat transfer characteristics. This allows to provide stable operation conditions for PWR-1000 reactor core fuel assemblies.

Literature:

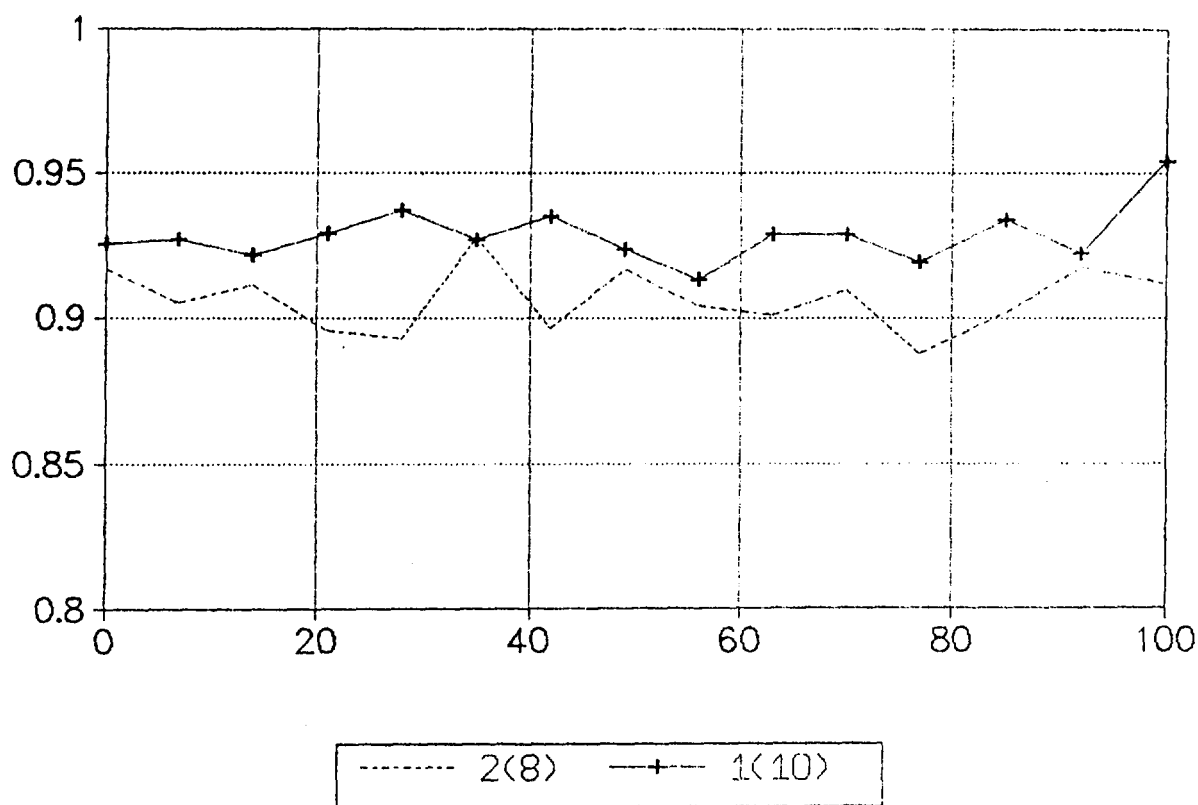
- 1. Ovchinnikov F.Ya., Voznesensky V.A. and others, NPP with PWR-1000 operational modes, Moscow, Energoizdat, 1992.*

Averaged values of heat transfer characteristics of SG PGV-1000 (in comparison with a comissioning value accepted as "1") for the begining and the end of fuel campaigns of Units 1 and 2.

<i>Fuel campaign</i>	<i>Unit 1</i>		<i>Unit 2</i>	
	<i>begining</i>	<i>end</i>	<i>begining</i>	<i>end</i>
3	==	==	0.97	0.96
4	==	==	0.94	0.92
5	==	==	0.92	0.90
6	0.95	0.94	0.89	0.87
7	0.94	0.96	0.94*	0.91
8	0.95	0.92	0.91	0.90
9	0.90	0.88	0.97*	0.96
10	0.93*	0.94	==	==
11	0.92	0.94	==	==
12	0.94	==	==	==

* — water-chemical washing was made during outage

Fig.1 Changing of averaged heat transfer characteristics of SG PGV-1000.



21. LAATIKAINEN, MARKKU. Stability of aqueous emulsions of synthetic and extracted wood pitches. 1992. 28 s.
22. SUN, ZHENG. Laser beam welding of austenitic-ferritic dissimilar steel joints. 1992. 87 s. Diss.
23. KOIKKALAINEN, PASI. Neurocomputing systems: formal modeling and software implementation. 1992. 142 s. Diss.
24. PIRTILÄ, TIMO. Empirical analyses of inventory intensity in the Finnish engineering industry. 1992. 118 s. Diss.
25. KOVANEN, M.A. Monte Carlo study of charged particle behaviour in Tokamak plasmas. 1992. U.s. Diss.
26. KALLAS, JUHA et al. Treatment technology of wastewater containing phenols and phenolic compounds. 1992. 40 s.
27. VAKKILAINEN, ESA K. Offdesign operation of kraft recovery boiler. 1992. 83 s. Diss.
28. LAMPINEN, JOUKO. Neural pattern recognition: distortion tolerance by self-organizing maps. 1992. U.s. Diss.
29. PUUMALAINEN, PERTTI. Paperin laadun ja siihen valmistusprosessissa vaikuttavien tekijöiden on-line mittaukset. 1993. 279 s. Väitösk.
30. Second International Seminar of Horizontal Steam Generator Modelling September 29 - 30, 1992, Lappeenranta, Finland. 1993. 195 s.
31. NYKÄNEN, TIMO. M_K -factor equations and crack growth simulations for fatigue or fillet-welded T-joints. 1993. 198 s. Diss.
32. KOSKINEN, JUKKA TAPIO. Use of population balances and particle size distribution analysis to study particulate processes affected by simultaneous mass and heat transfer and nonuniform flow conditions. 1993. U.s. Diss.
33. TUUNANEN, JARI. Thermal-hydraulic studies on the safety of VVER-440 type nuclear power plants. 1994. U.s. Diss.
34. ZHANG, ZHILIANG. A practical micro-mechanical model-based local approach methodology for the analysis of ductile fracture of welded T-joints. 1994. 151 s. Diss.
35. KÄLVIÄINEN, HEIKKI. Randomized Hough Transform: new extensions. 1994. U.s. Diss.
36. HEIKKONEN, JUKKA. Subsymbolic Representations, Self-Organizing Maps, and Object Motion Learning. 1994. 119 s. Diss.
37. KOSKINEN, JUKKA ANTERO. Knapsack sets for cryptography. 1994. 81 s. Diss.
38. TURUNEN, ESKO. A mathematical study of fuzzy logic; an algebraic approach. 1994. U.s. Diss.
39. JANHUNEN, ANTERO. Toimitustäsmällisyyden suunnittelumenetelmä. 1994. 161 s. Väitösk.
40. LARES-MANKKI, LAURA. Strategy implementation bottlenecks: identification, analysis and removal. 1994. 150 s. Diss.
41. French-Finnish Colloquium on Safety of French and Russian Type Nuclear Power Plants. 1994. 275 s.
42. KORPELA, JUKKA. An analytic approach to distribution logistics strategic management. 1994. U.s. Diss.
43. Third International Seminar on Horizontal Steam Generators October 18-20, 1994, Lappeenranta, Finland. 1995. 413 s.
44. AHOLA, JYRKI. Yrityksen strategiaprosessi: näkökohtia strategisen johtamisen kehittämiseksi konserniorganisaatiossa. 1995. 235 s., liitt. Väitösk.

45. RANTANEN, HANNU. The effects of productivity on profitability: a case study at firm level using an activity-based costing approach. 1995. 169 s., liitt. Diss.
46. Optics in Engineering: First Finnish-Japanese meeting Lappeenranta, 12-14th, June 1995 / ed. by P. Silfsten. 1995. 102 s.
47. HAAPALEHTO, TIMO. Validation studies of thermal-hydraulic code for safety analysis of nuclear power plants. 1995. U.s. Diss.
48. KYLÄHEIKO, KALEVI. Coping with technology: a study on economic methodology and strategic management of technology. 1995. 263 s. Diss.
49. HYVÄRINEN, LIISA. Essays on innovativeness and its evaluation in small and medium-sized enterprises. 1995. U.s. Diss.
50. TOIVANEN, PEKKA. New distance transforms for gray-level image compression. 1996. U.s. Diss.
51. EHSANI, NEDA. A study on fractionation and ultrafiltration of proteins with characterized modified and unmodified membranes. 1996. U.s. Diss.
52. SOININEN, RAIMO. Fracture behaviour and assessment of design requirements against fracture in welded steel structures made of cold formed rectangular hollow sections. 1996. 238 s. Diss.
53. OJA, MARJA. Pressure filtration of mineral slurries: modelling and particle shape characterization. 1996. 148 s. Diss.
54. MARTTILA, ESA. Ilmanvaihdon lämmönsiirtimien teknillinen ja taloudellinen mitoitus. 1996. 57 s. Väitösk.
55. TALONPOIKA, TIMO. Dynamic model of small once-through boiler. 1996. 86 s. Diss.
56. BACKMAN, JARI. On the reversed Brayton cycle with high speed machinery. 1996. 103 s. Diss.
57. ILME, JARNO. Estimating plate efficiencies in simulation of industrial scale distillation columns. 1997. U.s. Diss.
58. NUORTILA-JOKINEN, JUTTA. Choice of optimal membrane processes for economical treatment of paper machine clear filtrate. 1997. U.s. Diss.
59. KUHMONEN, MIKA. The effect of operational disturbances on reliability and operation time distribution of NC-machine tools in FMS. 1997. 133 s., liitt. Diss.
60. HALME, JARKKO. Utilization of genetic algorithm in online tuning of fluid power servos. 1997. 91 s. Diss.
61. MIKKOLA, AKI. Studies on fatigue damage in a hydraulically driven boom system using virtual prototype simulations. 1997. 80 s., liitt. Diss.
62. TUUNILA, RITVA. Ultrafine grinding of FGD and phosphogypsum with an attrition bead mill and a jet mill: optimisation and modelling of grinding and mill comparison. 1997. 122 s., liitt. Diss.
63. PIRTTILÄ, ANNELI. Competitor information and competitive knowledge management in a large, industrial organization. 1997. 175 s., liitt. Diss.
64. MEURONEN, VESA. Ash particle erosion on steam boiler convective section. 1997. 149 s. Diss.
65. MALINEN, HEIKKI. Forecasting energy demand and CO₂-emissions from energy production in the forest industry. 1977. 86 s., liitt. Diss.
66. SALMINEN RISTO T. Role of references in international industrial marketing - a theory-building case study about supplier's processes of utilizing references. 1997. 375 s. Diss.